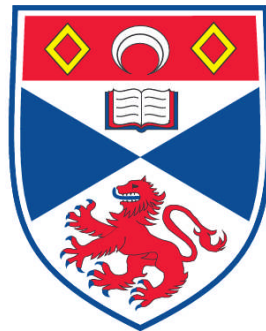


**STRUCTURE AND FUNCTION OF NITRATE AND NITRITE
TRANSPORTERS, N_{RTA} AND N_{ITa}, FROM
*ASPERGILLUS NIDULANS***

Vicki Frances Symington

**A Thesis Submitted for the Degree of PhD
at the
University of St. Andrews**



2009

**Full metadata for this item is available in
Research@StAndrews:FullText
at:**

<http://research-repository.st-andrews.ac.uk/>

Please use this identifier to cite or link to this item:

<http://hdl.handle.net/10023/748>

This item is protected by original copyright

**This item is licensed under a
Creative Commons License**

**Structure and Function of Nitrate and
Nitrite Transporters, NrtA and NitA, from
*Aspergillus nidulans***

Submitted to the University of St Andrews for the degree of Doctor of Philosophy

by

Vicki Frances Symington

Project Supervisor

Dr J. R. Kinghorn,
School of Biology,
Sir Harold Mitchell Building,
University of St Andrews,
Fife,
KY16 9TH.



University
of
St Andrews

February, 2009

Declarations

I, Vicki Frances Symington, hereby certify that this thesis, which is approximately 50,000 words in length, has been written by me, that it is the record of work carried out by me and that it has not been submitted in any previous application for a higher degree.

I was admitted as a research student in October 2004 and as a candidate for the degree of Doctor of Philosophy in October 2005; the higher study for which this is a record was carried out in the University of St Andrews between 2004 and 2009.

Date

Signature of candidate

I hereby certify that the candidate has fulfilled the conditions of the Resolution and Regulations appropriate for the degree of Doctor of Philosophy in the University of St Andrews and that the candidate is qualified to submit this thesis in application for that degree.

Date

Signature of supervisor

In submitting this thesis to the University of St Andrews we understand that we are giving permission for it to be made available for use in accordance with the regulations of the University Library for the time being in force, subject to any copyright vested in the work not being affected thereby. We also understand that the title and the abstract will be published, and that a copy of the work may be made and supplied to any bona fide library or research worker, that my thesis will be electronically accessible for personal or research use unless exempt by award of an embargo as requested below, and that the library has the right to migrate my thesis into new electronic forms as required to ensure continued access to the thesis. We have obtained any third-party copyright permissions that may be required in order to allow such access and migration, or have requested the appropriate embargo below.

The following is an agreed request by candidate and supervisor regarding the electronic publication of this thesis:

Access to Printed copy and electronic publication of thesis through the University of St Andrews.

Access to all or part of printed copy but embargo of all or part of electronic publication of thesis for a period of 1 year (maximum five) on the following ground:

publication would preclude future publication;

Embargo on both all of printed copy and electronic copy for the same fixed period of 1 year (maximum five) on the following ground:

publication would preclude future publication;

Permanent embargo of all or part of print and electronic copies of thesis (permission will be granted only in highly exceptional circumstances).

[Where part of a thesis is embargoed, please specify the part and the reasons. Evidence for a request for an embargo must be included with the submission of the draft copy of the thesis]

Date

Signature of candidate

Signature of supervisor

Acknowledgments

I would like to thank my supervisor, Jim Kinghorn for his ongoing help and support throughout my project. Jim has been encouraging and has helped me keep on with my project when sometimes it felt like there was no end in sight. Additionally, I acknowledge funds primarily from the Biology and Biotechnology Research Council who funded my studentship tuition fees as well as maintenance funds. Further funding was awarded for travel expenses and conference attendance from The Society for Experimental Biology, The Genetics Society of America, The Cross Trust, The Federation of European Microbiological Societies and The Minshull Award, all of which I am very grateful for.

Other members of the Fungal Genetics Group that I would like to acknowledge are as follows, Shiela Unkles, a fantastic molecular biologist who went above and beyond to help me when I was having difficulties. I can't thank her enough, particularly for her help with fungal transformations and Western blotting. Eugenia Karabika who arrived late in the course of my PhD, but, has been a fantastic support, in particular, her ability to 'sit on the fence' has been strangely comforting. For technical support I am thankful to Ray Stephenson, Harry Hodge, Lianne Baker, Maureen Cunningham and Murray Coutts.

Thanks to Richard Abbott and Alyson Tobin without whose supportive words I wasn't sure I would have made it through the past two years.

In the final year of my PhD I spent a lonely month in Vancouver, University of British Columbia where I worked with a wonderful team of people who were proficient in the use of ^{13}N , and struck fear into people who encountered their little red lead cart! I acknowledge Zorica Kotur, Ye Wang, Yaesh Siddiqi, and Tony Glass for their hands-on help with these assays. For accommodation and tourist trips in Vancouver I am indebted to Tony and Marg Glass, Mary Berbee, Dave and Brian Carmean. Once again, to Tony Glass for his discussions and support during a bomb threat and S.W.A.T. team evacuation of the U.B.C. Biological Sciences Building!

In a strange sort of way I wish to thank Stuart Hewlins and Stefania Angelino, if it wasn't for my year in industry I am not sure that I would have taken the PhD route, I am sure you didn't mean to do it, but you pushed me in the right direction and for that I am grateful.

My friends particularly, I thank Dan MacQueen for tirelessly reading drafts of my chapters mostly in return for food I am sure! One of the better friends a girl could ask for! Also, Stacey Munro, a star as always, a shoulder to cry on and a hand to hold, she can't get rid of me now! To Rach, Rich, Ruth MacQueen, Jodi, Jay, Shirley, Liz, Annie, Ollie Morton, Oli Walker, Gordon, Paty, Emma, Maria, Valentina, Jennie, Anne-Yael, Ruth Doherty, Tim, and Lee-Anne thanking you all for looking after me during the ups and the downs, and most of all for keeping life fun. May there be many more Burn's nights, Christmas dinners, holidays, birthdays, and muffins for us all to share!

My family, Mum and Dad, as always for financial support, a car and most of all hugs and encouraging words in the middle of the day or night, the phone calls to and from the lab, and for jumping in the car to drive up the coast to see if I was ok. Although they could never describe what I did to any of their friends, they tried, and they have always been supportive and proud of me for what I wanted to do and the time I had to take to do it. You are a wonderful pair and I am grateful for everything you have ever given me...except my stubbornness...that's just annoying! To Julie and Gail, the best big sisters ever and their partners Ian and Danny, who never knew what they had coming to them when they joined the Symington clan! Being the baby, my sisters have made the way for me and made my path through life a little easier and they have stuck up for me as big sisters should, many thanks.

My partner Dave who I have been with for almost six years, has helped me in so many ways, from looking after me when I was upset with my PhD to helping me with my calculations when I couldn't remember the formula! There are no words to say how much he means to me or how grateful I am to him for the love and support he has given me; I am looking forward to many, many more years together in our house with our dog and our freezer! Love always.

Peer reviewed publications

Wang, Y., Li, W., Siddiqi, Y., **Symington, V.F.**, Kinghorn, J.R., Unkles, S.E. & Glass, A. D. M. 2008 Nitrite transport is mediated by the nitrite-specific high-affinity NitA transporter and by nitrate transporters NrtA, NrtB in *Aspergillus nidulans*. *Fungal Genetics and Biology* **45**, 94-102.

I performed the preliminary work on this paper to generate a clear phenotype for the knock-out mutants.

Table of Contents

	Page
Abstract.....	1-2
 <u>Chapter One</u>	
1.0 General Introduction.....	3-43
1.1 Cell membranes: A historical perspective.....	3
1.1.1 Lipid rafts in biological membranes.....	5
1.1.2 Energy transfer of the cell membrane.....	5
1.2 Membrane proteins.....	5
1.2.1 General membrane protein structure.....	6
1.2.2 Protein translocation/insertion.....	6
1.2.3 The importance of membrane proteins.....	10
1.3 Membrane transport proteins.....	10
1.3.1 Transporter architecture, selectivity and coupling.....	10
1.4 Ion pumps and channels – Blurring the boundaries?	13
1.5 Which amino acid for where?.....	14
1.5.1 Glycine.....	15
1.5.2 Proline.....	16
1.5.3 Aromatics.....	17
1.5.4 Charged residues.....	17
1.5.5 Polar and non-polar amino acids.....	18
1.5.6 Protein oligomerisation and key amino acids.....	19
1.6 MFS and ATP Binding Cassette (ABC) protein super families.....	19
1.6.1 ABC Super-family.....	19
1.6.2 MFS.....	20
1.6.3 Comparison of ABC and MFS super-families.....	23
1.7 LacY structure and mechanism.....	23
1.7.1 Structure.....	24
1.7.2 LacY mutagenesis.....	26
1.8 GlpT.....	28
1.9 OxlT.....	28
1.10 Formate nitrite transporters (FNT)	30

1.11 <i>Aspergillus nidulans</i>: A model experimental organism.....	30
1.12 Nitrogen.....	32
1.12.1 Nitrogen and nitrogenous compounds in the environment.....	32
1.12.2 Nitrate assimilation.....	33
1.12.3 Nitrogen metabolite repression.....	34
1.12.4 Nitrate transport systems.....	35
1.12.5 Plant, yeast and protist systems.....	36
1.12.6 Nitrate transport in <i>A. nidulans</i> : Background.....	37
1.12.7 <i>NrtA</i> vs. <i>NrtB</i>	37
1.12.8 <i>NrtA</i>	38
1.12.9 Evolution, signature sequences and a duplication event.....	39
1.12.10 <i>NrtA</i> Mutagenesis.....	41

Chapter Two

2.0 Materials and Methods44-66

2.0 Introduction	44
2.1 <i>A. nidulans</i> strains and media.....	44
2.1.1 <i>A. nidulans</i> growth and storage.....	44
2.2 Plasmids.....	45
2.2.1 <i>V5TAGAGE/1</i>	45
2.2.2 <i>pMUT</i> and <i>V5MKNitA</i>	45
2.2.3 <i>WEBpyroA</i>	45
2.3 Bacterial cultures.....	46
2.3.1 Antibiotics.....	47
2.3.2 Preparation of competent cells.....	47
2.4 Molecular methods.....	47
2.4.1 Tissue preparation for fungal DNA extraction.....	47
2.4.2 DNA extractions.....	48
2.4.3 Plasmid DNA quantification	49
2.4.4 Polymerase chain reaction (PCR)	49
2.4.5 PCR product purification	50
2.4.6 Agarose gel electrophoresis.....	50
2.4.7 Restriction endonuclease digestion.....	50
2.4.8 Isolation of DNA fragments from agarose gel.....	51

2.4.9 <i>E. coli</i> transformation.....	51
2.4.10 Purification of plasmid DNA	52
2.4.11 DNA sequencing	52
2.4.12 <i>A. nidulans</i> transformation protocol.....	52
<i>Mycelia</i> preparation	52
Transformation	53
Strains.....	53
2.4.13 Southern blotting.....	55
Blot preparation	55
DNA hybridisation, membrane washing and autoradiography.....	56
2.4.14 Chemical mutagenesis.....	57
2.4.15 Generation of mutant amino acid constructs.....	58
2.4.16 Net nitrate/nitrite transport assays.....	59
2.4.17 Synthesis and purification of $^{13}\text{NO}_3^-$ tracer.....	60
2.4.18 Reduction of $^{13}\text{NO}_3^-$ to $^{13}\text{NO}_2^-$	60
Uptake assays using $^{13}\text{NO}_3^-$ and $^{13}\text{NO}_2^-$ tracers.....	60
2.4.19 Western blotting.....	62
<i>Aspergillus</i> crude plasma membrane preparation	62
SDS and Blue-Native PAGE.....	62
Standards and electrophoresis conditions.....	64
Western transfer	64
2.4.20 Construction of <i>A. nidulans</i> cosmid library.....	65
2.5 Chemicals.....	66

Chapter Three

Mutagenesis of the nitrate signature.....67-83

3.1 Introduction	67
3.2 Results	67
3.2.1 Alignments and secondary structure development	67
3.2.2 In-vitro mutagenesis	70
3.2.3 Alanine scanning mutagenesis.....	71
3.2.4 Further mutagenesis of G170	75
3.2.5 Further mutagenesis of L166	75
3.2.6 Further mutagenesis of N168	76

3.2.7 Chlorate and temperature sensitivity testing	76
3.3 Discussion	76
3.4 Summary	82

Chapter Four

Studies of the nitrate binding site84-92

4.1 Introduction.....	84
4.1.1 Background	84
4.1.2 Previous mutagenesis of NrtA.....	84
4.2 Results	85
4.2.1 Single mutant strains in the nitrate binding site.....	85
4.2.2 Multiple mutants in the nitrate binding site.....	86
4.2.3 ¹³ NO ₃ ⁻ uptake in mutant strain T83S	89
4.2.4 Modelling of NrtA, a view of the binding site.....	90
4.3 Discussion	90
4.4 Summary	92

Chapter Five

Post-translational modifications of nitrate transporter NrtA.....93-105

5.1 Introduction.....	93
5.1.1 Protein ubiquitination	93
5.1.2 Ubiquitination in membrane proteins.....	95
5.1.3 Protein phosphorylation.....	95
5.1.4 Phosphatases and kinases.....	96
5.1.5 Phosphorylation and nitrate transport.....	97
5.2 Results.....	98
5.2.1 Identification of putative PEST sequences in NrtA.....	98
5.2.2 Identification of putative phosphorylation sites in <i>A. nidulans</i> NrtA...	98
5.2.3 Single phosphorylation mutants.....	101
5.2.4 Multiple mutations.....	103
5.2.5 Chlorate and temperature sensitivity testing	104
5.3 Discussion	104

5.4 Conclusion	105
----------------------	-----

Chapter Six

Nitrate signalling.....	106-113
--------------------------------	----------------

6.1 Introduction	106
6.1.1 Nitrate signalling and assimilation.....	106
6.1.2 Photosynthetic organisms.....	107
6.1.3 Bacteria	108
6.1.4 Yeast	108
6.1.5 A fungal nitrate sensor?	108
6.2 Results.....	110
6.2.1 Vector and cosmid library construction.....	110
6.2.2 Strain development.....	110
6.3 Discussion	112

Chapter Seven

Nitrite transport and the NitA permease of <i>A. nidulans</i>.....	113-148
---------------------------------------------------------------------------	----------------

7.1 Introduction	114
7.1.1 Background	114
7.1.2 Nitrite permeases.....	114
7.1.3 FNT proteins in <i>E.coli</i> , <i>S. cerevisiae</i> and <i>A. nidulans</i>	115
7.2 Results.....	116
7.2.1 Growth and flux of nitrite in control strains on solid media and using $^{13}\text{NO}_2^-$	116
7.2.2 Two-dimensional model development and conserved motif analysis.....	118
7.2.3 Substrate specificity.....	120
7.2.4 Generation of strain VFS106 for high throughput transformation....	123
7.2.5 Residues replacements.....	124
7.2.6 'Wild-type' strains.....	124
7.2.7 Alteration of charged residues D88, K156 and K192.....	128
7.2.8 Alteration of histidine, H210.....	133
7.2.9 Alteration of conserved asparagines.....	134

7.2.10 Further expression analyses of N122 and N246.....	137
7.2.11 Net nitrite assays.....	137
7.2.12 Revertant studies	138
7.3 Discussion.....	138
7.3.1 Determination of enzyme kinetics and regulation.....	138
7.3.2 Predicted secondary structure of NrtA.....	140
7.3.3 Mutagenesis.....	141
7.3.4 Revertant studies.....	147
7.3.5 Previous reports of a nitrite transport gene in <i>A. nidulans</i>	147
7.4 Discussion.....	147

Chapter Eight

Future work and perspectives.....149-153

8.1 NrtA.....	149
8.2 Nitrate signalling in <i>A. nidulans</i>	151
8.3 NitA.....	152
8.4 Distribution and abundance of nitrate/nitrite transport permeases.....	152
8.6 Evolution of NrtA.....	153
8.7 And finally.....	153

Appendices.....153-168

Appendix One. Amino acid reference	153
Appendix Two. <i>Aspergillus</i> media and solutions.....	157
Appendix Three. General primers used in this study.....	160
Appendix Four. Mutagenic primers used in this study	162
Appendix Five. SDS-PAGE and BN-PAGE gel composition	165
Appendix Six. Accession numbers of proteins in NrtA alignment.....	166

Web References.....169-170

References.....171-203

List of Figures

	Page
Figure 1.1 Models of the lipid bilayer.....	4
Figure 1.2 Membrane protein translocation and integration by the translocon.....	8
Figure 1.3 Membrane protein folding and insertion	9
Figure 1.4 The ‘alternating access’ model for membrane transport.....	13
Figure 1.5 Topological representation of four crystallised ABC transporters.....	21
Figure 1.6 Structural representation of LacY based on C154G mutant with bound substrate.....	25
Figure 1.7 The internal hydrophilic cavity of LacY.....	26
Figure 1.8 The substrate binding site of LacY.....	27
Figure 1.9 Structural comparisons of LacY and GlpT.....	29
Figure 1.10 The life cycle of <i>A. nidulans</i>	31
Figure 1.11 Nitrate assimilation pathway for <i>A. nidulans</i>	34
Figure 1.12 Amino acid sequence alignment of <i>A. nidulans</i> nitrate transport paralogues NrtA and NrtB.....	38
Figure 1.13 Sequence comparison and analysis revealed distinct characteristics of NNP from different organisms.....	40
Figure 1.14 Comparison of the nitrate signature sequences in NrtA from MFS subfamily NNP.....	41
Figure 2.1 Plasmid vectors used in this thesis.....	46
Figure 2.2 Integration of mutant constructs at <i>argB</i>	54
Figure 3.1 Provisional secondary structure representation of the high-affinity nitrate transporter NrtA of <i>A. nidulans</i>	68
Figure 3.2 Alignment of NNP signature sequences and cladogram of these proteins.....	69
Figure 3.3 Southern blot of nitrate signature G167A mutants.....	70
Figure 3.4 Phenotypes of ‘alanine scanning’ mutants in the first nitrate signature of NrtA.....	74
Figure 3.5 Expression of mutant proteins in the first nitrate signature of NrtA.....	74
Figure 3.6 Phenotypes of G170 mutants in the first nitrate signature motif of NrtA.....	75

Figure 3.7	Phenotypes of L166 mutants in the first nitrate signature sequence of NrtA.....	76
Figure 3.8	Phenotypes of N168 mutants in the first nitrate signature sequence of NrtA.....	76
Figure 3.9	Modelling of NrtA based on GlpT.....	79
Figure 3.10	Trans membrane domains of NrtA in closed confirmation.....	80
Figure 3.11	Structural comparison of glycerol-3-phosphate and nitrate.....	81
Figure 3.12	Structural comparisons of chlorate and nitrate.....	82
Figure 4.1	Positioning of residues in the NrtA binding site investigated in this study.....	86
Figure 4.2	Phenotypes of single T83 mutants.....	87
Figure 4.3	Western blots of T83 mutants.....	87
Figure 4.4	Phenotypes of multiple binding site mutants.....	87
Figure 4.5	Nitrate influx in T83S using the $^{13}\text{NO}_3^-$ tracer.....	89
Figure 4.6	Cartoon representation of NrtA from two perspectives.....	90
Figure 5.1	Structural mechanism of plant aquaporin gating in plasma membrane.....	97
Figure 5.2	Illustration of NrtA minus the central loop domain.....	99
Figure 5.3	Alignment of NrtA with YNT1 and NIT10 from <i>H. polymorpha</i> and <i>N. crassa</i> respectively.....	100
Figure 5.4	Central loop domain of NrtA, including Tms 5 and 6.....	102
Figure 5.5	Phenotypic assessment of single phosphorylation site mutants in the loop of NrtA.....	111
Figure 6.1	Vector pTRAN3-1A.....	111
Figure 6.2	Illustration of colour produced on nitrate containing X-gluc media in the presence of pTRAN3-1A transformants with active and inactive signalling systems.....	112
Figure 6.3	Southern blot of putative signalling system mutants.....	117
Figure 7.1	Growth of wild-type T5275 and <i>ΔnitA</i> T26.....	117
Figure 7.2	$^{13}\text{NO}_2^-$ flux assays for control strains.....	119
Figure 7.3	Provisional secondary structure of the <i>A. nidulans</i> NitA permease.....	120
Figure 7.4	Direct comparisons of NrtA and NitA putative nitrate/nitrite signature sequences.....	121
Figure 7.5	Amino acid alignment of proteins from the FNT family.....	122

Figure 7.6	Chemical structures of FNT family substrates nitrite, formate and bicarbonate also showing nitrate as a structural comparison.....	123
Figure 7.7	Southern blot of <i>nitA</i> mutants integrated at the wild-type <i>nitA</i> locus.....	127
Figure 7.8	Growth and expression characteristics of wild-type (<i>nitA</i> ⁺) mutants L127V and C177T.....	128
Figure 7.9	Growth and expression characteristics of mutants in conserved charged amino acids in NitA.....	129
Figure 7.10	¹³ NO ₂ ⁻ tracer uptake assays of D88 mutants.....	130
Figure 7.11	¹³ NO ₂ ⁻ tracer uptake assays of D88 mutants, uncorrected for outliers.....	131
Figure 7.12	¹³ NO ₂ ⁻ tracer uptake assays of mutants K156R and K192R.....	133
Figure 7.13	Growth and expression characteristics of mutants in histidine residue H210 in NitA.....	134
Figure 7.14	Growth and expression characteristics of mutants N122, N173 and N246.....	135
Figure 7.15	¹³ NO ₂ ⁻ flux assays for N173 mutants N173A, N173S and N173Q.....	136
Figure 7.16	Expression characteristics for NitA proteins (10 % SDS-PAGE) which failed to show protein on BN-PAGE.....	137
Figure 7.17	Assessment of HNO ₂ concentration and NO ₂ flux.....	140

List of Tables

	Page
Table 1.1 Missense mutations in the nitrate signature of the high-affinity nitrate transporter NrtA from <i>A. nidulans</i>	42
Table 2.1 Genotypes of strains used in this study.....	44
Table 2.2 Timetable for ¹³ N assays.....	61
Table 3.1 Full mutagenic detail for mutations in the first nitrate signature of NrtA.....	72
Table 4.1 Single binding site mutations in residue T83 which resides directly above R87 in the NrtA binding site.....	88
Table 4.2 Multiple mutations in the putative NrtA binding site.....	89
Table 5.1 Conservation of putative phosphorylation sites of Nrt2 proteins shown by alignment comparison of proteins from <i>A. fumigatus</i> , <i>N. fischeri</i> , <i>A. terreus</i> , <i>A. oryzae</i> , <i>A. niger</i> , <i>N. crassa</i> and <i>Magnaporthe grisea</i>	101
Table 5.2 Summary of characteristics of single site phosphorylation mutants.....	103
Table 5.3 Summary of characteristics of mutants where multiple phosphorylation sites were altered.....	103
Table 7.1 Summary of mutations made to NitA.....	125
Table 7.2 Comparison of corrected and uncorrected uptake flux data using ¹³ NO ₂ ⁻ to study nitrite transport in D88 mutant strains.....	132
Table 7.3 Net nitrite uptake in control strains and in NitA mutant strains N173A and N173S.....	138
Table 7.4 Net nitrite uptake assays by comparison of induction conditions.....	139
Table 7.5 Kinetic data for nitrite flux of various <i>nrtA</i> , <i>nrtB</i> and <i>nitA</i> mutants.....	140

List of standard and non-standard abbreviations

2D	Two dimensional
3D	Three dimensional
Å	Angstroms
A	Alanine
ABC	ATP binding cassette
ADP	Adenosine diphosphate
Amp	Ampicillin
AnalR	Analytical grade (BDH)
APS	Ammonium persulphate
ATP	Adenosine triphosphate
bp	Base pair (s)
BN-PAGE	Blue native polyacrylamide gel electrophoresis
BPB	Bromophenol blue
BSA	Bovine serum albumin
C	Cysteine
CF	Cystic fibrosis
CFTR	Cystic fibrosis trans membrane conductance regulator
ClC	Chloride channel
CM	Complete media
CSM	Cysteine scanning mutagenesis
D	Aspartic acid
Da	Dalton (s)
DDM	Do-decyl maltoside
dNTP	Deoxyribonucleotide triphosphate
dCTP	Deoxycytidine triphosphate
DW	Distilled water
DMSO	Dimethyl sulphoxide
E	Glutamic acid
e.g.	<i>exempli gratia</i> (for example)
<i>et al.</i>	And others
etc.	Etcetera
ECL	Enhanced chemiluminescence
EDTA	Ethylene diamine tetra acetic acid

F	Phenylalanine
g	Gram (s)
G	Glycine
GANE	Global nitrogen enrichment
G3P	Glycerol-3-phosphate
Glt _{ph}	Sodium dependant glutamate transporter
GlpT	Glycerol-3-phosphate transporter
GPR	General purpose reagent (BDH)
h	Hour (s)
H	Histidine
I	Isoleucine
i.e.	<i>Id est</i> (that is)
<i>In vitro</i>	In glass (in an artificial environment)
<i>In vivo</i>	In the living organism
<i>Inter alia</i>	Amongst other things
K	Lysine
kDa	Kilo Dalton (s)
kg	Kilogram (s)
kb	Kilo base (s)
KO	Knock out
L	Litre or Leucine
LB	Luria broth/media
m	Metre
M	Methionine
MFS	Major facilitator superfamily
mg	Milligram (s)
µg	Microgram (s)
min	Minutes
MM	Minimal media
M	Molar
mM	Milli molar
µM	Micro molar
ml	Millilitre
mmol	Milli mols
MOPS	4-Morpholinepropanesulfonic acid
ng	Nano gram (s)

N	Asparagine or Normal
NEB	New England Biolabs
ND	Not determined
NERC	Natural environment research council
NQO	4-nitroquinoline-1-oxide
NRAMP	Natural resistance-associated macrophage protein
NTG	N-methyl-N'-nitrosoguanidine
nm	Nanometre
nmol	Nanomole
NNP	Nitrate nitrite porters
OD	Optical density
OSMO	Osmotic media
P	Proline
PABA	p-amino benzoic acid
PAGE	Poly acrylamide gel electrophoresis
pH	Measure of the acidity or alkalinity of a solution
PCR	Polymerase chain reaction
PEG	Polyethylene glycol
pi	Phosphate
PIPES	1, 4-Piperazinediethanesulfonic acid
PK	Protein kinase
PMF	Proton motive force
PMSF	Phenylmethanesulphonylfluoride
PTM	Post translational modifications
PVDF	Polyvinylidene Fluoride
PYRO	Pyridoxine
Q	Glutamine
R	Arginine
RIBO	Riboflavin
rpm	Revolutions per minute
RH	Right hand
RT	Room temperature
S	Serine
SAP	Shrimp alkaline phosphatase
SDS	Sodium dodecyl sulphate
SDS-PAGE	Sodium dodecyl sulphate poly acrylamide gel electrophoresis

SDW	Sterile distilled water
sec	Second (s)
SOB	2 % tryptone (w/v), 0.05 % yeast extract (w/v), 10 mM NaCl, 2.5 mM KCl, 10 mM MgSO ₄ , 10 mM MgCl ₂
SOC	2 % tryptone (w/v), 0.05 % yeast extract (w/v), 10 mM NaCl, 2.5 mM KCl, 10 mM MgSO ₄ , 10 mM MgCl ₂ , 2 mM glucose
SRP	Signal recognition peptide
SSC	3 M NaCl, 300 mM sodium citrate, pH 7
SSPE	750 mM NaCl, 50 mM NaH ₂ PO ₄ , 5 mM EDTA, pH 7.4
STC	1.2 M sorbitol, 10 mM Tris pH7.5, 10 mM CaCl ₂
T	Threonine
TAE	40 mM Tris, 1 mM EDTA, pH8-8.2 (acetic acid)
TBS	0.9 % w/v NaCl, 10 mM Tris pH 7.4
TBST	0.9 % w/v NaCl, 10 mM Tris pH 7.4, 0.1 % v/v Tween 20
TE	Tris EDTA
TEMED	Tetramethylethylenediamine
TM	Transformation media
Tm	Trans membrane domain
TRIUMF	Tri University Meson Facility
Tween 80	Polyoxyethylenesorbitan monooleate
Tween 20	Polyoxyethylene sorbitan
UBC	University of British Columbia
USA	Uniport, symport and antiport (Super family)
UV	Ultra violet
V	Volts or Valine
<i>Vide infra</i>	See below
W	Tryptophan
WT	Wild-type
XC	Xylene cyanol
Y	Tyrosine

Abstract

Membrane proteins play an integral role in the control of ion transport across the cell membrane in biological systems. However, due to experimental constraints, structural and functional data available for these proteins is limited, especially considering their importance. In this study, two membrane proteins which transport nitrate and nitrite into the model filamentous ascomycete *Aspergillus nidulans* were investigated.

Work on the twelve trans-membrane domain nitrate transport protein NrtA is well established. As a member of the major facilitator super family (MFS) the role of signature sequences characteristic of this family have previously been studied. Here, a series of point mutations were made to facilitate an understanding of key residues in the nitrate binding domain, the first nitrate signature motif and residues of the unique fungal central-loop domain. Using an expanded alignment package, the proposed secondary structure of NrtA was enhanced and used as a starting point for mutagenesis.

Alanine scanning mutagenesis showed that glycine residues in the conserved nitrate nitrite porter (NNP) motif were critical for NrtA function. This finding is paralleled in other membrane proteins suggesting that these residues provide a degree of flexibility and stability in otherwise compact regions. Also, the lack of expression in many of these mutants indicated that membrane packing, folding constraints or cellular trafficking caused protein degradation. Two asparagines in the NNP were investigated; N160 and N168. N168 was found to be critical for NrtA function as all mutants were devoid of growth on nitrate solid agar medium though they expressed in the membrane to varying degrees. Further, a central leucine residue (L166) in the NNP was postulated to be involved in structural support as a result of its considerable size. However, *in vitro* mutagenesis showed that L166 could be altered with no serious consequences to NrtA function.

The nitrate binding site has been studied previously, revealing the interaction of conserved arginine residues with the anion as it traverses the bilayer. Initially, the threonine (T83) situated directly above the first arginine (R87) in the NrtA binding site was altered in terms of residue size and charge. Though it was thought that mutations to a small, charge neutral, amino acid would substitute for T83, no alteration to enzyme kinetics in mutant T83S was found when using $^{13}\text{NO}_3^-$. Also, other nitrate binding site residues were 'rearranged'. For example, switching the position of R87 and R368, and the residues directly above those in the

helix, (T83 and N364 respectively) ablated nitrate transport, presumably due to an alteration in the size of the binding site preventing translocation of the substrate.

Putative post-translational modifications in NrtA were also investigated. It was hypothesised that conformational changes could be triggered by ubiquitination and/or phosphorylation. A computational examination showed no apparent ubiquitination sites in NrtA, although four putative phosphorylation sites were identified in the central loop domain which is specific to fungal NNP proteins. Candidate residues for phosphorylation were altered to alanine. All phosphorylation mutants grew well on nitrate, and nitrate uptake was only slightly reduced, possibly as a result of minor structural alterations. These phenotypes were paralleled in multiple phosphorylation mutants, with two to four putative sites 'knocked-out', ruling out an additive effect. Therefore this piece of work was inconclusive, although a critical role for phosphorylation at these sites seems unlikely.

Another major part of this thesis examined NitA which is part of a distinct nitrite transport family to NrtA (the Formate Nitrite Transporters, FNT). Little is known about proteins of the FNT family, which are composed of six trans-membrane domains. Recent work has established the kinetics of NitA, in particular its use of nitrite as a substrate. As FNT member proteins can transport both nitrite and formate, a study of motifs which may be characteristic for each substrate was performed. However, this experiment was hindered by a lack of experimentally characterised formate or nitrite transporters and modelling the sample set was thus problematic. A mutagenesis approach targeted NitA residues conserved amongst homologous proteins. Residues in position D88 in an alignment of homologues were conserved in terms of charge. Mutagenesis of D88 revealed that maintaining charge at this position was essential for NitA function, likely due to a role in salt-bridge formation during conformational changes. Mutations to asparagine, glutamine, serine and valine showed reduced growth on agar though the protein was expressed to approximately wild-type levels. Nitrite uptake assays using a $^{13}\text{NO}_2^-$ tracer were performed on D88N, D88E and D88Q and all showed wild-type K_m and V_{max} . Finally, the role of conserved asparagine residues found throughout NitA was investigated by mutagenesis. Expression studies revealed that mutants created in N122 and N246, changed to aspartic acid, lysine, glutamine and serine were generally not present in the membrane and thus did not grow on nitrite agar. However, mutations in N173 (in Tm 4) and N214 (in Tm 5), which are conserved in > 95 % of NitA homologues, showed varying degrees of growth and expression. Both of these residues are located in FNT signature motifs, so it is likely that they are involved with conformational changes or protein dynamics.

Chapter One

1.0 General Introduction

1.1 Cell membranes: A historical perspective

The membrane of a biological cell, or indeed an organelle, is one of the more important components of any biological system. It is likely that the first ever living cell came to exist when a membrane formed protecting its internal components from the environment (Mansey *et al.*, 2008). Membranes form divisions allowing for the segregation of cellular activities acting directly as barriers and control points for the transport of essential molecules (MacKinnon, 2004).

Early work by Gorter and Grendel (1925) resulted in the observation that red blood cells, from various animals, were surrounded by a fatty substance that they measured to be two molecules thick. They did this by measuring the area of occupancy of a dilated monolayer compared to the microscopic surface area of an erythrocyte, the resulting ratio being 2:1. By their extraction techniques they also demonstrated that these molecules were lipids, whose hydrophilic polar head-groups are directed to the inside and the outside of the cell. Their findings were not initially well accepted, notwithstanding, their conclusions were essentially correct. The first established model of a lipid bilayer, was proposed by Danielli and Davson (1935). This model illustrated the basic sandwich shape formed by lipid molecules; and also included a layer of globular protein which surrounded the bilayer. They noted that the membrane was accountable for the transport of different molecules into the cell, with the capability of distinguishing these molecules by size, charge and solubility characteristics. Singer and Nicolson discussed the structure of the cell membrane in 1972 when the 'fluid mosaic model' was initially suggested (Singer & Nicolson, 1972). This presentation of bilayer structure was the first to show the bilayer as a dynamic environment. The layer of seemingly static protein of Danielli and Davson's model being replaced with proteins which were attached to, traversed, or floated on the surface of the bilayer, allowing for a much more flexible model. Polar and charged residues were postulated to reside in the extra-membrane environment as a result of their thermodynamic restrictions. The predicted model of a fluid mosaic lipid bilayer expanse with dispersed membrane proteins has since been updated recently to include an increased density of membrane protein, variable bilayer thickness and a functionally independent range of both intra and extra-cellular membrane proteins (Engelman, 2005). The average area of occupancy of membrane proteins is as yet an unanswered question, though the protein/lipid composition of the cell membrane can be hypothesised

based on cell function (Engelman, 2005). For example, a bacterium which is performing several metabolic functions would have a higher percentage of membrane protein occupancy as compared to a myelin sheath, which has the sole function to protect the nerve. The Singer and Nicolson model and its update suggested by Engelman, are shown (Figure 1.1). It is important to note that the membrane is a dynamic environment and therefore this image conveys only a snap-shot of membrane structure and protein dynamics. The proteins, as shown in Figure 1.1 (b), represent examples of proteins that may be present in the bilayer. Engelman suggests that some proteins are largely contained in the bilayer, e.g. the *Escherichia coli* lactose and ammonia transporters LacY and AmtB (Abramson *et al.*, 2003b; Zheng. L. *et al.*, 2004), similarly some proteins may have large extra cellular domains e.g. the ATP synthase. While other proteins may be anchored in the membrane by a single transmembrane helix whilst the bulk of the protein remains extra cellular, such as the prostaglandin H2 synthetase-1 (Picot *et al.*, 1994).

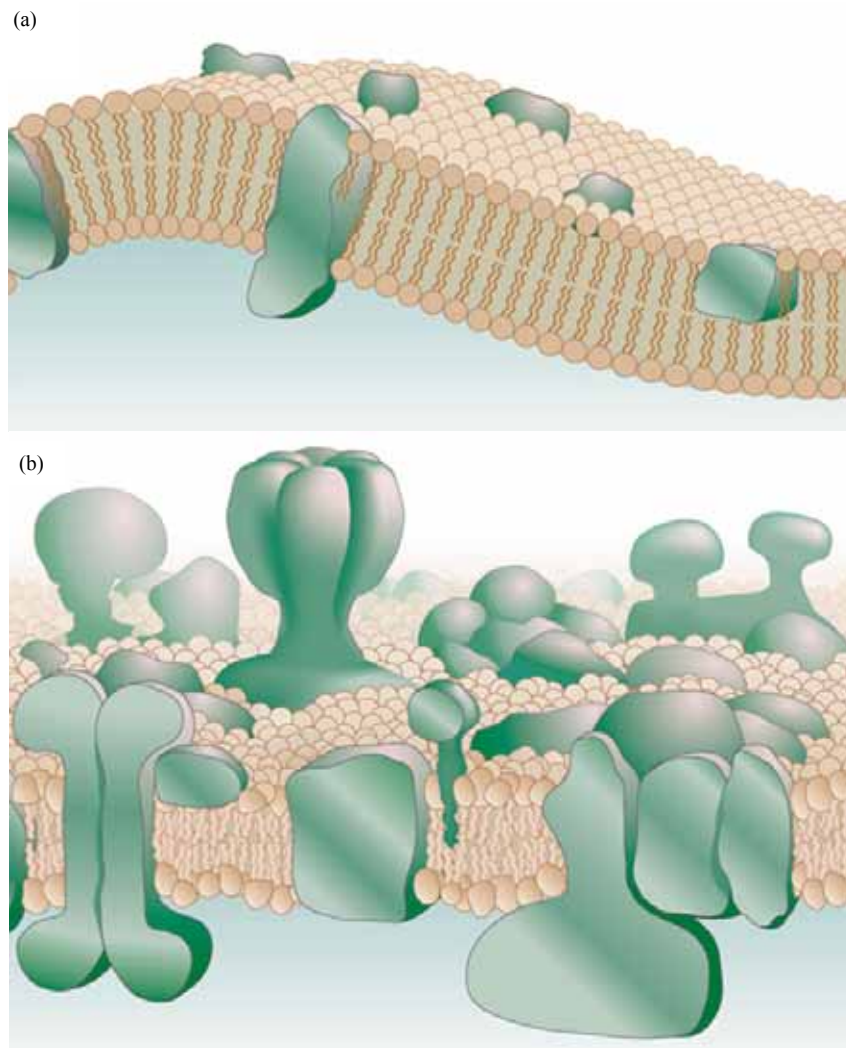


Figure 1.1 Legend on following page.

Figure 1.1 Models of the lipid bilayer (a) The Singer and Nicolson 'fluid mosaic model' (Singer & Nicolson, 1972) (b) An amended and updated fluid mosaic model by Engelman (2005). This figure was taken from Engelman (2005). The membrane is a dynamic environment and as such this image represents a snap-shot in time.

1.1.1 Lipid-rafts in biological membranes

According to its traditional definition, the lipid-raft is a "membrane domain which is resistant to extraction in cold 1 % Triton X-100 and floats in the upper half of a 5-30 % sucrose density gradient" (Pike, 2004). Over the past 20 years the idea of lipid-rafts in the membrane has been debated, though the variability among lipid-raft structure and function makes them difficult to define beyond these simple physical premises (Pike, 2004). However, it is undeniable that lipid-rafts are a collection of seemingly related domains with similar properties, which do not in-fact form uniform entities. Instead micro domains are created in cell membranes which are rich in cholesterol, lipids, glycolipids and sphingolipids (Simons & Ikonen, 1997; Pike, 2004). Specifically, a lipid-raft contains 3-5 times more cholesterol than the normal membrane, and 10-15 % more sphingomyelin, as well as a decreased density of glycerophospholipids (Pike, 2004; Sengupta *et al.*, 2007). The physiological roles suggested for the lipid-rafts are diverse, they include signal transduction (Pierce, 2002; Holowka, 2005; Kabouridis, 2006; Sengupta *et al.*, 2007), vesicle trafficking (Parton & Richards, 2003; Salaun *et al.*, 2004; Sengupta *et al.*, 2007), cellular adhesion and motility (Manes & Viola, 2003; Sengupta *et al.*, 2007) and passage of pathogens (Manes *et al.*, 2003; Lafont & van der Goot, 2005). Lipid-rafts will not be discussed further in this thesis though are an example of the dynamic nature of the cell membrane.

1.1.2 Energy transfer of the cell membrane

Energy transfer within the lipid bilayer raised the initially controversial hypothesis of chemiosmosis which has since been widely accepted. This theory suggests that during cellular respiration the movement of electrons along the electron transport chain is coupled to the outward pumping of protons across the inner mitochondrial membrane resulting in a proton gradient (pH gradient). The energy from this gradient, known as the proton motive force (PMF), is stored and later used to drive the phosphorylation of ADP (Mitchell, 1961). Though this theory is based on the generation of ATP in the chloroplast and mitochondria it can be applied to any charged species which creates a membrane gradient, and thus allows the transfer of the molecule across the lipid bilayer.

1.2 Membrane proteins

In genomes sequenced thus far, 20-30 % of all genes appear to encode membrane proteins (Mitaku *et al.*, 1999; Krogh *et al.*, 2001; Liu & Rost, 2001), which function as receptors,

anchors, enzymes and transporters. Regardless of their importance in all facets of life, less than 1 % of known protein structures are membrane proteins (Liu & Rost, 2001), the majority of which are bacterial. Indeed, Kaback and colleagues (2001) suggested that the level of understanding of membrane proteins was inversely proportional to their relative importance. In bacterial expression systems, eukaryotic proteins are not expressed to the same level as that of their prokaryotic homologues (Fleishman *et al.*, 2006). Add to this that ordered crystals are difficult to attain due to their hydrophobic and metastable nature, not to mention the post-translational modifications that they require, (Kaback *et al.*, 2001; Miller, 2003; Fleishman *et al.*, 2006) eukaryotic proteins certainly put up barriers to their research as a result of their complexity.

1.2.1 General membrane protein structure

The majority of membrane proteins belong to the α -helical class and fewer to the simpler β -barrel class, though some are α - β proteins which are composed of both α and β sub-units (White & von Heijne, 2005). Known protein structures are classified by the CATH system (Orengo *et al.*, 1997; Cuff *et al.*, 2008) whereby they are categorised by class, architecture, topology and homologous super families. The CATH database (<http://www.cathdb.info/>) is composed of proteins whose crystal structures have been solved to a resolution greater than 4 Å. Class is assigned based on the peptide's secondary structure and protein packing e.g. the α and β classes. Architecture ignores secondary structure and focuses on the overall protein shape, while topology refers to the domain topology in general, and finally homologous super family refers to proteins which group together as a result of a common ancestor.

The common motif of the α -helix is a right handed coil, the backbone being a hydrogen bonded chain of amino acids (Berg *et al.*, 2007). A single coil in the helix consists of 3.6 amino acids as each amino acid is 100° of each helical turn (Pauling *et al.*, 1951). Forming hydrogen bonds with amino acids above and below ensures tight packing of the helix. In membrane proteins a stable α -helix is common and a trans-membrane domain (Tm) consists of about 20 amino acids crossing 27-30 Å of membrane core (Wolin & Kaback, 2001; Guan *et al.*, 2002; White & von Heijne, 2005).

1.2.2 Protein translocation/insertion

After protein synthesis soluble proteins traverse biological membranes and membrane proteins become embedded in the bilayer. Protein translocation in both cases is energetically demanding and utilises specialised 'machinery'; a protein conducting channel complex known as a translocon (Simon & Blobel, 1991; Crowley *et al.*, 1993; Osborne *et al.*, 2005).

For eukaryotes this complex is known as the Sec61 translocon and prokaryotes, the SecY translocon (Hessa *et al.*, 2005). A significant feature of this channel is its ability to open both across the bilayer and 'into' the bilayer (Osborne *et al.*, 2005). The translocon is a heterotrimeric protein complex which is evolutionarily conserved in prokaryotes and eukaryotes (Snapp *et al.*, 2004; Osborne *et al.*, 2005). Both SecY and Sec 61 are named after the largest subunit in the complex (Rapoport *et al.*, 1996). The α and γ subunits are the only regions of the SecY/Sec61 complex which show sequence conservation in all organisms (Osborne *et al.*, 2005). Translocation takes three forms depending on the association of a partner which provides the driving force for protein translocation. The first method employs a signal recognition peptide (a protein-RNA particle that has the ability to recognise hydrophobic signal sequences emerging from the ribosome) (SRP) (Deshaies & Schekman, 1987; von Heijne, 2007). By this method the ribosome binds to the translocon and the nascent protein moves into the protein conducting channel (Deshaies & Schekman, 1987; Osborne *et al.*, 2005; von Heijne, 2007). Post-translational translocation can occur in eukaryotes whereby the ribosome does not provide the driving force, instead another protein complex, the Sec62/63 complex aids in creating a ratcheting effect which drives the protein into the membrane, this has been studied in the lower eukaryote *Saccharomyces cerevisiae* (Matlack *et al.*, 1999). There is a third mode of action for protein translocation, however, this only applies in the eubacteria (Osborne *et al.*, 2005) and shall not be discussed here. It should be noted that when a SRP is present, it is cleaved from the protein after it has fulfilled its role, though a signal can also be in the form of a recognition sequence which can later form a Tm which is not cleaved after insertion (Rapoport *et al.*, 2004).

Much of the structural information known about these translocon complexes has been garnered from the crystal structures of SecY which has been shown from *E. coli* and *Methanococcus jannaschii* by X-ray crystallography and electron microscopy (Breyton *et al.*, 2002; van den Berg *et al.*, 2004). During translation and insertion, a tight seal is formed at both sides of the membrane to prevent leakage of ions throughout this process (White & von Heijne, 2004), for membrane proteins the peptide must move from the channel through a lateral side gate to reach its destination in the lipid bilayer (van den Berg *et al.*, 2004). The channel is too small for several Tms to reside in the channel so instead they leave through this side gate either one by one or in pairs (Osborne *et al.*, 2005). Figure 1.2 shows the insertion of proteins into the membrane by Sec61 by the ribosome driven insertion method.

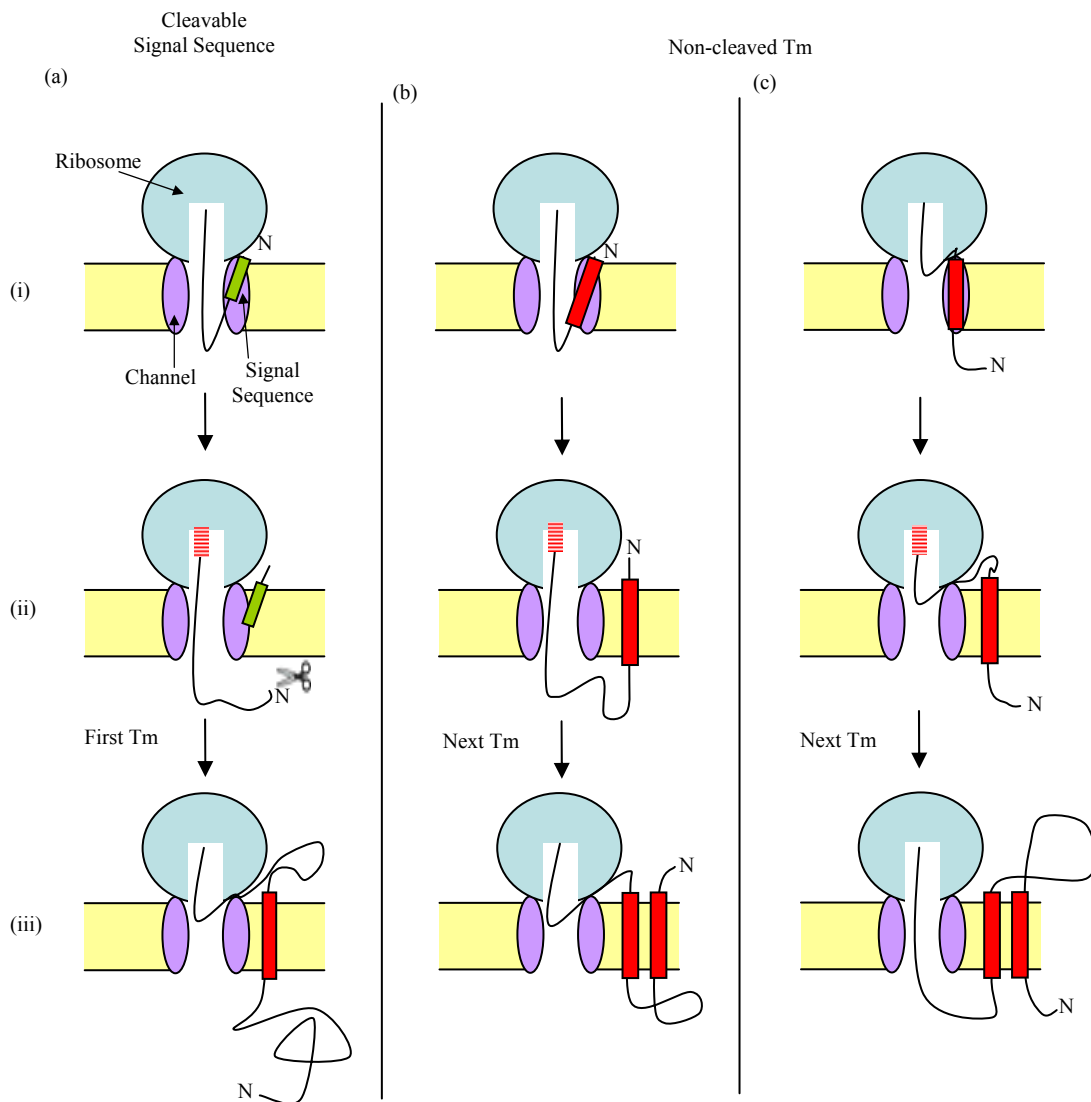


Figure 1.2 Membrane protein translocation and integration by the translocon (Sec61 is described here, though the method of SecY is thought to be similar). (a) Three stages of integration of a membrane protein with a cleavable signal sequence. (i) The signal sequence (green) has emerged from the ribosome (blue) and has inserted as a loop into the Sec61 channel (purple). (ii) At chain elongation, the signal sequence has been cleaved by signal peptidase (scissors), and a Tm segment (red stripes) is synthesised by the ribosome. (iii) The Tm (red) has emerged from the ribosome and has left the channel through the side gate and entered the lipid. (b) Three stages of integration of a membrane protein with a non-cleaved first Tm whose N terminus stays in the cytosol. (i) The first Tm has emerged from the ribosome and has inserted as a loop into the Sec61 channel. (ii) The first Tm has left the channel sideways and entered the lipid and a second Tm is synthesised. (iii) The second Tm has emerged from the ribosome, and has left the channel and entered the lipid. (c) Three stages of integration of a membrane protein whose N terminus is translocated. (i) The first Tm has emerged from the ribosome and the N terminus is translocated across the membrane. (ii) The first Tm has left the channel sideways and entered lipid, and a second Tm is synthesised. (iii) The second Tm has emerged from the ribosome and has left the channel and entered the lipid. Figure and legend modified from that by Rapoport *et al* (2004).

It is currently unclear if at this stage the protein is elongated or coiled, though it is likely that the secondary structure of the protein forms as it exits the ribosome (Hessa *et al.*, 2005). Membrane protein insertion and folding is commonly broken down into these two stages (Popot & Engelman, 1990; Popot & Engelman, 2000; Bowie, 2005) as shown in Figures 1.2 and 1.3. The translocon controls whether or not the nascent protein is secreted as it leaves the ribosome or ‘injected’ into the bilayer through the side gate (van den Berg *et al.*, 2004). The premise of this mechanism has been investigated through the use of specially designed polypeptide sequences (Hessa *et al.*, 2005; Hessa *et al.*, 2007). The amino acids isoleucine, leucine, phenylalanine and valine have been shown to promote membrane protein insertion whereas tryptophan and tyrosine when placed together centrally reduce membrane protein insertion (Hessa *et al.*, 2005). Likewise, the positioning of charged residues in the polypeptide is important for insertion. Traditionally, the protein enters the bilayer N-terminal first; therefore, this region should become situated outside the membrane surface. However, there is a fifty second window when the topology is not determined and the domain can ‘flip’, moving the N-terminal to the inside of the membrane, this is determined by the constitution of amino acids in this N-terminal region (Hessa *et al.*, 2005; Osborne *et al.*, 2005) (Figure 1.2). Signal anchor proteins direct and tether the nascent protein in the membrane; mutated key amino acids of the N-terminal of these proteins have been investigated. It has been found that positively charged residues are more likely to be cytoplasmic in eukaryotes (Goder & Speiss, 2001). When mutated to alter the overall charge of this region the protein has changed its membrane orientation, showing that charge is one of the important parameters during membrane insertion (Goder & Speiss, 2001; White & von Heijne, 2004). Length and hydrophobicity have also been implicated as important features of these protein anchors (White & von Heijne, 2004). While the confines of the bilayer may seem a restriction to transport, elegant structural adaptations have developed to accommodate these functions, and these are discussed for exemplified proteins.

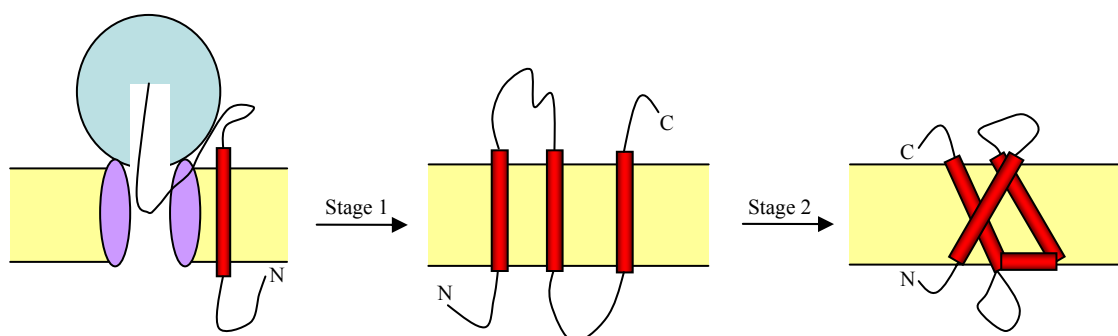


Figure 1.3 Membrane protein folding and insertion (Popot & Engelman, 1990). Stage 1. The protein is inserted across the bilayer; this is generally catalysed by the translocon. Membrane protein topology is partially formed in communication with the translocon complex. Stage 2. The protein is folded to form the tertiary and quaternary structures. This figure was adapted from (Bowie, 2005).

1.2.3 The importance of membrane proteins

Membrane proteins have been proven to be vital for many facets of life. For example, three of the most commonly prescribed drugs worldwide, Fluoxetine (Prozac), Lidocaine and Omeprazole (Prilosec), are targeted to membrane proteins, (le Coutre & Kaback, 2000; Abramson *et al.*, 2003b). To emphasise their importance from a human perspective, in addition to being drug targets, one must understand that when membrane proteins mutate they pose a threat to human life by causing disease. For instance, certain mutations in the Cystic Fibrosis Trans-membrane conductance Regulator (CFTR) gene cause the genetic condition Cystic Fibrosis (CF), which results in lung disease and premature death; it is the most common fatal genetic disease of Caucasians (McKone *et al.*, 2003). CFTR is an ion channel that controls the movement of primarily chloride, but also sodium ions, it belongs to the ATP-binding cassette (ABC) protein super-family. This is but one example of a medical condition caused by a defect in a membrane protein; there are several other conditions which are also associated with membrane proteins, though, this is not within the scope of this thesis.

1.3 Membrane transport proteins

The dielectric barrier which exists between the intra and extra-cellular solution allows the free transport of uncharged molecules across the bilayer but actively prevents the passive transport of ions. This is due to the natural stability of charged molecules in the aqueous extra-cellular environment compared to the 'oily' intra-cellular solution (MacKinnon, 2004). Charged molecules are actively monitored by the cell by way of integral membrane proteins which selectively mediate their passage in and out of the cell. Ion channels do not transduce energy but function exclusively as selective pores whereas gradients are built by ion pumps which provide energy for transporters to carry out the housekeeping functions of the cell (Gouaux & MacKinnon, 2005).

1.3.1 Transporter architecture, selectivity and coupling

Translocation takes the form of three mechanisms, namely uniport, symport and antiport (Jessen-Marshall *et al.*, 1995). Uniport refers to the facilitated diffusion of molecules by a channel or transporter one molecule at a time with a solute gradient. Symporters transport two different molecules in the same direction across a membrane, one against, one with its concentration gradient (Stryer, 1999). Finally, antiporters are like symporters though the two molecules are transported in opposing directions (Stryer, 1999). This dual movement allows one molecule to move with, and one move against a concentration gradient (Marger & Saier, 1993).

The α -helices of trans-membrane transporters (channels or pumps) are connected by a series of intra and extra-cellular loops. These are liable to vary in length and orientation to the membrane and may even be disjointed (Dutzler *et al.*, 2002). Membrane proteins are not rigid in the bilayer, as flexibility is required for substrate binding and conformational changes in the transport process; this will be discussed later in this chapter. It is important to note this flexibility, as an assumption of a rigid protein may result in the misinterpretation of crucial structural data. Transport proteins are known to form dimers, trimers etc. where it is possible for each monomer to form or contribute to the formation of a translocation pathway. The overall architecture of membrane channels and transporters is highly variable, even between proteins which seemingly share function. Gouaux and MacKinnon have reviewed some of these structures which I have briefly summarised here (Gouaux & MacKinnon, 2005). Basin and hourglass structures allow the aqueous transport of substrate to the selectivity filter through the first envelope of the membrane as in the case of sodium dependant glutamate transporter (Glt_{ph}), and chloride channel (ClC), as discussed later. Pumps such as the Ca²⁺ ATPase and the Glt_{ph} transporter have no obvious pathways for the substrate to move toward or through. While channels such as the potassium (K⁺) channel are open to the continual movement of ions, pumps require a conformational change to physically move the substrate across the membrane and thus have a lower through-put compared to ion channels.

The principle of selection, as regards membrane transporters, determines which ions are permitted to cross the membrane and which will be excluded. Major factors involved in ion selectivity are atomic composition and the stereochemistry of the binding site (Gouaux & MacKinnon, 2005). An ion must be physically detected, to be selected for or against; binding sites *a priori* must also be situated on the channel or pump at key locations to allow for substrate discrimination. When an ion is detected by a protein it is in a partially hydrated state as it is solubilised in the extra membrane solution. Following detection, and prior to translocation, the ion must be dehydrated to be translocated (Doyle *et al.*, 1998; Gouaux & MacKinnon, 2005). Dehydration of a substrate is an energy demanding step and as such must be of 'high value' to the organism. Therefore, selection occurs when the energetic compensation is more favourable to one ion over the other, allowing for its discreet determination. When the dehydrated substrate enters the binding site the surrounding molecules interact with it, either directly or indirectly from the surrounding solution. For instance, in the leucine transporter, LeuT, leucine and sodium are co-transported with the Na⁺ gradient i.e. this process provides the energy for the transport of leucine. There are two binding sites in LeuT where five and six oxygen atoms (both full and partial charges) are in direct contact with the Na⁺ atom as it is transported (Yamashita *et al.*, 2005). In the K⁺ channel, K⁺ is transported down an electrochemical gradient across four binding sites of the

channel where the dehydrated K^+ interacts exclusively with eight partial charges on the oxygen atoms of amino acids (Zhou *et al.*, 2001). In this instance water is removed from the ions, then they are caged in counter charges, this region is known as the selectivity filter (Doyle *et al.*, 1998). This shows that the protein selects for the particular cation by providing an oxygen-lined binding site of the appropriate cavity size for the trans-locating ion.

A feature of coupled transport systems is that the substrate is not permitted to collect within the receiving cells. Instead, it is quickly metabolised or stored for use later, though under controlled circumstances accumulation may be permitted (le Coutre & Kaback, 2000). Inbuilt 'imperfections' in biological systems can indirectly benefit organisms. For example, random mutation is the driving force behind natural selection and thus evolution. Likewise, the integral flaws of coupled transport can be beneficial to the cell. The stoichiometry of substrate and co-transporter(s) is system dependant. The stoichiometry of the mammalian divalent cation symporter, Dct1 (Nramp2), under normal conditions (pH 7) is 1:1 for Fe^{2+} : H^+ , where the protons drive the transport of the cation. However, in conditions of high proton concentration (low pH) the stoichiometric ratio is not necessarily maintained and can be as much as 18 protons to every iron molecule, this is referred to as a 'slip', whereby the protons slip through the driving force pathway uncoupled (Nelson *et al.*, 2002). Theoretically, at low pH, high proton concentration or negative membrane potential encourages the movement of excess protons across the transporter to no apparent detriment to substrate transport. This uncoupling can help to modulate the efficient functioning of the transport system and prevent the excessive accumulation of ions that may be damaging to the organism; this has been shown for other ions in addition to protons (Nelson *et al.*, 2002). Channels can be opened either as a result of ligand binding (where the ligand does not cross the membrane) or they can be pH dependant, (where the proton is considered to be the ligand) (Perozo *et al.*, 1999; le Coutre & Kaback, 2000). Ion channels although not involved with the transduction of energy can be involved with gating, whereby ions move with the concentration gradient as the gate is opened or closed (Miller, 2000). By contrast to the gating mechanism of the Major Facilitator Super-family (MFS), the machinery of the channel is abruptly altered in response to a stimulus (ligand binding or pH alteration) though the 'rocker switch' of the MFS is a slower fluid movement in answer to the proton electrochemical gradient (le Coutre & Kaback, 2000) (Figure 1.4).

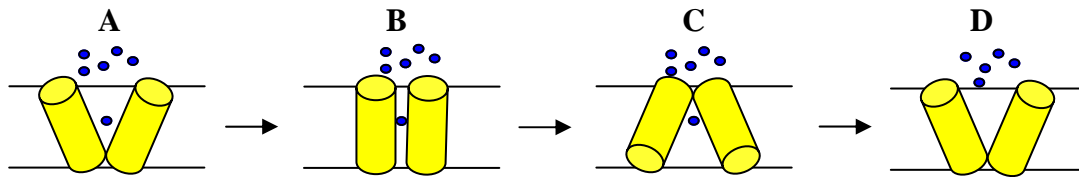


Figure 1.4 The ‘alternating access’ model for membrane transport. The membrane protein is represented by yellow barrels and substrate molecules are represented as blue circles. A. The substrate is up-taken from either the periplasm or the cytoplasm. B. Substrate binding induces conformational changes within the protein. C. It is then moved through the bilayer and deposited in its destination. D. The protein returns to its open conformation. Diagram based on that by Huang *et al* (2003)

In the case of permeases such as the lactose transporter (LacY) of *E. coli*, conformational changes are triggered in response to substrate binding (le Coutre & Kaback, 2000). With this substrate induced gating mechanism when substrate enters the binding site, protons on the other side of the membrane are already in position to be translocated. It is these protons which ‘hold’ the protein open to the extra-cellular environment (specific residues involved shall be discussed in Section 1.7) (le Coutre & Kaback, 2000; Sahin-Toth *et al.*, 2000). While remaining in this conformation, the substrate becomes bound between two helices at the membrane surface; it is this binding which induces the conformational changes to translocate the substrate. As the substrate moves through the membrane the affinity of the permease is reduced and the substrate is released (protons are also released at this stage). This cycle returns to its ‘starting’ position, i.e. open to the extra-cellular solution when protons become bound again (Sahin-Toth *et al.*, 2000).

1.4 Ion pumps and channels – blurring the boundaries?

“it seems that the structural boundary separating channels
and transporters is not as clear as generally thought”

(Accardi & Miller, 2004)

Membrane transporters may be separated from channels and receptors, by their expert functions in nutrient provision, ion gradient maintenance as well as their ability to seize neurotransmitters from pre synaptic terminals (DeFelice, 2004). ATP or protons are used as an energy source coupled to ion translocation in membrane pumps, whereas ion channels on the other hand, are passive and often hastily catalyse the movement of ions with a concentration gradient (Gouaux & MacKinnon, 2005). Active transport in a permease such as LacY may account for a turnover of 30-50 molecules of substrate per second whereas in channels the flux is significantly higher, (up to 10^6 - 10^7 molecules per second) (le Coutre &

Kaback, 2000). However, distinction between channels and pumps is becoming more and more difficult to determine (DeFelice & Blakely, 1996). At first glance the Lac permease and K^+ channel seem highly divergent; LacY is a monomer with no apparent electrophysiology, whereas the K^+ channel is a homo tetramer with channel-like electrophysiology (DeFelice, 2004). K^+ channels detect the rise in internal potassium and change their structure subtly to prevent further transport. Thus, in effect, K^+ channels gate in a similar manner to LacY, though the associated conformational changes are less extreme (DeFelice, 2004).

A subtle change (the substitution of a single amino acid) of a chloride channel can change it from a channel into a transporter. The high resolution structure of a bacterial analogue of a mammalian Cl^- channel (ClC-ec1) shows a low conductance of Cl^- with H^+ , where proton movement occurs by co-transport rather than by diffusion. A mutation in this protein (E148R) transforms this pump into a channel (Accardi & Miller, 2004). A second example would be a spontaneous mutation (G185R) in the divalent metal transport protein DMT1 (Nramp2) which changes this secondary Fe^{2+} transporter to a calcium channel; this was shown to underlie anaemia in rats (Xu *et al.*, 2004).

1.5 Which amino acid for where?

The main premise for the lipid bilayer is that it is semi-permeable; for proteins to operate efficiently they must not cause leakages of ions which could prove detrimental to the cell. Therefore, an effective membrane must have the correct packing of lipids and proteins, to ensure that the illegal immigration of ions across the bilayer is not permitted whilst the membrane transport proteins are free to pick up and deposit their cargo. When studying protein composition the features of the amino acids to consider are their charge, potential for hydrogen bonding, volume and the relative hydrophobicity of side-chains (Darby & Creighton, 1993). Refer to Appendix One for overview of amino acids.

Amino acids in trans-membrane proteins tend to be non-polar, as a result of their inability to solubilise with water molecules in the aqueous environments out-with the domain. Also, the side-chains of these amino acids are small and compact which cause little disturbance in the α -helix. As a result, alanine is common in the Tm whereas tyrosine and arginine are not. However, for functionality, amino acids which are neither small nor uncharged are required within this region. Consequently, determining the secondary structure of trans-membrane proteins can be problematic. The amino acids methionine, alanine, leucine, glutamic acid and lysine help to maintain the α -helix and are markers for this region. Conversely, proline and glycine disrupt the uniform nature of the helix backbone as a result of their unusual

conformation abilities (glycine has no side-chain and proline has no backbone, discussed below), consequently these amino acids are commonly found within the turns of the α -helix (Bailey & Manoil, 1998). In addition, other amino acids are less stable in an α -helix (tyrosine, tryptophan, phenylalanine, and valine) and tend to contribute to the formation of β -sheets (Wimley, 2002; Wimley, 2003; Waldispuhl *et al.*, 2008). Investigations into the function of specified amino acids tend to be carried out by chemical and site-directed mutagenesis techniques. A selection of typical residue functions shall be discussed briefly here as an introduction to the main mutagenesis experiments which were carried out in this thesis.

1.5.1 Glycine

The term helix breaker has been applied to glycine for its ability to form tight turns due to the absence of steric interactions in soluble proteins. Though, glycines have also been noted for their high frequency in the T_m regions of membrane proteins (Senes *et al.*, 2000; Liu, 2002), particularly their preponderance towards helix-helix interfaces showing an apparent function in the mediation of helix-helix interactions (Javadpour *et al.*, 1999). The high conservation of glycine residues in several transporters has been discussed, particularly in key motifs. The conformational changes in a membrane permease, like LacY, require the presence of amino acids which can interact directly with the substrate, however, a supporting role for glycine residues to aid conformational changes would also seem to be necessary (Jung *et al.*, 1995; JessenMarshall *et al.*, 1997). Specific functional analyses of conserved glycines in LacY showed that none were obligatory for function, though revealed the importance of side-chain bulk in some cases (Jung *et al.*, 1995; JessenMarshall *et al.*, 1997). Of the thirty-four glycine residues studied in LacY, (there are a total of thirty-six, however previous experiments had shown that G402 and G404 can be deleted with no loss of activity (Roepe *et al.*, 1989)), fifteen of the thirty-four mutants showed wild-type lactose transport, sixteen showed reduced, though significant transport and three showed loss of activity. These three residues (G64, G115 and G147) were targeted for further mutagenesis in both the wild-type construct and in the Cys-less construct. Overall, the results showed that none of the glycines in LacY are mandatory, though where loss of activity was observed it became apparent that side-chain bulk, not conformational flexibility, was critical in these positions (Jung *et al.*, 1995; JessenMarshall *et al.*, 1997). Later, suppressor analysis of G64 showed that it was likely to be located at the interface of the two halves of the LacY protein and is likely to be a key amino acid in facilitating conformational changes (JessenMarshall *et al.*, 1997). It would appear then, that in membrane proteins, glycine is not the helix breaker it is famed to be, though conversely is likely to have a more direct role in the maintenance of helix integrity.

In the four Tm multi-drug resistant homo-dimeric transporter EmrE from *E. coli*, the role of twelve glycine residues was investigated by site-directed mutagenesis (Elbaz *et al.*, 2008). Four of these residues were found to be mandatory for the protein to function effectively; two residues contributing to the formation of functional dimers as a result of close helix packing (G90 and G97), and the other two (G17 and G67) are thought to contribute to the formation of the binding site or to the conformational changes common for the alternating access mode of transport (Elbaz *et al.*, 2008). Over and above the conformational flexibility provided by glycine discussed here, in potassium channels glycine has been shown to act as a gating hinge (Jiang *et al.*, 2002) and in the photoreceptor rhodopsin, a conserved glycine has been shown to form part of the retinal binding pocket interacting directly with ligand (Han *et al.*, 1996; Han *et al.*, 1997). With unusually high frequency, glycine forms motifs which effectively stack glycine on a single α -helical face (Senes *et al.*, 2000; Elbaz *et al.*, 2008) these motifs have been shown to be functional, not only in the packing of domains, but also in the oligomerisation of proteins (Russ & Engelman, 2000; Kim *et al.*, 2004; Kim *et al.*, 2005; Arbely *et al.*, 2006).

Glycine residues in the Nitrate Nitrite Porter family (NNP) signature sequence (A-A-G-X-G-N-X-G-G-G) of MFS subfamily NNP are both highly conserved and of an unusually elevated density in this region, inferring function (Forde, 2000). These signature sequences and their purpose will be discussed further in Chapter Three. However, it is important to note at this point, that these signature sequences reside in trans-membrane regions and may be functionally important, potentially in substrate binding or recognition, and therefore this area may be in need of a certain degree of flexibility, this could be provided via these small putative 'helix breakers'. Specifically, the undertaking of this small amino acid is postulated to participate in close packing of trans-membrane helices in several other transporters, this may also be the case here.

1.5.2 Proline

Proline is an amino acid which is often key in protein-protein interactions (Kay *et al.*, 2000) though is known to be a helix breaker in soluble proteins (Chou & Fasman, 1974) it has been observed frequently within the Tm (Li *et al.*, 1996; Bywater *et al.*, 2001). Proline is unique, particularly because of its side-chain which is cyclic and attached to the backbone of the amino acid thus restricting conformational changes in this, and in neighbouring residues, this is one of the reasons for increased frequency of proline in β -sheet proteins (MacArthur & Thornton, 1991; Kay *et al.*, 2000; Orzaez *et al.*, 2004). Proline is commonly found to provide

a bend in a T_m helix which disrupts the α -helix, as suggested by the term helix breaker (Vonheijne, 1991; Ostermeier *et al.*, 1997; Orzaez *et al.*, 2004). Proline scanning *in vitro* mutagenesis in Glycophorin A (GpA) has shown the disruption of the α -helix when proline residues are located centrally in a T_m, while replacing residues at the ends of a helix with proline can allow for dimer formation, in-fact, when proline was located at the end of a helix it had the tendency to extend the T_m (Orzaez *et al.*, 2004).

1.5.3 Aromatics

Aromatic amino acids tend not to be uniformly distributed in the lipid bilayer. Instead they congregate on membrane interfaces, probably as a result of hydrogen bonding or anchoring mechanisms for membrane proteins which perform large conformational changes, such as, the alternating access mechanism of members of the MFS (Bailey & Manoil, 1998; Kelkar & Chattopadhyay, 2006). The introduction of aromatic amino acids to synthetic membrane proteins has been shown to be highly beneficial in optimising membrane protein insertion, orientation and channel activity (Kelkar & Chattopadhyay, 2006; Shank *et al.*, 2006). Aromatics have also been shown to be critically important in sugar transport (Kasahara & Kasahara, 2000). The galactose (Gal2) transporter in the yeast *S. cerevisiae* harbours an essential tyrosine which is involved with sugar binding. Additionally, a phenylalanine and another tyrosine, are thought to be involved in the translocation pathway and are therefore important for galactose transport (Kasahara & Kasahara, 2000). In *E. coli* the LamB maltosaccharide porin, an apolar stripe of six contiguous aromatic residues runs from the vestibule to the exit of the transporter (Denker *et al.*, 2005). This set of residues has been dubbed the 'greasy slide' (Dumas *et al.*, 2000; Denker *et al.*, 2005) and is conserved in a number of other proteins (Meyer *et al.*, 1997; Forst *et al.*, 1998). The greasy slide has been shown to be critical for the binding of translocating maltosaccharides and carbohydrates (Denker *et al.*, 2005). An additional tyrosine (Y118) is positioned opposite the greasy slide, and functions as a channel constrictor, regulating the control of movement through the porin. Alanine scanning *in vitro* mutagenesis suggested that each aromatic contributed to ion and carbohydrate transport (Denker *et al.*, 2005). It was found that the slide specifically helps to align the sugar as it enters the channel and facilitates its entry, binding and movement in concert with the polar tracks (Van Gelder *et al.*, 2002). Additionally, the greasy side and Y118 probably control the permeability of LamB to neutral solutes (Denker *et al.*, 2005).

1.5.4 Charged residues

Residues with complete charges are generally thought of as being disruptive in the T_m, so when they do exist in these regions they are thought to be functionally important. In LamB,

the 'greasy slide' works in tandem with the 'polar tracks'. The polar tracks are two lines of pair-wise ionisable residues which are located at the constriction zone of the channel (Dumas *et al.*, 2000). They are probably too far apart to be involved in salt-bridge formation, but may act as H-bond donors or acceptors with the translocating substrate (Wang *et al.*, 1997; Dumas *et al.*, 2000). While the maltosaccharide 'slides' over the aromatic residues in LamB it is facilitated by the making and breaking of hydrogen bonds with the hydroxyl groups of the sugars and the charged amino acids of the polar tracks (Dumas *et al.*, 2000). Alanine scanning mutagenesis indicated the importance of charged residues arginine, aspartic acid and histidine as a resulting decrease in sugar transport was observed when mutations were made individually and in tandem (Dumas *et al.*, 2000). It was thought that in this region only a few key connections were made to the substrate, as such these performed vital roles, so when a single mutation was made reducing the number of connections this altered the efficiency of the binding site (Dumas *et al.*, 2000). Additionally, structural determination of LamB revealed the H-bonding interaction of the polar tracks in the channel lining (Dumas *et al.*, 2000). The removal of H-bond partners from the channel resulted in decreased binding affinity of sugars in the channel and an increase in size of the pore, effectively increasing the rate of dissociation from the channel (Dumas *et al.*, 2000). Charged residues in this case are involved in the movement of the sugar in tandem with the aromatic greasy slide. In EmrE, a single charged residue is found in a T_m region, this residue is pivotal in substrate binding and translocation in this small transporter (Yerushalmi *et al.*, 1995; Yerushalmi & Schuldiner, 2000; Gutman *et al.*, 2003; Elbaz *et al.*, 2008). The involvement of charged residues is also discussed later in MFS pumps GlpT, OxlT and LacY, as well as nitrite transporters from another group of proteins discussed.

1.5.5 Polar and non-polar amino acids

As stated previously, charge is an important parameter in membrane proteins, often involved with substrate interactions and salt-bridge formation, amino acids which do not harbour full charges, i.e. polar and non-polar residues also play important roles. Specifically, polar amino acids when embedded in the bilayer amongst non-polar residues provide helical stability, helix-helix associations and contribute to the formation of oligomers through hydrogen bonding (Lear *et al.*, 2003; Hildebrand *et al.*, 2006). In particular large polar side-chains are involved with oligomerisation, it is thought that in the T_m, small polar residues act as apolar residues as a result of their small side-chains' failing to make the contacts necessary for hydrogen bonding (Lear *et al.*, 2003; Hildebrand *et al.*, 2006). An integral part of membrane proteins is that the T_m are formed by hydrophobic non-polar residues while hydrophilic polar residues locate at the membrane interfacial region and in the aqueous environment, though again, there are functional exceptions to this generalisation.

1.5.6 Protein oligomerisation and key amino acids

Among proteins embedded in the membrane, several are known to form higher order structures of dimers, trimers etc. (Liu *et al.*, 2004). These oligomeric structures are known to transport a wide variety of substrates and are not specific to channels or pumps. How these proteins efficiently oligomerise and form stable interactions in the membrane is determined by the amino acid sequence. As stated already, glycine contributes to the oligomerisation of membrane proteins, the GG4 motif (G-X-X-X-G) and related motifs (SS4 and AA4) along with single polar residue motifs which are known to contribute to the formation of substrate interaction sites (Senes *et al.*, 2004; Rath & Deber, 2008). These small residue motifs allow close packing of the T_m, while other residues such as aspartate, glutamic acid, asparagine and glutamine help to stabilise helix-helix interactions. It is thought that these small residue motifs (G/S/A-X-X-X-G/S/A) highlight protein-protein interaction sites as they frequently occur on the surface of oligomeric subunits.

1.6 MFS and ATP binding cassette (ABC) protein super-families

While several types of transporters are known to exist, the MFS and ABC dominate and are present throughout all kingdoms of life (Pao *et al.*, 1998). Members of the ABC family are multi-component primary transporters for the translocation of large and small molecules in response to ATP hydrolysis. Without protein phosphorylation, ATP hydrolysis is responsible for energising the transporter (Hollenstein *et al.*, 2007). Conversely, MFS proteins are simpler, single polypeptide carriers which catalyse the translocation of their substrate in response to electrochemical gradients (Pao *et al.*, 1998). Primary transporters (i.e. ABC's) are thought to have evolved from secondary transporters (i.e. MFS's) which are considered to be more energy efficient than their primary counterparts (Lemieux *et al.*, 2003). The need for generating an understanding of trans-membrane proteins is of utmost importance in many fields; their association with human diseases is profound. Mutations in MFS proteins are responsible for genetic hearing loss, some predispositions to cardiac arrhythmia and many other conditions (Guan & Kaback, 2006). However, it is not within scope of this thesis to go into specific detail on the pathologies associated with membrane proteins.

1.6.1 ABC Super-family

The ABC super-family is poorly understood compared to the MFS, and, at first, the system seems much more complicated. Members of this family are known to transport a highly diverse range of substrates, by influx (prokaryotes) and efflux (prokaryotes and eukaryotes) (Saier, 2000; Hollenstein *et al.*, 2007). ABC transporters are associated with human conditions such as CF and multi-drug resistance (Hollenstein *et al.*, 2007), and are also expressed in the human placenta (Dean *et al.*, 2001).

The structure of ABC proteins is variable; particularly the number and the organisation of the domains, the name ‘binding cassette’ comes from the formation of cassettes by four polypeptide loops. These domain regions function specifically in the sensing of the phosphate group, binding of the nucleotide in ATP bound and unbound states and in the conformational changes that occur within the peptide (Hollenstein *et al.*, 2007). A standard domain organisation is two trans-membrane regions of ten to twelve Tm, (twelve for ABC exporters) and two cytoplasmic nucleotide binding domains (Hollenstein *et al.*, 2007). For importers, these domains are on different polypeptide chains (Hollenstein *et al.*, 2007). However, for bacterial exporters one Tm and one binding domain are fused generating a half protein. For functionality the half protein must form a homo or hetero dimer with another ABC half protein (Hollenstein *et al.*, 2007). A highly conserved signature motif (L-S-G-G-Q) is also characteristic of ABC proteins and is located downstream of the ATP binding domain(s) (Szentpetery *et al.*, 2004). Protein mutation programmes have investigated key residues throughout the ABC proteins, particularly natural mutations occurring which cause disease (Frelet & Klein, 2006). In the ABC signature sequence, mutations, both natural in the case of CF sufferers and induced in the case of the bacterial transporter HisP, have shown the conserved serine residue and a glycine residue in the ABC motif to be particularly important for transport (Frelet & Klein, 2006). Four crystal structures are now known for ABC transporters shown in Figure 1.5. They are all importers aside from the *Staphylococcus aureus* Sav1866 exporter. This figure gives a representation of the topological scheme of the Tm, particularly how variable these examples are from one another (Hollenstein *et al.*, 2007).

The mechanism of the ABC transporters is not well understood, although it was postulated that when ATP is bound to each cassette, conformational changes are induced to allow the ATP binding domains to interact closely, inducing the Tm to shift and form a translocation pathway, known as the ‘powerstroke’ (Hollenstein *et al.*, 2007). At this point the affinity of the transporter is reduced and the substrate is released (Hollenstein *et al.*, 2007).

1.6.2 MFS

The MFS are an ancient family of highly diverse proteins which catalyse uniport, symport and antiport of diverse substrates (Kaback *et al.*, 2001). As a result, the MFS are also known as the USA super-family (Jessen-Marshall *et al.*, 1995). These proteins are known in eukaryotic organisms to constitute a considerable number of membrane proteins (Ward, 2001). MFS

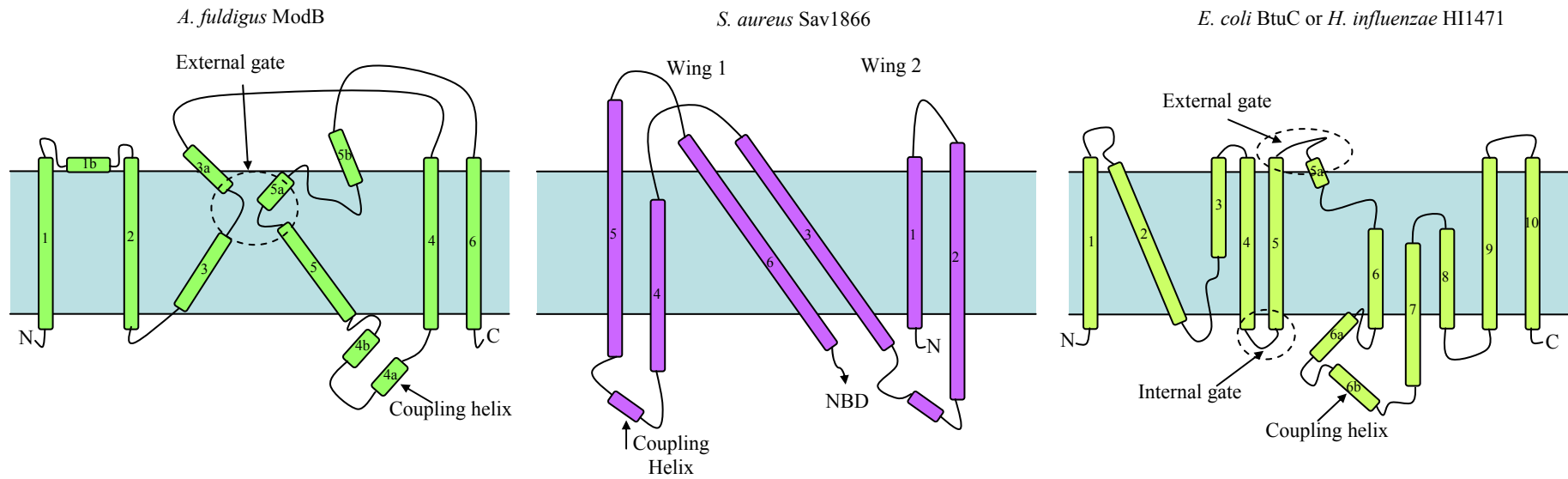


Figure 1.5 Topological representation of four crystallised ABC transporters. Here Tm's are numbered consecutively and short helices carry additional letters. For Sav1866, the schematic emphasises the 2 wings formed by Tm 1-2 and Tm 3-6 and the pseudo-two fold symmetry relating to Tm 1-3 and Tm 4-6. For ModB, the schematic emphasizes the conserved gate formed by Tm segments 3 and 5. For BtuC/HI1471 the schematic depicts the internal and external gates. The coupling helices in each domain are the main site of contact with the nucleotide binding domain in the assembled transporter. Figure and legend are adapted from Hollenstein *et al* (2007), to show the dramatic differences in the ABC transporters.

proteins specifically use the free energy liberated by movement of a 'driver' solute down its electrochemical potential gradient to energise the transport of their ions, LacY, GlpT and OxlT are examples of these (Abramson *et al.*, 2003b; Huang *et al.*, 2003; Hirai & Subramaniam, 2004). Currently, there are over one thousand sequenced members of the MFS which are sub-divided into fifty-four subfamilies (as detailed in the transporter classification database www.tcdb.org). The characteristics of these proteins include a characteristic signature sequence (G-X-X-X-D-K/R), and twelve trans-membrane α -helices composed of two sets of six Tm, one carboxyl, one amino (Locher *et al.*, 2003). While proteins containing twelve Tm are standard for this family, proteins of fourteen and twenty-four Tm have also been noted. An example of a twenty-four Tm protein is the nitrate transporter of *Parococcus pantotrophus*, composed of two homologous MFS proteins, NarK1 (NO_3^-/H^+ symport) and NarK2 ($\text{NO}_3^-/\text{NO}_2^-$ antiport) fused together, they are both required for the normal nitrate transport in *P. pantotrophus* (Wood *et al.*, 2002). A fourteen Tm tetracycline/ H^+ antiporter (TelL) has been noted in *Bacillus subtilis*, this protein has two additional central Tms, interestingly the removal of these additional Tms transforms the protein into a monovalent cation antiporter (Jin *et al.*, 2001). There is a two-fold axis of symmetry in members of the MFS which is represented both structurally and sequentially in the repetition of signature sequences (Locher *et al.*, 2003). This was probably due to a duplication of the existing initial six Tm structure (Maiden *et al.*, 1987; Abramson *et al.*, 2003a) and will be discussed further in Chapter Three. While there is strong homology between closely related members of this family, this becomes diffuse for distant relatives. The family has therefore been divided into subfamilies of similar transporters, where sequence identity over the whole polypeptide is not necessarily conserved but the MFS signature motifs (loops 2/3 and 8/9) persist (Jessen-Marshall *et al.*, 1995; Pazdernik *et al.*, 1997; Pazdernik *et al.*, 2000). It is unlikely that the MFS motif is involved in substrate binding since it is present among transporters of diverse substrates (Jessen-Marshall *et al.*, 1995; Pazdernik *et al.*, 1997; Pazdernik *et al.*, 2000). It is more likely that the motif is involved in the gating mechanism, conformational changes or solute accessibility (Jessen-Marshall *et al.*, 1995; Pazdernik *et al.*, 1997; Pazdernik *et al.*, 2000).

The MFS members have a characteristic 'alternating access' mode of transport where the protein undergoes a series of conformational transitions so the binding sites are only open on one membrane face at a time (Huang *et al.*, 2003; Majumdar *et al.*, 2007) (Figure 1.4). This was discussed originally by Jardetzky (1966) in its simplest form whereby the polymer must meet three structural conditions (i) the provision of an internal cavity for the translocating substrate (ii) it must be able to assume two configurations and (iii) it must contain a binding site with varying substrate affinities with conformational change. In the example of LacY it

has been shown that it is the binding of the sugar molecule that induces conformational change (Nie *et al.*, 2007; Smirnova *et al.*, 2007). Regarding substrate transport, the diversity and specificity of these proteins is immense; they are known to transport sugars, neurotransmitters, Krebs cycle intermediates, drugs, amino acids, organic and inorganic anions and many, many more. The secondary structure and mechanisms of these permeases are conserved across family members (Marger & Saier, 1993; Pao *et al.*, 1998). It is also possible that their tertiary structures and functional mechanisms are also conserved. Therefore, understanding these proteins can provide a vast number of comparisons and extrapolations to other systems. As the two main focuses of this work are the nitrate and nitrite permeases of *A. nidulans*, comparisons will be drawn throughout to proteins of other families transporting different substrates in different organisms.

1.6.3 Comparison of the ABC and MFS super-families

The structures of the ABC proteins are undoubtedly more complex, in addition there are - so far - no distinct rules for structure as opposed to the distinctive domain scheme of the MFS proteins. This is reflected in the crystallised forms of the ABC and MFS proteins. The MFS are ubiquitous in nature compared to the ABC proteins which are classified in terms of function, particularly, that influx of substrate is only catalysed in the prokaryotes. The ABC proteins are thought to have evolved from the MFS proteins and again this seems to reflect in the known structure and functional organisation of the proteins.

1.7 LacY structure and mechanism

LacY is a member of the MFS, and is considered to be a paradigm for membrane transport that has been intensely studied (Kaback *et al.*, 2001; Abramson *et al.*, 2003b; Guan & Kaback, 2006). *LacY* was the first gene of a polytopic membrane protein to be cloned and sequenced (Buchel *et al.*, 1980) and encodes the LacY permease, a 417 amino acid polypeptide that facilitates the proton coupled translocation of β -galactosides using energy released from an electrochemical proton gradient into substrate concentration gradient (Abramson *et al.*, 2003b; Kaback, 2005; Guan & Kaback, 2006). Like most MFS proteins, LacY has 12 α -helical hydrophobic Tms joined by extra-membrane loops with both the N and C termini on the cytoplasmic side of the membrane (Kaback *et al.*, 1994). Eight of the twelve helices line the hydrophilic substrate translocation pore, the remaining four hydrophobic helices - III, VI, VIII and XII - are imbedded in the bilayer (Abramson *et al.*, 2003b). LacY is unique in that it is solely responsible for all translocation reactions catalysed by the β -galactoside transport system (Kaback, 2005). Four β -galactoside molecules may be

transported simultaneously with protons in one reaction (Kaback *et al.*, 1994). Structurally and functionally LacY is a monomer *in vivo* (Vazquez-Ibar *et al.*, 2004).

1.7.1 Structure

The crystal structure of LacY was solved to 3.5 Å resolution (Abramson *et al.*, 2003b) (Figure 1.6 and Figure 1.7) which helped confirm the two domain theory, of two regions of six Tm, one a mirror image of the former. The crystallised protein mutant, where amino acid 154 (cysteine) was altered to glycine which was trapped in the inward facing conformation, with and without bound substrate (Abramson *et al.*, 2003b). Residue C154 is at the domain interface and when altered to glycine (a much smaller amino acid) allows for much tighter helix packing, therefore increased protein stability (Ermolova *et al.*, 2005). This stability has permitted the crystallisation of the permease (Abramson *et al.*, 2004). However, the mutation resulted in several physical and behavioural changes in the protein. Specifically increasing the binding affinity in a manner that is resistant to heat, and preventing aggregation in cold conditions unlike the wild-type protein. This is in addition to the lack of conformational changes which would otherwise be observed on ligand binding in the permease (Smirnova & Kaback, 2003). The structure illustrated the nature of distorted trans-membrane helices (once thought to be rigid) and the water filled internal cavity (Abramson *et al.*, 2003b). In addition to the mutant LacY structure, a wild-type structure of LacY has also been determined and is in agreement with the mutant protein crystallised previously (Guan *et al.*, 2007). This crystal structure was achieved after phospholipid composition was altered in the purified protein samples, an inward facing conformation was shown in this study, it is likely that this is the stable state of LacY that is crystallised showing the lowest free energy state of the protein (Guan *et al.*, 2007). The structure of the MFS protein GlpT (discussed, *vide infra*) was also solved (to 3.3 Å resolution) which illustrated the structural homology shared between these MFS proteins (Huang *et al.*, 2003). The substrate-binding site of LacY is located at the centre of the hydrophobic pore of the membrane envelope and is accessible to either side of the membrane (Abramson *et al.*, 2003b; Kaback, 2005), all of the amino acids which are involved in binding the substrate are arranged at the same level parallel to the membrane (Guan & Kaback, 2006). The dimensions of the crystal structure were calculated. With a known membrane thickness of 27 Å (Wolin & Kaback, 2001; Guan *et al.*, 2002), the heart shaped permease was estimated to be 30 Å by 60 Å and 60 Å deep when the cavity (25 Å by 15 Å) was open to the cytoplasmic side, this is detailed in Figure 1.6 (Abramson *et al.*, 2003b). Further work by Zhou *et al.* (2008) concluded that the maximum possible cavity size during translocation is approximately 17 Å as a result of cross-linking experiments.

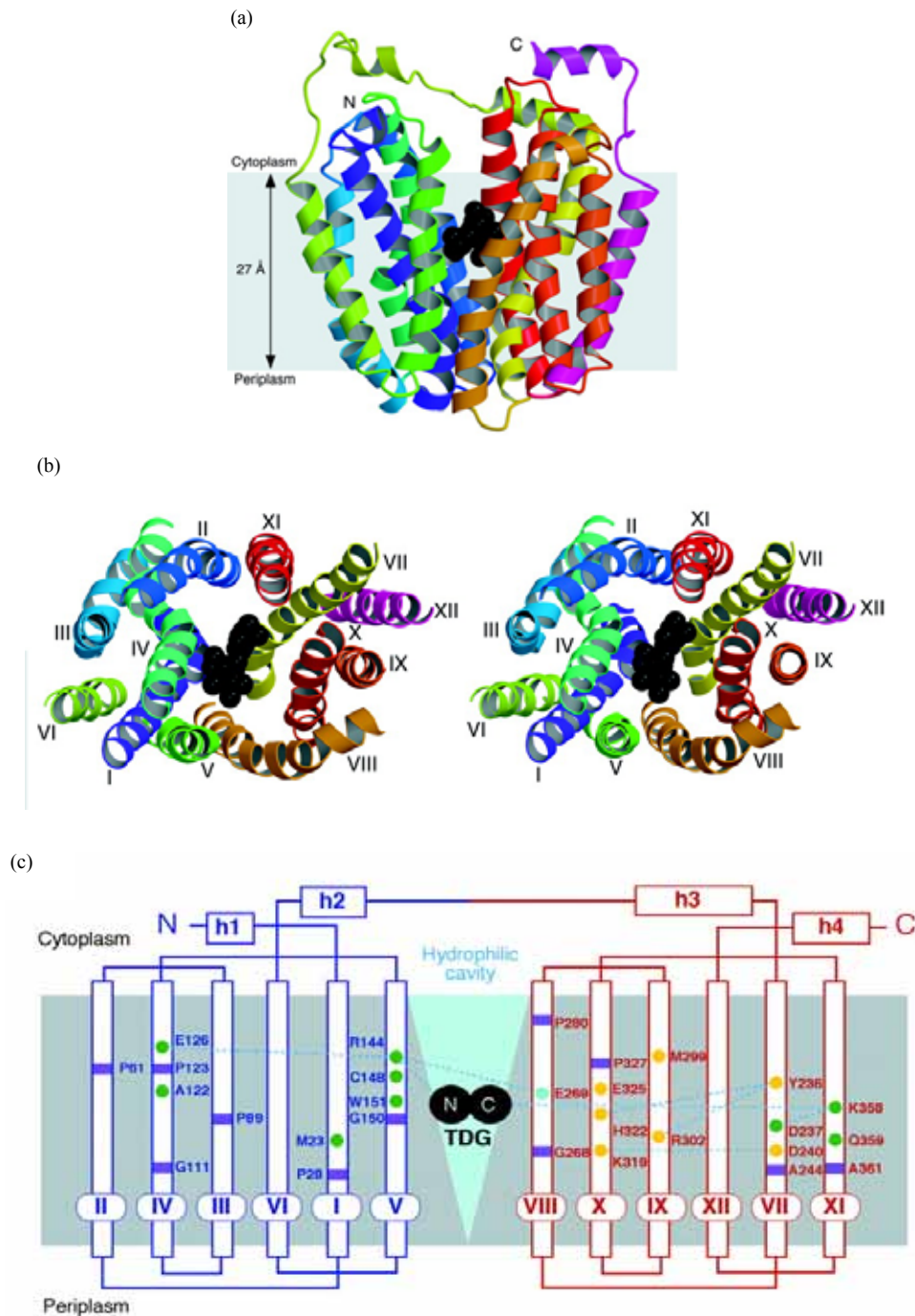


Figure 1.6 Structural representation of LacY based on the C154G mutant with bound substrate β -D-galactopyranosyl-1-thio- β -D-galactopyranoside (TDG) a high affinity homologue of lactose. (a) Ribbon demonstration of the mutant permease parallel to the membrane with substrate represented by black spheres. The illustration shows the 12 trans-membrane helices in pink (C-terminus) and purple (N-terminus). (b) Protein structure as in (a) in stereo along the membrane from the cytoplasmic side (loop regions omitted). (c) Secondary structure of LacY with N (blue) and C (red) terminals, specific residues are highlighted by function: green and yellow circles are involved in substrate binding and proton translocation in particular E209 is shown as a blue circle as it is involved in both functions. Purple rectangles represent points where the trans-membrane is disjointed forming kinks in the domain. The pale blue region represents the hydrophilic cavity where the TDG molecule is stationary in its transit. Finally, trans-membrane domains are numbered in (b) and (c) by Roman numerals and in (c) external loop regions are labelled h1-h4. Figure and legend adapted from Abramson *et al* (2003b).

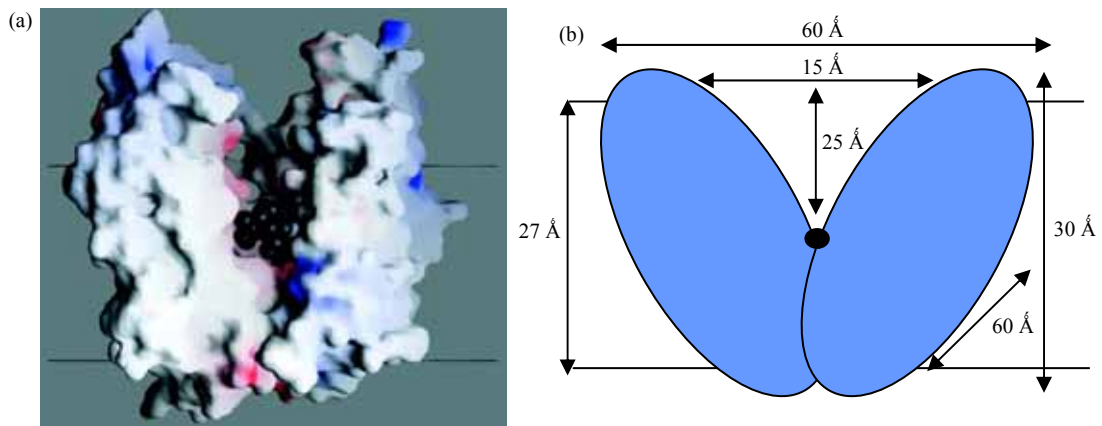


Figure 1.7 The internal hydrophilic cavity of LacY (a) LacY view parallel to the membrane (helices V and VII have been removed). Polar surfaces are coloured blue (positively charged) and red (negatively charged). The black spheres represent the bound TDG substrate. Adapted from Abramson *et al* (2003b) (b) Simplified model of LacY showing calculated dimensions (Abramson *et al.*, 2003b), it should be noted that the maximum cavity opening has now been estimated to be 17 Å (Zhou *et al.*, 2008).

Recent computer based modelling has facilitated in predicting the 3D structure of membrane proteins. While these provide an insight into the potential functionality of these proteins they should be treated with caution and cannot substitute for a biochemical approach. Although there are distinct homologies between these MFS proteins, where there are commonalities a programming approach would make definite assumptions whereas a protocol of mutagenesis may prove this otherwise, this has been shown in NrtA of *A. nidulans* (S.E. Unkles personal communication). Modelling, in NrtA has been of great benefit in highlighting potential mutagenesis regions, highlighting regions which can be tested in the laboratory as reinforcement for the model *in silico*. This will be discussed in Chapters Three and Four.

1.7.2 LacY mutagenesis

To understand the mechanism of a transporter, essential side-chains and their interactions must be determined (Zhang *et al.*, 2002). In LacY, six side-chains have been identified as critical for substrate translocation and energy transduction as a result of these mutagenesis studies – E126, R144 (substrate binding), E269, R302, H322 and E325 (proton coupling) (Frillingos *et al.*, 1998; Kaback & Wu, 1999). Crucial residues for substrate binding R144 and E269 are found close together within the trans-membrane region but not on the same domain (Frillingos *et al.*, 1998; Kaback & Wu, 1999). Specifically, R144 forms a tooth-like hydrogen bond with two oxygen atoms in the galactopyranosyl ring (O3 and O4) (Mirza *et al.*, 2006). It is thought that E269 may interact with oxygen 4, 5 or 6 of this ring via water molecules in the internal cavity of LacY (Frillingos *et al.*, 1997; Sahin-Toth *et al.*, 1999;

Kaback, 2005). Also, interactions between E269 in the C terminal domain and R144 and W151 may provide the energetic link between the N and C terminal bundles (Kaback, 1976; Kaback, 2005). Substrate recognition by W151, R144 and E126 and hydrogen bonding of R144 and W151 to E269 completes the binding site (Kaback *et al.*, 2001; Vazquez-Ibar *et al.*, 2004; Kaback, 2005). Substrate interaction is shown in Figure 1.8.

LacY is thought to be unstable in the outward facing conformation and is immediately protonated to induce substrate binding. Biochemical analysis has revealed three residues essential for proton coupling and translocation, R302 (Tm 9), H322 (Tm 10) and E325 (Tm 10) (Roepe *et al.*, 1989; Kaback *et al.*, 2001). Mutants lacking these residues have shown no ability to catalyse active transport (Frillingos *et al.*, 1998). Instant protonation occurs on E269 or is shared between E269 and H322 (Kaback *et al.*, 2001). After the substrate is recognised the proton is induced to transfer to H322 and subsequently E325 - which was previously charge paired to R302 - from where the proton is released (Kaback, 2005).

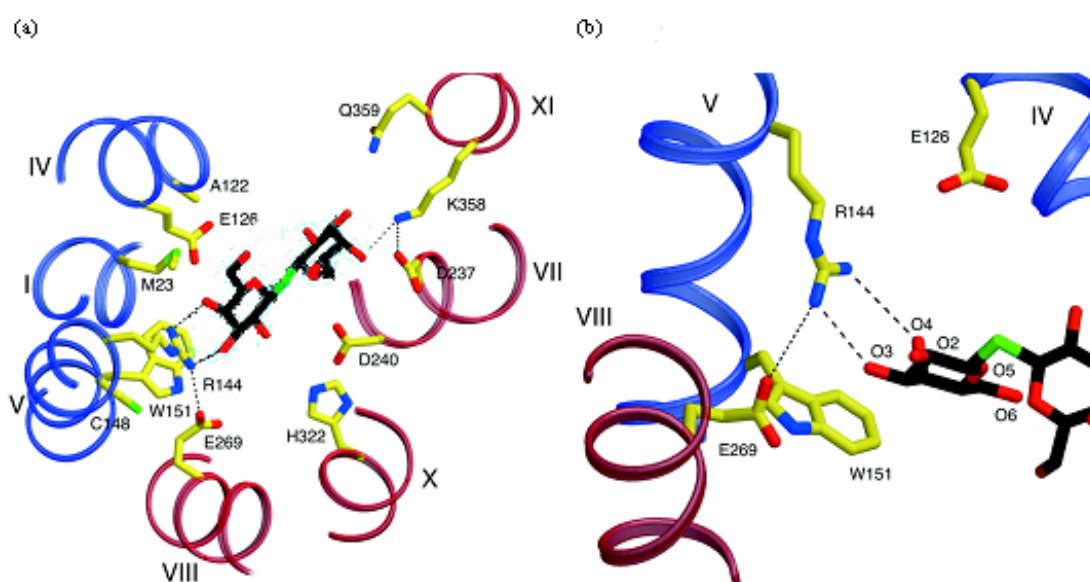


Figure 1.8 The substrate binding site of LacY. Possible hydrogen bonds and salt-bridges are represented by black dashed lines. (a) Residues involved in binding TDG viewed along the membrane from the cytoplasmic side. (b) Close up of the binding site in the N-terminal domain. Figure modified from Kaback (2005).

In LacY, the binding of protons and substrate induces conformational change (Kaback *et al.*, 2001) and salt-bridge formation between E269 and R144 (DeFelice, 2004). These conformational changes require a high degree of flexibility from the protein. Cysteine scanning mutagenesis (CSM) has been used to study complex side-chain interactions of substrate binding, translocation, and energy transduction (Frillingos *et al.*, 1998). These experiments have helped to determine the flexibility of the permease and quantitatively measure these conformational changes (Frillingos *et al.*, 1998; Abramson *et al.*, 2003a).

1.8 GlpT

The glycerol-3-phosphate (G3P) antiporter of *E. coli* is another member of the MFS, and is highly comparable to LacY (Abramson *et al.*, 2004). Abramson *et al.* (2004) published a structural comparison of LacY and GlpT, this illustrates the homologies discussed and also illustrates the extrapolations permitted between these crystal structures and other members of the MFS (Figure 1.9). As with LacY, GlpT is an inner membrane MFS transporter of *E. coli*. It is an organic/inorganic phosphate antiporter which is driven by the phosphate (Pi) gradient (Huang *et al.*, 2003). The structure of GlpT was solved to 3.3 Å resolution by X-ray crystallography (Huang *et al.*, 2003; Lemieux *et al.*, 2003) and was described as a “Mayan Temple,” with a flat top and bottom (Huang *et al.*, 2003). Like other MFS members, GlpT exhibits the pseudo 2-fold symmetry between N and C halves of the permease and was purified as a monomer (Huang *et al.*, 2003). It was suggested that GlpT functions as a monomer on the basis that the pure protein was monomeric in detergent solution (Auer *et al.*, 2001). The two halves of GlpT are connected by a long cytoplasmic loop and there are no salt-bridges and few H-bonds between domains (Huang *et al.*, 2003). However, there were many Van der Waals interactions on the periplasmic side. At the interface of the N and C terminal there are bulky side-chains that fit into ‘pockets’ on the C terminal side (Lemieux *et al.*, 2004). As with LacY, GlpT was studied in the inward facing conformation with its central pore at the interface between the N and C termini (Huang *et al.*, 2003). GlpT operates a single site alternating access mechanism which is activated in the presence of G3P (Lemieux *et al.*, 2004). It was proposed that substrate binding lowers the energy barrier allowing Pi to drive G3P transport (Huang *et al.*, 2003). Little is known regarding the substrate binding site of GlpT as the structure was solved in the absence of substrate. Though it was suggested the arginine residues in helices 1 and 7 (R45 and R269) interact directly with the phosphate molecule (Huang *et al.*, 2003; Law *et al.*, 2008).

1.9 OxIT

OxIT is an MFS protein from the anaerobic bacterium *Oxalobacter formigenes*, which is responsible for oxalate/formate exchange in the inner membrane (Heymann *et al.*, 2003). Similar to LacY and GlpT, OxIT is formed of 12 Tm α -helices in a pseudo-2-fold axis of symmetry, where 8 of the 12 helices form a central cavity for the transport of its substrate (Heymann *et al.*, 2003). Oxalate (the sole energy source for this bacterium) is removed from the periplasm by OxIT and is decarboxylated when it enters the cell (Heymann *et al.*, 2003). The bi-product of this reaction is formate which is removed from the cytoplasm by OxIT and deposited into the periplasm (Heymann *et al.*, 2003). The mechanism used by OxIT is the ‘rocker switch’, (as in Figure 1.4), which was expanded upon to explain the rocker switch as regards uniport, symport and antiport in an article by Hirai & Subramaniam (2004). Unlike

LacY and GlpT, crystal structures show this permease in the closed conformation (Heymann *et al.*, 2001; Heymann *et al.*, 2003). It was postulated that two charged residues interacted with the substrate in the internal cavity as in GlpT and NrtA (discussed later) (Heymann *et al.*, 2003). This was proven by Wang *et al* (2006), where the involvement of R272 (Tm 8) and K355 (Tm 11) in ligand binding was shown. Mutagenesis revealed that charged residues at this position are essential and it is also likely that the side-chain architecture is also critical as a result of the reduced activity of mutants R272K and K355R (Wang *et al.*, 2006).

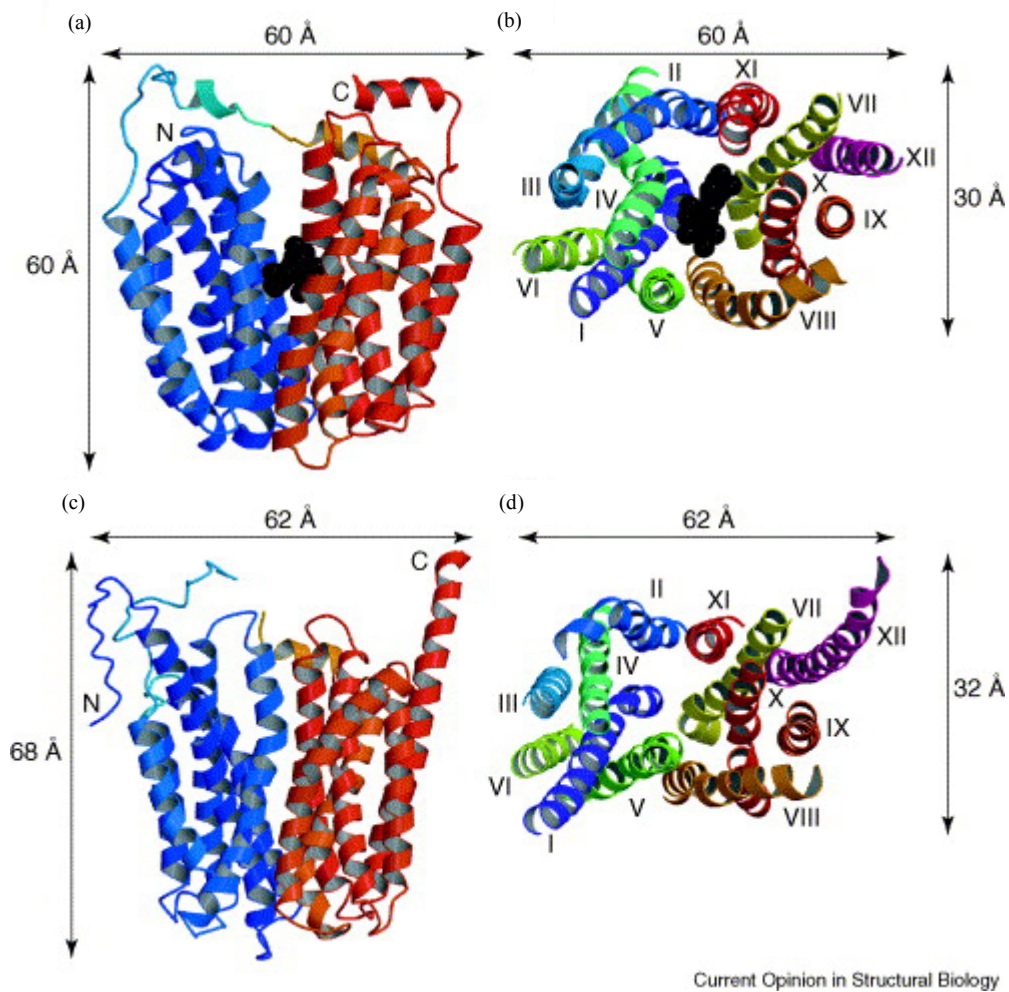


Figure 1.9 Structural comparisons of LacY and GlpT. (a) Ribbon demonstration of the mutant LacY permease parallel to the membrane with substrate represented by black spheres. The illustration shows the 12 trans-membrane helices in red (C-terminus) and blue (N-terminus). (b) Ribbon representation of LacY viewed from the cytoplasmic side. Each trans-membrane helix is a different colour; N-terminal is purple and the C-terminal pink. (c) Ribbon demonstration of GlpT. The colour scheme is as in (a). (d) Ribbon representation of GlpT viewed from the cytoplasmic side, colour scheme is as in (b) Figure taken from Abramson *et al* (2004).

1.10 Formate nitrite transporters (FNT)

A critical part of the work of this thesis involves the FNT family of proteins which are very different from proteins discussed here from the MFS and ABC families. The characteristics of members of this family will be discussed in Chapter Seven.

1.11 *A. nidulans*: A model experimental organism

Fungi have a long recorded history with man in both their beneficial and detrimental facets. They have been used in the production of food stuffs and antibiotics; but are also noted for their production of toxic metabolites (Timberlake & Marshall, 1989). The genus *Aspergillus* fits both these categories. *A. fumigatus* is the causative agent for the pulmonary condition Aspergillosis. Several other *Aspergilli* also cause disease particularly in immunocompromised patients (Lewis *et al.*, 1994). In Asia, *Aspergillus* has been used for centuries in the 'koji' stage of food fermentation in products such as saki, miso and soy sauce. Together with *Schizosaccharomyces pombe*, *S. cerevisiae* and *Neurospora crassa*, *A. nidulans* was one of the early eukaryotic model species (Samson, 1994). Indeed the first regulatory gene identified in eukaryotes - *nirA* - was identified in *Aspergillus* (Pateman *et al.*, 1964). The ease of handling, simple growth requirements and rapid life cycle of *A. nidulans* has made it an important eukaryotic model system. *A. nidulans* (also known as *Emericella nidulans*) is a common saprophyte found in soil, and decaying vegetation (Kozakiewicz & Smith, 1994). Its genome was recently sequenced by the Broad Institute (http://www.broad.mit.edu/annotation/fungi/aspergillus_nidulans/) and spans 31 Mb over 8 chromosomes.

The ability to grow on simple defined growth media has made *A. nidulans* an ideal candidate for biochemical and genetic analyses and is commonly used as the alternative to *N. crassa* (Casselton & Zolan, 2002). The *A. nidulans* life cycle is shown in Figure 1.10 (Casselton & Zolan, 2002). When using *A. nidulans* in the laboratory it is the haploid which is used for subculturing and mutagenesis, as the diploid is only a transitory phase (Martinelli, 1994). The asexual cycle of *A. nidulans* follows the mature hyphae with several nuclei which produces uninuclear haploid spores known as conidia or conidiospores (shown in orange in Figure 1.10) (Casselton & Zolan, 2002). The process of conidiation takes between 3 and 8 hours to germination at 37 °C; the entire asexual cycle taking around 48 hours (Martinelli, 1994). These conidiospores in the asexual cycle form haploid homokaryons which fuse with another homokaryon to produce a heterokaryon with different nuclei; it is this stage that allows for the exchange of genetic material during mitosis (Martinelli, 1994). This heterokaryon is unstable though can be maintained. The parasexual cycle employs mitosis from the fusion of haploid nuclei and further division by mitosis (Martinelli, 1994). From the mature colony there is

nuclear exchange and the formation of heterokaryons to form diploid nuclei, this diploid goes on to form conidiophores and thus conidia. During mitosis, crossing over events allow the exchange of genetic material and loss of chromosomes resulting in haploidisation (Martinelli, 1994). The sexual cycle in *A. nidulans* has been used extensively in genetic mapping and classical genetic analyses. In this pathway after 2-3 days cleistothecial (fruiting body) initials form, before the development of the mature cleistothecium which then produces the sexual spores, a pair of nuclei divide by meiosis to form a mass of cells, the ascogoneous hyphae. These hyphae branch at the tips to become a diploid ascus where two haploid nuclei fuse. Meiosis of this haploid nuclei results in the formation of eight haploid ascospores. The cleistothecium may hold tens of thousands of ascospores which are released (Casselton & Zolan, 2002).

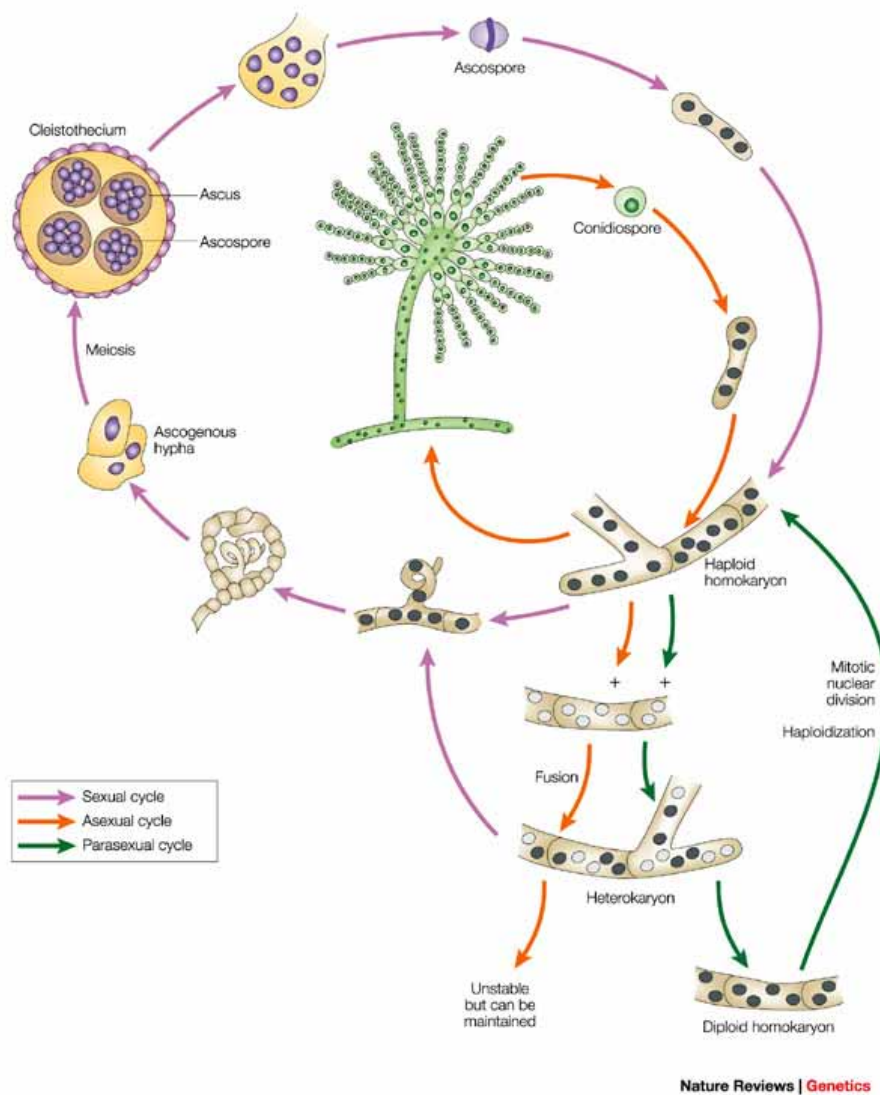


Figure 1.10 The life cycle of *A. nidulans*. Diagram taken from Casselton and Zolan (2002).

The 1980s brought about genetic engineering procedures for filamentous fungi, and due to its well characterised history in classical genetics, in studies of physiology and biochemistry *A. nidulans* (inter alia *N. crassa* and *S. cerevisiae*) came into its own as a model organism for eukaryotic genetic engineering (Galagan *et al.*, 2005). Specifically, *Aspergillus* has been exploited for its metabolic capabilities in the production of organic acids and enzymes (Galagan *et al.*, 2005). The production of heterologous proteins in the filamentous fungi and specifically *A. nidulans* have also been discussed extensively (Kinghorn & Unkles, 1994) and reviewed by Punt *et al* (2002).

Methods for the transformation of filamentous fungi have been an area of substantial research and many protocols have been devised and reviewed thereafter (Fincham, 1989; Kinghorn & Unkles, 1994; Ruiz-Diez, 2002). Genetic transformation systems allow the manipulation and incorporation of the genome and consequently the study of biological systems *in vivo*. Transformation methods for *A. nidulans* were devised by Balance *et al* (1983), Tilburn *et al* (1983), Yelton *et al* (1984) and Peberdy (1989). These approaches employed cell wall-degrading enzymes (a cocktail of chitinase and glucanases from the fungus *Trichoderma viridae* (Riach & Kinghorn, 1996)) to prepare protoplasts from fungal cells followed by transformation in the presence of polyethylene glycol and calcium chloride. This approach remains one of the most common methods for fungal transformation (Ruiz-Diez, 2002).

1.12 Nitrogen

Nitrate assimilation has been a subject of great public and scientific interest in recent years. Reviewed by Crawford & Glass (1998), Daniel-Vedele *et al* (1998) and Miller *et al* (2007). The Haber-Bosch process (the synthesis of ammonia from its elements) has been hailed as the most important invention of the 20th century (Smil, 1999). The issue of nitrogen pollution, often resulting from agricultural run-off, has recently been raised publicly via the Global Nitrogen Enrichment (GANE) programme funded principally by NERC. In an article in Nature (Giles, 2005), John Lawton, Chief Executive of NERC, proposed that nitrogen pollution is the 3rd major threat to the planet to date after climate change and loss of global biodiversity. It is this public awareness that helps to forward research into environmental nitrogen dynamics. Further reviews of nitrogen and its impact on the environment have been published by Galloway *et al* (2008) and Duce *et al* (2008).

1.12.1 Nitrogen and nitrogenous compounds in the environment

Production and use of nitrates has increased exponentially since the industrial revolution. To support a growing global population, agriculture has embraced artificial fertilisers. The population of the world has increased by 78 % since 1970, while production of reactive

nitrogen has increased by 120 % (Galloway *et al.*, 2008). However, the use of nitrogen is not evenly distributed, in some parts of the world nitrogen is used in excess to produce unused crops and contributes to a variety of environmental and health issues (Duce *et al.*, 2008; Galloway *et al.*, 2008). While in other parts of the world the lack of nitrogen fertiliser contributes to the lack of food to meet the basic nutritional requirements (Galloway *et al.*, 2008). Nitrogen is one of the most transitory of inorganic nutrients and is often the limiting factor in the growth of crop plants (Crawford & Glass, 1998; Daniel-Vedele *et al.*, 1998). The source of nitrogen is entirely species dependant though the 'preferred' sources tend to be ammonium and nitrate (Crawford & Glass, 1998). Soil nitrate availability has been shown to vary by up to five orders of magnitude in some environments (Crawford, 1995; Glass *et al.*, 2002). This variability can be seasonal and as a result of both biotic and abiotic factors (Crawford & Glass, 1998). To improve crop yield, nitrate fertilisers are supplied to land, in addition, nitrifying bacteria present in soils function to convert ammonia to nitrite and nitrate, these factors contribute to an excess of nitrate on farmland which is easily leached by rain water. This nitrate can enter the environment in several ways with sometimes devastating consequences. Environmental costs include eutrophication (algal blooms as a result of increased nutrient availability, which, if left untreated can reduce the dissolved oxygen resulting in suffocation of the ecosystem), acid rain, and shellfish poisoning. Health issues have also been well documented (Tsezou *et al.*, 1996; Vermeer & van Mannen, 2001). Nitrate itself is non-toxic but nitrous oxides that may be formed in the human gut can contribute to the formation of tumours and blue-baby syndrome (methyglobinaemia) (Tsezou *et al.*, 1996; Vermeer & van Mannen, 2001). These facts explain the growing public and scientific interest in the field. If there is a better understanding of how nitrate is assimilated by plants, algae, bacteria and fungi it is expected that problems occurring as a result of nitrate pollution may be prevented. Previous work on nitrate assimilation has focussed primarily on the functional genes and enzymes involved in the assimilation pathway, and have mainly neglected the mechanism of transport. Figure 1.11 shows the biochemical pathway of nitrate assimilation and the genes involved.

1.12.2 Nitrate assimilation

When nitrate is present in the extra-cellular environment, genes involved in nitrate assimilation in *A. nidulans* are expressed (Daniel-Vedele *et al.*, 1998). Generally, specific nitrate permeases transport nitrate into the cell. It is then either stored in vacuoles or reduced to nitrite and thence to ammonium by nitrate reductase and nitrite reductase enzymes respectively (Crawford & Glass, 1998). It is generally considered that fungal cells cannot store nitrate, it is only plants which store the nutrient in vacuoles (Unkles *et al.*, 2004b). Under anaerobic conditions nitrite can enter this pathway directly. In *A. nidulans*, nitrate may

be transported into the cell by nitrite permease NitA, or the nitrate permeases NrtA and NrtB, which are capable of transporting both nitrate and nitrite (Wang *et al.*, 2008). It is then directly reduced to ammonium by nitrite reductase and assimilated into organic nitrogenous compounds within the cell.

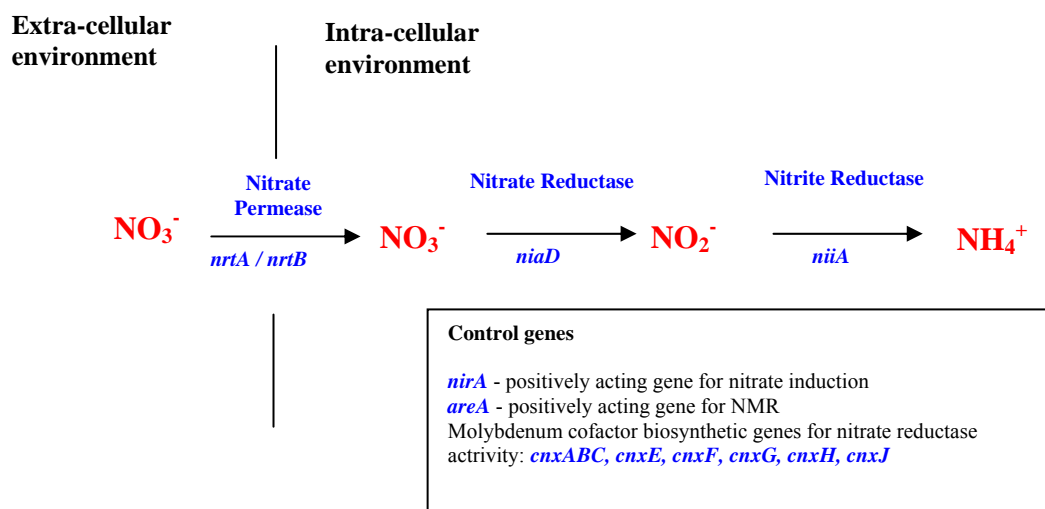


Figure 1.11 The Nitrate assimilation pathway for *A. nidulans*. Genes involved in this pathway are shown in blue and the nitrogen components are shown in red. For the transport of nitrate into the cell there are two nitrate permeases (NrtA and NrtB). Once inside the cell, nitrate is reduced to ammonium for use in various biosynthetic metabolite pathways. Diagram adapted from Kinghorn (1989).

1.12.3 Nitrogen metabolite repression

In *A. nidulans* the global control of nitrogen utilisation is known as nitrogen metabolite repression (NMR), in *S. cerevisiae* is known as nitrogen catabolite repression (NCR); NMR co-ordinates the enzymatic response to the nitrogen status of the cell (Wong *et al.*, 2008). GATA transcription factors are known to regulate nitrogen gene expression in all fungi though only those employed by *A. nidulans* are discussed here. Transcription factors AreA and NirA are required for the induction of nitrate assimilation genes (Kudla *et al.*, 1990; Burger *et al.*, 1991). At the protein level AreA and NirA are known to co-operate in the regulated expression of nitrate assimilation genes (Wong *et al.*, 2008). It is thought that AreA aids in the positioning of NirA to the bidirectional promoter of *niiA-niaD* when induced by nitrate (Wong *et al.*, 2008). NirA is known to accumulate in the nucleus upon nitrate induction and is exported from the nucleus to fulfil its function by binding to the *niiA-niaD* bidirectional promoter which has four NirA and ten AreA binding sites (Punt *et al.*, 1995; Strauss *et al.*, 1998; Muro-Pastor *et al.*, 1999; Bernreiter *et al.*, 2007). Upon binding of these transcription factors, the promoter undergoes various rearrangements of which AreA plays an important role (Bernreiter *et al.*, 2007).

AreA binds to the promoters of nitrate responsive genes via a single GATA zinc finger (Margelis *et al.*, 2001). Cellular levels of AreA are monitored through *areA* mRNA transcriptional alterations and transcript stability in addition negative regulation by NmrA which is thought to interact with the DNA binding domain at the C-terminus of AreA (Wong *et al.*, 2008).

Other genes involved in nitrate assimilation are the *cnx* family. Mutants originally isolated as defective in the synthesis of the molybdenum cofactor - which is essential for nitrate reductase and xanthine dehydrogenase activity - were selected on the basis of resistance to chlorate toxicity and were unable to utilise nitrate or purines as their sole nitrogen source (Unkles *et al.*, 1997). It was hypothesised that *cnx* mutants must be defective in the synthesis of a cofactor common to both nitrate reductase and xanthine dehydrogenase, hence their name *cnx* – common component for nitrate reductase and xanthine dehydrogenase. Initially, five un-linked *cnx* loci were identified *cnxABC*, *cnxE*, *cnxF*, *cnxG*, *cnxH* (Pateman *et al.*, 1964). However a further *cnx* gene was identified by Arst *et al* (1982), (*cnxJ*). It should be noted that *cnxJ* carries a different phenotype from the remaining loci (Arst *et al.*, 1982).

1.12.4 Nitrate transport systems

Nrt1 and Nrt2 are unrelated nitrate transport systems (Trueman *et al.*, 1996) which specifically classify low and high-affinity permeases respectively (Crawford & Glass, 1998; Orsel *et al.*, 2002). Constitutively expressed low-affinity transport systems (LATS) have linear kinetics that are not saturable at 50 mM nitrate, and only acquire nitrate at concentrations above 1 mM (Siddiqi *et al.*, 1989; Crawford, 1995), while high-affinity transport systems (HATS) acquire nitrate from low extra-cellular nitrate concentrations, typically less than 1 mM (Crawford, 1995). The HATS are further subdivided into inducible and constitutive subclasses (respectively iHATS and cHATS) (Crawford & Glass, 1998). The inducibility of the HATS is unique among mineral transporters, as others are de-repressed following a deficiency in their substrate (Clarkson & Luttge, 1991). Plants use these two mechanisms, which allow the acquisition of nitrogen in both organic and inorganic forms, and in environmental concentrations varying from 10 μ M to 100 mM (Crawford, 1995; Tischner, 2000; Miller & Cramer, 2005). Another dimension can be applied to proteins of the Nrt2 family, i.e. whether they function as one or two component systems (Galvan *et al.*, 1996; Zhou *et al.*, 2000a; Tong *et al.*, 2005; Okamoto *et al.*, 2006; Orsel *et al.*, 2006). In two component systems, proteins require an additional protein for efficient functioning e.g. Nar2 (Rexach *et al.*, 2002; Tong *et al.*, 2005; Okamoto *et al.*, 2006; Orsel *et al.*, 2006).

1.12.5 Plant, yeast and protist systems

In plants, the number and specific affinities of nitrate transport systems are variable. *A. thaliana* has several transporters belonging to the NNP. AtNrt1.1 (Chl1) is frequently studied, and is a dual affinity permease functioning in the range of HATS (K_m 50 μM) and the LATS (K_m \sim 4 μM) (Liu *et al.*, 1999; Guo *et al.*, 2002). In *Hordeum vulgare* (Barley), kinetics of the cHATS were measured as K_m 6-20 μM and V_{max} 0.3-0.82 $\mu\text{mol g}^{-1} \text{h}^{-1}$ and iHATS of K_m 20-100 μM and V_{max} 3-8 $\mu\text{mol g}^{-1} \text{h}^{-1}$ (Crawford & Glass, 1998). Few yeasts are known to assimilate nitrate; the model organisms *S. cerevisiae* and *Schizosaccharomyces pombe*, cannot use nitrate or nitrite as a sole nitrogen source since they cannot synthesise the molybdopterin cofactor required for nitrate reductase activity (Barnett *et al.*, 1990; Siverio, 2002). Nitrate transport in the yeast *Hansenula polymorpha* (a.k.a. *Pichia angusta* (Kurtzman, 1984)) is catalysed solely by the high affinity nitrate permease YNT1 (K_m 2-3 μM) (Perez *et al.*, 1997; Machin *et al.*, 2001; Machin *et al.*, 2004). YNT1 is a homologue of the plant and fungal nitrate permeases from the NNP (Forde, 2000; Siverio, 2002). As in *A. nidulans*, genes required for nitrate assimilation in addition to *ynt1* are clustered together in the genome and include regulatory transcription factors along with nitrate reductase and nitrite reductase enzymes (Siverio, 2002). It is thought that the clustering of genes for the nitrate assimilation process is a way for the organism to improve the efficiency of the process as clustering of genes from this pathway is observed in *H. polymorpha* (Perez *et al.*, 1997), *A. nidulans* (Zhuo *et al.*, 1999), *A. thaliana* (Zhuo *et al.*, 1999) and *C. reinhardtii* (Galvan & Fernandez, 2001), though the nitrate assimilation genes in *N. crassa* are not clustered (Okamoto & Marzluf, 1993). Similar to NrtA and NrtB, YNT1 can also transport nitrite to high affinity (Perez *et al.*, 1997). Further, a second system for nitrite transport has been identified in *H. polymorpha* (Machin *et al.*, 2001) and it was suggested that multiple nitrate uptake systems exist in this yeast (Machin *et al.*, 2004) though currently YNT1 is the only characterised.

The protist *C. reinhardtii* has thirteen putative nitrate/nitrite transport genes, of which six are related to Nrt2 and one Nrt1 on the sole basis of sequence homology, (Fernandez & Galvan, 2007). Nitrate permeases in plants are differentially expressed depending upon nutrient availability (Galvan *et al.*, 1996; Rexach *et al.*, 1999). In *Chlamydomonas* there are four systems for high affinity nitrate/nitrite uptake; I is a bispecific $\text{NO}_2^-/\text{NO}_3^-$ permease (CrNrt2.1) which requires Nar2 (Zhou *et al.*, 2000a; Fernandez & Galvan, 2007); II is a nitrate specific permease (CrNrt2.2), again requiring Nar2 (Galvan *et al.*, 1996; Zhou *et al.*, 2000a); III is thought to be a high affinity nitrite/low affinity nitrate transporter (Nrt2.3) (Quesada *et al.*, 1998; Rexach *et al.*, 1999) and finally system IV is a bispecific $\text{NO}_2^-/\text{NO}_3^-$

permease (Rexach *et al.*, 1999; Navarro *et al.*, 2000). Systems I-III are inducible and IV is constitutively expressed and differential expression of these systems is induced in response ammonia, carbon dioxide and chloride (Fernandez & Galvan, 2007). The remaining six transport systems in *C. reinhardtii* belong to the Nar1 family of the FNT (Peakman *et al.*, 1990; Suppmann & Sawers, 1994; Rexach *et al.*, 2000; Fernandez & Galvan, 2007) which will be discussed further in Chapter Seven.

1.12.6 Nitrate transport in A. nidulans: Background

Brownlee and Arst (1983) established the early kinetic data for nitrate transport in *A. nidulans*. Previous to their work, it had been found that strains which were deficient in the *crnA* (also known as *nrtA*) gene were resistant to the toxic nitrate analogues, chlorate and bromate (Tomsett & Cove, 1979). Additionally, the regulation of *crnA* was shown to be by the transcription factors *nirA* and *areA* (Arst & Cove, 1973; Cove, 1979; Tollervey & Arst, 1981). Brownlee and Arst (1983) as well as Tomsett and Cove (1979) showed that nitrate uptake was a “separate and distinct” process from intra-cellular nitrate reduction; they also noted the presence of another system for nitrate uptake (Brownlee & Arst, 1983). Subsequently, genes encoding two nitrate transporters designated *nrtA* and *nrtB* were cloned from *A. nidulans* (Unkles *et al.*, 1991; Unkles *et al.*, 2001). NrtA was reported as a 12 Tm protein independent from membrane proteins known previously at this time. Also, the transcription regulation of *nrtA* by *nirA* and *areA* were confirmed by Northern blot analyses (Unkles *et al.*, 1991; Unkles *et al.*, 1995). Kinetic data shall be discussed for these nitrate permeases in *A. nidulans* also in reference to nitrate uptake in other systems.

1.12.7 NrtA vs. NrtB

NrtA and NrtB are of comparable size (507 amino acids/57 kDa, and 497 amino acids/54 kDa respectively) and are structurally similar to the MFS permeases discussed earlier (Unkles *et al.*, 2001). The genes *nrtA* and *nrtB* appear to be the only genes which encode nitrate transporters in *A. nidulans* (both Nrt2 type). By comparison, *A. thaliana* has no less than eleven nitrate permeases of both Nrt1 and Nrt2 types (Unkles *et al.*, 2001). So, does functional redundancy exist in these permeases? The *nrtA* and *nrtB* genes are clearly paralogous based on their high sequence identity of 59.8 % and similarity of 73.2 % (Figure 1.12) and their regulation is identical (Refer to *Section 1.12.9* for definitions of homologous, orthologous and paralogous in reference to genes/proteins in this thesis). Knock-out of each gene also has no detectable phenotype on concentrations of nitrate from 1-10 mM (Unkles *et al.*, 2001). However, these proteins have different K_m and V_{max} for nitrate as determined using the nitrate tracer $^{13}\text{NO}_3^-$ (Unkles *et al.*, 2001). The rationale for the presence of two Nrt paralogues was that NrtA functions more efficiently at high nitrate concentrations and NrtB at

reduced nitrate concentrations. Thus, due to the variability of nitrate in the environment, loss of either NrtA or NrtB would be a disadvantage (Unkles *et al.*, 2001). Functional differences in NrtA and NrtB may also extend to their preferences for nitrite and nitrate. NrtA, NrtB and NitA (the nitrite specific protein in *A. nidulans*) each have different affinities and capacities for nitrite as shown from net nitrite studies (Wang *et al.*, 2008) (discussed in Chapter Seven).

```

NrtA      ---MDFAKLLVASPEVNPNNR KALTI PVLNPFNTYGRVFFF SWFGFMLAFLSWYAFPPLL
NrtB      MKPTQVLR LAVAAPDVNPQTRKARSIPVLNPF DLYGRVFFF SWIGFLVAFLSWYAFPPLL
          :. : *  ** : * : *** : . *** : ***** : ***** : * : *****
NrtA      TVTIRDDLMSQTQIANSNI IALLATLLVRLICGPLCDRFGPRLVFVIGLLL VGS IPTAMA
NrtB      SVTIKKDLHMSQDDVANSNI VALLGTFVMRFIAGPLCDRFGPRLV FVGLLICGAVPTAMA
          : *** : . ** : * * * : : ***** : * * * : * : : * : * . ***** : * * * : * : * * * *
NrtA      GLVTSPQGLIALRFFIGILGGTFVPCQVWCTGFFDKSIVGTANSLAAGLGNAGGGITYFV
NrtB      GLVTTPOGLIALRFFVIGILGATFVPCQVWCTGFFDKNIVGTANSLAGGFGNAGGCITYFV
          * * * : * * * * * * * : * * * . * * * * * * * * * * * . * * * * * * * * * * *
NrtA      MPAIFDSLIRDQGLPAHKAWRVAYIVPFILIVAAALGMLFTCDDTPTGK WSERHIWMKED
NrtB      MPAIYDSFVHDRGLTPHKAWRVSYIVPFIIVSIALAMLFTCPDTPGKWAD-----
          * * * : * * : : * : * . * * * * * * * * * * * * * : * . * * * * * * * * * * :
NrtA      TQTASKGNIVDLSSGAQSSRPSGPPSIIAYAI PDVEKKGTTETPLEPQSQAIGQFDFRAN
NrtB      REKTSGQSI VDLSSTPNASSAN---SINISSEKKA VHPVTDSEAQVHVRAGQIESSDA
          : : * . * * * * * * * : : * . . * * : : : * * * : . .
NrtA      AVASPSRKEAFNVIFSLATMAVAVPYACSF GSELAINSILGDYDKNFPYMGQTQTGKWA
NrtB      VIEAPTIKRYSIALDPSALAVAVPYACSF GAELAINSILGAYYLLNFPLLGQTQSGRWA
          : : : * : * . : : : . : : * * * * * * * * * * * * * * * * * * * * * * * *
NrtA      AMFGFLNIVCRPAGGFLADFLYRKTNTPWAKKLLLSFLGVVMGAFMIAMGFSDPKSEATM
NrtB      SMFGLVNVVFRPMGGFIADLIYAR TNSVWAKKMWLVVLGLAMSGMAILIGFLDPHRESVM
          : * * : : * * * * * * * : * * : * * : * * * * * * * * * * * : * : * * * * * : * : *
NrtA      FGLTAGLAFFLESCNGAIFSLVPHVHPYANGIVSGMVGGFGNLCGIIIFAIIFRYSHHDYA
NrtB      FGLVVLMAFFIAASNGANFAIVPHVHPSANGIVSGIVGGMGNFGGIIFAIIFRYNGTQYH
          * * * . . : * * * : : * * * * : * * * * * * * * * * * * * * * * * * * * * * * *
NrtA      RGIWILGVISMAV FIVSVWVRPVPK SQMRE
NrtB      RSLWIIGFII LGCTLFFSWVRPVPK QNH--
          * . : * * : * * . : . : * * * * * * * * :

```

Figure 1.12 Amino acid sequence alignment of *A. nidulans* nitrate transport paralogues NrtA and NrtB. This alignment was prepared using ClustalW (Chenna *et al.*, 2003) software available from www.ebi.ac.uk. Conserved residues are shown as: * represents a conserved residue, . a conserved substitution and : a semi conserved substitution. MFS signature motifs are shown in yellow, while NNP motifs are shown in blue.

1.12.8 NrtA

A. nidulans NrtA was the first eukaryotic iHATS to be isolated and has acted as a paradigm for plant high-affinity systems as well as providing a springboard to the cloning and identification of a number of orthologous genes from a number of species (Quesada *et al.*, 1994; Trueman *et al.*, 1996; Perez *et al.*, 1997; Quesada *et al.*, 1997; Amarasinghe *et al.*, 1998; Filleur & Daniel-Vedele, 1999; Zhuo *et al.*, 1999; Fraiser *et al.*, 2000). It belongs to a large family of high-affinity nitrate carriers (Brownlee & Arst, 1983; Unkles *et al.*, 1991; Forde, 2000) and it has been shown that *nrtA* mutants isolated on the basis of resistance to chlorate, grew as wild-type on nitrate medium but had reduced uptake, this was as a result of the presence of the second nitrate permease NrtB which appears to be impermeable to chlorate (Cove, 1979; Brownlee & Arst, 1983).

Contiguous with *niiA* and *niaD*, in the gene order *nrtA-niiA-niaD*, *nrtA* is located on chromosome VIII interrupted by three introns (Tomsett & Cove, 1979; Johnstone *et al.*, 1990; Unkles *et al.*, 1991) – *nrtB* is also located on chromosome VIII. Like other NNP MFS permeases, NrtA forms an α -helical 12 Tm structure that is well conserved. Each of these 12 helices weaves through the membrane connected by trans-membrane loops, leaving both N and C termini on the cytoplasmic side of the membrane. The primary structure of NrtA is shown in Chapter Three (Figure 3.1). Note the presence of a large central loop domain absent from plants or bacteria that is critical for function in *A. nidulans* (Unkles. *S.E. Personal Communication*). The cluster of NNPs can be subdivided into three categories by structure (Figure 1.13). Type I are the smaller prokaryotic nitrate carriers, type II, fungal and yeast Nrt2 proteins are classified by their large central loops (Forde, 2000; Siverio, 2002), and finally, type III the plant proteins which do not have the large central loop of the fungi, but have an extended C (or N) terminal domain (Trueman *et al.*, 1996; Forde, 2000; Kinghorn *et al.*, 2005).

Studies of the electrophysiology of NrtA have shown that it transports two protons with every molecule of nitrate, and in the absence of substrate, it rests in the inward facing conformation (Boyd *et al.*, 2003). Electrophysiology experiments carried out by another research group also showed that nitrate, nitrite and chlorite are all transported by NrtA and that this transport is dependant upon pH, substrate availability and membrane potential (Zhou *et al.*, 2000b).

1.12.9 Evolution, signature sequences and a duplication event

In this thesis reference shall be made to homologous, orthologous and paralogous genes and proteins. Homologous refers to similarity as a result of shared ancestry. Orthologous refers to genes/proteins which share a common ancestor. While paralogue, refers to genes/proteins which are related by gene duplication within a species.

Conserved regions, named the “signature sequences” are regions which are highly conserved amongst families of proteins. These sequences tend to characterise the group as a whole, presumably playing a structural or functional role. The first of two signature sequences discussed here is the MFS signature sequence. This motif is formed between Tm 2 and 3 of MFS proteins, that is repeated in the second half of the protein between Tm 8 and 9 although this is less phylogenetically conserved (Griffith *et al.*, 1992).

The role of this motif has been studied by site-directed mutagenesis in LacY (Jessen-Marshall *et al.*, 1995; Pazdernik *et al.*, 1997; Pazdernik *et al.*, 2000) and Tet (tetracycline transporter) (Yamaguchi *et al.*, 1992). While well conserved, additional residues may be inserted in the

domain (Jessen-Marshall *et al.*, 1995). The role of the glycine residues particularly in the first position are found to be functionally important in maintaining conformational changes within this structure (Yamaguchi *et al.*, 1992; Jessen-Marshall *et al.*, 1995) or they act as stabilising agents within the helix (Wickner, 1988; Henry & Sykes, 1990). Highly conserved basic residues were thought to have no critical role in sugar transport, though have now been shown to play a part in sugar translocation (Jessen-Marshall *et al.*, 1995; Pazdernik *et al.*, 1997; Pazdernik *et al.*, 2000). In LacY and Tet the aspartic acid is essential; mutants in this site experience reduced activity (Yamaguchi *et al.*, 1992; Jessen-Marshall *et al.*, 1995; Pazdernik *et al.*, 2000). As this motif is present in transporters with diverse substrates, it is not likely that these residues are involved directly in substrate binding, but in conformational changes to allow close packing or charge pairing between molecules or the lipid head groups during translocation (Maiden *et al.*, 1987; Pazdernik *et al.*, 1997; Pao *et al.*, 1998; Pazdernik *et al.*, 2000).

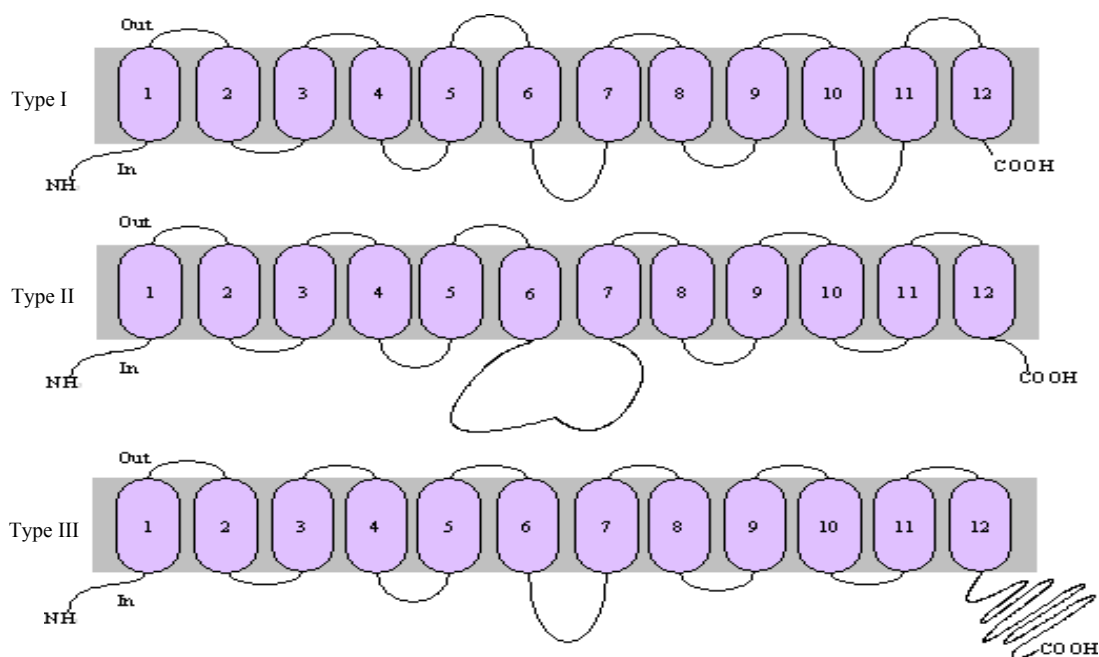


Figure 1.13 Sequence comparison and analysis revealed distinct characteristics of NNP from different organisms. This representation of NNP topology predictions is for generalised members of subfamily types I-III. Type I members are characterised by their small size by comparison to the other sub families and are found in bacteria e.g. NarK from *E. coli* (Jia & Cole, 2005). Fungal and yeast NNP members belong to the second type displaying a large central loop such as NrtA (Siverio, 2002). Type III, the plant proteins, have a comparably longer C-terminal domain such as Nrt2.1 from *A. thaliana*. Type III proteins can be further subdivided by a conserved N-terminal domain (Type IIIb). Phosphorylation recognition sequences for protein kinase C are found on some of these intracellular domains, such as the N or C terminal fragments or the large central loop of the Type II proteins, which are thought to be necessary for function. This diagram was redrawn based on work by Trueman *et al* (1996) and Forde (2000).

The repetition of the signature sequence is potentially a reflection of the evolutionary origin of the MFS. The MFS were thought to have evolved from 6 Tm domain proteins, following a duplication or fusion event where the ancestral structure doubled to form a 12 Tm (Maiden *et al.*, 1987; Pao *et al.*, 1998). This two domain theory was proven by the crystallisation of LacY, showing that the N and C terminal domains can be superimposed with an root mean square deviation of 2.2 Å for 149 Cα atoms (Abramson *et al.*, 2003a). Thus, a common domain origin exists despite seemingly low sequence homology (Henderson, 1990). The NNP subfamily of MFS contains an additional motif in Tms 5 and 11, the nitrate signature sequence (A-A-G-X-G-N-X-G-G-G) (Trueman *et al.*, 1996; Forde, 2000; Kinghorn *et al.*, 2005) (Figure 1.14). It is notable that this motif is also conserved in other transport proteins outside the MFS such as nitrite permease NitA (refer to Chapter Seven).

NNP Motif	A-A-G-X-G-N-X-G-G-G
NNP I	A-A-G-L-G-N-A-G-G-G
NNP II	V-G-G-F-G-N-L-G-G-I

Figure 1.14 Comparison of the nitrate signature sequences in NrtA from MFS subfamily NNP. Residues highlighted in yellow show conservation with the signature sequence which is conserved throughout the NNP family. NrtA harbours two nitrate signature sequences, NNP I and NNP II, one in each half of the protein.

1.12.10 NrtA Mutagenesis

Progress was made using random chemical mutagenesis when studying the LacY permease (Bailey & Manoil, 1998), and later on NrtA. The highest density of functionally important mutations was found in the cytoplasmic loop joining Tm 4 and 5, in agreement with previous studies (Manoil & Bailey, 1997). Essential residues for function were identified and included E126 and R144, again in agreement with previous LacY mutageneses (Frillingos *et al.*, 1997). This region is the site of the NNP signature sequences which is lacking in the sugar transporter LacY. It is suggested here that this region may be the site of further subfamily specific signature sequences. In NrtA, chemical mutagenesis established the first of the two nitrate signature sequences as a prime target for further work as they suffered frequent mutagenesis (26 % of the total mutants were in this region) using the primary base change mutagens NTG and 4-nitroquinoline-1-oxide (NQO) (Kinghorn *et al.*, 2005). This work established the need for high frequency of small non-polar glycine residues in this region presumably for tight packing of the α-helix at a seemingly crucial point for nitrate transport (Kinghorn *et al.*, 2005).

In the first nitrate signature, relatively conservative mutations result in reduced function indicating the requirement of tight packing at this junction (Kinghorn *et al.*, 2005) (Table 1.1). By comparison, in this study by Kinghorn *et al.* (2005) no mutations in Tm 3 - region of high density glycine residues - were represented. This reflects the relatively reduced importance of

this region in the transport process, the observation was made that this region is not part of the binding site, instead Tms 3, 6, 9 and 12 of NrtA are embedded within the bilayer (Kinghorn *et al.*, 2005) this is in agreement with work on LacY and GlpT (Abramson *et al.*, 2003b; Huang *et al.*, 2003).

Residue Substitution	Nucleotide change	Specific Change	Net nitrate uptake (nmol min ⁻¹ mg ⁻¹ DW)	Expression
G157R	GGG → CGG	Gain of charge	2.29 ± 0.38	+
G157E	GGG → GAG	Gain of charge	3.62 ± 0.59	+
G167S	GGT → AGT	Conservative	6.89 ± 0.78	+
A169P	GCT → CCT	Conservative	3.36 ± 1.28	+
G170R	GGT → CGT	Gain of charge	3.66 ± 0.55	+
G170S	GGT → AGT	Conservative	3.03 ± 0.45	+
G170C	GGT → TGT	Polar-SH*	5.28 ± 1.75	+
G170Y	GGT → TAT	Size increase	3.72 ± 1.26	+
G172D	GGT → GAT	Gain of charge	5.73 ± 0.80	+
G172C	GGT → TGT	Polar-SH*	4.22 ± 0.03	+
G172S	GGT → AGT	Conservative	3.34 ± 0.61	+

Table 1.1 Missense mutations in the nitrate signature of the high-affinity nitrate transporter NrtA from *A. nidulans*. Table adapted from Kinghorn *et al* (2005). The basal nitrate uptake in a loss-of-function *nrtA* mutant is 3-4 nmol min⁻¹ mg⁻¹ under the standard employed for net nitrate uptake to account for uptake of NrtB (Brownlee & Arst, 1983; Kinghorn *et al.*, 2005). Therefore, the only mutants showing significant nitrate uptake are G167S and G170C. The results represent a mean of 3 independent experiments with standard deviations. The presence or absence of NrtA protein was estimated by Western blot in indicated by + or -, respectively. *SH, sulfhydryl group of cysteine. Specific changes are assessed here, and where stated as 'gain of charge' this an amino acid without a complete charge i.e. a polar or non-polar residue which has been altered to a fully charged residue. In the case of changes to cysteine in this table these have been referred to as Polar-SH changes, i.e. a gain of a sulfhydryl group. In the case of G170Y there is a dramatic increase in side chain size. Finally, a 'conservative' mutation is one where little size or charge alteration has been elicited by the mutagenesis.

Chemical and site-directed mutagenesis are two distinct approaches which have been known to complement each other, for example in NrtA chemical mutagenesis (reversion) of mutant strain R87T revealed the importance of asparagine (459) in the second nitrate signature (Unkles *et al.*, 2004a) as discussed above. While the main advantage of using chemical mutagenesis is that it targets potentially important - and likewise does not target less important - regions in proteins that may not be highlighted by conservation analyses. However, a major disadvantage of using a chemical mutagen is that the mutagenesis produces a disproportionate number of deletion mutants and only a small number of mutants in the sense strain of the coding protein which is the target of the study. Therefore, can be labour intensive for a relatively small return. The mutagen NTG which has been used for NrtA

studies (Kinghorn *et al.*, 2005) is known to target guanine rich residues only, therefore, producing a bias towards guanine based codons. Guanines are replaced in the sense strand with NTG which pairs with thymine (as opposed to cytosine) therefore, making sense strand mutations phenotypically visible (Adelberg *et al.*, 1965), similarly mutagenesis in *A. nidulans* can also employed NQO as a mutagen (Bal *et al.*, 1977; Kinghorn *et al.*, 2005) though this mutagen has the same target set, i.e. guanines (Bal *et al.*, 1977).

The research carried out as presented in this thesis investigates the amino acids that may be involved with the different stages of anion translocation. Site-directed mutagenesis and biochemical analyses were used to gain insights into NrtA and NitA. Additionally, there was a brief attempt to investigate the signalling system which is involved with the transport of these molecules.

Chapter Two

Materials and Methods

2.0 Introduction

In this chapter, the main methodologies used during this thesis are described. Basic media preparation and tabulated lists are included in appendices where stated.

2.1 *A. nidulans* strains and media

The genotypes of specific strains used in this study are shown in Table 2.1. Gene symbols used are described previously (Clutterbuck, 1974). All strains were derived from the Glasgow University stocks, held by Dr. John A. Clutterbuck, which were themselves derived from the single wild-type isolate of *A. nidulans*, NRRL 194 (Pontecorvo, 1953). Strain A1150 was purchased from the Fungal Genetics Stock Centre.

Strain	Genotype
T110	<i>nrtA747; nrtB110</i>
T474	<i>nrtA747; nrtB110; nrtA::argB; pyroA4; pabaA1; yA2</i>
G01	<i>biA1</i>
T600	<i>nrtA747, nrtB110, pyroA4, pabaB1, yaA2</i>
JK1060	<i>nrtA747; nrtB110; argB2; ya2; pyroA4; pabaA1</i>
VFS50	<i>nrtA747; nrtB110; nitA26; argB2; yA2</i>
VFS106	<i>nrtA747; nrtB110; yA2; argB2; nkuA::argB*; pyroA4</i>
T19	<i>nrtA747; nrtB110; pyroA4; pabaA1; pTRAN3-1^a::argB; yA2</i>
T20	<i>nrtA747; nrtB110; pyroA4; pabaA1; pTRAN3-1^a::argB; yA2</i>
A1150	<i>pyroA4; argB2; nkuA::argB*; riboB2</i>
T26	<i>nrtA747; nrtB110; nitA26; yA2</i>

Table 2.1 Genotypes of strains used in this study.

2.1.1 *A. nidulans* growth and storage

Routine *Aspergillus* growth media and handling techniques used were as described previously (Clutterbuck, 1974). Shake flask cultures for nitrate uptake assays, genetic transformation, and DNA preparation were grown in liquid minimal medium (Cove, 1966) containing the appropriate nitrogen and vitamin supplements as stated in the specific methods. Static cultures for fungal DNA extractions were prepared when using the cell disrupter method (see DNA extraction methods). *Aspergillus* media was as described in Appendix Two.

Harvesting of mycelium grown from shake flask cultures was through a Buchner funnel using a sterile Miracloth. Samples were frozen in liquid nitrogen and stored at -80 °C. *A. nidulans* conidial preparations for liquid culture were prepared in sterile bijous or McCartney bottles using saline-tween 80 (0.9 % (w/v) NaCl, 0.1% (v/v) tween 80) as a carrier solution. To obtain pure single colonies from *A. nidulans*, dilute conidial suspensions were prepared in saline-tween 80 and a small aliquot of this suspension was spread on complete media (CM) agar plates (Appendix Two). After 2 days growth at 37 °C, well separated colonies were obtained, selected and their phenotype assessed. Fungal stock cultures were maintained at 4 °C on CM agar slopes. For long-term storage, spores were held on silica gel at 4 °C.

2.2 Plasmids

Standard procedures were used for the propagation of plasmids, sub cloning and maintenance. Plasmids were amplified in *E. coli* strain *DH5 α - F ϕ 80dlacZAM15 Δ (lacZYA-argF)U169 deoR, recA1 endA1 hsdR17(r_k⁻ m_k⁺ phoA supE44 λ thi-1 gyrA96 relA1*. In the preparation of the cosmid library, *E. coli* strain EPI305 was used. This strain is genetically deficient in both recombination and restriction systems to minimise the rearrangement and loss of clones *in vivo*, these cells were both recommended and supplied with Epicentre Technologies (Madison, WI, U.S.A.) pWEB::TNC deletion cosmid cloning kit which was used to produce the cosmid library.

2.2.1 *V5TAGAGE/I*, was the primary vector for producing mutants in *nrtA*. It encodes the *nrtA* coding region fused in-frame at the 3' end with a sequence encoding the V5 epitope (Invitrogen, Renfrewshire, U.K.). The whole gene was flanked by *EcoRI* sites in pUC19. Mutations to *nrtA* were inserted using unique restriction sites (Unkles *et al.*, 2005) (Figure 2.1).

2.2.2 *pMUT* and *V5MKNitA*, were used for the integration of *nrtA* and *nitA* mutations into *A. nidulans* respectively. They encoded 1.3 kb of *nrtA* promoter sequences including putative regulatory protein binding sites and 350 bp of *nrtA* terminator sequence. Unique restriction sites were used for the insertion of mutant coding sequences. These vectors also encoded the *argB* gene (i.e. *argB*^{*}) to allow for the targeting of the construct to the *argB* locus. This allowed comparison of single copy integrations of *nrtA* or *nitA* in the *argB* system (Unkles *et al.*, 2005). The coding region of *nrtA* is not included in pMUT; it is cloned in for use using the *EcoRI* site in pMUT. *V5MKNitA* includes the 1 kb *nitA* coding region (Figure 2.1).

2.2.3 *WEBpyroA*, was used for the preparation of a cosmid library for investigations into the nitrate signalling system. Plasmid pWEB::TNC was provided as part of Epicentre Technologies deletion cosmid cloning kit in a pre-cut (*SmaI*) dephosphorylated state. Before use this plasmid was phosphorylated using T4 polynucleotide kinase as per the manufacturer's

instructions (NEB, Hertfordshire, U.K.) and amplified in *E. coli*. It was then purified, cut with *EcoRV* (unique site) by standard restriction conditions, again as per manufacturer's instructions (Promega, Hampshire, U.K.) and dephosphorylated using shrimp alkaline phosphatase following manufacturer's instructions (Promega). A 2.5 kb *pyroA* fragment cloned from *A. fumigatus* provided by Dr. S. E. Unkles was introduced into the vector for use as a selectable marker, producing vector *WEBpyroA* for use (Figure 2.1).

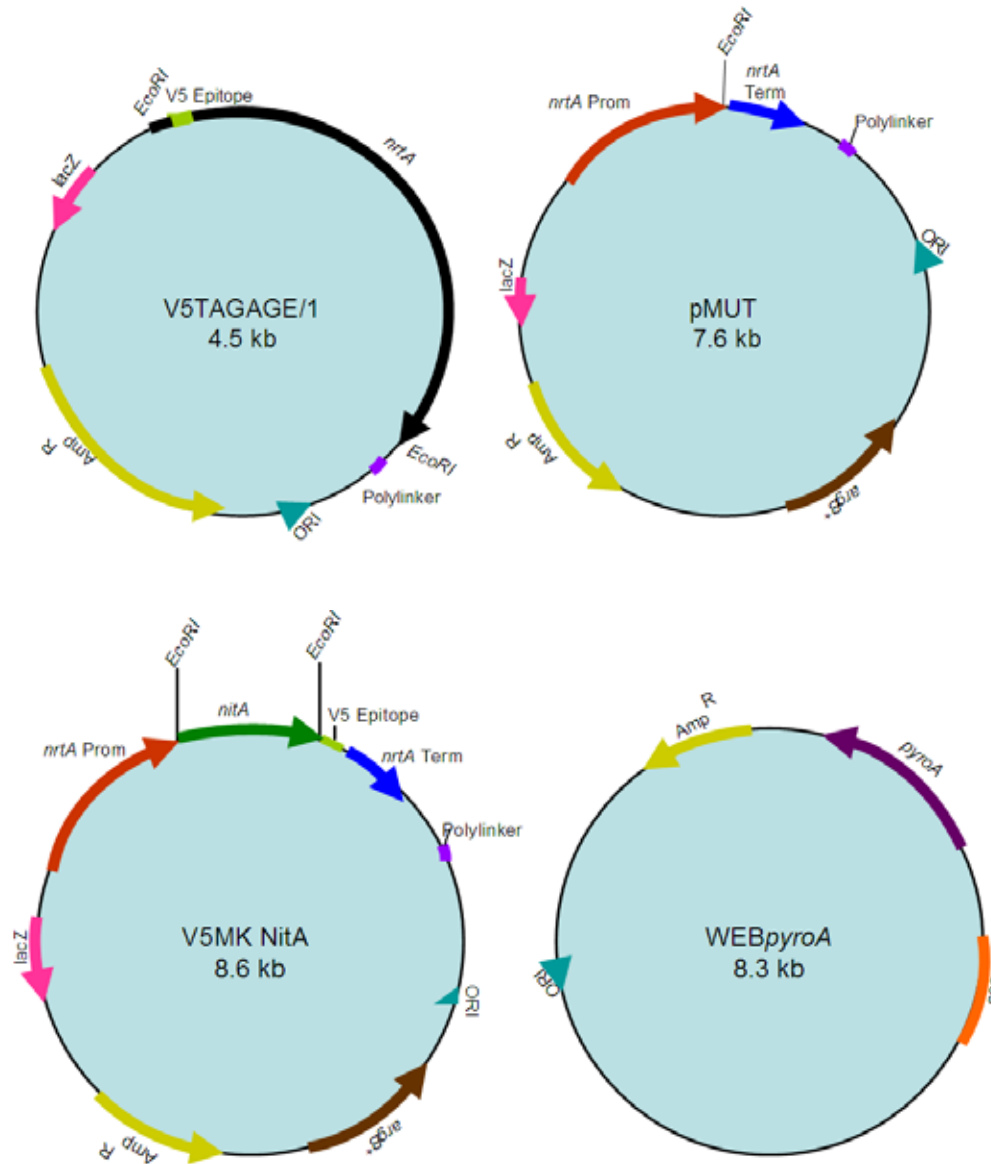


Figure 2.1 Plasmid vectors used in this thesis (as described in section 2.2). Diagrams are not to scale.

2.3 Bacterial cultures

Luria Broth (Miller's Modification) (Sigma, Dorset, U.K.) was prepared as per manufacturer's instructions, adding 1.2 % agar for solid media.

2.3.1 Antibiotics

Ampicillin (Melford, Suffolk, U.K.) was used as a selectable marker for *E. coli* transformations. Liquid ampicillin (sodium salt) stock solution of 10 mg ml⁻¹ in sterile distilled water was added to 4.5 ml Luria broth in McCartney bottles to a final concentration of 0.1 mg ml⁻¹. This stock solution was stored at 4 °C and kept for no longer than one week. Solid ampicillin was also added directly to cooled molten agar to a final concentration of 0.1 mg ml⁻¹.

All bacterial cultures were grown overnight aerobically at 37 °C in Luria broth, unless otherwise stated. Growth was either on an orbital shaker or a static incubator for liquid and solid culture respectively. For short-term storage, bacterial strains were spread on agar plates and placed at 4 °C. For long-term storage, bacterial strains were placed in Luria broth containing 20 % glycerol and stored at -80 °C.

2.3.2 Preparation of competent cells

The preparation of competent cells was based on the method of Cohen *et al.* (1972). A single colony of *E. coli DH5 α* was transferred to 4.5 ml Luria broth and grown overnight at 37 °C in an orbital shaker at 250 rpm. 1 ml of this culture was transferred to 100 ml SOB (2 % tryptone (w/v), 0.05 % yeast extract (w/v), 10 mM NaCl, 2.5 mM KCl, 10 mM MgSO₄, 10 mM MgCl₂) in a 1 L Erlenmeyer flask and incubated at room temperature (250 rpm) until an OD₆₀₀ of 0.4-0.8 was achieved when measured using a spectrophotometer (Perkin Elmer UV/Vis Lambda II, Waltham, Massachusetts). The flask was then placed on ice for 10 min and the cells harvested by centrifugation (750 x g, 15 min, SS-34 at 4 °C). The pellet was suspended in 40 ml of transformation buffer (10 mM PIPES (C₈H₁₈N₂O₆S₂), 15 mM CaCl₂, 250 mM KCl, pH 6.7 (KOH), and 55 mM MnCl₂·4H₂O) and incubated on ice for a further 10 min before the centrifugation step was repeated. These cells were then re-suspended in 4 ml of transformation buffer. 300 μ l dimethyl sulphoxide (DMSO) was then added to this mixture which was gently agitated and placed on ice for 10 min. The cells were then dispensed in 100 μ l aliquots and placed directly into a pre-cooled metal tray for freezing and storage at -80 °C.

2.4 Molecular methods

2.4.1 Tissue preparation for fungal DNA extraction

Plates inoculated from a single point were prepared for DNA extraction. Conidia from half a plate were grown overnight on an orbital shaker then washed with sterile distilled water through a sterile Miracloth (Calbiochem, Darmstadt, Germany.). Mycelia were collected and

snap-frozen in liquid nitrogen. Approximately 300 mg wet-weight mycelium was ground to a fine powder using a pestle and mortar.

2.4.2 DNA extractions

The Nucleon II Kit (Scotlab, Strathclyde, U.K.) was used as standard for fungal DNA extractions; it was superseded by the cell disruption method for DNA extraction for sequencing (due to its speed) described below.

The ground material was placed in a 5 ml polypropylene screw cap tube with 2 ml Nucleon Reagent B (400 mM Tris pH 8, 120 mM ethylene diamine tetra acetic acid (EDTA), 150 mM NaCl, 1 % (w/v) sodium dodecyl sulphate (SDS)) and 1 μ l (10 mg ml⁻¹) RNase A. The tube was mixed thoroughly and incubated for 30 min at 37 °C. After incubation 0.5 ml 5 M sodium perchlorate was added and agitated before 2 ml of 100 % v/v chloroform (-20 °C) was added. Fully homogenised samples were centrifuged at 1800 x g for 3 min (MSE Mistral 1000) before the upper aqueous layer was removed and placed in a 15 ml centrifuge tube. 2 ml of ethanol 96 % v/v (-20 °C) was added to the sample, the precipitated DNA was collected using a sealed glass Pasteur pipette. The DNA was purified using 0.5 ml of 70 % v/v ethanol, and air dried for 30 min. The DNA was re-suspended in TE (10 mM Tris, 0.1 mM EDTA, pH 8) buffer.

The Qiagen DNeasy[®] Plant Mini Kit (Qiagen, West Sussex, U.K.) was used to isolate DNA from fungal tissue following the plant tissue protocol according to the manufacturer's instruction, including optional steps. This method was employed for the preparation of DNA from strain T110 for the construction of the cosmid library.

DNA extraction using a cell disrupter was used for DNA extraction from fungal cells for sequencing. By this method, approx. 10⁵ spores were inoculated into 2 ml liquid MM with 5 g L⁻¹ yeast extract, 10 mM NH₄T and vitamins. This was grown for 16-20 h as a static culture at 37 °C. The mycelial matt was dried between paper towels and added to 300 μ l glass beads, 500 μ l chloroform : isoamyl alcohol (24:1) at 4 °C, 500 μ l breaking buffer (2 % v/v Triton X-100, 1 % w/v SDS, 100 mM NaCl, 10 mM Tris pH 8, 1 mM EDTA pH 8) at 4 °C. This was shaken at full speed (6.5 m sec⁻¹) for two 1 min intervals in a MP FastPrep 24 (MP Biomedicals, Cheshire, U.K.). Tubes were then centrifuged in a bench-top centrifuge at 22,000 x g, for 10 min at room temperature. The upper aqueous phase was then added to two volumes of ice cold ethanol (96 %) for DNA to precipitate. This mixture was centrifuged at 22,000 x g, for 10 min at room temperature. The ethanol was then poured off and the pellet

was purified in 70 % ethanol before being dried at room temperature. Dried pellets were solubilised in 50 µl TE, and then incubated at 65 °C for 20 min to inhibit DNase activity.

2.4.3 Plasmid DNA quantification

The Beer-Lambert Law - i.e. the linear relationship between absorbance and the concentration of a sample at a specific wavelength of light - was used to calculate the concentration of DNA samples. Where A is absorbance, ϵ is the coefficient of absorbance for a given substrate, l is the path length (cm), and c is the sample concentration (g l^{-1}):

$$A = \epsilon l c$$

The optical density of plasmid DNA was measured spectrophotometrically (Perkin Elmer UV/Vis Lambda II) to ascertain the approximate concentration. The DNA concentration was calculated based on the rearrangement of the above equation with dilution as a separate entity i.e.:

$$A_{260 \text{ nm}} \times 50 \times l \times \text{dilution factor} = \text{DNA concentration } \mu\text{g ml}^{-1}$$

Where 50 is a constant representing the coefficient of absorbance (ϵ) of DNA at 260 nm, and a 1 cm light path is used (l). Thus an absorbance of 1 would represent a $50 \mu\text{g ml}^{-1}$ sample of DNA (c) in a sample diluted 1000 times, assuming that absorbance is linear with concentration.

2.4.4 Polymerase chain reaction (PCR)

PCR reactions were carried out using Vent Polymerase (NEB) and Phusion Polymerase (Finnzymes, Espoo, Finland) enzymes and their appropriate buffers using either a ThermoHybaid Omne thermo cycler or Gstorm GS1 thermo cycler (Essex, U.K.). Non-mutagenic primers are documented in Appendix Three and mutagenic primers in Appendix Four, specifics for the manufacture of mutant constructs are given in Section 2.4.15. Reaction conditions were experiment dependant, though as standard when using Vent Polymerase for the production of mutant constructs 100 µl PCR reactions were carried out (100 ng DNA, buffer to concentration recommended by manufacturer, 2 mM MgSO_4 , 0.2 mM dNTP, 40 µM of each primer and 2 units of enzyme) and Phusion polymerase reactions as standard for fungal DNA amplification were in 50 µl reactions, DNA concentration in these reactions was experiment dependant though was often, 1 µl of DNA extracted by cell disruptor method or 1 µl extracted DNA digested by Nucleon method after genomic digest (5 µl DNA digested in 30

µl reaction), otherwise the PCR reaction contained buffer – concentration as per manufacturer’s instruction, 0.2 mM dNTP, 0.4 µM of each primer and 0.5 unit of Phusion polymerase.

2.4.5 PCR product purification

Purification of PCR products was carried out using the Marligen Biosciences (Ijamsville, MD, U.S.A.) PCR purification kit as per the manufacturer’s instructions. Latterly, PCR products were purified using Invitex MSB Spin PCRapace Kit (Berlin, Germany). Where product needed concentration, for example for sequencing reactions, a Philip Harris Gyro Vap GL11 (Cheshire, U.K.) was used.

2.4.6 Agarose gel electrophoresis

Agarose gel electrophoresis was carried out basically as described by Sambrook *et al* (1989). Size of gel and agarose concentration was dependant upon samples and the requirement’s of the gel. Slabs were poured routinely as 1 % agarose made in solution using 1 x TAE buffer (40 mM Tris, 1 mM EDTA, pH 8-8.2 (acetic acid)). Higher concentrations of agarose i.e. 1.5 % were poured for the resolution of fragments less than 800 bp. Agarose was solubilised by heating in a microwave then cooled before the addition of ethidium bromide (0.5 µg ml⁻¹) (Sharp *et al.*, 1973). Once set, the gel was submerged in 1 x TAE in an electrophoresis tank. Samples to be loaded were prepared with the appropriate loading buffer and placed into the wells. *HindIII* digested λ-phage DNA and Promega 100 bp molecular size markers were used routinely. Voltage and time for electrophoresis was experiment dependant. Gels were visualised using a UV light and photographed using a UV-trans illuminator and photographic suite (Herolab E.A.S.Y. Photographic Suite, Scotlab). Before loading DNA on agarose, loading dye was added (1 µl for every 10 µl) xylene cyanol (0.25 % (w/v) bromophenol blue, 0.25 % (w/v) XC, 40 % (w/v) sucrose) (XC) for fragments less than 800 bp and bromophenol blue (BPB) (0.25 % BPB 40 % (w/v) sucrose) for larger fragments as described by Sambrook *et al* (1989).

2.4.7 Restriction endonuclease digestion

Restriction digests were carried out using Type II restriction endonucleases (Promega, Hybaid and NEB) at the temperature and timings recommended by the manufacturer in their supplied buffers, or in double digests as directed. For genomic DNA digestion, DNA was digested overnight at the temperature required by the enzyme. Phosphatase treatment was carried out using Shrimp Alkaline Phosphatase (SAP) and its corresponding buffer according to the Promega instruction manual.

2.4.8 Isolation of DNA fragments from agarose gel

This protocol is based on the methods of DNA adsorption to silica as described by Vogelstein and Gillespie (1979). DNA was separated by gel electrophoresis and required bands were excised by scalpel and gel purified using the Qiagen QIAEXII gel extraction kit. An additional step of drop-dialysis of the solubilised DNA on a Millipore (Hertfordshire, U.K.) type VS 0.025 μm filter was carried out. The filter was placed in a Petri dish half filled with sterile distilled water for 10-15 min to remove any salt residue from the sample.

For the preparation of vectors, digested fragments - mutant PCR products or vector fragments - were ligated using a Rapid DNA ligation kit (Roche, Sussex, U.K.). Cut insert and cut vector (total volume 10 μl) were incubated for 5 min at room temperature with 5 μl ligation buffer (2 x) and 2.5 u T4 DNA ligase then incubated on ice for a further 3 min prior to bacterial transformation.

2.4.9 *E. coli* transformation

An aliquot of plasmid - or a complete ligation reaction - was added to 10-50 μl of chemically competent *E. coli* DH5 α cells and incubated on ice for 20 min before heat shock at 42 °C. Transformed cells were plated out onto LB-Ampicillin (50 mg ml⁻¹) media and grown overnight. Plasmids with a low transformation efficiency were incubated for 1 h shaking at 200 rpm at 37 °C with 1 ml SOC (2 % tryptone (w/v), 0.05 % yeast extract (w/v), 10 mM NaCl, 2.5 mM KCl, 10 mM MgSO₄, 10 mM MgCl₂, 2 mM glucose) before being centrifuged briefly and spread on LB-Ampicillin (50 mg ml⁻¹) (Sambrook *et al.*, 1989). Bacterial transformants were lysed using 'cracking buffer' and voltage applied to check that plasmids transformed were of the correct size before sequencing or restriction digest of inserted plasmids (Adapted from a Promega method (1991)). Using a 96 well microtitre plate 20 μl sterile distilled water was pipetted into each well required (typically 12 wells per transformation). Using a blunt tooth-pick, colonies were picked off and suspended in the water; this tooth-pick was then used to inoculate a fresh Luria broth agar plate with ampicillin (50 mg ml⁻¹). This was carried out for several colonies per bacterial transformation. In the 12th well approximately 0.25 μg marker plasmid was added, commonly a control plasmid with insert or similarly sized plasmid for transformation assessment. Further to this 20 μl of cracking buffer (1.25 M NaOH, 20 % w/v sucrose, 0.5 % w/v SDS, with a few crystals of bromocresol green) was added to each well. The Luria broth agar plate was incubated overnight at 37 °C and the samples run on a thick 1 % agarose gel. Colonies with the correct plasmid - when compared to the marker - were grown up for plasmid preparation.

2.4.10 Purification of plasmid DNA

The QIAprep[®] Miniprep Kit (Qiagen) was used to purify plasmid/cosmid DNA according to the manufacturer's instructions. For the preparation of higher concentrations of plasmid DNA the Qiaprep Midi and Maxi plasmid purification kits were used (Qiagen). Following the manufacturer's instructions.

2.4.11 DNA sequencing

DNA sequencing was performed by either The Sequencing Service (School of Life Sciences, University of Dundee, Scotland, <http://www.dnaseq.co.uk>) or Macrogen Sequencing Service (Seoul, Korea, <http://www.macrogen.com>). Both companies employ Applied Biosystems Big-Dye Version 3.1 chemistry on an Applied Biosystems model 3730 automated capillary DNA sequencer. Returned sequences were analysed using Sequencher[™] software (Version 4.0.5, Gene Codes Corporation 91-99).

2.4.12 *A. nidulans* transformation protocol

Transformation method was based on methods described by Balance *et al* (1983), Tilburn *et al* (1983), John and Peberdy (1984), Yelton *et al* (1984) and Peberdy (1989). This final method was reviewed in Riach and Kinghorn (1996) and references therein. Mutant constructs were transformed into the appropriate recipient strain and plated out on selective media for growth of transformant colonies. This method was standard for all transformations carried out. For mutant constructs in *nrtA*, the *argB* transformation was used as shown in Figure 2.2; while *nitA* transformations were as described in Chapter Seven.

Mycelia preparation

A single colony inoculum of transformation strain was grown for 4-7 days prior to transformation on agar at 37 °C. Plates were left on the bench at room temperature to mature for approximately 7 days. Conidiospores were grown at room temperature on an orbital shaker (250 rpm), for approximately 12 h in liquid media with vitamin supplements, and nitrogen sources. If mycelia had not started to germinate at this time they were re-incubated with orbital shaking at 37 °C to produce immature mycelia for protoplast preparation. Mycelia were harvested through an ethanol sterilised Miracloth (Calbiochem) and washed with cold (4 °C), sterile, 0.6 M MgSO₄ for protoplast preparation. The resulting material was placed in a pre-cooled, sterile 250 ml Erlenmeyer flask and re-suspended in 5 ml cold osmotic media (OSMO) (1.2 mM MgSO₄, 10 mM Na₂HPO₄ (pH 7.0), pH 5.8 with 0.2 M Na₂HPO₄). 2 ml Novozyme 234 (Novozyme Prods Ltd) solution (50 mg ml⁻¹ OSMO) was added to the cell suspension and incubated for 5 min on ice. Next 0.25 ml BSA solution (12 mg ml⁻¹ OSMO) was added to the suspension. The mixture was incubated at 30 °C for 3.5 h with gentle orbital

shaking at 80 rpm. The mixture was placed on ice to stop the reaction. Flasks were gently mixed to free protoplasts from the mycelial debris. Using a 10 ml glass pipette, equal volumes of protoplast suspension were placed in two pre-cooled 30 ml corex tubes. The flask was rinsed with 5 ml OSMO to ensure that all the protoplasts had been collected and added to the corex tubes. An equal volume of trapping buffer (0.6 M sorbitol, 100 mM Tris pH 7.0) was overlaid on the suspension ensuring that the two phases did not mix. Protoplasts were separated from the cellular debris by centrifugation at 4100 x g for 20 min in a refrigerated (4 °C) Sorval RC-5 centrifuge using an HB-4 swing-out rotor. The protoplasts at the interface of the two liquids were removed using a plastic pastette and pooled in a third corex tube. 20 ml cold STC (1.2 M sorbitol, 10 mM Tris pH 7.5, 10 mM CaCl₂) was added to wash the protoplasts which were then centrifuged at 10,500 x g for 5 min at 4 °C (Sorval RC-5, Rotor HB-4). The protoplast pellet was re-suspended in n x 90 µl STC where n is the number of transformations. DNA concentration is reaction dependant (i.e. depending upon the quality of the protoplasts and the number of transformants required), though for a typical *argB* transformation 5-7 µg DNA per reaction was used with 90 µl protoplasts.

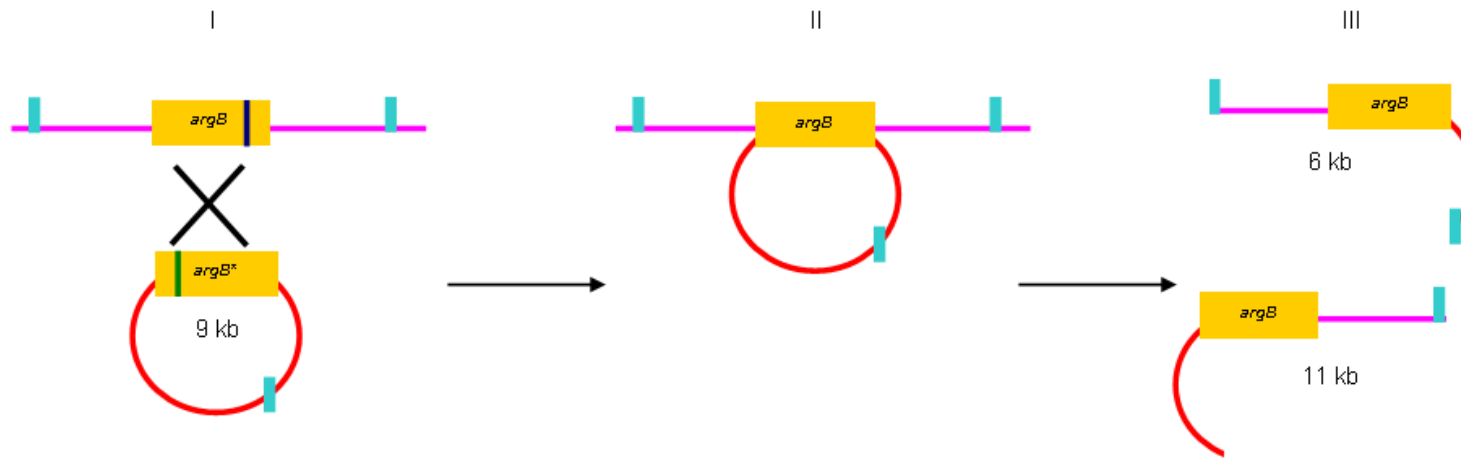
Transformation

DNA and protoplasts were placed in 15 ml centrifuge tubes in preparation for transformation. 25 µl 60 % PEG 6000 was added to each sample and gently mixed by pipetting, this was left on ice for 20 min. A further 1 ml 60 % PEG 6000 was added to each tube which was then inverted gently to mix and this was left at room temperature for 20 min. 5 ml cold STC was added to each tube and the resulting suspension was centrifuged at 2500 x g for 5 min using a MSE Mistral 1000 centrifuge at room temperature. The supernatant was removed and the pellet re-suspended in 100 µl STC. The suspension was split between two selection plates that were grown at 37 °C for up to 7 days. Selection was carried out on transformation medium containing a nitrogen source suitable for the selection of transformants and vitamin supplements. Copy number and plasmid integration was further assessed using Southern analysis of digested genomic DNA.

Strains

Strains used for fungal transformation were JK1060 (*nrtA747; nrtB110; argB2; ya2; pyroA4; pabaA1*), VFS50 (*nrtA747; nrtB110; nitA26; argB2; yA2*) and VFS106 (*nrtA747; nrtB110; yA2; nkuAΔ; pyroA4*). JK1060 and VFS50 were used for the transformation of *nrtA* and *nitA* mutant constructs respectively for integration at the *argB* locus. VFS106 was developed for the integration of *nitA* mutant constructs at the wild-type *nitA* locus.

(a) Single Copy Integration



(b) Multiple Copy Integration

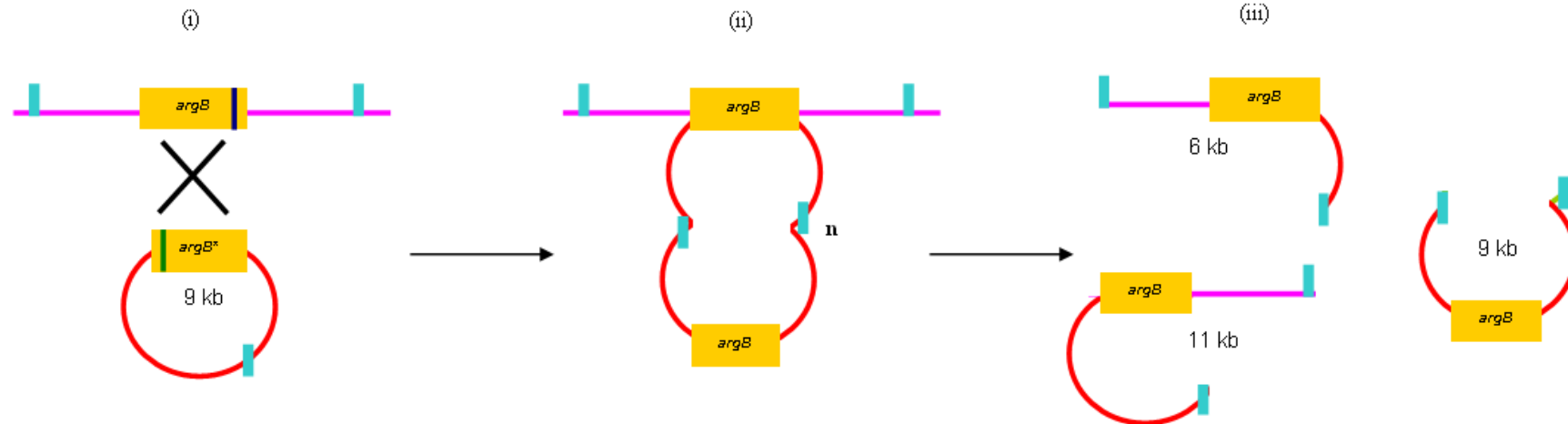


Figure 2.2 Legend on following page.

Figure 2.2 Integration of mutant constructs at *argB*. Plasmid is shown in red, chromosomal DNA in pink and *BamHI* sites in blue. Both plasmid and chromosomal copies of *argB* harbour mutations in the *argB* gene; these are represented by as dark green and dark blue lines respectively. Southern blotting was used to determine single copy integrations using *BamHI* digestion of genomic DNA. (a) Step (I) showing the single crossover event for plasmid integration, (II) Crossover produces the wild-type *argB* due to exchange of wild-type genetic material (III) Southern blotting is performed on *BamHI* digested transformant DNA. For single copy integration two fragments are produced (6 and 11 kb). (b) For multiple integrations at *argB*, the plasmids join prior to transformation. (i) Single crossover event for plasmid integration, (ii) As the plasmid was joined to another (possibly several i.e. to the power of n) plasmid, the integration only happens once but the DNA integrated is n times the size. (iii) *BamHI* digested Southern blot reveals three bands for multiple copy integration (6 kb, 9 kb, and 11 kb); the intensity of the 9 kb band relative to the others reflects the number of integrations. This integration method was as described by Unkles *et al* (2005).

2.4.13 Southern blotting

Southern blotting was performed on transformants harbouring mutant constructs as to confirm site integration and copy number, after phenotypic analysis of these transformants. Single copy strains were sought for biochemical studies. Transforming constructs harbour one *BamHI* site allowing enzymatic digests using the corresponding *BamHI* enzyme. The *argB* gene (*XbaI* fragment, 1 kb) can be used to probe these blots to reveal single copy integrations of the 9.3 kb construct into the *argB* locus disrupting the local *argB* fragment (9 kb) to produce two fragments of 11.7 kb and 6.6 kb. For multiple integrations an additional band of 9.3 kb is observed, and its intensity is relative to the number of tandem integrations at *argB* (Unkles *et al.*, 2005). VFS106 transformants were targeted to the wild-type *nitA* locus. As a result of high efficiency in this gene targeting system for single copy integrations (Szewczak *et al.*, 2006) it was not deemed necessary to screen for single copy integration with the same vigour of that of *argB* integrations. As a check on the integrations, *BglIII* genomic digests were performed on sequenced NitA transformants and these were probed with *nitA* (*EcoRI*, 1.7 kb) with the expectation of a 3.4 kb fragment for single copy integration. DNA transfer was carried out using the capillary method of Southern (1975) and by Sambrook *et al* (1989).

Blot preparation

DNA samples were incubated at 65 °C for 20 min to destroy potential DNase activity, around 10 µg DNA was then digested and equalised by eye for DNA concentration. Digested fragments were separated by agarose gel electrophoresis on 1 % gels. The gel was viewed on a transilluminator and trimmed to remove the meniscus, wells and top right hand corner for orientation. A photograph of the stained gel was also taken for record (Herolab E.A.S.Y. Photographic Suite, Scotlab). The DNA was then depurinated by washing with 0.25 M HCl for 20 min. DNA was then denatured using denaturing solution (1.5 M NaCl, 0.5 M NaOH) for 30-40 min and finally neutralised in neutralising buffer (1.5 M NaCl, 1 M Tris-EDTA, pH

7.4) for 30-40 min. A long piece of Whatman (Kent, U.K) 3MM paper was wetted with 20 x SSC (3 M NaCl, 300 mM sodium citrate, pH 7) solution and draped over a Perspex stand. Atop this the gel was placed DNA side up and an equal size of nylon Hybond-N membrane (Amersham) was placed on the gel (RH corner cut). On top again 3 pieces of 3MM paper were wetted with SSC and 3 dry pieces of 3MM placed on top. A bundle of cut to size paper towels placed on top of the last pieces of 3MM and finally, a weight. This was left overnight to allow for DNA transfer. The set-up was dismantled the following day and the gel was re-stained with an ethidium bromide solution ($0.5 \mu\text{g ml}^{-1}$). The Hybond-N membrane was rinsed in 2 x SSC and placed on a piece of 3MM paper to dry. The membrane was placed in a crosslinker (Spectrolinker XL-1500 UV Crosslinker) to crosslink the DNA to the nylon substrate.

^{32}P Labelling was carried out by the method of Feinberg and Vogelstein (1983) with high stringency hybridisations. Double stranded probes (25-30 ng) were denatured in water for 2 min and then chilled on ice before the addition of the remaining reaction ingredients (0.2 mM dCTP, 1x labelling buffer (Promega), Klenow 2.5 u (Fermentas, Yorkshire, U.K.). $2.5 \mu\text{l}$ of $\alpha^{32}\text{P}$ (1 MBq) was added to the reaction, gently mixed and placed on heating block at 37°C for 30 min. Assessment of the label was carried out using a NICK gel filtration column (GE Healthcare, Buckinghamshire, U.K.) which was washed using TE buffer before assessment. Blue dextran was added to the probe ($4 \mu\text{l}$ of a saturated solution) as a tracker dye. The dyed probe was added directly to the column membrane, followed by a few drops of TE, once the dye had passed through the membrane 4-5 ml TE was applied to the column. The blue label was caught in an Eppendorf. The radioactivity of this sample was compared to the same volume of wash which followed through the column to assess how the label had incorporated to the DNA. Successfully labelled probe was boiled for 5-10 min and then chilled on ice.

DNA hybridisation, membrane washing and autoradiography

The nylon membrane was incubated overnight in a 65°C water-bath shaking at 80 rpm in hybridisation buffer (9 % v/v PEG 3000, 0.5 % w/v powdered milk (Marvel) solution, 0.1 % w/v SDS, 0.2 mg ml^{-1} Herring sperm DNA, 5 x SSPE (750 mM NaCl, 50 mM NaH_2PO_4 , 5 mM EDTA, pH 7.4)) with radio-active probe. This was performed at 65°C at 80 rpm.

Membranes were washed in washes of increasing stringency to rinse un-hybridised probe. Specifically, membranes were washed for 20 min in 5 x SSC, then 2 x SSC, then 0.5 x SSC. All washes performed at 65°C at 80 rpm until the background radiation was negligible. Washed filters were placed in an autoradiography cassette against photographic film (Kodak

Biomax MX film) and stored at -80 °C. Films were developed in Fugi RG II X-ray film processor with signal dependant exposure time. Phosphoimaging software was later employed to replace the use of photographic film. In this case the Phospho-screens were 'Kodak Imaging Screen K', the imager was a Bio-Rad Molecular Imager FX and the software used was Quantity One.

Once single copy transformants were determined they were purified, phenotypically assessed and the coding regions were amplified and fully sequenced. This sequence was then quality control checked by another member of the group.

2.4.14 Chemical mutagenesis

Chemical mutagenesis was employed in the development of revertants in NitA mutant studies and also when trying to identify genes involved in the nitrate signalling system. Strains were treated with N-methyl-N'-nitro-N-nitrosoguanine (NTG) (Adelberg *et al.*, 1965) and mutants were plated and screened on selective media as described previously. The mutagen NTG, when incorporated into DNA replaces guanine and pairs with thymine not cytosine. The mutations are therefore made 'selectively at random' as the only nucleotide targeted is guanine. This method preferentially targets G-rich codons (e.g. glycine) over C-rich codons such as proline (Kinghorn *et al.*, 2005). Usually, NTG replaces guanine only in the sense strand. If a change occurs in the anti-sense strand the mutation is not phenotypically visible. Sense strand base alterations can be inhibited by DNA repair mechanisms. Further single base changes that are synonymous do not change the amino acid due to the degeneracy of the genetic code. Selection in this method allows only for amino acid alterations which restore the activity which is targeted.

The strain to be mutagenised was grown on a plate from a single point inoculum and harvested into 10 ml saline-tween 80 (0.9 % w/v NaCl, 0.1 % v/v tween 80). The spores were warmed to 36-37 °C in a water bath. To check the efficiency of the mutagenesis at this stage, a 10-fold dilution series was performed using the non-mutagenised harvested spores. They were plated out on media containing the required nutrients and dilutions were grown to be counted. 10-20 mg of NTG mutagen was fully solubilised in 10 ml saline-tween 80 and the spores added to the mutagen, and mixed at 2 min intervals over 20 min to avoid spore aggregation. This mix was then centrifuged at 1670 x g for 5 min (Jouan B4 I centrifuge, rotor S40) and the mutagen was removed by 3 sequential washes in 10 ml saline-tween 80. In the final mixture the mutagenised spore suspension was placed in a clean centrifuge tube. The 10-fold dilution series was repeated with the mutagenised cells and dilutions 4, 3 and 2 were plated out to calculate the spore survival rate, which was approximately 0.1 %. The

surviving viable cells were grown at 37 °C for 3-4 days for recovery and conidiation before the survival rate could be established. In all cases spores were plated onto media which, in addition to the required nutrients, also contained 0.08 % w/v deoxycholate as to increase the number of colonies screened per Petri dish. In the case of NitA revertants, mutagenised cells were spread onto minimal media agar at pH 7.5 (Appendix Two) containing 1.5 mM NaNO₂, with vitamins and an additional dose of p-amino benzoic acid. Revertants which grew on this media were then phenotypically assessed against control strains. They were then grown further to obtain DNA to sequence the *nitA* gene for mutants (as described).

For studies on the signalling system, mutagenised cells of strain T19 were plated onto media containing 10 mM proline, vitamins and 0.08 % w/v deoxycholate. Afterwards, the survival rate was calculated and when less than 1 %, colonies were plated onto media to screen for mutants in the nitrate signalling system. This media contained either 10 mM NaNO₃, 10 mM proline with 0.08 % w/v deoxycholate, vitamins and X-Glucuronidase (0.05 mg ml⁻¹) or 3 mM NaNO₂ with 0.08 % w/v deoxycholate, vitamins, p-amino benzoic acid supplements (1 x) and X-Gluc (0.05 mg ml⁻¹).

2.4.15 Generation of mutant amino acid constructs

Warrens *et al.* (1997) describe the method for site-directed mutagenesis by PCR overlap extension. Amino acid mutations were carried out in both NrtA and NitA proteins of *A. nidulans*. Plasmid DNA was amplified in two parallel PCR reactions; the first employing an upstream forward primer with a reverse mutant primer, the second with a complementary forward mutant primer and a downstream non-mutagenic primer (One cycle 98 °C 1.30min, followed by 30 cycles of denaturing 98 °C, 0.10 min; annealing 60 °C, 0.20 min; and, elongation 72 °C, 0.10 min, annealing temperature was occasionally modified for primers with higher annealing temperatures). It was common that these external primers were in the region of a unique restriction site for *nrtA*, primers NrtAF1.2, and NrtAR2.10 located on the *HindIII*, and *NcoI* with forward and reverse primers NrtAF1.7 and NrtAR2.4 both located on the *Sall* restriction site were standard for mutagenesis. These external primers were used in combination with mutant primers described in Appendix Four. For *nitA* mutagenesis, external primers NitAF1.5, NitAR2.1 located on restriction sites *NheI* and *BstEII* respectively and in combination with mutant primers as described in Appendix Four. After the generation of these PCR products they were purified as described, and, the resulting fragments placed together in a third PCR which amplified a final fragment using external primers described. This fragment was then purified from agarose to ensure only one single band for restriction digestion. These mutant fragments were then ligated back into to the plasmid via the selected restriction sites. Successfully cloned mutants were sequenced (as described previously) to

confirm the presence of the intended mutation and to confirm that no other PCR-induced mutations had occurred, the coding region of *nitA/nrtA* were sequenced in full in both plasmid and single copy transformant in all cases.

2.4.16 Net nitrate/nitrite transport assays

Net $\text{NO}_3^-/\text{NO}_2^-$ assays were carried out by the method of Brownlee and Arst (1983), which specifically measures $\text{NO}_3^-/\text{NO}_2^-$ depletion from media, therefore accounts for both influx and efflux reactions vs. actual uptake experiments which measure flux using $^{13}\text{NO}_3^-$. Mutants were grown from a single point inoculum on a Petri dish until growth covered the dish. Half of this growth was used to inoculate 200 ml MM with 5 mM urea and vitamins in a 1 L flask. This culture was grown for 4 h 50 min in an orbital shaker at 37 °C, 200 rpm until germination. After this period, 10 mM NaNO_3 was added to induce the cells over a 100 min period. The flasks were removed from the incubator and a 50 ml aliquot was removed and filtered under vacuum through a pre-weighed Whatman GF/C glass fibre filter. This aliquot was used to measure the dry weight of the cells and was stored overnight at 70 °C to dry. A second aliquot was measured and filtered rapidly through a cellulose acetate filter not allowing compaction of the mycelium. Mycelium were washed with 4 aliquots of 50 ml pre-warmed nitrogen free MM with vitamins. This filter was added to a 250 ml Erlenmeyer flask containing 50 ml pre-warmed MM, with vitamins and 500 μM NaNO_3 . (Net nitrite assays were performed with 100 μM and 2 mM NaNO_2). The flask was then shaken to free the mycelium. A 3 ml aliquot was removed and filtered rapidly through a Whatman GF/C glass fibre filter. The assay flask was then placed in a shaker at 37 °C, 200 rpm. This filtrate was the zero sample, after a 20 min interval a 3 ml sample was removed again and processed as before. For nitrate assays, 50 μl of each filtrate was added to 3 separate test tubes with 950 μl 5 % perchloric acid for absorbance measurements at 204 nm. Based on a standard curve for nitrate uptake was calculated as $\text{nmol mg}^{-1} \text{ ml}^{-1}$. Each assay was carried out at least 3 times with 2 mutants in tandem with a positive (T474) and negative control (T110). For nitrite assays 100 μl indicator solution (50 μl Reagent A (1 g sulphanilamide (BDH) in 100 ml 40 % HCl) plus 50 μl Reagent B (0.1 g N-[1-naphthylene] ethylenediamine (BDH) in 100 ml water) was added to 900 μl of diluted filtrate before being left to incubate at room temperature for 5 min. Absorbance was read at 543 nm and, based on a standard curve for nitrite; uptake was calculated nmol mg^{-1} of dry weight mycelium per hour ($\text{nmol mg}^{-1} \text{ DW h}^{-1}$).

For net nitrate uptake assays, outliers were selected as experiments where the positive or negative controls did not produce the expected result, or, where strains appear to grow well on

solid medium they produced an uncharacteristic lack of uptake, particularly when compared to replicates.

2.4.17 Synthesis and purification of $^{13}\text{NO}_3^-$ tracer

$^{13}\text{NO}_3^-$ was generated by proton irradiation of water at the TRIUMF cyclotron facility at the University of British Columbia (UBC). The tracer was purified of contaminating isotopes ($^{13}\text{NH}_4^+$, $^{13}\text{NO}_2^-$, ^{18}F) (Siddiqi *et al.*, 1989; Kronzucker *et al.*, 1995) and was then (approx. 5 ml) placed in a beaker and 1 ml of 2 M KOH was added and adjusted to pH 11-12. The solution was boiled for 2-3 min to volatilise $^{13}\text{NH}_3^+$ before the addition of 0.2 ml 10 % (v/v) H_2SO_4 (pH of 1-2) to drive off residual NO_x gases. 1 ml of 20 % (v/v) H_2O_2 was added, and the mixture was boiled for 2.5 min. 2 M KOH was then added to neutralise the pH. The mixture was then cooled to room temperature on ice bath. The final pH was approximately 6; this was measured with pH indicator paper (EMD Chemicals, U.S.A.). Finally, 1 ml catalase (Sigma) (2 mg ml^{-1}) was added to the mix to remove residual H_2O_2 .

2.4.18 Reduction of $^{13}\text{NO}_3^-$ to $^{13}\text{NO}_2^-$

A cadmium column was used for the reduction of the $^{13}\text{NO}_3^-$ tracer to $^{13}\text{NO}_2^-$ (McElfresh *et al.*, 1979). The column was washed with distilled water to remove NH_4Cl . On the arrival of the tracer, 1 ml catalase was added (2 mg ml^{-1}) for 2 min to liberate oxygen. The tracer was then applied to the column followed by 25 ml distilled water. The eluate was collected in a beaker below the column and 0.1 ml of 2 N NaOH was added. This mixture was boiled for 2.5 min to liberate residual $^{13}\text{NH}_3^+$. The solution was cooled to room temperature on an ice bath and then pH neutralised with sulphuric acid.

Uptake assays using $^{13}\text{NO}_3^-$ and $^{13}\text{NO}_2^-$ tracers

^{13}N assays were undertaken at UBC using tracers prepared at the TRIUMF cyclotron facility. Synthesis of the $^{13}\text{NO}_3^-$ tracer and influx method have been described before (Siddiqi *et al.*, 1989; 1995; Unkles *et al.*, 2001). Work on the $^{13}\text{NO}_2^-$ tracer will be described here. Growth of strains and assay of nitrate influx at the routine concentration range of 10-250 μM were as detailed in Unkles *et al* (2001).

Mutants for assays were grown from a single point inoculum in two Petri dishes until the growth covered the plates. All of this growth was used to inoculate 200 ml MM with 5 mM urea and vitamins in a 1 L flask. This culture was grown for 4 h in an orbital shaker at 37 °C at 200 rpm. After this period 10 mM NaNO_3 was added to induce the cells over a 100 min period. For nitrite assays, induction was with 5 mM potassium nitrite, with an additional 1 x p-amino benzoic acid for 3 h. The flasks were removed from the incubator and the mycelium

washed with 300-400 ml MM plus vitamins (minus salts) through a sterile Miracloth to remove contaminating inducer. The mycelia were then re-suspended in fresh nitrogen free MM, and aliquoted into 250 ml Erlenmeyer flasks with vitamins. 3 aliquots of 30 ml mycelial suspension were reserved for vacuum filtration through glass fibre filters for the calculation of dry weight. These flasks were incubated in a water bath at 37 °C with shaking at 80 rpm. At time intervals shown in Table 2.2 the flasks were inoculated with stock nitrate or nitrite to bring the medium to concentration followed by an aliquot of the tracer which was of negligible concentration. After 5 min, five 10 ml aliquots were filtered through vacuum filtration units with Whatman GF/C glass fibre filters and washed twice with 200 ml 200 μ M KNO₃ (KNO₂) to remove any unabsorbed tracer from the cell wall. This has been shown to be effective at removing all but miniscule quantities of tracer from both the mycelia and the filters (Unkles *et al.*, 2001). The glass fibre filters were then placed in scintillation vials and radioactivity measured with a Canberra Packard Gamma counter to measure their activity. Three aliquots (50 μ l) of the stock tracer were also taken to measure the specific activity of the tracer. Dry weight was calculated by rapidly filtering three 30 ml aliquots of reserved mycelium in MM through a pre-weighed PVDF membrane (Millipore), this was performed on completion of uptake assay. These were left to dry overnight.

Final concentration (μ M)	250	200	150	100	50	25	10
Add nitrite (min)	0	4	8	12	16	20	24
Take sample (min)	5	9	13	17	21	25	29
Volume of stock (μ l)	100 mM nitrite/nitrate					10 mM nitrite/nitrate	
	157.5	126	94.5	63	31.5	157.5	63
Tracer (ml)	3	3	3	3	3	3	3

Table 2.2 Timetable for ¹³N assays. Due to the short half life of ¹³NO₂⁻ ($t_{1/2}$ = 10 min) a strict timetable was adhered to. At given times nitrite and tracer were added and samples were taken. The assay period was 5 min which was carefully monitored. At all times stock nitrate (nitrite) was added approximately 10 seconds before the addition of tracer nitrite, the time points were counted from the time that the tracer was added.

Values for influx are expressed as nmol mg⁻¹ of dry weight mycelium per hour (nmol mg⁻¹ DW h⁻¹). Influx assays were repeated at least in duplicate. Values of K_m and V_{max} were determined by linear regression of a Hoffstee analysis (v against v/s) with five replicates at each of the seven concentrations used. For each transformant a completely separate experiment was run twice and results were highly reproducible. Michaelis-Menton curves were generated using MicroCal Origin software.

2.4.19 Western blotting

Strains were grown up for Western blotting at least twice independently and the protein extract analysed and compared for consistency. Values for NitA are shown in brackets and NrtA is shown in the main text.

Aspergillus crude plasma membrane preparation

Crude membrane preparations were made as described by Unkles *et al* (2004a), with modifications. Mutants for blots were grown from a single point inoculum on one to two Petri dishes until the growth covered the plates. All of this growth was used to inoculate 400 ml MM with 10 mM proline and vitamins in a 1 L flask. This culture was grown for approximately 5 h 20 min (or longer if necessary to obtain the ideal growth phase) in an orbital shaker at 37 °C at 200 rpm. After this period 10 mM NaNO₃ (10 mM NaNO₂ with 1x p-amino benzoic acid supplement) was added to induce the cells over a 100 min (3 h) period. The mycelia were harvested through sterile Miracloth and washed with cold sterile water, then pressed in paper towels to dry before being frozen in liquid nitrogen in individual 300 mg pouches.

Mycelia (300 mg) were ground to a fine powder in liquid nitrogen and added to 10 ml of cold extraction buffer (NrtA protein extraction buffer, 50 mM sodium phosphate, 300 mM NaCl, 10 % v/v glycerol, 200 mM PMSF, 1 mM benzamidine, pH 7 with protease inhibitor tablet (Roche), NitA protein extraction buffer 20 mM Tris pH 7.5 (at 4 °C), 100 mM 6-amino hexanoic acid, 5 % (v/v) glycerol, 1 mM benzamidine). This was centrifuged at 3000 x g for 15 min at 4 °C in a Sorval SS-34 rotor (Sorval RC-6 plus). The supernatant was transferred to a fresh cold centrifuge tube and was centrifuged at 37,000 x g for 35 min at 4 °C. The supernatant was discarded and the pellet re-suspended in 80 µl cold extraction buffer. This extract was stored at -80 °C until ready for Western blotting.

SDS and blue native PAGE

Aliquots of each protein sample (50 µg) were run 10 % SDS-PAGE gels (see Appendix Five) at 200 V with 1 x sample buffer (60 mM Tris pH 6.8, 25 % v/v glycerol, 5 % w/v SDS, 1 % v/v saturated bromophenol blue) using 1x PAGE running buffer (250 mM Tris pH 8.3, 500 mM glycine, 1 % w/v SDS) with pre-stained protein size markers (New England Biolabs). This gel was then stained with Simply Blue Safe Stain (Invitrogen), following the manufacturer's instructions to ascertain protein load. Once determined, a standardised aliquot of protein (50 µg) was loaded onto a gel for Western blot. Proteins were quantified with more accuracy using the Pierce Protein Quantification BCA kit following the manufacturer's

instructions whereby 50 µg protein aliquots were used as standard for all Western analyses. For Western blotting of NrtA mutants, 10 % SDS-PAGE gels were run as standard. Gels were run with a low range protein size marker (Bio-Rad, Hertfordshire, U.K.) and each sample set was run in tandem with a positive and a negative control.

Sambrook *et al* (1989) discuss fully the theory and methods involved with SDS-PAGE. In SDS-PAGE, SDS is a dissociating agent which is used to coat the protein in charge. SDS denatures the protein's tertiary structure and coats it in negative charge which is in proportion to mass; therefore allows proteins of differing charge to mass ratio run according to their size. Poly acrylamide gel is a synthetic gel which has variable pore size depending upon the concentration of acrylamide and crosslinker (bisacrylamide) used. PAGE is a discontinuous system whereby two gels of different buffered pH are employed to create an ion gradient, the first is known as the stacking gel, and the second, the separating or resolving gel. The function of the stacking gel and the ion gradient is to concentrate the proteins in a thin, sharp band. This is achieved by the preparation of the stack two pH units lower than the separating gel and electrophoresis buffer, also, the large pore size in the stack and small pore size in the separating gel. The running buffer used in PAGE contains glycine which is contains a source of trailing ion (glycinate) which runs behind the slowest of the proteins in the pH range.

For NitA mutants it was necessary to determine their quaternary structure using Blue Native-Polyacrylamide Gel Electrophoresis (BN-PAGE). BN-PAGE refers to an electrophoresis performed using Coomassie blue in cathode buffer. Native gels employ non-denaturing conditions unlike SDS-PAGE gels; therefore separation is based on the protein's native charge to mass ratio. The methodology for BN-PAGE was originally discussed in Schägger and van Jagow (1991) and is further discussed in Eubel *et al* (2005).

In BN-PAGE experiments here the detergent dodecyl maltoside (DDM) was used to lyse lipid membranes, not to provide charge unlike SDS in SDS-PAGE systems. The other noteworthy difference with BN-PAGE is that the running buffer contains Coomassie blue dye which is used to charge the protein for electrophoretic separation (Eubel *et al.*, 2005). In this method the proteins remain in their native state as regards their secondary structure.

The gels for BN-PAGE were prepared using a multi-gel caster with a gradient former (SG Series, Hoeffer Scientific, Holiston, MA, U.S.A.) and a peristaltic pump. The 17 % gel was

loaded into the reservoir furthest from the pump and the 5 % added to the closest reservoir, with the stirrer bar active (in 5 % reservoir) the gel was allowed to mix as it was pumped into the multi-gel caster to create a linear gradient. Gels were overlaid with water-saturated isobutanol to allow polymerisation. BN-PAGE was performed with a different buffering system to that of SDS-PAGE.

Standards and electrophoresis conditions

As there are no internal standards that can be employed for membrane proteins - particularly when studying the quaternary structure - standard proteins are employed as size standards. Proteins used here were maintained at concentrations of 10 mg ml⁻¹, 1 µl of each protein was loaded into one well on a gel with sample buffer (100 mM BisTris (Fluka, Hannover, Germany), 500 mM 6-amino hexanoic acid (Fluka), 5 % w/v Coomassie Blue G250 (Serva, Oxon, U.K.) pH 7) and extraction buffer to run alongside proteins in analysis. The standard proteins were Ferritin from equine spleen (440 kDa), Bovine serum albumin (66 kDa and 132 kDa) and Thyroglobulin from porcine thyroid (669 kDa). Protein extracts were incubated for one hour prior to electrophoresis with 1 % w/v DDM. Once the sample buffer was added they were then loaded into the 4 % stacking gel and run halfway into the separating gel at 100 V using Blue Cathode buffer (15 mM BisTris (Fluka) 50 mM Tricine (Fluka), 0.02 % w/v Coomassie Blue G250 (Serva), pH 7 at 4 °C) and separate anode buffer (50 mM BisTris (Fluka), pH 7 at 4 °C). At this point both the anode and cathode buffers were exchanged for fresh anode and cathode buffers (minus Coomassie) and the gel was then run to the end at 130 V. Once the run was complete, the gel was equilibrated in transfer buffer (25 mM Tris pH 8.3, 192 mM glycine, 20 % v/v methanol, 0.1 % w/v SDS) prior to Western transfer.

Western Transfer

Once protein gels had run they were prepared for Western transfer. Prior to transfer, gels were equilibrated in transfer buffer for 20 min. Hybond-P membranes were used for blotting and the apparatus for transfer was assembled using 3 MM paper and blotting pads. Hybond-P membrane was activated using methanol and equilibrated in transfer buffer. The transfer was performed on ice using a BioRad Mini Protean II system at 100 V for 50 min.

BN-PAGE membranes were washed in PAGE destain (45 % v/v ethanol, 10 % v/v acetic acid) for 10 min prior to washing in TBST (0.9 % w/v NaCl, 10 mM Tris pH 7.4, 0.1 % v/v Tween 20) to remove residual Coomassie blue which has a tendency to quench the reaction from the detection reagents. Membranes were washed for two intervals of 15 min in TBST at room temperature, and then incubated in 5 % block (GE Healthcare membrane blocking agent) in TBS (0.9 % NaCl, 10 mM Tris pH 7.4), overnight at 4 °C. After this incubation the

membranes were washed further in TBST for two periods of 10 min at room temperature. The membranes were then exposed to anti-V5HRP antibody (anti-V5HRP 1/5000 in TBS containing 0.5 % block) for at least 4 hr at room temperature). The probed membranes were then washed in TBST for two periods of 5 min and two periods of 20 min. TBST was drained from the membrane, placed protein side up, and was immersed in ECL plus detection solution (GE Healthcare Buckinghamshire, U.K.). After a 5 min incubation the detection solution was drained off and the membrane was placed in plastic bagging in an autoradiography cassette. A piece of Hyper-film ECL was applied to the gel, initially for a 30 second period though this was altered depending upon the resolution of bands on Hyperfilm ECL.

For this immunological detection an engineered sequence encoding the V5 epitope was fused to the 3' end of the NrtA (and NitA) coding regions (Unkles, unpublished) (refer to Figure 2.1), using an anti-V5 antibody (Invitrogen) proteins on nylon membranes could be immunologically detected when the antibody was used in tandem with a Western blotting detection kit.

2.4.20 Construction of *A. nidulans* cosmid library

An *A. nidulans* cosmid library was constructed using pWEB::TNC™ Deletion Cosmid Cloning Kit (Epicentre technologies). pWEB::TNC cosmid vector was supplied with the cosmid cloning kit. This was altered by the cloning of the *pyroA4* gene from *A. fumigatus* into pWEB::TNC using the unique *EcoRV* restriction site to produce the vector - WEB*pyroA*. This vector was digested using *SmaI* (unique site) to produce a linear vector which was used to carry insert DNA (see below) and packaged as per the Epicentre protocol.

DNA from T110 - which is double mutant in both nitrate transport proteins NrtA and NrtB (*nrtA747*, *nrtB110*) - (grown overnight in 5 mM urea) was extracted using the DNeasy plant mini kit, (Qiagen) including any optional steps to optimise DNA extraction. The DNA was repaired using END-It DNA End-Repair Kit (Epicentre Technologies) following the manufacturer's instructions. This created blunt-ends for efficient ligation into the WEB*pyroA* cosmid vector, approximately 0.3 µg DNA was then ligated into the prepared WEB*pyroA* cosmid vector and transformed into plating cells EPI305.

This cosmid library was created with the intention of transforming it into a 'nitrate signalling system' mutant strain for the identification of the genes involved with signalling.

2.5 Chemicals

All chemicals were supplied by BDH and Sigma unless otherwise stated, and of AnalR, or GPR grade where necessary.

Chapter Three

Mutagenesis of the nitrate signature

3.1 Introduction

Brownlee and Arst (1983) laid the foundations for our current understanding of nitrate transport in *A. nidulans* as presented in Chapter One. Recent work by Unkles and colleagues (Unkles *et al.*, 2004a; Kinghorn *et al.*, 2005; Unkles *et al.*, 2005) has provided insights into important amino acids involved with substrate binding in the high-affinity nitrate transport protein NrtA. The objective of the present study is to delve deeper into the functionality of NrtA, in particular, the first nitrate signature sequence in this protein. An alanine-scanning approach was used initially to target amino acids in this motif followed by additional *in vitro* mutageneses to other amino acids to assess the function of key residues. Alanine scanning mutagenesis is a very simple technique which is widely employed to determine the catalytic or structural contribution of target amino acids in a protein (Lefevre *et al.*, 1997; Dumas *et al.*, 2000; Denker *et al.*, 2005; Guerra *et al.*, 2007). Alanine, as discussed before, is a small, somewhat simple amino acid which does not alter the main-chain conformation of the α -helix unlike some residues of comparable size e.g. glycine and proline. With alanine there are no issues with imbalance of electrostatic charge or steric hindrance (Lefevre *et al.*, 1997). Further, these mutants were biochemically assessed for phenotypic alterations and protein expression in membrane protein extracts.

3.2 Results

3.2.1 Alignments and secondary structure development

An alignment and provisional structure of 52 NNP homologues for prokaryotes and eukaryotes was used as previously published by Kinghorn *et al* (2005). This model was updated by Dr. Mamoru Okamoto using 118 homologous proteins from both prokaryote and eukaryote taxa (Figure 3.1) – a list of accession numbers from these proteins is shown in Appendix Six. In Figure 3.2, an alignment of the NNP signature sequences from NrtA homologues in other organisms is shown along with a neighbour distance cladogram to show the relatedness of these proteins from different species. A second nitrate signature is located in Tm 11 in NrtA (Figure 3.1). This sequence is not as well conserved as the first motif as in MFS signature sequences.

Figure 3.1 Provisional secondary structure representation of the high-affinity nitrate transporter NrtA of *A. nidulans*. This model is based on the original scheme proposed by Kinghorn *et al* (2005), which used model prediction software by Claros and von Heijne (1994) to assess the distribution of both charged and hydrophobic amino acids. This model has been developed to include a larger alignment of 118 homologous protein sequences (Appendix Six). Residues shown in red represent > 95 % conservation in both prokaryotes and eukaryotes, purple > 95 % conservation in eukaryotes, green > 90 % conservation in prokaryotes and eukaryotes and blue > 90 % conservation in eukaryotes. In Lp 2/3 and 8/9 MFS signature motifs are highlighted with yellow dashed lines, in Tm 5 and 11 sequence highlighted in blue indicates the NNP signature sequences discussed. Caution should be exerted when examining the precise location of the membrane domains (Unkles *et al.*, 1991; Unkles *et al.*, 1995; Trueman *et al.*, 1996).

(a)	NNP 1	NNP 2
<i>A. nidulans</i> NrtA	A-A-G-L-G-N-A-G-G-G	V-G-G-F-G-N-L-G-G-I
<i>A. nidulans</i> NrtB	A-G-G-F-G-N-A-G-G-G	V-G-G-M-G-N-F-G-G-I
<i>N. fischeri</i> CrnA	G-G-T-C-G-G-A-G-C-G	G-C-T-C-G-C-T-A-T-C
<i>H. polymorpha</i> YNT1	S-A-G-W-G-N-A-G-G-G	T-G-A-M-G-N-L-G-G-I
<i>C. reinhardtii</i> Nar4	A-A-G-W-G-N-M-G-G-G	V-A-Q-G-L-H-Q-G-S-M
<i>C. reinhardtii</i> Nar5	A-G-G-W-G-N-M-G-G-G	V-A-D-G-L-H-H-T-S-L
<i>E. coli</i> NarU	N-G-G-L-G-N-L-G-V-S	I-S-A-I-G-A-V-G-G-F
<i>E. coli</i> NarK	N-G-G-L-G-N-M-G-V-S	I-S-A-I-G-A-I-G-G-F
<i>A. thaliana</i> Nrt2.1	G-G-A-A-A-T-C-G-A-G	C-C-G-C-G-C-C-A-A-C
<i>T. thermophilus</i> NarK1	L-V-G-L-G-A-T-G-G-	L-A-L-L-L-L-A-L-G-L
Consensus Sequence	A-A-G-X-G-N-X-G-G-G	A-A-G-X-G-N-X-G-G-G

(b)

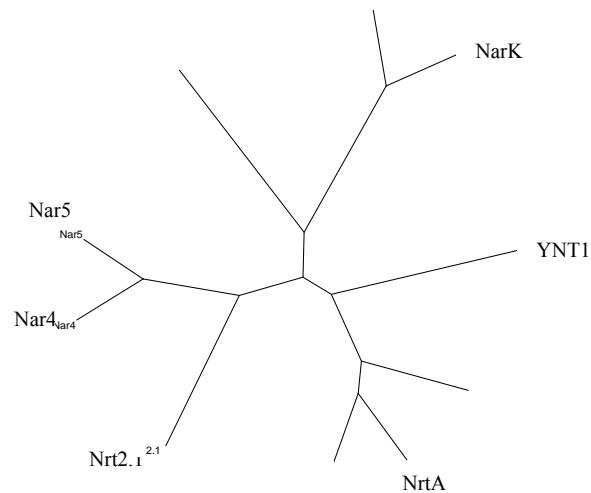


Figure 3.2 Alignment of NNP signature sequences and neighbour joining cladogram of these proteins. (a) Illustrated sequences are from fungi (*A. nidulans*, *Neosartorya fischeri*, *H. polymorpha*), protists (*C. reinhardtii*), bacteria (*E. coli*), plants (*A. thaliana*) and archaea (*Thermus thermophilus*). Regions highlighted in yellow show conservation with the NNP motif (A-A-G-X-G-N-X-G-G-G). Accession numbers P22152, XP_658008, XP_001264479, CAA11229, EDP00896, EDP02491, P37758, CAA34126, NP_172288, CAB65479 respectively. In NrtA this motif represents residues A163-G172 and V454-I463 inclusive. Sequences were obtained by BLASTp using NrtA as an *in silico* probe and then aligned. Data in figure (b) shows neighbour joining cladogram to provide a graphical

representation of the evolutionary relationships of these NNP proteins; branch lengths do not represent evolutionary distance.

3.2.2 *In-vitro* mutagenesis

Mutant plasmids were prepared by site-directed mutagenesis as described in Chapter Two. The sequenced constructs were transformed into the recipient strain (JK1060) and targeted towards the *argB* locus; the phenotypes of the resulting mutants were assessed on MM agar containing 100 mM NaNO₃ as the sole nitrogen source. The reason for using 100 mM NaNO₃ instead of the conventional concentration of 10 mM was that a pronounced phenotype was achieved more rapidly. DNA from these strains was extracted and prepared for Southern blotting. After the identification of single copy strains (Figure 3.3), their purification and phenotypic assessment, the DNA was extracted and the full 1.7 kb *nrtA* gene was amplified by PCR and sequenced to confirm the integrity of the *nrtA* gene. This was confirmed in all cases and the gene was as predicted with no additional mutations. Net nitrate assays were performed on strains which showed growth on 100 mM NaNO₃. The mutant identifiers (transformant numbers), along with phenotypic results, nitrate uptake, and Western analysis data is shown in Table 3.1. Additionally, Western blots were carried out using Anti V5-HRP to detect the N-terminal V5 epitope tag on the mutant NrtA protein.

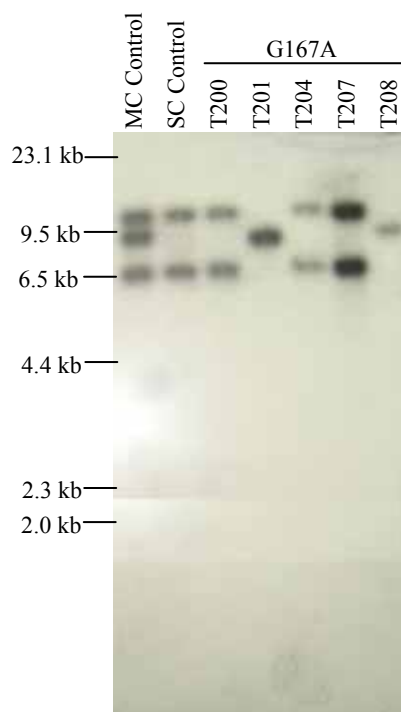


Figure 3.3 Southern Blot of Nitrate Signature G167A mutants. Image shows multi and single copy controls (MC and SC respectively) which were samples from laboratory stocks of historic single and multiple copy strains.

Multiple copy integrations show band sizes of 11 kb, 9 kb and 6 kb, while single copies have only the 11 and 6 kb fragments as discussed in *Section 2.4.12*. DNA marker is representative of λ phage DNA cut with *HindIII*.

In previous work by Kinghorn *et al* (2005) nitrate uptake showed basal uptake in all mutant strains at 3-4 nmol mg⁻¹ DW h⁻¹ accountably for nitrate uptake in the NrtB permease which was functional. Therefore, the wild-type uptake between 10-12 nmol mg⁻¹ DW h⁻¹ was inclusive of NrtB uptake and was therefore 7-8 nmol mg⁻¹ DW h⁻¹ minus NrtB contributions, consistent with nitrate uptake assays performed in this study whereby the double mutant (*nrtA747, nrtB110*) had no nitrate uptake compared to the NrtA wild-type (*nrtB110*) strain which demonstrated uptake of 8.76 ± 2.55 nmol mg⁻¹ DW h⁻¹ as shown in Table 3.1.

3.2.3 Alanine scanning mutagenesis

Though the nitrate signature sequence is proposed to begin at A163 (Kinghorn *et al.*, 2005), the high conservation of residues G157 (99 % conserved in prokaryotes and eukaryotes) and N160 (100 % conserved in eukaryotes) suggest they are essential to this motif (Figure 3.1). Alanine scanning mutagenesis was thus performed on all non-alanine residues in the nitrate signature sequence, including G157 and N160.

Phenotypic studies showed that most residues in the nitrate signature were critical for growth on nitrate (Figure 3.4, Table 3.1). However, altering N160 failed to affect growth on nitrate (Figure 3.4, Table 3.1). Net nitrate assays showed that the nitrate uptake of N160A mutant was 68 % of wild-type (Table 3.1). Expression of the N160A mutant protein was also comparable to wild-type (Figure 3.5). It is notable that in plate growth assays, although the ‘++’ designation of N160A is akin to L166A, N160A appeared to conidiate and grow at a slightly faster rate than L166A on agar (Figure 3.4). Mutant G171A shows very poor growth on nitrate, this is reflected in the very low uptake of nitrate in this strain relative to the wild-type value (Table 3.1). Western blot analysis of G171A showed wild-type level of expression of protein which was smaller than that of the wild-type band by ~10 kDa (Figure 3.5). The remaining mutants do not show growth on nitrate, protein expression was variable and in most cases the band was 10 kDa smaller than wild-type (Figure 3.5).

Mutant	Transformant No.	Codon Change	Side Chain Alteration	Phenotype			Nitrate Uptake (nmol min ⁻¹ mg ⁻¹ DW)	Expression	Main Band Size (kDa)
				Chlorate	25 °C	37 °C			
WT	T474	N/A	-	-	+++	+++	8.76 ± 2.55	Good	45
<i>ΔnrtA</i>	T110	Δ	-	+++	-	-	-0.01 ± 0.86	Poor	0
G157A	T1065	GGG → GCA	Conservative	+++	-	-	ND	Moderate	35
N160A	T2250	AAC → GCC	Volume reduction	+++	++	++	5.94 ± 2.42	Good	45
G165A	T504	GGT → GCC	Conservative	+++	-	-	0.27 ± 1.02	Moderate	35
L166A	T2458	CTA → GCA	Volume reduction	+++	++	++	3.28 ± 0.67	Poor	35
L166F	T5	CTA → TTC	Volume increase	+++	++	++	1.80 ± 1.02	Poor	ND
L166T	T3240	CTA → ACA	Non-polar → polar	+++	++	++	ND	ND	ND
L166W	T782	CTA → TGG	Large volume increase	+++	++	++	2.99 ± 0.77	Poor	ND
G167A	T200	GGT → GCC	Conservative	+++	-	-	ND	Moderate	35
N168A	T2726	AAC → GCC	Volume reduction	+++	-	-	ND	Poor	35
N168S	T1352	AAC → TCC	Slight volume reduction	+++	-	-	ND	Good	35
N168L	-	AAC → CTC	Polar → non-polar	+++	-	-	ND	ND	ND
N168Y	T1421	AAC → TCC	Volume increase	+++	-	-	ND	Poor	35
G170A	T1707	GGT → GCC	Conservative	+++	-	-	ND	Good	35
G170N	T1622	GGT → AAT	Volume increase	+++	-	-	ND	Poor	ND
G171A	T100	GGC → GCT	Conservative	+++	+	+	0.56 ± 0.38	Good	35
G172A	T2525	GGT → GCC	Conservative	+++	-	-	ND	Good	35

Table legend on the following page.

Table 3.1 Details of mutations in the first nitrate signature sequence of NrtA. The mutants are given along with their transformant numbers, and codon changes. Transformant number is not specified for mutant strain N168L as it is in the process of being sequenced. A general comment about the mutation is made in each case. Where 'conservative' is stated, the change does not alter the charge or the size of the amino acid significantly. Size and charge alterations are noted along with 'SH', whereby the amino acid is altered with the addition of a sulfhydryl group. Phenotypes '+' represents slight growth, '++' less than wild-type and '+++ wild-type, and '-' no growth. Growth tests for nitrate were performed on MM (pH 6.5) with 100 mM NaNO₃ as the sole source of nitrogen and vitamin supplements for 2 days at 37 °C (or 25 °C for temperature sensitivity testing). Chlorate resistance was tested on MM with 10 mM proline, vitamins and 150 mM sodium chlorate, at 37 °C for two days, while the wild-type is shown to be '-' here it could be leaky on occasion, as such a non-transformed wild-type (G01) was used as the control which was consistent in its lack of growth on chlorate. Net uptake experiments were performed only on strains which produced appreciable growth on 100 mM NaNO₃ agar plates (+ → +++). Where 'ND' is shown nitrate uptake assays were not performed for these mutants and as such uptake was not determined. Young conidiospores were grown for uptake assays to germination in 5 mM urea as the sole nitrogen source and induced with 10 mM NaNO₃ for 100 min. Outliers were excluded from the data set. For each nitrate uptake experiment, at least three uptakes were performed, standard deviations are shown. Western blots were carried out on membrane protein fractions which were extracted from cells which had grown to germination in 5 mM urea with vitamins, then induced for 100 min with 10 mM NaNO₃. Approximately equal concentrations of protein were loaded onto these gels and as such an approximate measurement of expression is given here as 'poor', 'moderate' or 'good' by comparison to the wild-type transformant representing: little to no expression, expression of around half of the wild-type and wild-type expression respectively, there is no internal control for membrane proteins used currently. Most proteins expressed were approximately 10 kDa smaller than the wild-type this shall be discussed though sizes are noted here. In addition to *nrtA* mutations described all strains were *nrtB*. Refer to Appendix One for a full overview of amino acid structure and charge.

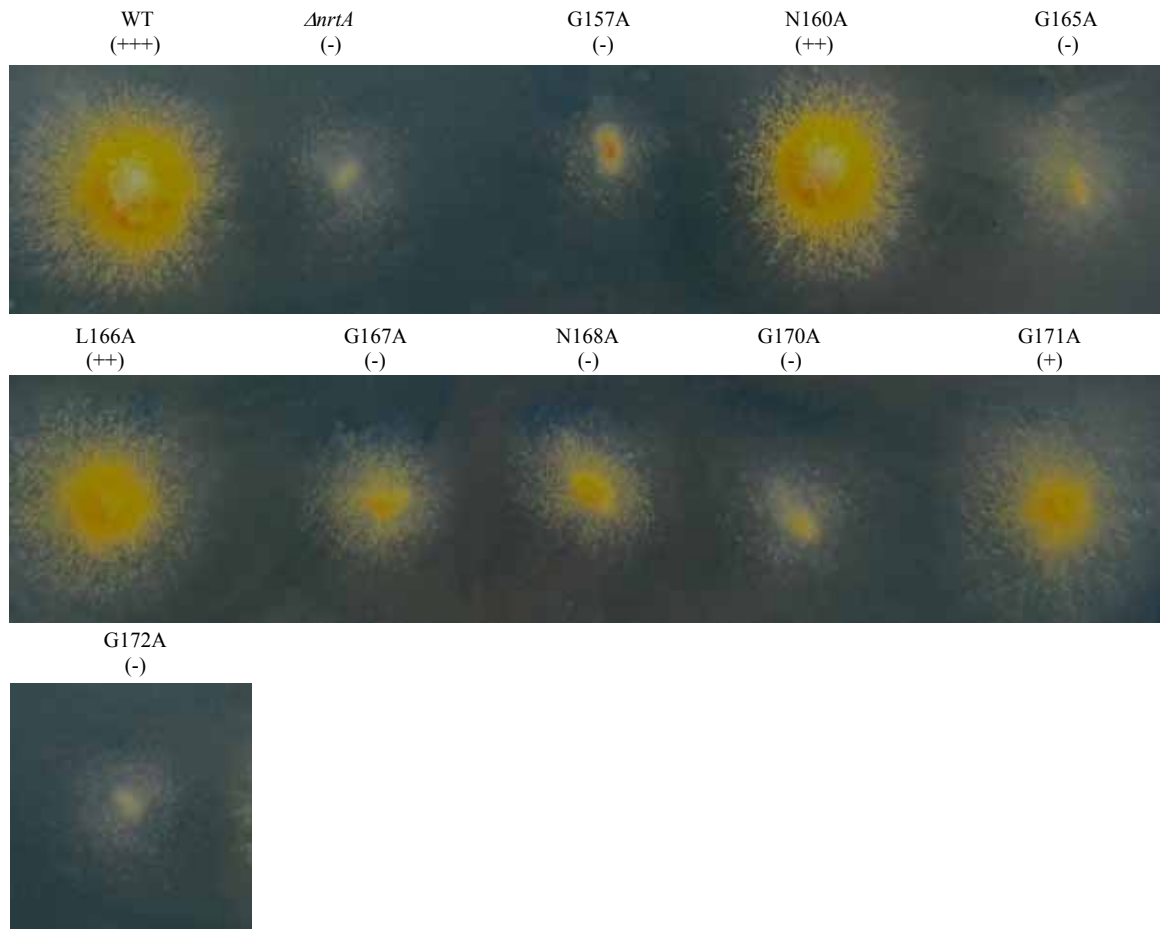


Figure 3.4 Phenotypes of ‘alanine scanning’ mutants in the first nitrate signature sequence of NrtA. Phenotypes were assessed on MM (pH 6.5) containing 100 mM NaNO₃ as the sole nitrogen source with vitamins supplements. Growth was allowed for 2 days at 37 °C. Wild-type strain shown here, and in all cases of phenotypic assessment, was a wild-type transformant strain produced in the same way as the mutant strains that are compared directly to it. Grading shown here are on the same scale as those in Table 3.1.

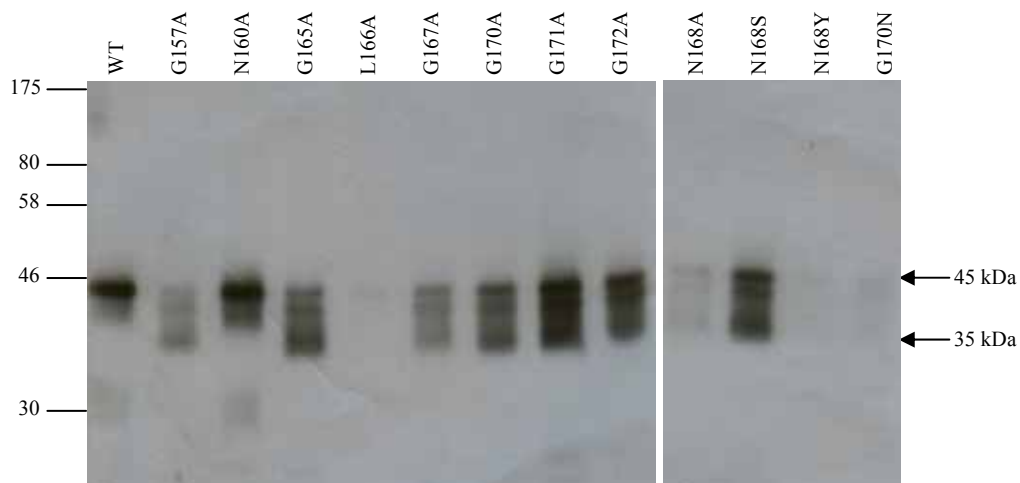


Figure 3.5 Expression of mutant proteins in the first nitrate signature of NrtA as shown on 10 % SDS-PAGE, Refer to Section 2.4.19. Conidiospores for Western blots were grown initially in 5 mM urea, followed by 100 min with

10 mM nitrate induction prior to being harvested and prepared for Western blotting. Anti-V5 antibody was used to probe blots. The wild-type band is approximately 45 kDa with mutant strains showing bands of varying levels though the majority show a smaller band of approximately 35 kDa. Molecular marker is shown in kDa. Western blots were carried out using crude membrane protein extracts from two independent growths.

This series of alanine replacement mutant strains revealed largely non-complementing strains, i.e. those which did not produce growth on nitrate. While net nitrate assays were not performed routinely on these strains, G165A was subjected to a set of assays, which confirmed the lack of nitrate uptake expected with this strain (Table 3.1).

3.2.4 Further mutagenesis of G170

Further to the alanine scanning mutagenesis of residue G170 (98 % conserved in eukaryotes and prokaryotes) an additional mutation of G170N was examined. Growth studies with nitrate (100 mM) showed that mutagenesis to asparagine gave no growth on nitrate (Figure 3.6). Poor level of expression was observed for G170N implying that this protein had not been inserted into the membrane (Figure 3.5).

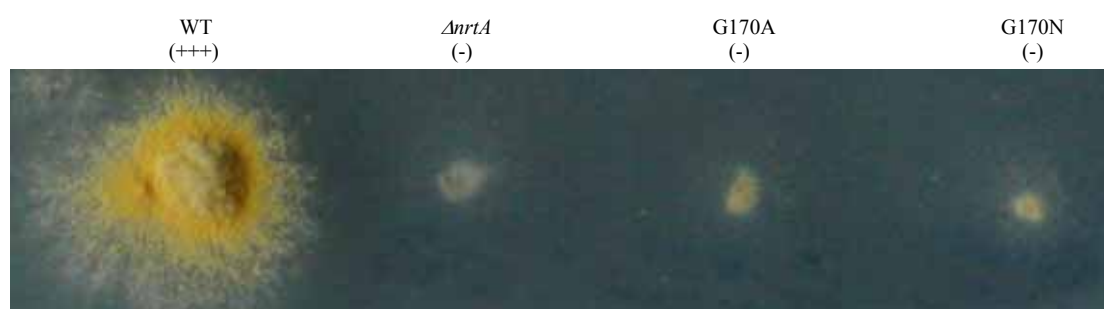


Figure 3.6 Phenotypes of G170 mutants in the nitrate signature sequence of NrtA. Phenotypes are assessed here as described for Figure 3.4. Grading shown here are on the same scale as those in Table 3.1.

3.2.5 Further mutagenesis of L166

Mutation in this position to alanine showed no particular detriment to the phenotype of the transformant with growth comparable to wild-type (Figure 3.7). Phenotypes of all L166 mutations are shown (Figure 3.7). Net nitrate uptake was approximately half of the wild-type for mutants L166F and L166W (Table 3.1). Expression profiles of the mutants showed a 35 kDa band for L166A at levels < 5 % of wild-type and L166F and L166W were expressed to similar levels (data not shown). Initial phenotypic assessment of L166T agrees with alanine, phenylalanine and tryptophan results though nitrate uptakes and Western analysis were not performed on this strain. Km and Vmax were not calculated for any L166 mutants since they are unlikely to be involved with substrate interactions and should not alter enzyme kinetics.

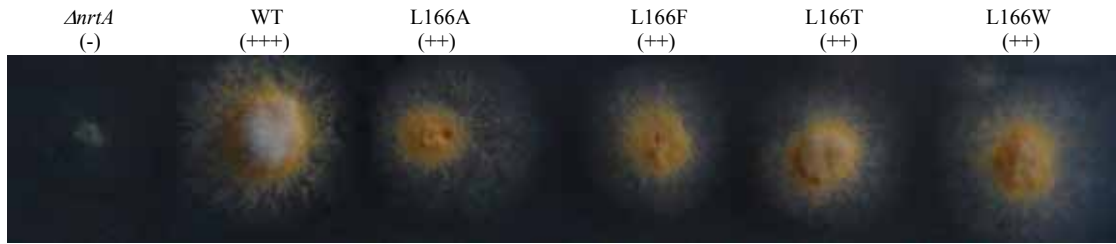


Figure 3.7 Phenotypes of L166 mutants in the nitrate signature sequence of NrtA. Phenotypes are assessed here as described for Figure 3.4. Grading shown here are on the same scale as those in Table 3.1.

3.2.6 Further mutagenesis of N168

When N168 was altered to alanine, serine, lysine and tryptophan no growth was observed on nitrate (Figure 3.8). In addition, Western analysis showed a 35 kDa band as for many other mutants (Figure 3.5). N168A and N168Y showed approximately 5 % of wild-type protein expression whereas expression of N168S was similar to wild-type (Figure 3.5). Caution should be exerted over the N168L phenotypic result as sequencing of this mutant is ongoing as a result of time constraints; this result of non-growth on nitrate is in agreement with other mutagenesis performed on this residue.

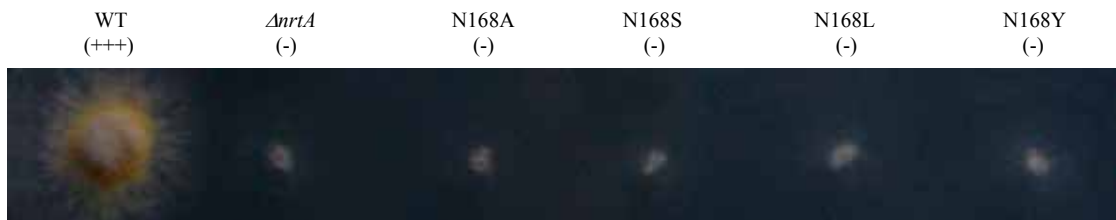


Figure 3.8 Phenotypes of N168 mutants in the first nitrate signature sequence of NrtA. Phenotypes are assessed here as described for Figure 3.4.

3.2.7 Chlorate and temperature sensitivity testing

All mutants in this study were tested on MM with 150 mM sodium chlorate with 10 mM proline as the sole nitrogen source. All mutants grew well on chlorate. Further to this, all mutants were assessed for growth at 25 °C on nitrate as the sole nitrogen source, and without exception showed growth at 37 °C (Table 3.1).

3.3 Discussion

Chemical mutagenesis has highlighted the first nitrate signature as a particular region susceptible to change, stressing the need for particular residues, and, the potential requirement for tight packing in this region (Kinghorn *et al.*, 2005). Most likely a structural role is performed, particularly by N168 and glycine residues (i.e. G157, G160, G165, G170, G171,

and G172). Phenotypic analysis showed that mutation in the first nitrate signature was not well tolerated (Figure 3.4), as expected from the high conservation of these residues and previous chemical mutagenesis work (Kinghorn *et al.*, 2005). The only glycine change which was tolerated was G171A which grew weakly on nitrate agar but showed negligible levels of nitrate uptake ($0.56 \pm 0.38 \text{ nmol mg}^{-1} \text{ DW h}^{-1}$) and was expressed (35 kDa) to wild-type levels (Figure 3.4). Work by Kinghorn *et al.* (2005) is in agreement with mutations in positions G157 (arginine and glutamic acid), G170 (arginine, serine and tyrosine) and G172 (serine) all of which showed no nitrate uptake. However, some mutants made by Kinghorn *et al.* (2005) (G167S, G170C, G172D and G172C) showed uptake at 50 % of wild-type level illustrating a certain need, but not essential requirement, for these residues i.e. G167, G170 and G172 (Table 1.1). It is notable that G172 seems to be more tolerant to change particularly to negatively charged aspartic acid. In all mutants from the study by Kinghorn *et al.* (2005) mentioned here, the protein was expressed as wild-type in both size and expression levels.

The asparagine residues in the NNP motif are highly conserved and were thought to play an important role in substrate binding or translocation (Unkles *et al.*, 2004a). When N160 was altered to alanine, the mutant displayed wild-type growth (Figure 3.4) and uptake ($5.94 \pm 2.42 \text{ nmol mg}^{-1} \text{ DW h}^{-1}$, Table 3.1). This makes it unlikely that this residue contributes to protein function or stability as the 40 % reduction in amino acid side-chain volume is quite significant. Ideally, further mutagenesis to alter the charge of this residue would be performed to establish a specific requirement at this position; it is unlikely that there is a particular space constraint due to its position on an extra membrane loop domain. Conversely, N168 seems to be crucial for protein function (Figure 3.8). Protein expression studies of mutants N168A and N168Y was poor whereas expression of N168S was shown to be approximately wild-type (Figure 3.5); although none of these mutants produced growth on nitrate (Figure 3.8). The construction of N168 mutants was also carried out by Unkles *et al.* (2004a), who showed that the mutations N168C, N168Q and N168R all failed to grow on nitrate though were expressed to wild-type levels in the membrane. It seems that this asparagine at N168 is critical for function, as conservative mutations such as glutamine and leucine were not tolerated. In the second nitrate signature motif of NrtA, asparagine has been shown to replace the charge of R87 (R87T) in reversion studies when mutated to lysine (N459K), revealing that these residues are close together in the folded protein (Unkles *et al.*, 2004a). These studies were also confirmed by site-directed mutagenesis (Unkles *et al.*, 2004a). However, site-directed mutagenesis which essentially created the same mutants in the first signature (i.e. N168K/R368T instead of N459K/R87T) did not produce transformants on nitrate showing a lack of symmetry in this instance. Work on LacY has shown apparent structural symmetry of these MFS proteins which is not reflected in function. Suppressor

analysis frequently reveals compensatory amino acids in the opposing half of the protein, revealing a structural symmetry. As regards function, Tms 2, 7 and 11 in LacY are more sensitive to mutation and/or seem to show an increased necessity for specified residues reflecting a functional asymmetry (Green *et al.*, 2003). The replacements discussed here for N168, seem to disrupt the protein as no growth is observed on nitrate (Figure 3.8) where expression is wild-type in N168S, the size of the protein is 10 kDa less than that of the wild-type, whether this is the contributing factor to lack of nitrate uptake in these mutants is uncertain and further analysis on these mutants is necessary. It is likely that as with the other residues in this region the asparagine contributes to protein stability whereas substrate interaction is improbable since no current mutations have been found which can partially substitute at this position to result in altered kinetics.

At the beginning of this work it was postulated that in the heart of the nitrate signature where the small glycine residues are perhaps working as a cushion for a highly conserved asparagine residue, L166 could be helping to provide stability to aid substrate translocation. The positioning of L166 relative to asparagine and the corresponding residues in the second nitrate signature are illustrated in Figure 3.9. L166 is not known to be highly conserved and was investigated to understand the essentiality of side-chain bulk at this position – the data in Figure 3.7 show the phenotypes of L166 mutants. In eukaryotic homologues, tryptophan is conserved in position 166 in 96 % of sequences; leucine and phenylalanine make up the remaining 4 %. Thus, it seems likely that side-chain bulk is essential at this position in homologues even if the side-chain of leucine is considerably smaller than that of tryptophan, it is, what might be regarded as a medium sized amino acid with a side-chain volume of 114 (tryptophan is 187) compared with alanine (72) and threonine (102) for example. However, mutants in this residue, all of which cause side chain volume alteration were shown not to be critical for function, only reducing net nitrate uptake slightly (Table 3.1 and Figure 3.7). This is probably as a result of minor structural alteration though expression in these mutant strains was low relative to wild-type (Figure 3.5). This result is unusual considering the net nitrate uptake in these mutants; this reduction in expression could be accountable for the reduction in uptake. It would seem that this residue plays no crucial role in substrate binding and translocation. It is possible that a minor degree of structural stability is provided by this residue, though it is not essential for function. The expression of this mutant is problematic: when altered, the mutant protein is seemingly cleaved as in other mutants in this region and it is expressed to reduced levels. This suggests that the protein is not reaching the membrane and after attempted insertion, or incorrect folding after insertion, the protein is targeted by the proteasome. Future work should establish the final expression characteristics of the mutants, particularly as regards degradation.

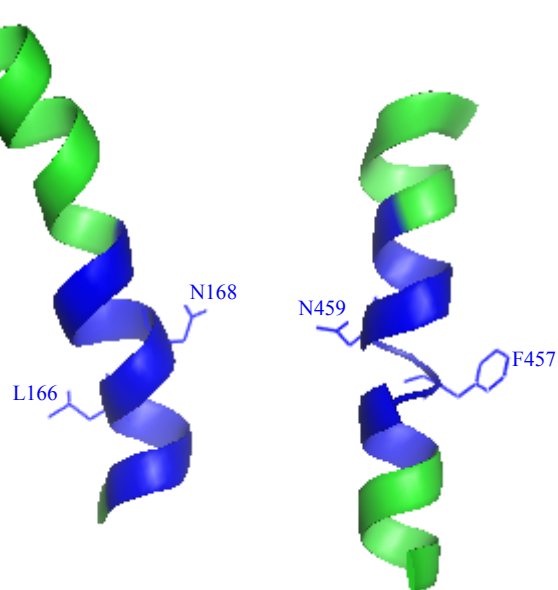


Figure 3.9 Modelling of NrtA based on GlpT. Positions of non-conserved residues in the NNP binding sites relative to residues thought to be important with substrate binding are indicated. Nitrate signature motifs are shown in blue, whilst the remaining sections of the helices are shown in green. Only Tms 5 (left) and 11 (right) are shown in this diagram for clarity. This model was built using the inward facing conformation of the MFS GlpT transporter from *E. coli* as a template in collaboration with Dr. S.E. Unkles and Dr. J. Perry. This figure was prepared using PyMOL version 0.99 (Delano, 2002).

The first nitrate signature is clearly intolerant of change (Figure 3.4). However, the second nitrate signature appears to be more malleable and mutagenesis performed thus far has largely produced complementing mutants (data not shown). This asymmetry reflects possible neofunctionalisation of this motif following its duplication from the progenitor. It also appears from this alanine scanning mutagenesis, in addition to other mutagenesis performed here, that the first NNP signature motif plays a structural role in ion translocation. This fits with previous discussions by Kinghorn *et al* (2005). It will be necessary to employ alanine scanning in this entire Tm.

The model shown in Figure 3.10 serves as an illustration of the relative positions of the transmembrane domains in NrtA. In collaboration with Dr. S. E. Unkles and Dr. J. Perry 3D modelling of NrtA based on GlpT will be developed to include the results here along with further developments in parallel projects. Figure 3.8 shows the relative positions of L166 and N168, and N459 and the NNP 2 counterpart of L166 (F457). Modelling of NrtA, in particular the binding site is discussed further in Chapter Four. Figure 3.10a shows the protein in the closed, inward facing, conformation as viewed from outside the cell. Note that Tms 2 and 8 seem to allow a passage for substrate through the bilayer, as viewed from inside the cell

(Figure 3.10b) Tm 5 and 11 lean in towards each other, presumably helping in the coordination of the substrate providing support to Tm 2 and 8 which are more widely spaced in relation to the cavity, this assumption should be confirmed by measurements of the binding site which will come from the ongoing project of CSM. As discussed in the Introduction, membrane proteins are not rigid in the bilayer and are often bent. This is illustrated here for Tms 1, 4, 10 and 11 (Figure 3.10). Differences in substrate structure for GlpT and NrtA are illustrated (Figure 3.11).

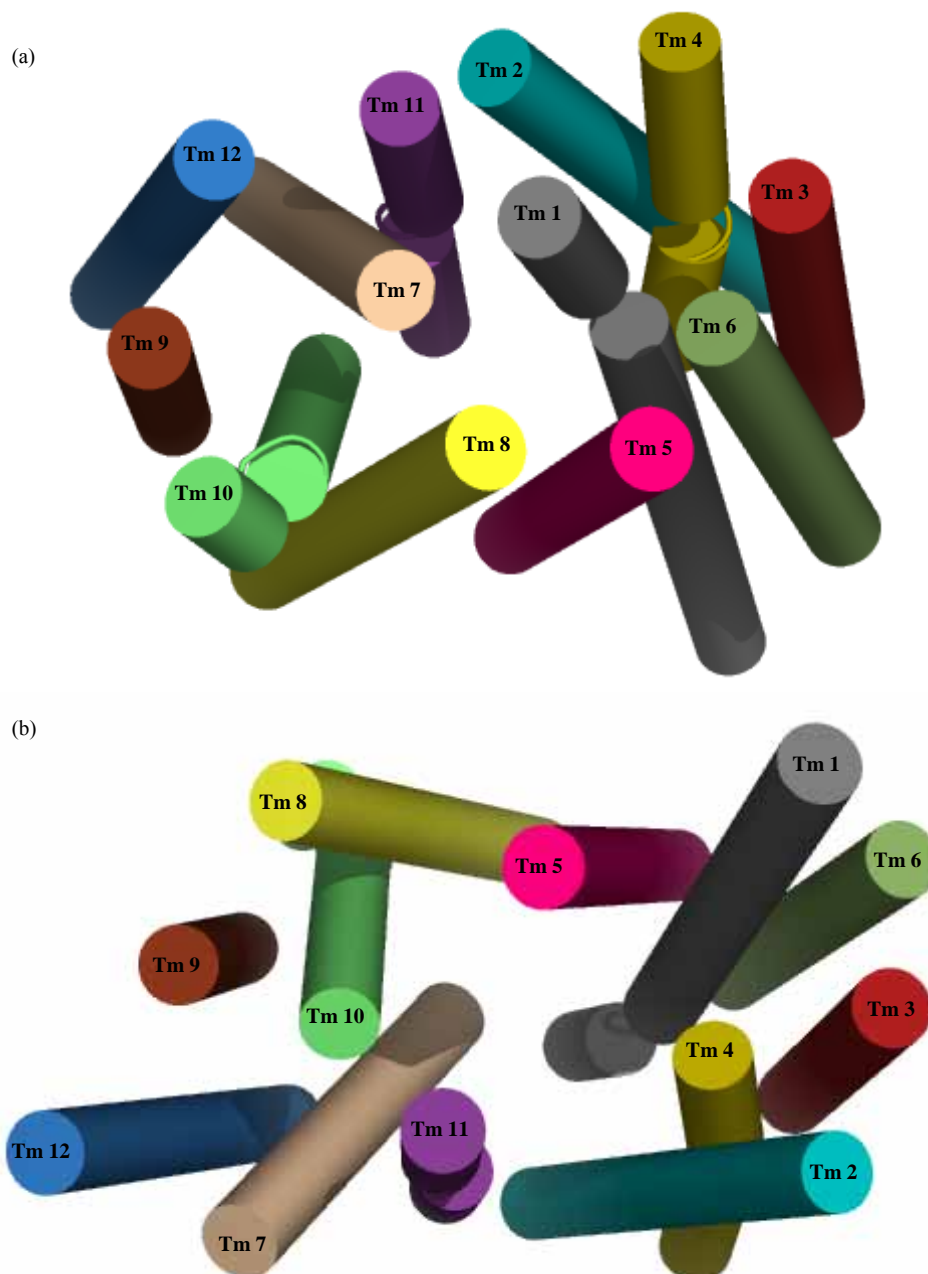


Figure 3.10 Trans membrane domains of NrtA in closed conformation. Domains are coloured individually with their domain numbers (a) Viewed from extra-cellular environment and (b) from inside the cell. This model was built using the inward facing conformation of the MFS GlpT transporter from *E. coli* as a template and was prepared using PyMOL version 0.99 (Delano, 2002).

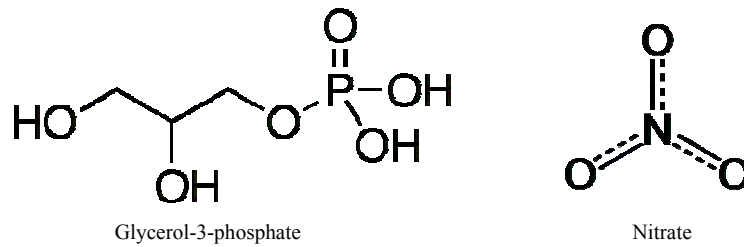


Figure 3.11 Structural comparisons of glycerol-3-phosphate and nitrate.

In this current study, Western blotting results were unexpected since the majority of the mutant proteins were ~10 kDa smaller than wild-type (Figure 3.5). This also occurred in mutants studied in the nitrate binding site (Chapter Four). This phenomenon has not been observed in previous mutageneses of NrtA (*Kinghorn personal communication*). To test whether the apparent cleavage is as a result of the denaturing conditions or a factor of the protein, future work would aim to analyse these proteins using non-denaturing gels. It is possible that the protein was cleaved at the N-terminal but remained functional in some cases e.g. L166 mutants. If mutations have interrupted the protein so that folding or membrane insertion were affected then the protein would be degraded by the cell. As the membrane preparations were crude extractions then the band observed may be an incomplete protein located elsewhere in the cell that may not have reached the cell membrane. A further investigation with pure plasma membrane protein extracts might provide an answer. This method requires a high concentration of protein and thus is ineffective for proteins expressed at sub-wild-type levels. An alternative method such as trypsinolysis could be employed whereby the mutant protein, due to its supposed misfolding, should be more susceptible to proteolysis and when separated on SDS-PAGE the band would be further digested or absent depending on the incubation period. Guerra *et al* (2007) carried out a similar experiment on alanine scanning mutants from the M8 domain of the H⁺-ATPase Pma1 from *S. cerevisiae*. These mutants were expressed to varying degrees in the post-Golgi secretory vesicles and had been constructed to prevent plasma membrane fusion using a temperature-sensitive block (Guerra *et al.*, 2007). Mutants were expressed < 10 % of wild-type protein levels and the authors suggested that this was due to misfolding. This theory was tested by trypsinolysis and since mutants were trypsin sensitive the targeted residues were probably important for permease folding (Guerra *et al.*, 2007).

In LacY, residues E126 and R144 of helices 4 and 5, were found to be crucial for transport, potentially through the stabilisation of the binding site or a direct interaction with the substrate (Frillingos *et al.*, 1997). R144 is also critical for substrate binding in LacY (Frillingos *et al.*, 1998; Kaback & Wu, 1999; Kaback *et al.*, 2001; Vazquez-Ibar *et al.*, 2004; Kaback, 2005;

Mirza *et al.*, 2006). Thus, this region's importance may also be reflected in a similar role in NrtA. While the role of Lp 4/5 may have differentiated during evolution of MFS proteins it can be speculated that its necessity holds true for different substrates. On the completion of this current project focussing on the second nitrate signature, should *a priori* further an understanding of these key motifs.

It is noteworthy that a factor affecting protein transcription would be the sequence of the promoter. In this mutagenesis - and in mutageneses discussed in Chapters Four and Five - mutants were made in V5TAGAGE/1 (Section 2.2, Figure 2.1) before being ligated into V5M which contained the *nrtA* promoter sequences, thus the potential for generating mutant promoters was negligible. Another avenue for future work would be to conduct Northern Blots to analyse the expression of these mutant genes, though it is expected that they would be wild-type, it may be necessary to confirm this.

Results from growth on chlorate, while difficult to explain, do allude to the complexity of this system. In strains which show growth on nitrate, growth on chlorate is wild-type. Chlorate, once taken into the cell is toxic, thus it cannot be uptaken in these mutants. Chlorate as a molecule is similar in structure to nitrate though it seems that the permease interacts differently with chlorate than nitrate (Figure 3.12). With chlorate the lone pair of electrons is likely to interact where nitrate cannot and vice versa, due to the imbalance in charge whilst in the nitrate molecule charge is evenly distributed. The lone pair from chlorate could potentially provide extra attraction to positive sites and thus have a propensity to form bonds to the chlorine atom over the nitrogen atom, this could lead to tight bond formations which may prevent release of the ion on translocation and hence prevent toxicity. There are currently no plans to investigate this further though as stated it highlights some of the intricacies of this system.

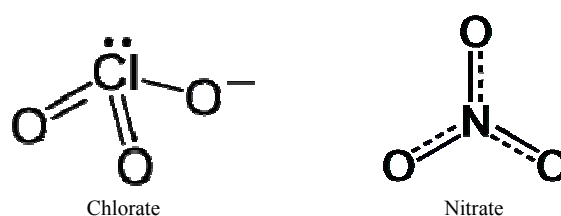


Figure 3.12 Structural comparisons of chlorate and nitrate.

3.4 Summary

This study has shown the importance of a high density of glycine residues in the first nitrate signature motif of NrtA. This may be significant for the close compaction of this region in

reference to substrate binding and translocation. This domain may also be involved in a structural capacity and aid protein folding. The highly conserved asparagine (N168) was shown to be important at some stage of activity, most likely providing support to the cavity and reacting residues. As suppressors of this residue were not found in previous studies (Unkles *et al.*, 2004a) to reflect symmetry of function with N459 in Tm 11 it is suggested that functional asymmetry exists in NrtA as has been observed for LacY. The non-conserved amino acid, L166, does not appear to perform the structural role initially thought as a result of near wild-type growth and nitrate uptake shown in mutants. Expression studies showed an unexpected protein of reduced size in many cases which will clearly require further investigation.

Chapter Four

Studies of the nitrate binding site

4.1 Introduction

4.1.1 Background

When studying an anion transporter, it is necessary to observe how that anion interacts with the permease and how it is taken from the cytoplasm across the membrane. During translocation in MFS proteins, it is thought that the anion moves through a binding site, a core which is alternately accessible from either side of the membrane (Jardetzky, 1966; Abramson *et al.*, 2003b; Abramson *et al.*, 2004; Unkles *et al.*, 2004a). In *A. nidulans* NrtA, the interaction of two perfectly conserved arginines with the substrate has been shown (Unkles *et al.*, 2004a). With regard to the NarU protein in *E. coli*, it was also found that charged arginine species (R87 and R303) are involved directly in nitrate and nitrite transport. NarU is responsible for both nitrate import and nitrite export in the bacterium (Jia & Cole, 2005).

4.1.2 Previous mutagenesis studies of NrtA

Comparison of crystal structures of MFS proteins has shown that Tm helices 1, 2, 4, 5, 7, 8, 10 and 11 are the most likely domains to form the translocation pore in NrtA (Unkles *et al.*, 2004a). While Tms 3, 6, 9 and 12 are embedded in the membrane performing a structural role. As a result, these domains are unlikely to contribute to the substrate binding site in NrtA due to their positioning on the outskirts of the folded protein (Kinghorn *et al.*, 2005). The conserved arginine residues (R87 and R368) from Tms 2 and 8 were altered in accordance with size, hydrophobicity and side-chain bulk, it was shown that these residues are functionally important, but not mandatory in NrtA (Unkles *et al.*, 2004a). While an isofunctional mutation to lysine at position 87 demonstrated a decrease in substrate affinity, a loss-of-charge mutation in position 87 (or 368) ablated function completely (Unkles *et al.*, 2004a). It was concluded that side-chain charge was essential for NrtA activity and that side-chain size also contributed to function (Unkles *et al.*, 2004a). It is thought that R87 and R368 interact directly with the substrate during translocation (Unkles *et al.*, 2004a). Putative salt-bridge partners were also investigated for R87 and R368 that would act as stabilisers for their charges, although none were proved to be mandatory (Unkles *et al.*, 2004a). It was suggested that the substrate could act as a dynamic salt-bridge as it passes through the binding site (Unkles *et al.*, 2004a). Unkles and colleagues also included a second site suppressor study using mutant strains R87T and R368T as the host strains. R87T (Tm 2) gained a mutation in

the second nitrate signature, namely N459K (Tm 8), replacing the charge of the absentee arginine i.e. R87 (Unkles *et al.*, 2004a). This change implied that these helices were in close proximity to one another. As this suppressor was generated, it had to be involved in making the substrate binding site accessible to the nitrate molecule since this strain (i.e. R87T N459K) was functional for nitrate uptake (Unkles *et al.*, 2004a). An *in vitro* study changing N459 to arginine in an otherwise wild-type *nrtA* construct reported loss of function (Unkles *et al.*, 2004a). However, this is probably a reflection of space constraints in this region, illustrated by the prevalence of small glycine residues. This result was in agreement with crystallography data on MFS proteins (Abramson *et al.*, 2003b; Hirai *et al.*, 2003; Huang *et al.*, 2003). Growth is not supported in other mutations at N459, again showing its importance to NrtA function (Unkles *et al.*, 2004a). On the opposite side of the pathway, Tm 5 and 8 form the mirror image to Tm 2 and 11. However, conservative mutations to lysine and arginine of the N459 counterpart, N168, failed to compensate for the R368T change in Tm 8 (Unkles *et al.*, 2004a). This functional asymmetry has been previously reported for LacY (Green *et al.*, 2003).

Here, T83 and N364 present respectively above R87 in Tm 2 and R368 in Tm 8 of NrtA were targeted by mutagenesis to investigate their involvement in the nitrate binding site of NrtA. It was thought that these polar amino acids, may contribute to hydrogen bonding with the substrate as it passes through the binding site. Additionally, the positioning of both of these residues and the conserved arginines was investigated.

4.2 Results

4.2.1 Single mutant strains

Mutant plasmid constructs were prepared by site-directed mutagenesis, followed by the selection, sequencing and phenotypic assessment of purified single copy transformants as described previously in Section 3.2.2 and example shown in Figure 3.3. Mutants were prepared to the same standard i.e. all single copy mutants were successfully sequenced with no additional mutations. Mutant positions in relation to other Tms are shown in Figure 4.1 and results of the single site mutagenesis approach are reported in Table 4.1. Mutagenesis of T83 to A, Q, R, S, and V accounted for conservative change, along with an increase in size and the inclusion of a full positive charge in the case of arginine mutants. T83Q, R and V showed no growth on 100 mM NaNO₃ (at 37 °C and 25 °C) whereas T83A and S showed moderate growth (scores of + and ++ respectively vs. +++ of the wild-type) (Figure 4.2). Net nitrate uptake assays were performed on T83A and T83S which were approximately 50 % of wild-type uptake (Table 4.1). Expression of the mutant protein was assessed in these strains as

before, using the anti-V5 HRP antibody (Invitrogen). As in Chapter Three, the band generated for strains expressing mutant plasmids was approximately 10 kDa smaller than the wild-type, hinting at protein cleavage. However, a faint wild-type band was apparent in mutants T83 A, Q, R and V (Figure 4.3).

4.2.2 Multiple mutants in the *NrtA* binding site

Next, multiple mutant constructs were sought, to investigate the importance of the polar residues above the conserved arginine in the *NrtA* binding site. A double mutant, which switched the positions of T83 and R87 (i.e. T83R R87T) showed loss of function, further the complementary positions in the second half of the protein were also exchanged (i.e. N364R R368N). The quadruple mutant strain (T83R R87T N364R R368N) was shown to produce no growth on 100 mM NaNO₃ (Figure 4.4). A double mutant in the second half of *NrtA* (N364R R368N) was not constructed due to time constraints. The hypothesis for reorganising all four positions was to allow for space as shown for *NrtA* previously (Unkles *et al.*, 2004a).

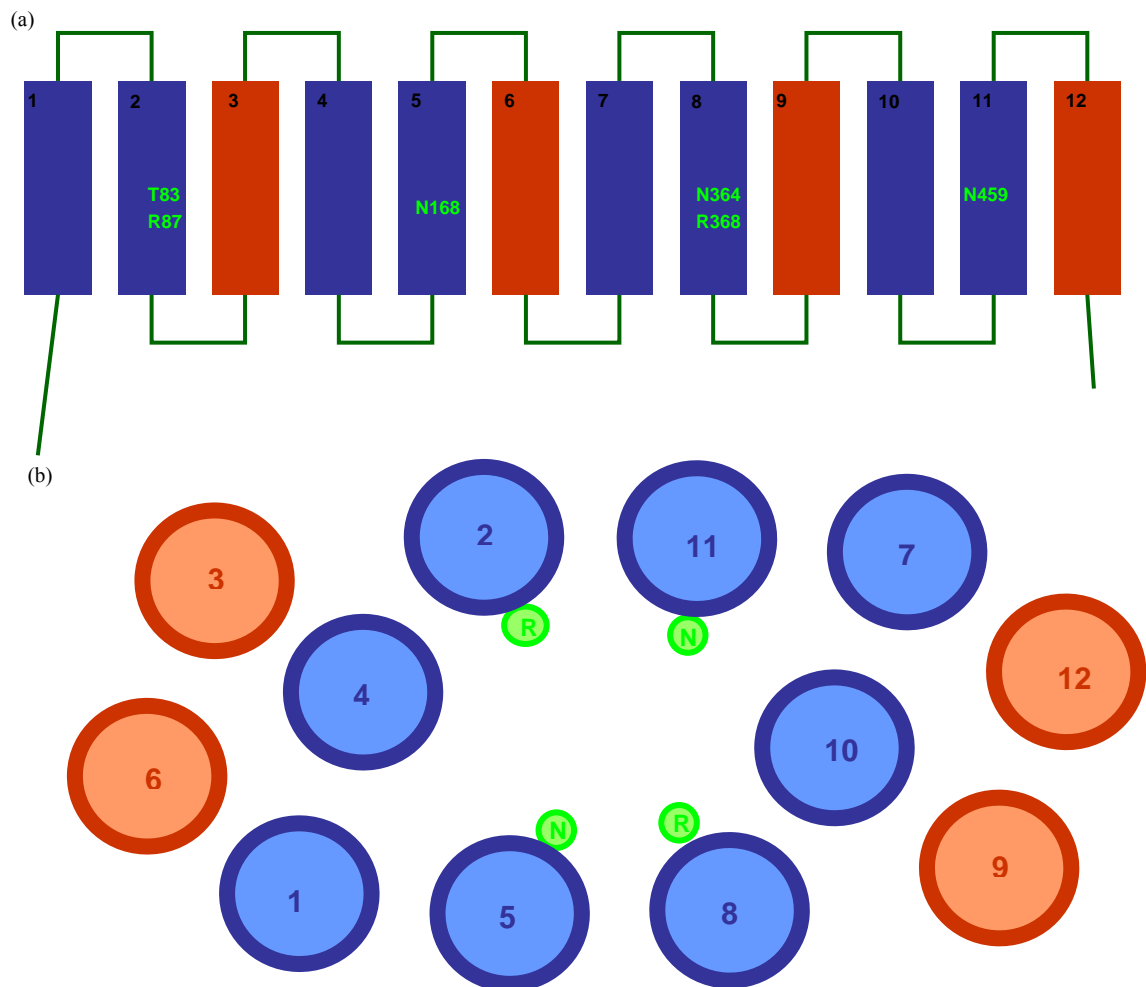


Figure 4.1 Positioning of residues in the NrtA binding site investigated in this study. (a) Representation of secondary structure of NrtA highlighting residues of interest here. (b) View through the permease from the extra-cellular environment into the cell. Helices shown in blue are thought to contribute to the formation of the binding site whereas helices in red are likely to perform more of a structural role in their positions embedded in the bilayer. Asparagines from Tm 5 and 11 are from the nitrate signature motifs and residues shown in Tms 2, 5, 8 and 11 are of focus here in particular. Diagram (b) does not show the threonine residues studied here which are positioned above the arginines.

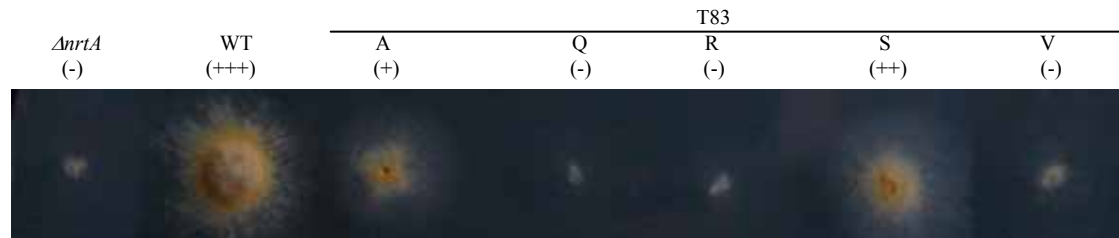


Figure 4.2 Phenotypes of single T83 mutants. Phenotypes were assessed on MM (pH 6.5) containing 100 mM NaNO₃ as the sole nitrogen source with vitamins supplements. Growth was allowed for 2 days at 37 °C. Scores shown are as in Table 4.1. Wild-type strain shown here, and in all cases of phenotypic assessment, was a wild-type transformant strain produced in the same way as the mutant strains that are compared directly to it.

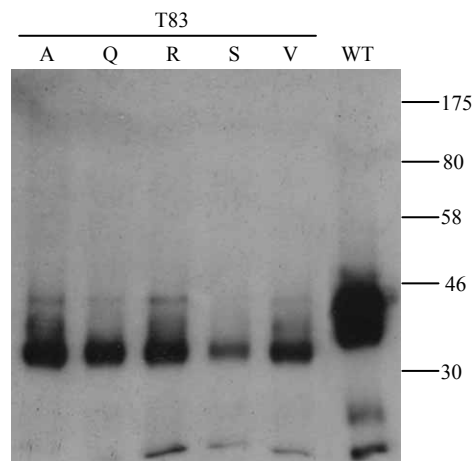


Figure 4.3 Western blot of T83 mutants. Conidiospores for Western blots were grown initially in 5 mM urea, followed by 100 min with 10 mM nitrate induction prior to being harvested and prepared for Western blotting. Anti-V5 antibody was used to probe blots. The wild-type band is approximately 45 kDa with mutant strains showing 35 kDa bands of wild-type levels as discussed in Chapter Three. Molecular marker is shown in kDa.

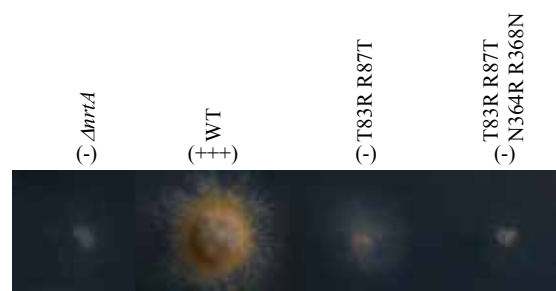


Figure 4.4 Phenotypes of multiple binding site mutants. Phenotypes were assessed as in Figure 4.2. Scores shown are as in Table 4.2.

Mutant	Transformant No.	Codon Change	Side Chain Alteration	Phenotype			Nitrate Uptake (nmol mg ⁻¹ DW min ⁻¹)	Expression
				Chlorate	25 °C	37 °C		
WT	T474	N/A	-	-	+++	+++	8.76 ± 2.55	Good
$\Delta nrtA$	T110	Δ	-	+++	-	-	-0.01 ± 0.86	-
T83A	T2855	ACG → GCG	Conservative	+++	+	+	3.60 ± 1.95	Good
T83Q	T103	ACG → CAG	Increase in size	+++	-	-	ND	Good
T83R	T5	ACG → CGG	Polar- +ve charge	+++	-	-	ND	Good
T83S	T605	ACG → AGG	Conservative	+++	++	++	2.09 ± 1.73	Good
T83V	T98	ACG → GTG	Conservative	+++	-	-	ND	Good

Table 4.1 Single binding site mutations in residue T83 which resides directly above R87 in the NrtA binding site. The phenotypes of each transformant were assessed on MM with 150 mM chlorate, 10 mM proline and vitamins, and MM with 100 mM NaNO₃ and vitamins, standard growth conditions were two days at 37 °C and for temperature sensitivity testing, 4 days at 25 °C. Conidiospores for uptake assays were grown initially in 5 mM urea, followed by 100 min with 10 mM nitrate induction, followed by 20 min uptake assays in 250 μM nitrate. Nitrate uptake experiments were performed in triplicate. Similarly, conidiospores for Western blots were grown initially in 5 mM urea, followed by 100 min with 10 mM nitrate induction prior to being harvested and prepared for Western blotting. Anti-V5 antibody was used to probe blots. Approximately equal concentrations of protein were loaded onto these gels and as such an approximate measurement of expression is given here, ‘Good’ expression represents expression comparable to the wild-type, though it is notable that T83S is slightly reduced, with expression approximately 80 % of the wild-type strain. No internal control is currently available for studying expression in these membrane proteins. All proteins expressed were approximately 10 kDa smaller than the wild-type (discussed in Chapter Three). All strains shown are *nrtB*⁻, the wild-type strain is *nrtA*⁺, *nrtB*⁻ and finally the $\Delta nrtA$ strain is *nrtA*⁻, *nrtB*⁻.

Mutant	Transformant No.	Phenotype		
		Chlorate	25 °C	37 °C
WT	T474	-	+++	+++
$\Delta nrtA$	T110	+++	-	-
T83R R87T	T543P	+++	-	-
T83R R87T N364R R368N	T1261	+++	-	-

Table 4.2 Multiple mutants in the putative NrtA binding site. The phenotypes of each transformant were assessed on MM with 150 mM chlorate, 10 mM proline and vitamins, and MM with 100 mM NaNO₃ and vitamins, standard growth conditions were two days at 37 °C and for temperature sensitivity testing, 4 days at 25 °C. Nitrate uptake experiments were not performed on these strains as no growth was shown on agar. All strains shown are as described in Table 4.1.

4.2.3 ¹³NO₃⁻ uptake in mutant strain T83S

The short lived nitrate tracer ¹³NO₃⁻ (t_{1/2}=10 min) was then used on mutant T83S to investigate its potential to interact with substrate (Figure 4.5). Employing this tracer has been shown to be efficient at measuring nitrate transport previously (Siddiqi *et al.*, 1989; Kronzucker *et al.*, 1995; Unkles *et al.*, 2001; Unkles *et al.*, 2004a). This experiment involves the growth and induction of strains in standard conditions for uptake assays followed by concurrent uptakes at a range of nitrate concentrations including the addition of radioactive ¹³NO₃⁻ to facilitate the measurements. Km and Vmax were determined by computer using direct fits to a rectangular hyperbolae as in Unkles *et al.* (2004a). Km and Vmax, (calculated by Hofstee analysis) were the same as in the wild-type (Km 47.39 ± 4.50 μM and Vmax 94.64 ± 4.40 nmol mg⁻¹ DW h⁻¹) making it unlikely that T83 interacts directly with nitrate as it passes through the substrate binding site (Table 4.1).

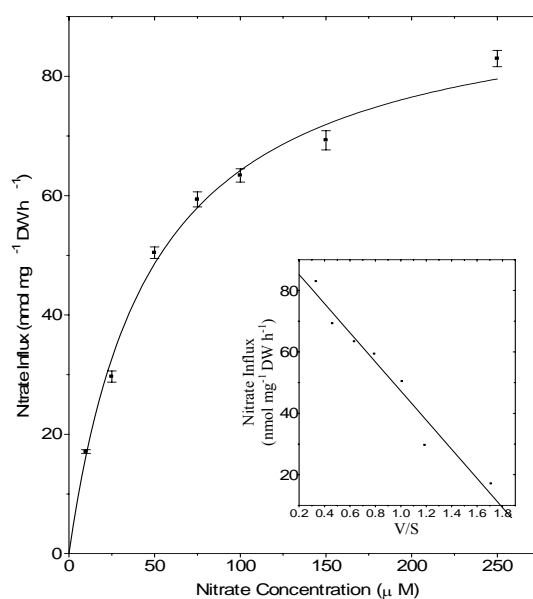


Figure 4.5 Legend on following page.

Figure 4.5 Nitrate influx in T83S using the $^{13}\text{NO}_3^-$ tracer. Flux data were analysed by Hofstee plot which is shown as an insert in this graph. By Hofstee analysis, reaction velocity is shown plotted against the velocity vs. substrate concentration ratio. Here, V_{max} is the y-intercept, and K_m the negative of the slope of this line. Assays were carried out using $^{13}\text{NO}_3^-$ as described in Chapter Two. Two replicates were performed for this mutant and the experiment with the highest r^2 is shown here. K_m and V_{max} were obtained by Hofstee Analysis as $47.39 \pm 4.50 \mu\text{M}$ and $94.64 \pm 4.40 \text{ nmol mg}^{-1} \text{ DW h}^{-1}$, K_m .

4.2.4 Modelling of NrtA: a view of the binding site

In collaboration with Jennifer Perry (National Institute of Environmental Health Sciences, MD, USA) and Shiela Unkles some modelling work based on the *E. coli* GlpT in the closed conformation, was carried out. The cartoon representation in Figure 4.6a shows the basic structure of NrtA as viewed along the bilayer, (open to the cytoplasm). Figure 4.6b shows the view through the permease from the cytoplasm with MFS, NNP and reactive arginine residues shown in each case.

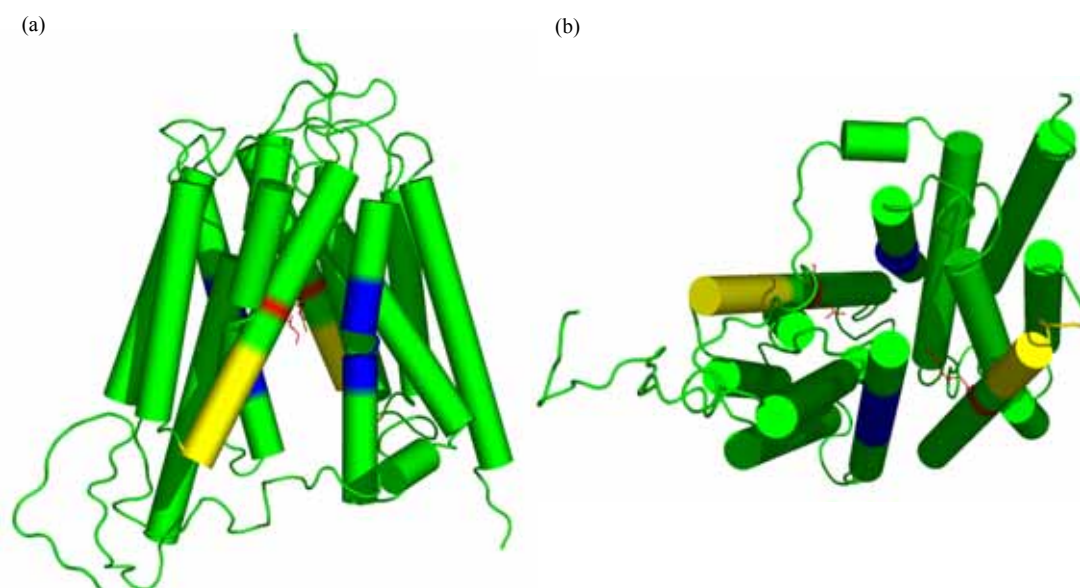


Figure 4.6 Cartoon representation of NrtA from two perspectives. Regions shown in blue, yellow and red respectively show the nitrate signature sequences the MFS motifs and the amino acids known to interact directly with nitrate as it traverses the bilayer, (R87 and R368) (Unkles *et al.*, 2004a). Representation of NrtA along the bilayer (a), and through the permease from the cytoplasm (b). This model was built using the inward facing conformation of the MFS GlpT transporter from *E. coli* as a template. This figure was prepared using PyMOL version 0.99 (Delano, 2002).

4.3 Discussion

From amino acid alignments of 118 orthologous proteins from eukaryotes and prokaryotes as performed in Chapter Three, Section 3.2.1, T83 was shown to be conserved in just 25 % of eukaryotic and 29 % of prokaryotic NrtA homologues studied. This site is generally occupied by serine or alanine in eukaryotes (respectively 55 and 17 % of the time) whereas glycine is

more frequent in prokaryotes (68 % occurrence), alanine is rare (3 % occurrence). Thus, it seems that a small residue is required at this site to provide flexibility to the arginine residue as it interacts with the substrate. Here T83 was targeted for mutagenesis to analyse its function. T83 was altered to alanine, valine, serine, glutamine and arginine with varying degrees of complementation. Phenotypic data presented in Figure 4.1 suggest that changes to alanine and serine are permitted by the protein. Alanine and serine residues are common in this position in prokaryotic homologues. Further, serine seems to be tolerated more than alanine, though nitrate uptake studies showed alanine to transport more nitrate than serine (Table 4.1). However, accounting for experimental error, uptake in these mutant strains can probably be considered similar. Tracer uptake studies were carried out on T83S to determine if an alteration in this position altered the K_m or V_{max} of NrtA. However, uptake kinetics were unaffected (Figure 4.5), implying that this residue is unlikely to interact with nitrate. Valine is of comparable size to threonine, and it would be expected that mutants to valine would complement on nitrate containing agar. Unexpectedly, this was not the case (Figure 4.2). Valine is commonly found in β -pleated sheets and it is possible that properties that favour valine in these regions are unfavourable in the α -helix, potentially the split C side-chain could affect available space. As stated Western analysis of these mutants produced an apparently cleaved protein, though the reason for this is currently under investigation. However, as activity is observed in both T83A and T83S it is apparent that nitrate was transported by NrtA. However, whether the reduction in nitrate uptake is as a result of the point mutation or protein cleavage is unclear from these results.

The importance of the relevant position of the arginine residues (R87 and R368) in relation to the polar residues T83 and N364 was investigated, initially by the construction of a double mutant which effectively swapped the positions of the T83 and R87. This mutant did not show growth on nitrate media, indicating that the positioning of these residues is critical for NrtA function. Further to this it was thought that if the position of the arginine was elevated in the helix then the interactions with nitrate might not occur on the same plane of the bilayer while the opposite arginine remained in a lower position (for residue positioning see Figure 4.1). All amino acids involved with substrate binding in LacY are located on the same plane in the transporter (Guan & Kaback, 2006) and therefore it is likely that this will be the case for NrtA. To test this, a quadruple mutation was created which moved the threonine and arginine in Tm 2 in addition to exchanging the positions of N364 and R368 in Tm 8. This mutant did not show growth on nitrate, suggesting that the positioning of these residues is critical for the efficient functioning of the substrate binding site. Perhaps as the substrate is moved towards or out of the binding site, there are additional interactions that are required for

the transit of nitrate which are unavailable in this mutant. As a final note of interest, mutagenesis work in parallel, on the polar residue (N364) above second interactive arginine (R368), preliminary results show that mutations to alanine and glutamine are tolerated in this position while cysteine, lysine and arginine are not, this too fits in with the theory that drastic size alterations are not permitted at these positions above the arginines.

To study the binding site, parallels are best drawn to previous studies on NrtA as have been done here. While LacY and GlpT are models for MFS proteins it is notable that the substrates in these permeases are structurally very different from nitrate as discussed in Chapter Three. While modelling of GlpT has provided clues as to the orientation of specified amino acids and their relationship to the binding site this model has to be backed up by experimental evidence on NrtA. For example in LacY the key residues known to be involved directly with the substrate are located in helices 4, 5, 8, 9 and 10 (i.e. substrate binding residues E126, R144 located at the intracellular edge of Tms 4 and 5, and residues involved with proton coupling E269, R302, H322 and E325, located on Tm 8, 9 and 10) (Frillingos *et al.*, 1998; Kaback *et al.*, 2001; Vazquez-Ibar *et al.*, 2004; Kaback, 2005; Mirza *et al.*, 2006). While charged residues in NrtA are known to reside on Tms 2 and 8 (R87 and R368 respectively), residues involved in proton coupling have yet to be identified in NrtA. This shows that although it is possible to employ these models as a guide for the targeting of residues caution should be exerted when drawing parallels.

The significance of results for growth on chlorate was as discussed in Section 3.3.

4.4 Summary

It would appear that the precise positioning of residues in the NrtA binding site is important for substrate binding. In particular the size of the residues directly above the interactive arginine (R87) is important; these residues above the critical charges probably provide both flexibility and stability in these active regions.

Chapter Five

Post-translational modifications of nitrate transporter NrtA

5.1 Introduction

For an organism to respond to, and survive in, a changing environment a degree of metabolic plasticity is essential (Huber & Hardin, 2004). Post-translational modifications can help to control enzyme activity, localisation, stability and interactions with other proteins (Mann & Jensen, 2003; Huber & Hardin, 2004). These modifications involve the covalent processing events which add chemical groups to specific amino acids or, alternatively, are involved with proteolytic cleavage of specified motifs (Mann & Jensen, 2003). A few examples of these modifications include phosphorylation, the reversible addition of a terminal phosphate group to serine, threonine or histidine; acetylation, the addition of an acetyl group to the N-terminus of a protein; glycosylation, the addition of a glycosy group to specified amino acids to produce a glycoprotein; and ubiquitination, the covalent linkage of ubiquitin to a protein. These are just four examples of a large variety of modifications which can be performed on a protein post-translationally. Each single modification can be responsible for a range of activities. In this chapter ubiquitination and phosphorylation which are known to relay signals in almost all cellular events (Peng, 2008) were investigated in relation to transport of nitrate by *A. nidulans* NrtA.

5.1.1 Protein ubiquitination

Ubiquitin is a seventy-six amino acid protein which is both highly conserved and ubiquitously expressed in eukaryotic cells, including *A. nidulans*. Ubiquitylation or ubiquitination involves the reversible, stable, covalent attachment of ubiquitin to a lysine residue in the target substrate via the carboxyl group on its C-terminal glycine (Hicke & Dunn, 2003). The conjugation of ubiquitin is commonly known as the ‘kiss of death’ for a peptide, as it ‘tags’ the substrate for degradation by targeting it to the proteasome (Govers *et al.*, 1999). However, this addition, depending on the site of conjugation, can also regulate protein stability, activity or location (Hicke & Dunn, 2003).

The addition of ubiquitin requires several enzymatic steps starting with its activation by ubiquitin activating enzyme (Hershko & Ciechanover, 1998; Catic *et al.*, 2004). Next, ubiquitin conjugating enzyme, in combination with ubiquitin ligase, transfers ubiquitin to a lysine side-chain on the target substrate. The highly specific ubiquitin ligases present in *A. nidulans*, control this process by monitoring the timing and substrate selection events (Hicke

& Dunn, 2003); for a comprehensive review see Hershko and Ciechanover (1998). Ubiquitinated lysine residues are exposed at the surface of the substrate and are easily accessible (Catic *et al.*, 2004). Further, loop regions show an increased propensity for ubiquitination (Williams *et al.*, 1987; Wilmot & Thornton, 1988; Catic *et al.*, 2004). Ubiquitination is a reversible process and several deubiquitinating enzymes can precisely cleave ubiquitin from its substrate (Wilkinson, 2000; Nijman *et al.*, 2005). It has been suggested that deubiquitination is largely used to recycle ubiquitin moieties from proteins which are to be degraded (Hicke & Dunn, 2003). In the cell, ubiquitin-targeted proteasome degradation and processing is known to control a large variety of basic cellular processes including regulation and development, differentiation, proliferation, cell cycling, apoptosis, gene transcription, signal transduction, senescence, antigen presentation, immune activation, and, inflammation and stress response (Kisselev *et al.*, 1999; Naujokat & Hoffmann, 2002; Kruger *et al.*, 2004; Wolf & Hilt, 2004; Naujokat *et al.*, 2007). Ubiquitination, without degradation, is known to regulate processes such as the internalisation of proteins in eukaryotes and sorting proteins to be secreted or routed elsewhere in the cell (Hicke & Dunn, 2003).

Poly-ubiquitination refers to the sequential addition of several ubiquitins to the target substrate. These link via lysine residues (of which seven are available) on the previously conjugated ubiquitin (Peng *et al.*, 2003). Chains of more than four ubiquitin moieties linked at K48 on the ubiquitin protein are known to target proteins to the 26S proteasome for degradation. The specificity of proteasomal degradation is dependant upon the poly-ubiquitin side-chains i.e. a minimum of four ubiquitins must be present at K48 for the 'tagging' to be complete (Chau *et al.*, 1989; Thrower *et al.*, 2000). It should be noted that non-ubiquitinated proteins can be targeted for proteasomal degradation, though this mechanism is not currently known.

Different types of ubiquitination underlie the different cellular functions. Chains of ubiquitins at residue K63 are involved in basic cellular processes such as protein localisation, in addition to endocytosis (Galan & Haguener-Tsapis, 1997; Fisk & Yaffe, 1999; Hoegge *et al.*, 2003). Proteolysis mediated by poly-ubiquitin is independent of protein sequence and sub-cellular environment. In contrast, non-proteasomal functions of ubiquitination are dependant upon both substrate sequence and sub-cellular environment, in addition to the presence of ubiquitin (Johnson, 2002). Finally, mono-ubiquitination is known to be involved in cellular events as a regulatory signal (Hicke, 2001; Salghetti *et al.*, 2001; Hoegge *et al.*, 2003).

5.1.2 Ubiquitination in membrane proteins

Yarden *et al.* (1986) were the first to show membrane proteins conjugated with ubiquitin (Govers *et al.*, 1999). Ubiquitination has been implicated in the internalisation of membrane proteins and their subsequent vacuolar degradation (Govers *et al.*, 1999; Horak, 2003; Dupre *et al.*, 2004) and has also been linked with protein stability, function and localisation (Staub *et al.*, 1997). Reizman (2002) proposed that mono-ubiquitination could control conformational change in target proteins in the same manner as phosphorylation. The high affinity nitrate transporter YNT1 of the yeast *H. polymorpha*, which is orthologous to NrtA, is ubiquitinated in the central hydrophilic domain (Navarro *et al.*, 2006). Specifically, residues K253 and K270 are involved with internalisation and vacuolar degradation of the protein, as opposed to 26S proteasomal degradation, and, is as a result of down regulation by glutamine (Navarro *et al.*, 2006). The ubiquitination motif for yeast plasma membrane proteins is thought to be (D/K)-X-K-(S/T) (Horak, 2003; Dupre *et al.*, 2004). Hydrophilic stretches known as PEST sequences are also known to be near to or hold part of ubiquitination motifs, these are of variable length and are rich in proline, glutamic acid, serine and threonine, flanked by acidic residues (Rogers *et al.*, 1986; Rechsteiner & Rogers, 1996). Proteins with PEST tagged motifs are targeted for degradation in the vacuole and not proteasomal digestion (Horak, 2003). According to Navarro *et al.* (2006) the large central loop of NrtA has putative PEST-like sites. As part of this chapter PEST-like sites in NrtA were investigated using PESTfind (<https://emb1.bcc.univie.ac.at/toolbox/>) (Rechsteiner & Rogers, 1996) and the PPSearch Protein Motif search algorithm at the European Bioinformatics Institute's web server (<http://www.ebi.ac.uk>).

5.1.3 Protein phosphorylation

The second post-translational modification investigated in this chapter was phosphorylation which is defined as the reversible, covalent attachment of the terminal phosphate (PO₃) group of ATP to a specific protein. At any one time, more than one third of the proteins in a eukaryotic cell appear to be phosphorylated (Mann *et al.*, 2002; Murray *et al.*, 2004; Schulenberg *et al.*, 2004). Phosphorylation has been shown in eukaryotic systems to be an important factor in the regulation of enzyme activity (Huber & Hardin, 2004). Phosphorylation triggers major changes within protein dynamics, for example by converting a hydrophobic protein into a hydrophilic protein (Pawson, 1994). Phosphorylation can act as a switch for functions, by turning enzymes on or off, or by activating or deactivating transport mechanisms (Huber & Hardin, 2004).

5.1.4 Phosphatases and kinases

Protein kinases and phosphatases are responsible for phosphorylation and dephosphorylation respectively. These enzymes are present in high cellular titres and form one of the largest super-families of homologous proteins (Hanks & Hunter, 1995). Protein kinases may be dedicated to trigger one function, or a small group of related functions, or can trigger a range, or cascade, of protein phosphorylation events (Cohen, 2002). Protein kinases and ubiquitin ligases are similar in terms of the specificity and wide level of cellular control they confer (Hicke & Dunn, 2003). Phosphorylation is highly effective for the cell for a number of reasons and can vary widely in rate, depending on the physiological context, over a scale of seconds to hours (Berg *et al.*, 2007). Phosphorylation induces highly significant conformational changes and the activity of a single protein kinase can evoke reactions from several targets almost simultaneously (Berg *et al.*, 2007). Also, the ability of the phosphate to form three hydrogen bonds can make the interactions highly directional (Berg *et al.*, 2007). It is common for proteins to cycle between a phosphorylated and dephosphorylated state, for example, the gating mechanism of transport proteins such as the spinach aquaporin, SoPIP2.1 (Tornroth-Horsefield *et al.*, 2006). During conditions of flooding and drought stress the protonation and phosphorylation state of SoPIP2.1 alters in response to these environmental changes, this is detailed in Figure 5.1 and illustrates the importance of post-translational modifications in this example (Tornroth-Horsefield *et al.*, 2006). Most proteins are phosphorylated at multiple sites and the phosphorylation target has a consensus motif. For example the recognition motif of protein kinase A (PKA) is R-R-X-S/T-Z, where X is a small residue, and Z a large hydrophobic residue (Hardie, 1993). The amino acid phosphorylated in this example is serine or threonine; this is not an entirely rigid motif as arginine is interchangeable for lysine, with lesser effect (Berg *et al.*, 2007).

Some examples of the actions of phosphorylation include the activation of sucrose synthetase and cytosolic pyruvate kinase which are implicated in the targeted degradation of proteins (Hardin *et al.*, 2003; Hardin & Huber, 2004; Hardin *et al.*, 2004). When phosphorylated, DARPP-32 (a dopamine and cyclic AMP regulated phosphoprotein) can function as either a kinase or phosphatase inhibitor depending on which threonine residue (T34 or T75) is phosphorylated (Bibb *et al.*, 1999). There have been several studies linking phosphorylation with different facets of ion translocation through channels (Esguerra *et al.*, 1994; Wang *et al.*, 1996; Beguin *et al.*, 1999; Kwak *et al.*, 1999; Schiff *et al.*, 2000). For example, phosphorylation is required for the binding of eukaryotic regulatory proteins, the 14-3-3 proteins, that have wide roles in regulating multiple cellular processes (Fuglsang *et al.*, 1999; Svennelid *et al.*, 1999). These are just a few examples of the role of phosphorylation in the wide range of cellular activities critical for cellular upkeep and maintenance.

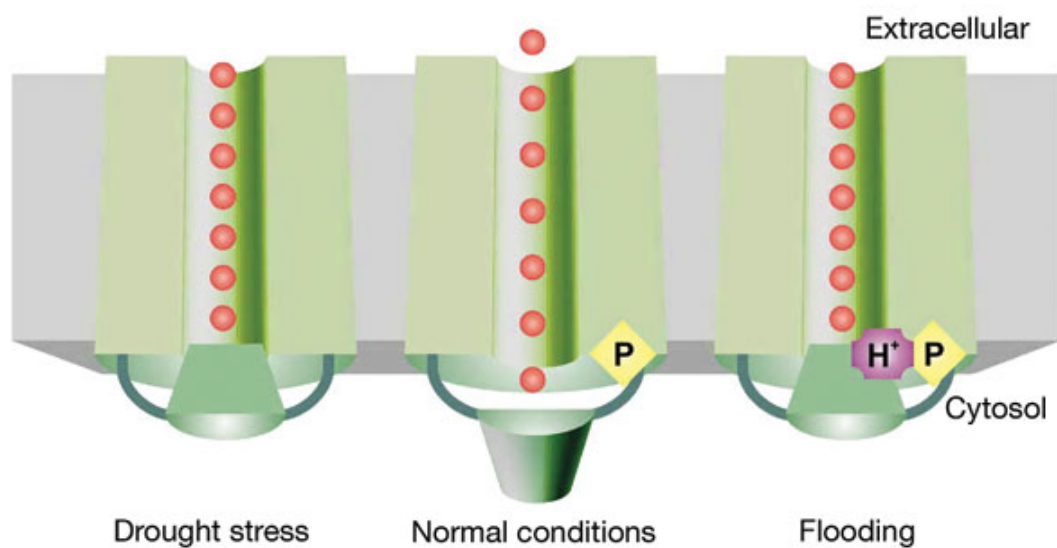


Figure 5.1 Structural mechanism of plant aquaporin gating in plasma membranes. During drought stress, the channel closes in response to the dephosphorylation of two highly conserved serine residues. During flooding it closes in response to the protonation of a highly conserved histidine. Figure taken from Tomroth-Horsefield *et al* (2006).

5.1.5 Phosphorylation and nitrate transport

Regarding the *Arabidopsis* nitrate transporter AtNrt1.1 (also designated Ch11), phosphorylation acts to switch the protein between low and high affinity transport (Liu & Tsay, 2003). High and low affinity phases occur respectively when AtNrt1.1 is phosphorylated or dephosphorylated at cytoplasmic T101 (Liu & Tsay, 2003). This residue resides in the PKA consensus motif R-X-X-T/S (Liu & Tsay, 2003) within intra-cellular loop 2/3 of AtNrt1.1 (Liu & Tsay, 2003). Phosphorylation of AtNrt1.1 provides a rapid response to changing environmental conditions, and is more subtle than the up-regulation of inducible permeases which have their own specific affinities for different conditions (Liu & Tsay, 2003). Dual affinity is not a characteristic feature of AtNrt1.1 paralogues. For example AtNrt1.2 which functions at low affinity only, lacks the phosphorylation sequence motif present in AtNrt1.1 (Huang *et al.*, 1999; Liu & Tsay, 2003). Phosphorylation is also thought to occur in the central loop domain of YNT1, the *H. polymorpha* nitrate transporter although its role in nitrate regulation remains elusive (Navarro *et al.*, 2006).

Forde (2000) highlighted the occurrence of protein kinase C (PKC) recognition sites present at the N and C terminal domains and central loop domain of Nrt transporters from different taxa suggesting that the presence of these motifs may be significant in Nrt regulation. However, mutagenesis of PKC recognition motifs in the plant Nrt1.1 and Nrt2.1 proteins has

not confirmed an involvement with protein regulation (Vidmar *et al.*, 2000; Okamoto *et al.*, 2003; Wirth *et al.*, 2007). On the large intra-cellular loop between Tm 6 and 7 of *A. nidulans* NrtA, four residues have been identified as putative phosphorylation sites based on functional protein sequence analysis using programs on the ExPASy proteomics server (<http://www.expasy.org>). A domain deletion mutant in residues Q239 to L314 of the *A. nidulans* NrtA loop domain (Figure 5.2) demonstrated that this region was essential for protein function. Transformants harbouring this mutant did not grow on nitrate agar, using nitrate as the sole nitrogen source (Unkles personal communication). Therefore, this loop might be subject to post-translational modifications. The second aim of this chapter therefore, was to gain an insight into putative phosphorylation sites which are thought to be present in the conserved fungal central loop domain of NrtA, taking an initially computer based approach to predict potential target regions followed by a laboratory based mutagenesis approach.

5.2 Results

5.2.1 Identification of putative PEST sequences in NrtA

PESTfind software (Rechsteiner & Rogers, 1996) (<https://embl.bcc.univie.ac.at/toolbox/>) was employed to identify putative ubiquitination sites in *H. polymorpha* YNT1, *N. crassa* NIT10 and *A. nidulans* NrtA. Regions identified were defined as ‘poor-PEST’ sequences in both YNT1 and NrtA. PPSearch Protein Motif identification software on the European Bioinformatics Institute’s web server (<http://www.ebi.ac.uk>) was used to further investigate putative ubiquitination sites and again no PEST domains were identified in either protein. However, a ‘potential-PEST’ site was found for NIT10. These results are highlighted in Figure 5.3 in addition to known ubiquitination sites essential to YNT1 function along with the corresponding aligned residues in NrtA and NIT10. It is interesting to note that ubiquitination sites known in YNT1 are in regions common to NIT10 and NrtA as predicted ‘poor-PEST’ sites. However, in NrtA only one potential lysine is present, i.e. K274. Also, while most ‘poor-PEST’ sites were found on regions that were part of, or very close to, Tms as shown in Figure 5.3, the loop region was the most likely place for ubiquitination as a region easily accessible intra-cellularly. No further work was carried out on potential ubiquitination sites in NrtA.

5.2.2 Identification of putative phosphorylation sites in *A. nidulans* NrtA

Putative phosphorylation motifs in the central loop domain of NrtA were identified using functional databases on the ExPASy proteomics server (<http://www.expasy.org/>) and were

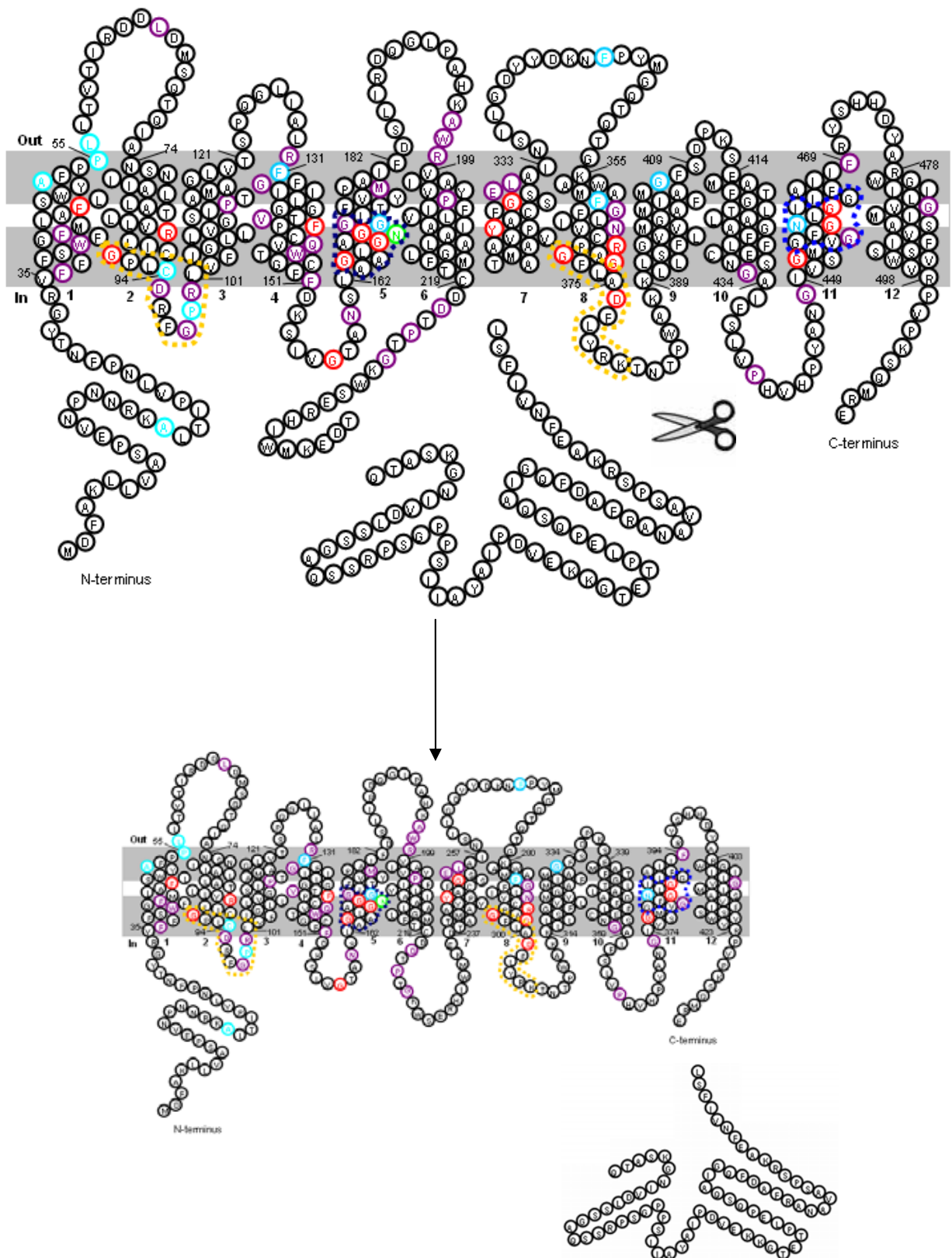


Figure 5.2 Illustration of NrtA minus the central loop domain. In the initial part of the diagram the deleted region is shown following domain excision and a smaller Lp 6/7 is evident. Conservation is shown here as residues in red representing > 95 % conservation in both prokaryotes and eukaryotes, purple > 95 % conservation in eukaryotes, green > 90 % conservation in prokaryotes and eukaryotes and blue > 90 % conservation in eukaryotes.

	Position of phosphorylated residues in <i>A. nidulans</i>			
	224	228	255	303
<i>A. nidulans</i>	TGK	SER	SSR	SRK
<i>A. fumigatus</i>	TGK	SER	STR	SRK
<i>N. fischeri</i>	TGK	SER	STR	SRK
<i>A. terreus</i>	TGK	SER	SVR	SFK
<i>A. oryzae</i>	TGK	SER	SSH	TFK
<i>A. niger</i>	TGK	SER	--I	TRK
<i>N. crassa</i>	TGR	RDR	AET	S--
<i>M. grisea</i>	TGK	SER	DKG	TFG

Table 5.1 Conservation of putative phosphorylation sites of Nrt2 proteins shown by alignment comparison of proteins from *A. fumigatus*, *N. fischeri*, *A. terreus*, *A. oryzae*, *A. niger*, *N. crassa* and *Magnaporthe grisea*. Motifs were identified in NrtA using a combination of KinasePhos (<http://kinasephos.mbc.nctu.edu.tw/>) (Huang *et al.*, 2005), Net Phos (<http://www.cbs.dtu.dk/services/NetPhos/>) (Blom *et al.*, 1999), MyHits (<http://myhits.isb-sib.ch/cgi-bin/index>) (Pagni *et al.*, 2004) and Prosite (<http://www.expasy.ch/prosite/>) (Hulo *et al.*, 2006; Hulo *et al.*, 2008) software. Residues in yellow highlight characteristics of the PKC recognition sequence (S/T-X-R/K).

5.2.3 Single phosphorylation mutations

Putative NrtA phosphorylation sites (as shown in Figure 5.4) were identified *in silico* and knocked-out by altering the target residue to alanine in each case. Mutagenic primers used in this study are shown in Appendix Four. Plasmids containing these putative phosphorylation mutants were transformed into JK1060 (*nrtA747*; *nrtB110*; *argB2*; *ya2*; *pyroA4*; *pabaA1*) using the arginine selection system described previously. Mutant strains found to be single copy after Southern blotting (as example shown in Figure 3.3) were phenotypically assessed on 100 mM NaNO₃ and the *nrtA* gene was fully sequenced. All of these mutant strains were found to grow well on nitrate (Figure 5.5). Specifically, net nitrate uptake in these mutants is around 50 % of the wild-type (Table 5.2). Western analyses were not carried out on these mutant strains because of time constraints which resulted from the unexpected results of apparent protein cleavage shown in Chapters Three and Four. These experiments shall be conducted for publication to confirm if minor modifications in protein expression are the justifications for reduced growth on nitrate.

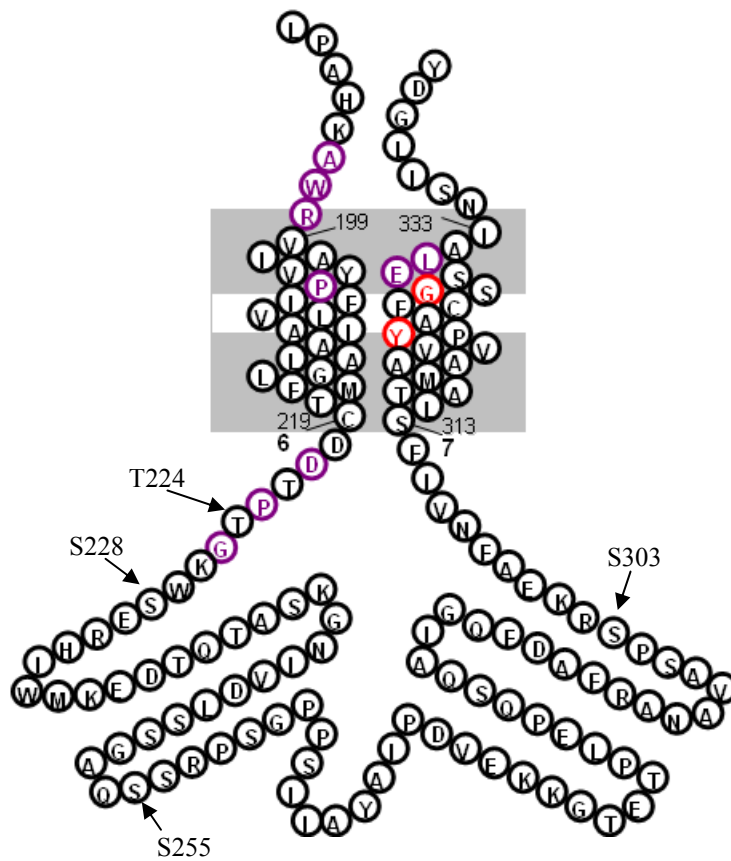


Figure 5.4 Central intra-cellular loop domain of NrtA, including Tms 5 and 6. Conservation is shown here as in Figure 5.2. Of relevance here are the putative phosphorylation sites T224, S228, S255 and S303, all of which are intra-cellular. This loop region is only conserved in fungi.

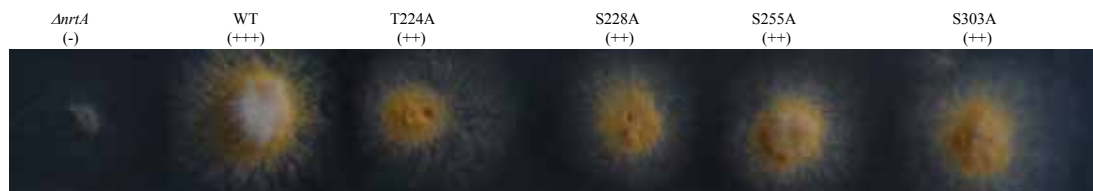


Figure 5.5 Phenotypic assessment of single phosphorylation site mutants in the loop of NrtA. Phenotypes are assessed here on MM (pH 6.5) containing 100 mM NaNO₃ as the sole nitrogen source with vitamins supplements. Growth was allowed for two days at 37 °C. Wild-type strain shown here, and in all cases of phenotypic assessment, was a wild-type transformant strain produced in the same way as the mutant strains that are compared directly to it. All strains shown are *nrtB*⁻, the wild-type strain is *nrtA*⁺, *nrtB*⁻ and the *ΔnrtA* strain is *nrtA*⁻, *nrtB*⁻.

Mutant	Transformant No.	Codon Change	Position	Phenotype			Nitrate Uptake (nmol min ⁻¹ mg ⁻¹)
				Chlorate	25 °C	37 °C	
WT (<i>nrtB</i>)	T474	N/A	-	-	+++	+++	8.76 ± 2.55
<i>ΔnrtA</i>	T110	Δ	-	+++	-	-	-0.01 ± 0.86
T224A	T2901	ACT → GCC	Lp 6/7	+++	++	++	4.90 ± 3.45
S228A	T1	TCC → GCC	Lp 6/7	+++	++	++	3.57 ± 0.87
S255A	T2573	TCC → GCC	Lp 6/7	+++	++	++	3.48 ± 1.07
S303A	T500	TCC → GCC	Lp 6/7	+++	++	++	3.74 ± 2.06

Table 5.2 Summary of characteristics of single site phosphorylation mutants. Each codon change ‘knocked-out’ a phosphorylation site by changing that residue to alanine. The phenotypes of each transformant were assessed on MM with 150 mM chlorate, 10 mM proline and vitamins, and MM with 100 mM NaNO₃ and vitamins. In each case, standard growth conditions were used (two days at 37 °C and for temperature sensitivity testing, 4 days at 25 °C). For uptake experiments conidiospores were grown initially in 5 mM urea, followed by 100 min 10 mM nitrate induction, 20 min uptake assays in 250 μM nitrate. Uptake assays were performed in three independent experiments and then standard deviation calculated on this basis. Mutant T224A showed a high degree of variation; however the uptake reflected that of the other mutations on agar and in net assays so this experiment was not repeated further.

5.2.4 Multiple mutations

On the basis of the growth phenotype of mutants carrying alanine residues at putative phosphorylation sites, it was thought that phosphorylation might occur through multiple sites and thus single site mutants were functionally redundant. Accordingly, quadruple mutants in all putative phosphorylation sites, were sought (Figure 5.5). Thus, in seeking this multiple mutant, two double mutant strains were also made, designated T224A/S228A and S255A/S303A. Growth of these mutant strains on 100 mM NaNO₃ was shown to be similar to the wild-type, although this data should be accepted with caution awaiting sequencing confirmation. However, the initial phenotypic assessment was consistent with the single mutant strains. This data is summarised in Table 5.3.

Mutant	Transformant No.	Position	Phenotype		
			Chlorate	25 °C	37 °C
WT (<i>nrtB</i>)	T474	-	-	+++	+++
<i>ΔnrtA</i>	T110	-	+++	-	-
T224A S228A	T4203	Lp 6/7	+++	++	++
S255A S303A	-	Lp 6/7	+++	++	++
T224A, S228A, S255A, S303A	T4252	Lp 6/7	+++	++	++

Table 5.3 Summary of characteristics of mutants where multiple phosphorylation sites were altered. Codon changes and assay conditions are as described for Table 5.2. Multiple mutations were made by the cloning of mutant DNA fragments using unique restriction sites. The phenotypes of each transformant were assessed as

described in Table 5.2. Transformant number is not specified for mutant strain S255A S303A because it is currently awaiting sequencing, however, the initial phenotypic assessment is shown here.

5.2.5 Chlorate and temperature sensitivity testing

All mutants in this study were tested on MM with 150 mM sodium chlorate with 10 mM proline as the nitrogen source. All mutants grew well on chlorate. Further to this, all mutants were assessed for growth at 25 °C on nitrate as the sole nitrogen source, this was shown to be similar to growth at 37 °C, and again this is shown in the corresponding tables.

5.3 Discussion

The large loop region of NrtA is conserved in fungi, but is absent in plants and bacteria. As such, comparisons to other MFS proteins, and indeed other Nrt proteins from other taxa reveal little as to the structure of the NrtA loop, and no modelling based on the GlpT crystal structure could be performed. This loop is critical for function in NrtA, as shown by deletion of this loop domain (Figure 5.2 and 5.3). In contrast, the loop domain of YNT1 has been deleted and the transformants maintained their ability to transport nitrate (Navarro *et al.*, 2006) (Figure 5.3). However, the expression of the mutant YNT1 protein lacks down-regulation by glutamine as a result of the absence of the ubiquitination sites discussed (Navarro *et al.*, 2006). Based on the possibility of ubiquitination sites in the loop region of NrtA an investigation into putative ubiquitination sites was performed *in silico*. However, aligning NrtA and YNT1 proteins showed that the first residue that is necessary in YNT1 (Navarro *et al.*, 2006) is not conserved in NrtA. In the second instance lysine at position 274 (K270 in YNT1) was conserved. As computational methods did not highlight putative PEST sequences in NrtA, this investigation was terminated.

Using computer based phosphorylation site prediction software; four putative phosphorylation sites were identified in the central loop region of NrtA. In particular, sites T224 and S228 were highly conserved (Table 5.1), as previously noted (Forde, 2000). Phosphorylation has been shown to control the mode of action of AtNrt1.1 in *A. thaliana* (Liu & Tsay, 2003), though no control has been shown in nitrate permeases such as NrtA. While it is common to carry out immuno-precipitation or mass spectrometry to assess protein phosphorylation, this simple mutagenesis approach was aimed at identifying residues critical for function within the fungal central loop domain. Wang *et al* (2007) have previously attempted to use anti-serine phosphate and anti-threonine phosphate immunoglobulin against crude membrane proteins in strains which were mutant and wild-type for nitrate reductase, but were unable to observe any difference in phosphorylation on Western blots. In this study, growth of both single and multiple mutant strains was less than wild-type (at both 37 °C and 25 °C), as was nitrate

uptake in single mutant strains. These mutants were also tested for growth on media containing chlorate, the toxic analogue of nitrate. Growth in each strain was shown to be as in *nrtA* strain T110 (*nrtA747*, *nrtB110*), and no growth was shown in *nrtA* wild-type transformant strain T474. This was expected, since mutants have been noted as chlorate resistant previously (*J.R. Kinghorn: personal communication*). Though this is difficult to explain as one would expect to find some chlorate sensitive mutants this has not been the case. It is likely that chlorate interacts differently with the permease to nitrate as it enters the cell; this was discussed thoroughly in Section 3.3.

Western blots were not performed on any of these strains, although their good growth phenotype suggests protein expression close to wild-type. Reduced nitrate uptake was as a result of these loop region modifications performed which may have been responsible for potentially minor structural roles in the NrtA protein. However, a cumulative effect was not observed in multiple mutant strains, making it unlikely that these sites are phosphorylated. To investigate the effect of single mutants on the loop further, other amino acids in this region should be modified to assess for the same effect.

5.4 Conclusion

Of the four putative phosphorylation sites identified, none were critical for function of NrtA despite their conservation. Mutants were also assessed for temperature sensitivity and phenotypes were approximately consistent at both temperatures. In summary, these regions may perform minor structural roles in the central loop domain. Unfortunately, this experiment was not conclusive; although it is evident that these regions are not involved with phosphorylation.

Chapter Six

Nitrate Signalling

6.1 Introduction

Nitrate is ubiquitous in nature though its concentration is known to vary across five orders of magnitude (Crawford, 1995; Glass *et al.*, 2002). In addition to being a substrate for nitrogen assimilation, nitrate acts as an essential signalling molecule which regulates cellular differentiation, and metabolic development (Crawford, 1995; Camargo *et al.*, 2007). In response to nitrate availability, plants alter root-shoot balance (Scheible *et al.*, 1997b), root development (Zhang & Forde, 2000), stomatal opening (Guo *et al.*, 2003), development of nascent organs in both roots and shoots (Guo *et al.*, 2001), and carbon and nitrogen metabolism (Scheible *et al.*, 1997a). In the photosynthetic protista *C. reinhardtii*, gametogenesis is also known to be influenced by nitrate availability (Pozuelo *et al.*, 2000; Camargo *et al.*, 2007). In this chapter, nitrate as a signalling molecule for nitrate assimilation shall be discussed.

The availability of nitrate or nitrite up-regulates genes involved in the assimilation pathway in response to an apparent nitrate/nitrite signalling system (Wang *et al.*, 2003; Wang *et al.*, 2007). Microarray analysis of the *Arabidopsis* transcriptome has shown over 1000 genes in roots and shoots were up-regulated in response to low levels of nitrate (Wang *et al.*, 2003). These genes are involved in glycolysis, iron transport/ metabolism, sulphate uptake/ reduction, and trehalose-6-phosphate metabolism (Wang *et al.*, 2003). This is in addition to genes known to be nitrate responsive, i.e. nitrate reductase, nitrite reductase and the nitrate transporter genes which are directly involved with nitrate uptake and metabolism (Wang *et al.*, 2003).

Nitrite has also been shown to provide a signal for nitrate assimilation, and increases mRNA levels in induced cells as rapidly as nitrate (Wang *et al.*, 2007). Genes from different families in *Arabidopsis* have been shown to react to nitrogen starvation and nutrition, though their specific roles are not established (Scheible *et al.*, 2004).

6.1.1 Nitrate signalling and assimilation

In fungi, the transcription factors NirA and AreA are involved as positive and negative regulators of nitrate assimilation (Marzluf, 1997). While nitrate regulatory genes in *A. nidulans* are well documented (Crawford & Arst, 1993; Marzluf, 1997), in the photosynthetic

organism *C. reinhardtii* *Nit2* is the only known nitrate signalling transcription factor (Camargo *et al.*, 2007). Showing no homology to known transcription factors, *nit2* contains motifs common to regulatory proteins (Schnell & Lefebvre, 1997). *A. thaliana* homologues of the *A. nidulans* regulatory proteins have been sought without success. Homologues of *nirA* and *areA* have only been identified in the fungi and yeasts (Marzluf, 1997). *ANR1* is a MADS-box gene in *A. thaliana* that was identified as a possible downstream transcription activator of a putative signal transduction pathway, that links between external nitrate availability and gene expression (Zhang & Forde, 2000). However, *ANR1* has since been shown to respond to nitrogen starvation and not nitrate availability *a priori* cannot be involved with receiving nitrate signals (Gan *et al.*, 2005).

6.1.2 Protista and planta organisms

The gene *nit2* in *C. reinhardtii* has been shown to be an essential signalling transcription factor for nitrate assimilation which requires intra-cellular nitrate to activate *nial* (coding nitrate reductase) gene expression (Llamas *et al.*, 2002; Camargo *et al.*, 2007). Mutants in *nit2* are unable to grow on nitrate as the sole nitrogen source since this *C. reinhardtii* mutant does not express known genes required for nitrate assimilation e.g. *nial*, *nrt2.1*, *nrt2.2*, *nii1*, *nar2* and *nar1* (Galvan & Fernandez, 2001; Camargo *et al.*, 2007). The product of the *nit2* gene has not been characterised and further nitrate assimilation regulatory genes have not been identified in this organism (Galvan & Fernandez, 2001; Camargo *et al.*, 2007). Nitrate sensing in *C. reinhardtii* occurs intra-cellularly and is dependant on the nitrate permeases *Nrt2.1* and *Nar2* (Camargo *et al.*, 2007). Repression of this pathway in this organism is thought to be under the control of pathway specific genes *Nrg1* and *Nrg2*, though these genes show no homology to fungal *areA* (Prieto *et al.*, 1996). The DNA binding protein *Nit2* is unrelated to fungal nitrogen assimilation regulatory proteins (Crawford & Arst, 1993; Marzluf, 1997; Siverio, 2002; Camargo *et al.*, 2007) but does show conserved domains found in other *C. reinhardtii* regulatory proteins (Ferris *et al.*, 2002; Lin & Goodenough, 2007) and *Arabidopsis* (Schäuser *et al.*, 1999; Schäuser *et al.*, 2005).

In addition to roles associated with nitrate signalling, an involvement for nitrate with relieving seed dormancy has been discussed in *Arabidopsis* (Alboresi *et al.*, 2005). It is thought that *Nrt1.1* (*Chl1*) may convey the signal into seeds to promote germination in favourable conditions (Alboresi *et al.*, 2005). This protein has also been suggested to be a key nitrate sensor in the roots of *Arabidopsis* (Remans *et al.*, 2006). In root growth assays it has been shown that nitrate stimulates lateral root development, and it has been suggested that *Nrt2.1* may be a sensor or transducer for nitrate in the root, independent of its transport mechanism

(Little *et al.*, 2005). Dual function for substrate uptake and sensing have also been noted for sugar transport in plants (Lalonde *et al.*, 1999).

6.1.3 Bacteria

In *E. coli*, nitrate signalling is accomplished via a dual two-component phospho-relay system (Noriega *et al.*, 2008). By this method nitrate is sensed extra-cellularly by the transmembrane histidine kinase sensor proteins NarQ and NarX which are phosphorylated in response to extra-cellular nitrate in addition to other stimuli (Rabin & Stewart, 1993; Stewart, 1994; Cavicchioli *et al.*, 1996; Williams & Stewart, 1997; Lee *et al.*, 1999; Forde, 2002; Stewart *et al.*, 2003). These proteins form a dual two-component phospho-relay system which encompasses the paralogous sensor-response regulators NarX-NarL and NarQ-NarP (Rabin & Stewart, 1992). The phosphorylation state of NarL and NarP is controlled by NarX and NarQ (Rabin & Stewart, 1993; Walker & Demoss, 1993; Schroder *et al.*, 1994; Cavicchioli *et al.*, 1995; Noriega *et al.*, 2008), and the phosphorylated forms of NarP and NarL regulate transcription of anaerobic gene expression where nitrate and nitrite act as the preferred terminal electron acceptors (Darwin *et al.*, 1997). NarX and NarQ are central to nitrate sensing and are composed of a periplasmic region with 2 Tm helices where nitrate is sensed (Walker & Demoss, 1993; Cavicchioli *et al.*, 1996; Williams & Stewart, 1997; Appleman *et al.*, 2003; Appleman & Stewart, 2003; Anantharaman *et al.*, 2006; Noriega *et al.*, 2008). This domain also encodes signal transduction motifs and a further central domain with no known function (Noriega *et al.*, 2008).

6.1.4 Yeast

Although regulation of nitrogen assimilation is more extensively characterised in the yeast and fungi as opposed to plants (Crawford & Arst, 1993; Marzluf, 1997; Siverio, 2002), little is known about signalling systems for nitrate in fungi. It is thought that in the yeast *H. polymorpha*, nitrate signalling is likely to be associated with a high affinity nitrate transport mechanism and not with nitrate reductase (Navarro *et al.*, 2003). *H. polymorpha* encodes two transcription factors which are thought to be involved with the transcriptional activation of nitrate assimilation genes, namely *YNA1* and *YNA2* (Avila *et al.*, 1998; Avila *et al.*, 2002; Siverio, 2002), though no link has been made to signalling systems for nitrate in this organism.

6.1.5 A fungal nitrate sensor?

In *A. nidulans* the regulated degradation of *areA* mRNA in response to ammonia or glutamine acts as a nitrogen metabolite signalling system (Morozov *et al.*, 2001). In response to intra-cellular levels of ammonia, as well as glutamine, aspartic acid, asparagine, glutamic acid, and

nitrite the mRNA of *areA* is degraded. The rate of this degradation is proportional to extra-cellular glutamine concentration, a major end product of nitrogen metabolism. However nitrate does not elicit a degradation response. Morozov and colleagues (2001) proposed that nitrogen signalling in the cell may be multi-faceted as, in addition to *areA* transcript degradation, two other signalling pathways for the regulation of *areA* were implied involving the negative regulatory protein NmrA which is known to repress *areA* in response to intra-cellular glutamine (Platt *et al.*, 1996; Andrianopoulos *et al.*, 1998), and glutamate dehydrogenase (*gdhA*) which is thought to control intra-cellular glutamine levels (Morozov *et al.*, 2001).

Homologues of bacterial nitrate sensors are found in *A. nidulans*, although no role in nitrate assimilation has been demonstrated. However, they are thought to control spore formation (*tcsA*) (Appleyard *et al.*, 2000) and possibly act as an osmosensor histidine kinases (*tcsB*) (Furukawa *et al.*, 2002).

A plasma membrane sensor has been raised as the most likely target of nitrate in *A. nidulans*. As nitrate transporters tend to be located at the forefront of the root in plants or at the hyphal tip in fungi they are the primary colonisers of virgin territory. Unkles *et al* (2001) reported that a nitrate minus strain (*nrtA747*, *nrtB110*) expressed the *nrtA* gene to wild-type levels and *niaD* and *niia* to 40-45 % of wild-type. This showed that nitrate does not need to enter the pathway to induce the enzymes involved, ruling out the possibility that nitrate transporters in *A. nidulans* are nitrate sensors.

Nitrate assimilation in *A. nidulans* is well understood and a degree of understanding has been made to the mechanism of nitrate transport through NrtA has been discussed; however, the signalling system in *A. nidulans* is elusive at present. It appears that in the organisms discussed here very different mechanisms of nitrate signalling are employed. In this chapter, a cosmid library was constructed using DNA from the nitrate non-growth strain T110 (*nrtA110*, *nrtB747*) with the intention of transforming it into a nitrate signalling system deficient mutant, in order to identify mutant strains which were involved with nitrate signalling.

6.2 Results

6.2.1 Vector and cosmid library construction

Using the Epicentre Technologies pWEB::TNC vector with the addition of *A. fumigatus* *pyroA4* cloned into the *EcoRV* site - a cosmid library was constructed using DNA from nitrate non-growth strain T110.

6.2.2 Strain development

A 'signalling system minus' strain was required to receive the cosmid library DNA. To this end, strain T19 (*nrtA747*; *nrtB110*; *pyroA4*; *pabaA1*; *pTRAN3-1A::argB*), was employed. T19 is a nitrate non-growth strain which harbours two copies of pTRAN3-1A (Figure 6.1) (Punt *et al.*, 1991). This vector is a twin reporter vector which, when transformed into *A. nidulans* is integrated at the *argB* locus. As shown in Figure 6.1 the *niaD* (coding for nitrate reductase) gene promoter is fused to the reporter gene *uidA* and the promoter of *niiA* (coding for nitrite reductase) is fused to the reporter gene *lacZ*. Thus when nitrate is present in the surrounding media, β -glucuronidase is produced by *uidA* translation, which is excreted to the media digesting the resident X-Gluc (5-bromo-4-chloro-3-indoly glucuronide) resulting in a blue coloured staining in the vicinity of the colony. An active signalling system should activate these promoters producing the blue colour, whereas an inactive signalling system would not (Figure 6.2). The β -glucuronidase reporter gene (*uidA*) was employed in this study as one would expect inherent β -galactosidase (*lacZ*) activity in *A. nidulans*. It is a suitable reporter system for use here as fungi have no inherent β -glucuronidase activity (Jefferson, 1989b; Jefferson, 1989a).

T19 was targeted with the chemical mutagen N-methyl-N'-nitrosoguanidine (NTG) (Adelberg *et al.*, 1965), to produce a signalling system minus strain in the nitrate minus background. In chemical mutagenesis experiments, kill rates of > 99 % were required. Surviving conidia from these experiments were plated on MM with X-Gluc and either nitrate (with proline) or nitrite. After a sufficient incubation period, strains which failed to produce blue colour were selected. After several mutageneses, six putative signalling system mutants were selected from several hundred colonies screened. These strains were purified and their phenotypes rigorously tested on omission media. The four remaining strains were designated VFS1, VFS2, VFS3 and VFS4. Southern blots were performed on *BamHI* digested genomic DNA from these strains to ascertain that two copies of pTRAN3-1A remained at the *argB* locus. Only VFS2 harboured two copies (Figure 6.3).

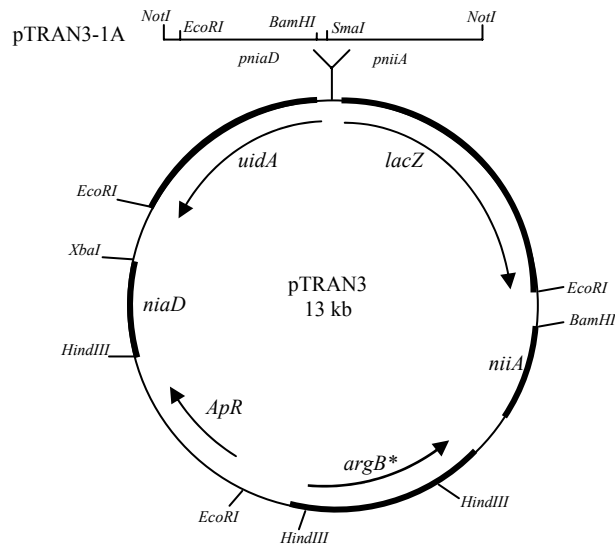


Figure 6.1 Vector pTRAN3-1A, pTRAN3 with fragment 1A is 14.3 kb in size. Diagram based on that of Punt *et al* (1991).



Figure 6.2 Illustration of colour produced on nitrate containing X-Gluc media in the presence of pTRAN3-1A transformants with active and inactive signalling systems.

Further tests of VFS2 included the sequencing of *uidA*, and *niaD* and *niiA* promoter sequences (primers used for amplification and sequencing are shown in Appendix Three), all were confirmed to be wild-type. Additional phenotypic assessment on hypoxanthine, proline and arginine were conducted to ensure that there was no *areA* mutation, as repressor mutations in *areA* would not grow on media without ammonia or glutamine. Finally, nitrate reductase assays were performed by Dr. S. Unkles. These showed that VFS2 had wild-type nitrate reductase activity; therefore, as the signalling system appeared to be active, it was thought that VFS2 was a sugar transport mutant which could not transport β -glucuronidase and that the reporter system was not functional.

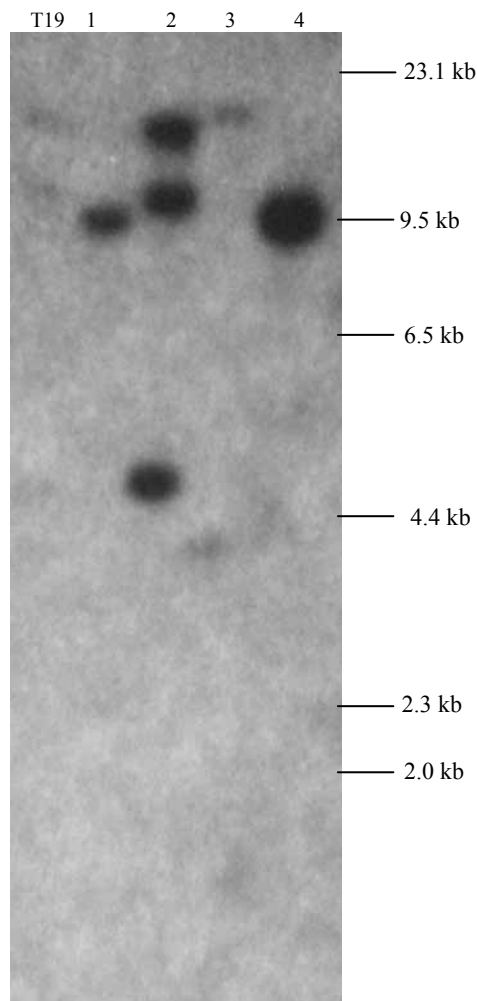


Figure 6.3 Southern blot of putative signalling system mutants. T19 represents the positive control strain which harbours two copies of pTRAN3-1A at the *argB* locus represented by three bands of 6, 10 and 14.3 kb, where the even intensity of the 14.3 kb band is representative of a double integration of pTRAN3-1A (a single copy integration of pTRAN3-1A would not reveal the 14.3 kb band shown here). A direct comparison of T19 to the mutant in lane two, which represents the putative signalling system VS2, this mutant harbours two copies of pTRAN3-1A at *argB*. This integration as shown here was discussed by Punt *et al* (1995) and a diagrammatic representation of possible recombination events was shown by Brakhage and van den Brulle (1995). The remaining mutants did not show any copies of pTRAN3-1A. Ladder shown is *HindIII* digested phage λ DNA.

6.3 Discussion

In the introduction to this chapter, putative nitrate signalling systems and investigations in this direction were described in a range of organisms. Nitrate signalling is the missing piece in the puzzle of nitrate assimilation. In terms of ecological importance, the assimilating organism's ability to detect nitrate is central to the induction of assimilation enzymes, as such the response of the signalling system is pivotal in the efficient use of nitrate in the environment. To this aim, nitrate signalling was investigated here. A cosmid library was successfully constructed using DNA from nitrate non-utilising strain T110. The intention was

to use this library to identify genes which may be involved in nitrate signalling in *A. nidulans*. A nitrate signalling system mutant strain had to be identified by chemical mutagenesis, however this was unsuccessful. Several hundred colonies were screened though the mutant proved to be elusive. The library is stored at -85 °C while an alternative strain is developed; which is outside the scope of the current studies.

Chapter Seven

Nitrite transport and the NitA permease of *A. nidulans*

7.1 Introduction

7.1.1 Background

The anion nitrite may be used by certain organisms as their sole source of nitrogen (Lee, 1979; Kielland, 1994), and in *E. coli* nitrite is used for respiration (Darwin *et al.*, 1997). Nitrite is drawn into the nitrate assimilation pathway, where it is reduced by assimilatory nitrite reductase to ammonium for use in the formation of organic nitrogenous compounds. Under certain environmental conditions, for example in water-logged soils, nitrite, as well as organic nitrogen from amino acids, can make a significant contribution to the nitrogen available to a plant (Lee, 1979; Kielland, 1994; Suppmann & Sawers, 1994; Delomenie *et al.*, 2007), though nitrate and ammonium remain the staple source.

7.1.2 Nitrite permeases

Nitrite specific permeases have been found to exist in the archaebacteria, eubacteria, protista and the fungi, for example, NirC from *E. coli*, (Clegg *et al.*, 2002; Jia & Cole, 2005), the six Nar1 proteins from *C. reinhardtii* (Rexach *et al.*, 2000; Mariscal *et al.*, 2004; Mariscal *et al.*, 2006), and NitA from *A. nidulans* (Wang *et al.*, 2008). Formate transporting proteins such as EgFth from *Euglena gracilis* (Delomenie *et al.*, 2007) and FocA and FocB from *E. coli* are known (Suppmann & Sawers, 1994; Andrews *et al.*, 1997). As members of the Formate Nitrite Transporter family (FNT) each of these permeases is composed of 6 Tm.

Recent work has reported that nitrite crosses the cell membrane in *A. nidulans*, through the bifunctional permeases, NrtA and NrtB, which transport both nitrate and nitrite, and also through a nitrite specific permease NitA (Wang *et al.*, 2008). FNT proteins transport either formate or nitrite (Suppmann & Sawers, 1994), and no bifunctional members are known for both these substrates, though Nar1.2, from *C. reinhardtii* transports both bicarbonate and nitrite (Mariscal *et al.*, 2006). There is little mechanistic insight into the FNT proteins and comparisons cannot be made to the MFS NNP subfamily due to the primary amino acid sequence and by extension considerable structural differences. Extrapolations discussed in this chapter are from FocA (Suppmann & Sawers, 1994).

7.1.3 FNT proteins in *E. coli*, *S. cerevisiae* and *A. nidulans*

Studies in *E. coli* have revealed three polytopic membrane proteins involved in the movement of nitrate and nitrite in both directions across the membrane, namely NarK, NarU and NirC (Clegg *et al.*, 2002). NarK and its paralogue NarU are 12 Tm proteins, homologous to NrtA and NrtB and are involved in the import of nitrate and the export of nitrite (Clegg *et al.*, 2002). NarK is also involved with nitrite uptake (Clegg *et al.*, 2002). The flux of nitrate and nitrite in NarK is higher than NarU (Jia & Cole, 2005). NirC is a 6 Tm polytopic protein, first identified as a possible nitrite transporter by Peakman *et al* (1990). NirC has since been shown to be the principle permease involved with nitrite transport in *E. coli* with the flux being approximately 5-fold higher than NarK (Jia & Cole, 2005). NarK and NirC are the dominant carriers for nitrate and nitrite respectively in *E. coli* (Jia & Cole, 2005). A defining role for NarU is that in oxygen-limited conditions, it transports nitrate with greater efficiency than NarK (Clegg *et al.*, 2002). As regards formate transport, FocA was recognised on the basis of hypophosphite resistance (Suppmann & Sawers, 1994) and FocB was identified by sequencing of the *hyf* operon in *E. coli* (Andrews *et al*, 1997). The presence of a second formate transporter in *E. coli* was rationalised by the additional formate uptake in *focA* mutants, though no specific transport activity has been determined for FocB (Andrews *et al.*, 1997). Further, neither of these proteins is currently known to transport nitrite.

The *C. reinhardtii* genome encodes nitrate/nitrite transporters from three protein families (Fernandez & Galvan, 2007). There are six paralogous genes which encode proteins homologous to FocA and NirC from *E. coli* (Suppmann & Sawers, 1994; Galvan *et al.*, 2002; Jia & Cole, 2005; Fernandez & Galvan, 2007) that are differentially regulated by carbon and nitrogen (Mariscal *et al.*, 2006). The first gene found to encode a high affinity chloroplast nitrite transporter was *nar1.1*, which is critical for cell survival when nitrate is limited (Mariscal *et al.*, 2004). The majority of work on *C. reinhardtii* Nar proteins has focussed on Nar1.1, though, Nar1.2 has been revealed as a high affinity nitrite transporter/low affinity bicarbonate transporter which is located in the chloroplast membrane along with Nar1.1 and Nar1.5. Nar1.3, Nar1.4 and Nar1.6 are thought to be plasma membrane proteins (Mariscal *et al.*, 2006; Fernandez & Galvan, 2007). Additionally, Nar1.1 is involved with the maintenance of metabolic balance of nitrogenous compounds, through the regulation of high affinity nitrate transporters, nitrate and nitrite reductase, and glutamine synthetase (Mariscal *et al.*, 2004; Mariscal *et al.*, 2006). While the cellular location and regulation of these proteins has been studied, the specific substrates have only been identified for Nar1.1 and Nar1.2 (Mariscal *et al.*, 2006). No work has yet established the functional mechanisms and residue interactions in these proteins.

In the fungus *A. nidulans* nitrate loss of function double mutants for *nrtA* and *nrtB* are unable to grow on MM containing 10 mM NaNO₃ (Unkles *et al.*, 1991; Unkles *et al.*, 2001). However, double mutant strains can grow on MM containing 2 mM NaNO₂ as wild-type, indicating the possibility of an independent nitrite carrier. The presence of a saturable nitrite transporter and the kinetics of this permease were reported by the St Andrews/Vancouver group (Wang *et al.*, 2008). These authors used the *E. coli* NirC gene as a probe to identify an orthologue in *A. nidulans* which was then cloned (Accession No. AN8647). This gene was designated *nitA*. The NitA protein shares 32-38 % identity with the discussed nitrite transporter genes from the *C. reinhardtii* NarI family (Wang *et al.*, 2008).

Currently, there is no information on FNT family proteins regarding critical amino acids for substrate binding and translocation. With a lack of suitable models, a comparison to existing protein structures would be unfruitful as proteins from different families exhibit different structural folds. Indeed, a comparison to NNP proteins such as NrtA and NrtB which possibly share a signature sequence is not an option due to the differences in secondary and quaternary structure of these proteins. Without conserved arginine residues there is no obvious candidate for anion interaction in NitA.

NitA is 310 amino acids in length corresponding to the predicted 33.6 kDa (*S.E. Unkles personal communication*). A thorough assessment of conserved residues in NitA was undertaken to deliver functional data about this protein. There are a number of highly conserved residues in NitA relative to its orthologues. Of particular interest are the highly conserved asparagines in Tm 2, 4, 5 and 6 (N122, N173, N214 and N246 respectively) and charged amino acids such as D88 in Tm 2, and K156 and K192 in loop regions 3/4 and 4/5 respectively. While this chapter formed part of the results in the Wang *et al.* article (2008), the main aim of further work described here in this thesis was to establish function of these conserved residues by the production and characterisation of mutant strains.

7.2 Results

7.2.1 Growth and flux of nitrite in control strains on solid media and using ¹³NO₂⁻

The *nitA* deletion strain T26 was generated by gene disruption by Dr S.E. Unkles in a *nrtA*, *nrtB* double mutant background, as described by Wang and colleagues (2008). After the identification of a gene disruption strain by Southern blot, the mutant phenotype was optimised on agar solid medium. At pH 6.5 (with 2 mM NaNO₂ as the sole nitrogen source) - the triple mutant strain was somewhat 'leaky' (Figure 7.1), possibly as a result of nitrous acid diffusion, as at low pH nitrous acid has been shown to move across the cell membrane

passively (Wang *et al.*, 2008), as shall be discussed here. This phenotype was altered at pH 7.5 which ablated growth relative to wild-type (Figure 7.1). It should be noted that a minor complication arose with this phenotypic assessment, this was that p-amino benzoic acid (PABA) appears to be destroyed in the presence of nitrite. However, an additional PABA supplement circumvented this technical difficulty. It is appropriate to add that PABA cannot be used as a nitrogen source (data not shown) but had to be added to MM to supplement the *pabaA1* auxotrophy.

The flux of $^{13}\text{NO}_2^-$ in non-transformant wild-type *nitA* strain T600 (*nrtA747*, *nrtB110*, *pyroA4*, *pabaB1*, *yaA2*), and in $\Delta nitA$ T26 control strains were carried out using ^{13}N ($t_{1/2} = 10$ min) supplied by TRIUMF, UBC, Vancouver (Figure 7.2). Kinetics for NitA were determined as $19.17 \pm 0.88 \mu\text{M}$ and $148.77 \pm 2.01 \text{ nmol mg}^{-1} \text{ DW h}^{-1}$ for K_m and V_{max} respectively ($r^2 = 0.92$). Low level flux in T26 is attributed to diffusion by nitrous acid ($pK_a = 3.6$).

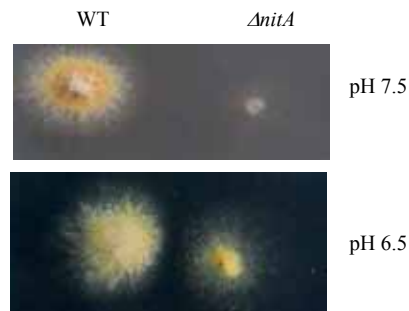


Figure 7.1 Growth of wild-type T5275 and $\Delta nitA$ T26, on minimal agar media at pH 6.5 and pH 7.5 with 2 mM NaNO_2 as the sole nitrogen source with vitamin supplements, and additional dose of 1 x PABA. Growth was permitted for 2 days at 37 °C. Both of these strains are in the *nrtA*, *nrtB* double mutant background.

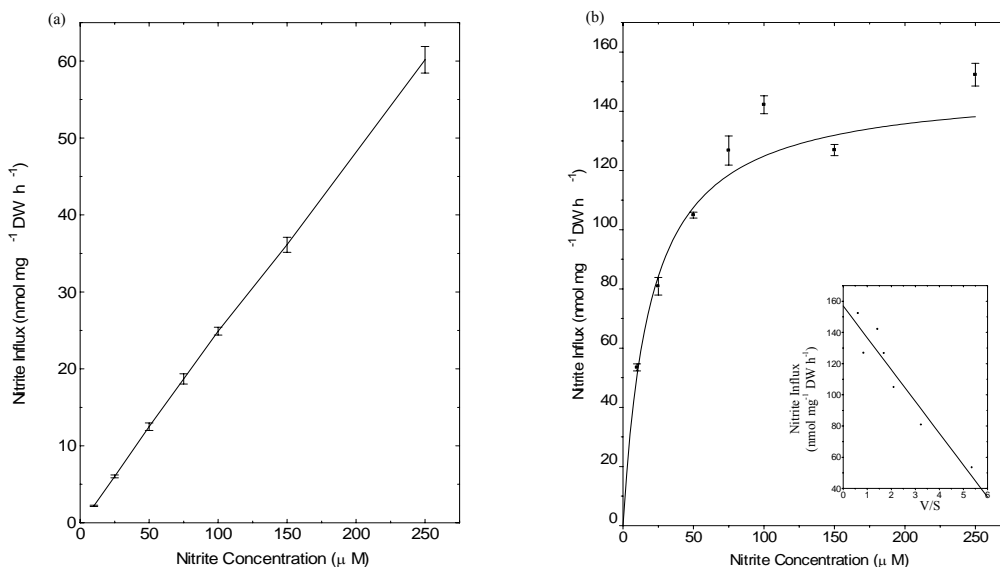


Figure 7.2 Legend on following page.

Figure 7.2 $^{13}\text{NO}_2^-$ flux assays for control strains. (a) Strain T26 (*nitAA*) shows linear kinetics ($r^2 = 0.99$) (b) Strain T600, a non-transformed *nitA* wild-type strain (*nrtA747*, *nrtB110*, *pyroA4*, *pabaB1*, *yaA2*). Flux data were analysed by Hofstee plot shown as an insert to figure (b) ($r^2 = 0.92$). Strains were grown in MM pH 6.5 for 4 h on urea followed by 3 h induction by KNO_2 before 10 min assays at pH 6.5 of 10-250 μM KNO_2 .

7.2.2 Two-dimensional model development and conserved motif analysis

A provisional secondary structure for NitA was developed using TMHMM, TmPred and TopPred algorithms on the ExpASy Proteomics Server (<http://www.expasy.org>) to determine the distribution of charged and hydrophobic amino acids, and thus, the number and distribution of Tms (Figure 7.3). Also, a comparison to FocA helped determine the Tm boundaries (Suppmann & Sawers, 1994) (Figure 7.3). An alignment of 373 available NitA homologues from 258 species (Pfam Protein Families Database - Accession No: PF01226, (Finn *et al.*, 2006)), including FocA, was investigated to ascertain the conservation of key NitA amino acids from the archaeobacteria, eubacteria, fungi and protista. Ten residues with almost perfect conservation are indicated in red in Figure 7.3. Further residues with relatively high levels of conservation were shown in green (> 90 %) and purple (> 60 %). Additionally, it was noted that some isofunctional substitutions were present in terms of charge. Specifically, charge conservation exceeded 80 %, in D88, D209, K156 and K192, (Figure 7.3 yellow shading).

A number of characteristic motifs are also apparent (Figure 7.3). NitA contains signature motifs unique to the FNT group of proteins which may be critical for structure or function, including FNT1 ((L/I/V/M/A)-(L/I/V/M/Y)-X-G-(G/S/T/A)-(D/E/S)-L-(F/I)-(T/N)-(G/S), FNT2 ((G/A)-X-X-(C/A)-N-(L/I/V/M/F/Y/W)-(L/I/V/M/F/Y/W)-V-C-(L/V)-A and FNT3 (F-(I/V/F/A)-X-(L/I/S)-G-(L/E/Y/T)-(E/Q)-H-(S/V/C/Y)-(V/I)-(A/G)-(N/D)-(M/L/Q) (Galvan *et al.*, 2002) (Figure 7.3). An additional motif is conserved in Tm 6 (G/A)-(G/A/S)-(G/A/M/E)-(N/T/D/A)-(V/M/L/F/T)-(V/M/L/F/T)-G-(G/A/S)-(G/V/A/I) (Figure 7.3). This NS-like sequence shows remarkable similarity to the nitrate signature sequences found in the NNP family (Unkles *et al.*, 1991; Trueman *et al.*, 1996; Unkles *et al.*, 2001; Unkles *et al.*, 2004a). As already discussed in Chapter Three, the nitrate signature sequences of NrtA are thought to be intimately linked to the substrate binding site, possibly in a structural capacity (Chapter Three).

Comparing the NitA NS-like sequence to the nitrate signature sequences of NrtA, shows an apparent conservation of glycine residues (Figure 7.4).

Figure 7.3 Provisional secondary structure of the *A. nidulans* NitA permease. Conservation is shown by coloured residues; red indicates > 95 % conservation, green > 90 % conservation and purple > 60 % conservation when compared to homologues. Signature sequences are shown with coloured lines, characteristic of the FNT family, the FNT signature sequences are shown in blue (FNT1), pink (FNT2) and green (FNT3) while the putative NNP signature sequence is shown in orange (Tm 6). Amino acid positions, which show an isofunctional substitution in terms of charge in over 80 % of residues, are shaded yellow.

NrtA	NS I	AGLCNAGGG
	NS II	GGFGNLGGI
NitA	NS-like seq	TLLGNIVGG

Figure 7.4 Direct comparison of NrtA and NitA putative nitrate/nitrite signature sequences, showing conservation of glycine residues (yellow) which are thought to be involved with close packing of the Tm, and the conserved asparagine (blue).

7.2.3 Substrate specificity

Figure 7.5 shows an alignment of nitrite, formate and nitrite/bicarbonate FNT transporters, elucidating similarities and differences of family members in comparison to their specific substrates (Figure 7.6). The conservation between these proteins is interesting though substitutions in relation to specific substrates may equally reveal functional information. Of the three substrates discussed here, nitrite is the smallest molecule; it is bent from the central nitrogen with the charge shared equally between the two oxygen atoms (Figure 7.6). Formate and bicarbonate share a similar overall trigonal planar structure of a central carbon atom surrounded by hydrogen atoms and 3/2 oxygens respectively in bicarbonate/formate (Figure 7.6). Using MEME (motif discovery tool) (<http://meme.sdsc.edu/meme/intro.html>) (Bailey & Elkan, 1995; Bailey *et al.*, 2006)), independent analyses were performed on known nitrite (NitA, Nar1.1 and NirC) and formate (FocA and *M. formicum* FdhC) transporters, with the intention of using Motif alignment and search tool (<http://meme.sdsc.edu/meme/mast.html>) (MAST) to search unknown FNT protein sequences for motifs identified from the MEME analyses. However, this sample number of transporters was insufficient for a successful MAST analysis. Specifically, only known FNT motifs were identified for each group of substrate specific transporters.


```

EcFocA      MVLPMVAMFVASGF EHSIANMFMI PMGIVIRDFASPEFWTAVGSAPENF SHLTVMNFITDNLIPVTIGNI IGGGLLVGLTYWVIYLRENDHH----- 285
EcFocB      MILPITL FVASGF EHCIANLFVIPFAIAIRHFAPPPFWQLAHSSADNF PALTVSHFITANLLPVMLGNI IGGAVLVSMCYRAIYLRQEP----- 282
MfFdhC      IWFPIAMAFVCI GF EHVVANMF FIPVGI FIGG-----VTWSQFFINNMIPATLGNIVGGAI FVGC IYWF TTYLRGT-----NKAKA----- 280
EgFth       CWFPPVALFAVMRYEHVVVNM YTVPCSMALGSG-----VSWG LFWGWSIAPSTLGNMVGASLLVAFPMWVTHGHEYRQKQREAKQIDDKLTGSSSSDGLMNAEEAIPP 293
AnNitA      IWLPIYA FVSLGFDHVVANTFIPLAIWLDAPG-----ISVGLYIWKGI I PTLLGNI VGGGLFVGTYYWYMYLLQTNPVTLTGLRKT KAGESEGTVT PRQDDVEANAG 298
EcNirC      IWWCLLAFIASGYEHSIANMTL FALS WFGNHS-----EAYTLAGIGHNLLWVTLGNTLSGAVFMGLGYWYATPKANRPVADKFNQTETAAG----- 268
PfNitA      VFFAVYAFAIAGYEHI IANIYTLNIALMVNTK-----ITVYQAYIKNLLPTLLGN YIAGAI VLGLPLYFIYKEHYYNFERSKRDNDDAQMKSL SIELRN----- 309
CrNar1.1    AYLPMVAFITL GLEHSVANMF FCSL GIVQGAP-----VSWGAF LTNLLPVTLGNTLAGVLCMAAAYCACFGAAGNKPAATAAPAAK----- 355
CrNar1.2    LWPCITAFVAI GLEHSVANMF VIPLGMMLGAE-----VTWSQFFFNLI PVTLGNTIAGVLMMAIAYSISFGSLG---KSAKPATA----- 336
CrNar1.3    VYLPVSAFVTLGTEHVIANQF ELSLAKMLG-----SGMSLHTI IRDNWVPATIGNI IGGAFFVGTLYAGVYGTLYERMWLRCLQVYVWVLPRAVRERIHAARTAVYE 439
CrNar1.4    IWLPI SAFAMLGFEHSIANMF LFLMAWAMGAN-----ITAKQFIWDNLI PATLGNFFGGVCLGT VYAFAYGRTPKLMGAWIDQKLKRS----- 406
CrNar1.5    MWMPVTA FVTV GLEHSIANMWV IPI GMALGAP-----VSAGAPLTANLIPVTLGNVFAGAVL TAGSYSLAFGR LG---AAFNGEAAK----- 343
CrNar1.6    VLI PVTL FVASGF EHCIANQF I PGMRLGGAA-----QYVTTSEAI VKNYI PVTLGN SVAAMIFIVGFYFFS IGS GHD MVVNSWNSGVTRYLP PMLAGWLQTGDVVAE 330
      : *      :* :.*      .      : ** . . . .

```

```

EcFocA      -----
EcFocB      -----
MfFdhC      -----
EgFth       TYPDGSFVDEAPEAL YSGNNAAPNT PDVRHY-----
AnNitA      TVQGV EGSKMGG-----
EcNirC      -----
PfNitA      -----
CrNar1.1    -----
CrNar1.2    -----
CrNar1.3    KLFGWVDWDYI TTPADVIRETAGQDLNEDSPGPHDHAAIAKAGVSSAGGNSDNAGALDRKTGASTGAASQRGGVSRAGTSG LGRGGPARAISSMLVDVAVRNPMP TPF EKQRTEAALGSD 559
CrNar1.4    -----
CrNar1.5    -----
CrNar1.6    GGLQPLPGKFIG-----DISVHYGGVAGGGGTPSHRGISAALRAL T--SSMRG-----THAPPPAAV VSAQPQAATG-----EGANGKS 403

```

```

EcFocA      --
EcFocB      --
MfFdhC      --
EgFth       --
AnNitA      --
EcNirC      --
PfNitA      --
CrNar1.1    --
CrNar1.2    --
CrNar1.3    VV 561
CrNar1.4    --
CrNar1.5    --
CrNar1.6    MV 405

```

Figure 7.5. Legend on the following page.

Figure 7.5 Amino acid alignment of proteins from the FNT family, known to transport formate, nitrite and/or bicarbonate. Regions underlined represent putative Tm domains predicted by Topcons (<http://topcons.net/>). *C. reinhardtii* is proposed to have an additional Tm (Mariscal *et al.*, 2006) (shown in italics). EcFocA and MfFdhC transport formate or its analogue hypophosphite (White & Ferry, 1992; Suppmann & Sawers, 1994) and EcFocB and EgFth are putative formate transporters based on sequence conservation (Andrews *et al.*, 1997; Delomenie *et al.*, 2007). AnNitA, EcNirC and CrNar1.1 are nitrite transporters (Clegg *et al.*, 2002; Mariscal *et al.*, 2006; Wang *et al.*, 2008). PfNitA is uncharacterised and CrNar1.2 is a bifunctional nitrite/bicarbonate transporter (Mariscal *et al.*, 2006). No substrate is defined for CrNar1.3, CrNar1.4, CrNar1.5 or CrNar1.6 (Mariscal *et al.*, 2006). Conserved residues are shown where ‘*’ represents a conserved residue, ‘.’ a conserved substitution and ‘.’ a semi conserved substitution.

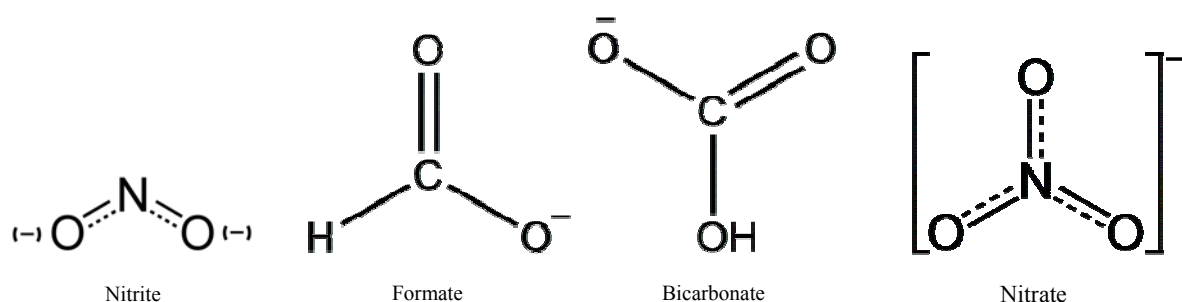


Figure 7.6 Chemical structures of FNT family substrates nitrite, formate and bicarbonate also showing nitrate as a structural comparison.

7.2.4 Generation of strain VFS106 for high throughput transformation of *nitA* mutants

As a result of low transformation efficiency targeting mutant constructs to the *argB* locus using the JK1060 strain, a new transformation system was developed following Szewczyk *et al* (2006). By means of traditional genetic techniques A1150 (*pyroA4; argB2; nkuA::argB*; riboB2*) was crossed with JK1060 (*nrtA747; nrtB110; argB2; ya2; pyroA4; pabaA1*). From here progeny were purified and tested on various growth media to identify a strain with the genotype *nrtA747; nrtB110; ya2; argB2; nkuA::argB* pyroA4*, this was designated VFS106 (Vicki Frances Symington-106). This method provided increased transformation frequency and single copy construct integration at the wild-type *nitA* locus. This method uses PCR product instead of plasmid integration for genetic integration.

The fragment was produced using primers described in Appendix Three for Fusion PCR. The initial stage was to prepare four independent fragments following the standard PCR reaction as described in Section 2.4.4 with reaction conditions of 1 cycle of 98 °C 1.30 min followed by 30 cycles of 98 °C 10 sec, 55 °C 20 sec 72 °C 10 sec. Products from this stage were pooled and added to a second reaction to fuse fragments together using only external nested primers FNitA1.1 and FNitA1.2 with reaction components as described and reaction cycles: 1 cycle of 98 °C 1.30 min followed by 25 cycles of 98 °C 10 sec, 55 °C 20 sec 72 °C 2.00 min. This product was then purified and

transformed into strain VFS106 as described in *Section 2.4.12*. With the expectation that successful transformants were to be selected for pyridoxine prototrophy. By this method homologous crossover events would produce single copy integrations at the wild-type *nitA* locus.

The main advantage here is the increased frequency of successful transformation and the need to produce only a PCR product and not high plasmid concentrations for standard *argB* transformations.

7.2.5 Residue replacements

Mutant PCR products were transformed into strain VFS106 to replace the wild-type *nitA* gene. Transformants were selected for on MM containing pyridoxine as the selective marker. Phenotypes of the resulting transformants were tested on 2 mM NaNO₂ as the sole nitrogen source (pH 7.5). The coding regions of each purified mutant were amplified by PCR and the entire *nitA* gene sequenced to confirm the desired mutation and to ensure that no other mutations had arisen in the gene. The data presented in Table 7.1 summarises *nitA* mutations made, including codon changes, phenotypes on 2 mM NaNO₂ minimal media at pH 7.5 at both 25 °C and 37 °C and protein expression results together with any kinetic data obtained from assays performed using ¹³NO₂⁻. Fusion PCR and gene targeting using VFS106 were used to produce single copy integrations at the wild-type *nitA* locus (Szewczyk *et al.*, 2006). Southern blotted genomic DNA was studied in a selection of mutants to ensure single copy integration of fusion PCR product; this was achieved (Figure 7.7). Strains which showed good growth on 2 mM NaNO₂ (+++/++) were selected for influx assays. No mutant demonstrated an alteration in either Km or Vmax. Table 7.1 shows the Km and Vmax generated for key strains.

7.2.6 'Wild-type' strains

Alterations to non-conserved residues L127 and C177 were performed as internal positive controls to test the system, to ensure that both vector and transformation system were appropriately constructed. As such, conservative mutations to valine and threonine in L127 and C177 respectively, demonstrated wild-type growth on 2 mM NaNO₂ and wild-type expression of the respective mutant proteins after Western blot analysis (Figure 7.8). As internal controls for the system, these mutants were shown to be fully functional by both growth tests and expression studies. ¹³N assays were not carried out for these strains.

Mutant	Transformant No.	Codon Change	Position	Side Chain Alteration	Phenotype		Expression	¹³ NO ₂ ⁻ Assay Results		
					25 °C	37 °C		Km (μM)	Vmax (nmol mg ⁻¹ DW h ⁻¹)	r ²
<i>AnitA</i>	T26	Δ	-	-	-	-	Poor	Linear kinetics		0.99
WT	T5275/T600	N/A	-	-	+++	+++	Good	19.17 ± 0.88	148.77 ± 2.01	0.92
D88E	T2655	GAC → GAG	Tm 2	Conservative	++	+++	Good	32.36 ± 5.38	120.29 ± 8.73	0.90*
D88N	T2621	GAC → AAT	Tm 2	Loss of charge	++	++	Moderate	42.44 ± 9.60	80.31 ± 9.60	0.87**
D88Q	T5004	GAC → CAA	Tm 2	Loss of charge and volume increase	++	++	Good	28.69 ± 7.67	91.98 ± 11.15	0.82**
D88S	T5313	GAC → TCC	Tm 2	Loss of charge	++	++	Moderate	ND	ND	ND
D88V	T5326	GAC → GTG	Tm 2	Loss of charge	+/-	+/-	Poor	ND	ND	ND
N122D	T2681	AAC → GAT	Tm 3	Gain of charge	-	-	Poor	ND	ND	ND
N122Q	T2123	AAC → CAA	Tm 3	Conservative	-	-	Poor	ND	ND	ND
N122S	T2111	AAC → TCC	Tm 3	Conservative	-	-	Poor	ND	ND	ND
N122K	T5183	AAC → AAA	Tm 3	Gain of charge	-	-	Poor	ND	ND	ND
L127V	T5021	TTA → GTC	Tm 3	Conservative	+++	+++	Good	ND	ND	ND
K156Q	T5232	AAA → CAG	Lp ¾	Loss of charge	-	-	Good	ND	ND	ND
K156R	T5075	AAA → CGA	Lp ¾	Conservative	+++	+++	Good	34.14 ± 7.27	162.03 ± 14.54	0.82
K156S	T5050	AAA → TCA	Lp ¾	Loss of charge and volume decrease	-	-	Good	ND	ND	ND
N173A	T2484	AAC → GCC	Tm 4	Loss of charge	++	++	Good	Linear kinetics		0.99
N173C	T2407	AAC → TGC	Tm 4	Addition of SH	++	++	Moderate	ND	ND	ND
N173D	T5150	AAC → GAT	Tm 4	Gain of charge	+	+	Good	ND	ND	ND
N173K	T2454	AAC → AAA	Tm 4	Gain of charge	-	-	Poor	ND	ND	ND
N173Q	T2154	AAC → CAA	Tm 4	Conservative	-	-	Moderate	Linear kinetics		0.99
N173S	T2040	AAC → TCC	Tm 4	Conservative	++	++	Good	Linear kinetics		0.99
N173T	T2428	AAC → ACA	Tm 4	Conservative	+	+	Good	ND	ND	ND
N173Y	T2500	AAC → TAT	Tm 4	Loss of charge	-	-	Moderate	ND	ND	ND

Mutant	Transformant No.	Codon Change	Position	Side Chain Alteration	Phenotype		Expression	¹⁵ NO ₂ ⁻ Assay Results		
					25 °C	37 °C		Km (μM)	Vmax (nmol mg ⁻¹ DW h ⁻¹)	r ²
<i>ΔnitA</i>	T26	Δ	-	-	-	-	Poor	-	-	0.99
WT	T5275/T600	N/A	-	-	+++	+++	Good	19.17 ± 0.88	148.77 ± 2.01	0.92
C177T	T2175	TGT → ACC	Tm 4	Conservative	+++	+++	Good	ND	ND	ND
K192Q	T2532	AAG → CGA	Lp 4/5	Loss of charge	+++	+++	Good	ND	ND	ND
K192R	T5100	AAG → CAA	Lp 4/5	Conservative	+++	+++	Good	39.87 ± 12.95	98.28 ± 14.17	0.84
K192S	T2617	AAG → TCA	Lp 4/5	Loss of charge and volume decrease	+++	+++	Good	ND	ND	ND
H210Q	T2029	CAC → CAG	Tm 5	*	-	-	Poor	ND	ND	ND
H210K	T5131	CAC → AAG	Tm 5	*	-	-	Poor	ND	ND	ND
H210S	T2250	CAC → TCC	Tm 5	Volume decrease	-	-	Good	ND	ND	ND
N214D	T5581	AAC → GAC	Tm 5	Gain of charge	+++	+++	Good	ND	ND	ND
N214Q	T5503	AAC → CAA	Tm 5	Conservative	-	-	Poor	ND	ND	ND
N214S	T5400	AAC → TCC	Tm 5	Conservative	+	+	Poor	ND	ND	ND
N214K	T5450	AAC → AAG	Tm 5	Gain of charge	-	-	Poor	ND	ND	ND
N246D	T2720	AAT → GAT	Tm 6	Gain of charge	-	-	Good	ND	ND	ND
N246Q	T2302	AAT → CAA	Tm 6	Conservative	-	-	Poor	ND	ND	ND
N246S	T2341	AAT → TCC	Tm 6	Conservative	-	-	Poor	ND	ND	ND
N246K	T5353	AAT → AAA	Tm 6	Gain of charge	-	-	ND	ND	ND	ND

Table 7.1. Legend on next page.

Table 7.1 Summary of mutations made to NitA. The mutants are shown with their transformant numbers, codon changes and general position within the permease. Where ‘conservative’ is stated, the change does not alter the charge or the size of the amino acid significantly. Alterations to side chain volume are noted along with loss or gain of charge. Growth characteristics are shown on a scale where ‘-’ represents no growth, ‘+/-’ is negligible, though not as low as the negative control, ‘+’ is a slight improvement on ‘-’, ‘++’ is less than wild-type and ‘+++’ is wild-type growth. Approximately equal concentrations of protein were loaded onto gels and an approximate measurement of expression is given here as ‘poor’, ‘moderate’ or ‘good’ by comparison to the wild-type. All mutants are *nrtA*, *nrtB* (*nrtA747*, *nrtB110*). The control strain T5275 harbours a transformed wild-type copy of *nitA* at the wild-type locus. T600 is a nitrate knock-out mutant which is naturally *nitA* wild-type (*nrtA747*, *nrtB110*, *pyroA4*, *pabaB1*, *yaA2*), and T26 is a *nitA* knock-out in the *nrtA*⁻*nrtB*⁻ (*nrtA747*, *nrtB110*) background. ¹³N tracer assay results are shown for assayed mutants. These assays were performed at least in duplicate and a representative experiment is shown here. * This r^2 and corresponding data represents 0-200 μ M nitrite, 250 μ M is excluded as an outlier. ** This r^2 and corresponding data represents 0-150 μ M nitrite, 200 μ M and 250 are excluded as outliers; refer to plots of this data, Figure 7.10 and 7.14. Where a result shows ‘ND’ this data has not been determined.

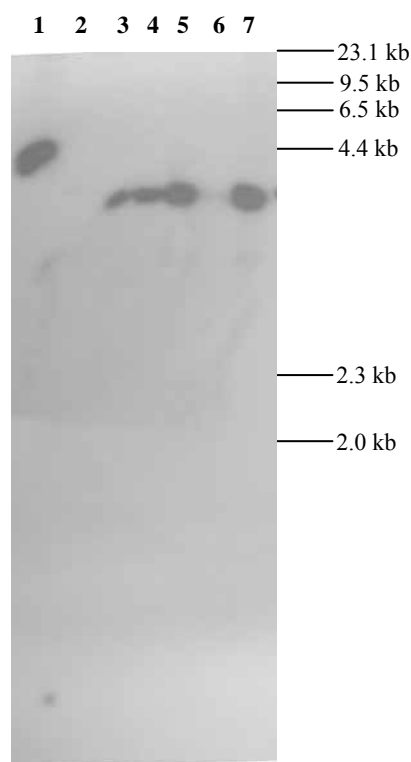


Figure 7.7 Southern blot of *nitA* mutants integrated at the wild-type *nitA* locus. *BglII* digests of genomic DNA shows a fragment size of 3.4 kb indicating the single copy integrations (3-7); *BamHI* digests of the wild-type acts as a size marker control showing 4.3 kb for comparison (1). No DNA is shown in lane two due to DNA loading. Of the strains investigated all showed the 3.4 kb band of the *BglII* digest as expected. While *HindIII* phage λ DNA is shown as a size marker, the *BamHI* digested D88N T2621 was shown as the size marker control.

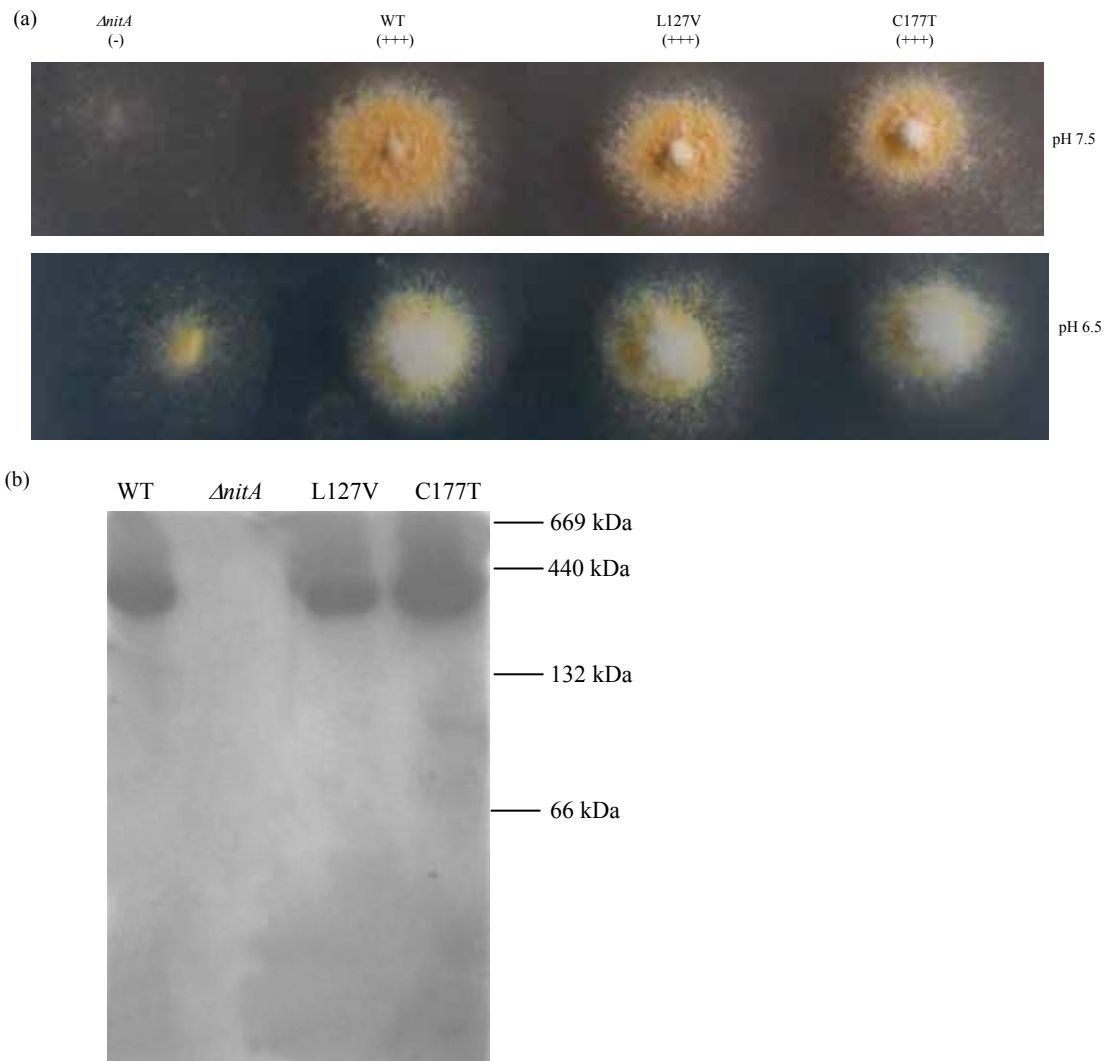


Figure 7.8 Growth and expression characteristics of wild-type (*nitA*⁺) mutants L127V and C177T. All strains are in an *nrtA*, *nrtB* double mutant background. (a) Growth tests shown were performed as described in Figure 7.1 (b) Western Blot showing the expression of the NitA protein in the membrane fraction of mutant strains after growth for 5-6 h in 5 mM urea followed by a 3 h induction with NaNO₂ at 37 °C. The complete gel is shown for these mutants; it can be observed that NitA is a tetramer based on its size, approximately four times the size of the predicted 33.6 kDa. At least two independent experiments were completed. Grading as in Table 7.1.

7.2.7 Alteration of charged residues D88, K156 and K192

The charges in positions D88 (Tm 2), K156 (Lp 3/4), K192 (Lp 4/5), and D209 (Tm 5) are conserved in 93 %, 87 %, 96 % and 81 % of 373 aligned proteins respectively, codons of these residues were targeted for mutagenesis. Residue D88 was altered to asparagine, glutamic acid, arginine, serine and valine representing conservative replacements, loss of charge and alterations to residue size. Growth of each mutant was reduced compared to wild-type on 2 mM NaNO₂ (pH 7.5) with the exception of D88E (Figure 7.9). Western blot showed that D88 mutant expression was approximately wild-type for D88E and D88Q and

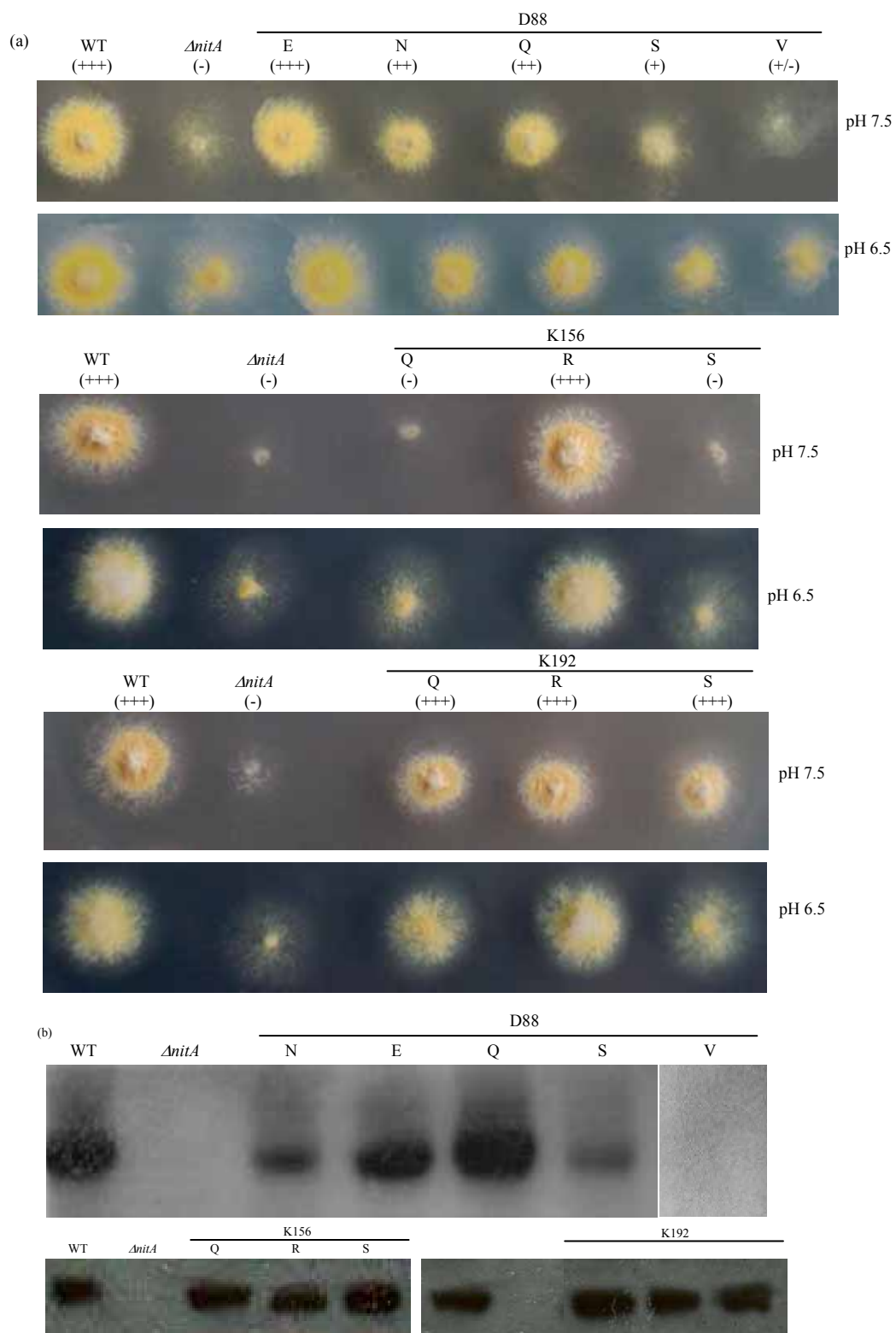


Figure 7.9 Growth and expression characteristics of mutants in conserved-charged amino acids in NitA. (a) Growth tests carried out as Figure 7.8. (b) Western blots carried out as Figure 7.8.

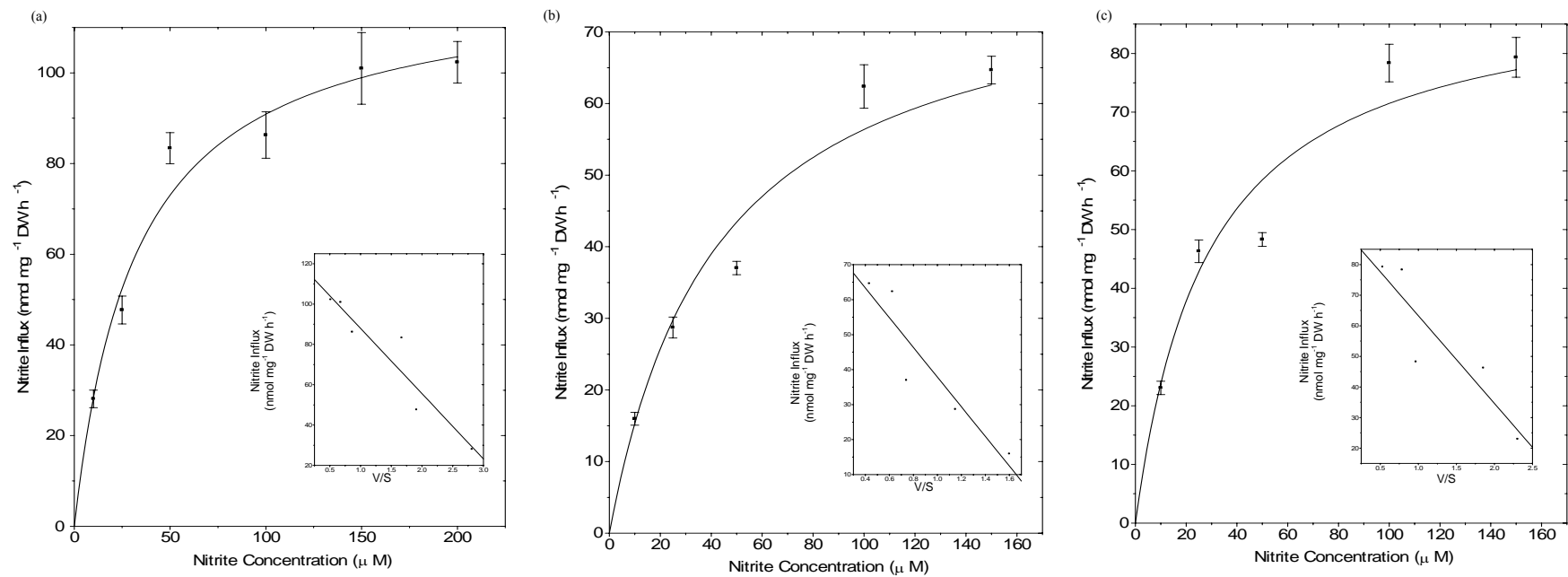


Figure 7.10 ¹³NO₂ tracer uptake assays of D88 mutants, corrected for outliers. Flux data were analysed by Hofstee plot which are shown as inserts in each graph. At least two replicates were performed for each mutant and the experiment with the highest r² is shown. (a) D88E (b) D88N (c) D88Q.

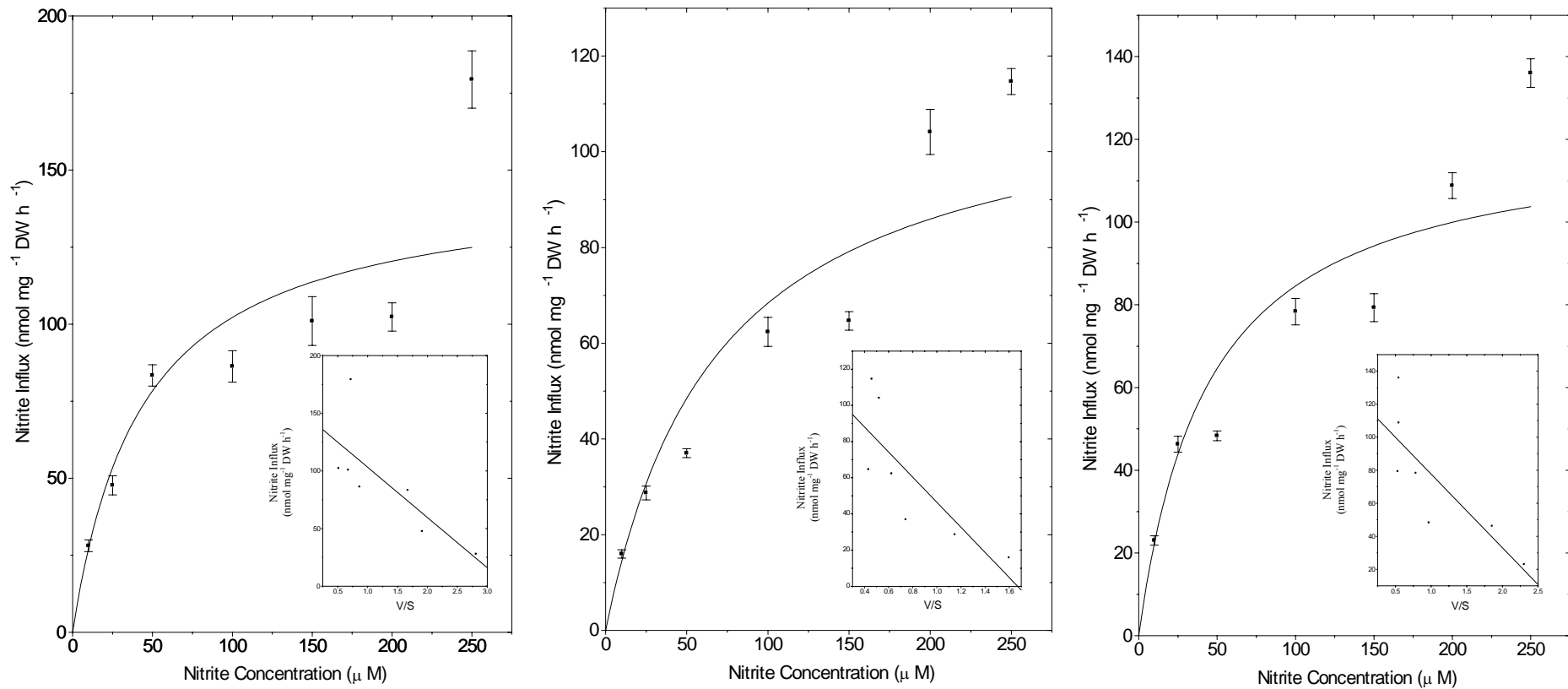


Figure 7.11 ¹³NO₂ tracer uptake assays of D88 mutants, uncorrected for outliers based on experiments in the range of 10-250 μM KNO₂ Flux (a) D88E (b) D88N (c) D88Q

Mutant	Km (μM)		Vmax ($\text{nmol mg}^{-1} \text{DW h}^{-1}$)		r^2	
	Corrected	Uncorrected	Corrected	Uncorrected	Corrected	Uncorrected
T26	Linear Kinetics	-	-	-	0.99	-
T5275	19.17 ± 0.88	-	148.77 ± 2.01	-	0.92	-
D88E	32.36 ± 5.38	43.58 ± 16.25	120.29 ± 8.73	146.71 ± 24.80	0.90	0.58
D88N	42.44 ± 9.60	69.25 ± 23.20	80.31 ± 9.60	115.71 ± 20.53	0.87	0.64
D88Q	28.69 ± 7.67	44.66 ± 14.04	91.98 ± 11.15	122.24 ± 17.72	0.82	0.67

Table 7.2 Comparison of corrected and uncorrected uptake flux data using $^{13}\text{NO}_2^-$ to study nitrite transport in D88 mutant strains. All assays were performed on young germlings grown for 5 h in MM (pH 6.5) containing 5 mM urea followed by a 3 h induction in 5 mM KNO_2 . Uptake assays were performed for 10 min at each specified concentration. Wild-type *nitA* transformant T5275 and *nitA* knock-out strain T26 are shown here for comparison only.

moderately expressed for D88N and D88S (Figure 7.9b) while D88V was not expressed in the membrane.

The augmented growth phenotype of D88E compared to D88N, D88Q, D88S and D88V identified a putative requirement for charge position. To further examine this finding, assays were performed using $^{13}\text{NO}_2^-$, on mutants D88N, D88E and D88Q. If this residue was involved with anion interaction or salt-bridge formation an alteration to Km or Vmax would be expected. However, all showed hyperbolic curves with no apparent alteration to Vmax or Km (Table 7.1). Each of these mutants had outliers at the end of the concentration set, 200-250 μM KNO_2 (Figure 7.11) in contrast to the wild-type hyperbolic curve (Figure 7.2b) implying sigmoidal, not hyperbolic kinetics. Removing these from the data improved r^2 , Km and Vmax values became more comparable to wild-type. The uncorrected data (shown in Figure 7.11) was compared to corrected data (see Table 7.2). It is unclear at this stage whether or not the outlying value is a true value or an outlier. As a true value this would imply sigmoidal kinetics and therefore it would be very interesting to look at these mutants over an extended concentration range. This, it is hoped could be performed in the future.

Additionally, conserved lysines present on loops 3/4 (K156) and loop 4/5 (K192) were altered to arginine, glutamine and serine, each showed expression comparable to wild-type (Figure 7.9b). Again, growth of these mutants was assessed on 2 mM NaNO_2 (pH 6.5 and 7.5) (Figure 7.9a). When K156 was altered to glutamine and serine no growth was observed, though was wild-type when altered to R, implying that at this position charge is required. Without exception, K192 mutants showed wild-type growth on NaNO_2 .

K156R and K192R mutants were selected for $^{13}\text{NO}_2^-$ transport assays but again, had no apparent alteration to K_m or V_{max} (Figure 7.12). Both mutants showed hyperbolic kinetics over the concentration range shown with no real alteration to either K_m or V_{max} (Figure 7.12).

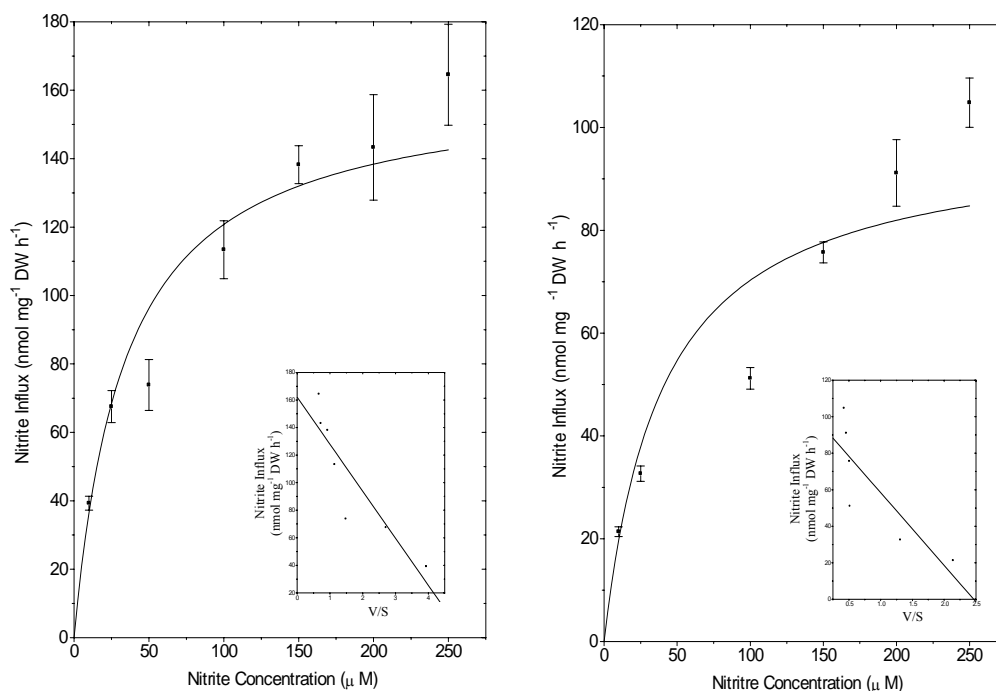


Figure 7.12 $^{13}\text{NO}_2^-$ tracer uptake assays of mutants K156R and K192R. Flux data were analysed by Hofstee plot which are shown as inserts in each graph. Assays were carried out using $^{13}\text{NO}_2^-$ as described. At least two replicates were performed for each mutant and the experiment with the highest r^2 is shown. (a) K156R (b) K192R

7.2.8 Alteration of histidine, H210

H210 is a 'special case' amino acid and is present in Tm 5 of FNT proteins (in motif FNT 3). There is no charge status defined for H210 in Table 7.1 because its charge is dependant upon the protonation of the imidazole side-chain, which in turn is dependent on the internal pH. In NitA, if H210 is charged it would be an ideal candidate for substrate binding. It is conserved in 357 of 373 NitA proteins studied (96 %). Interestingly, of the sixteen aligned proteins which did not have histidine in position 210, ten of these proteins had glutamine (polar). However, alone this does not answer whether there is a charge required at this position or if the side-chain is polar. This histidine residue was altered to glutamine, serine and lysine, none of these changes permitted growth on 2 mM NaNO_2 (Figure 7.13). Further, mutants H210Q or K were not expressed while H210S was expressed near to wild-type levels.

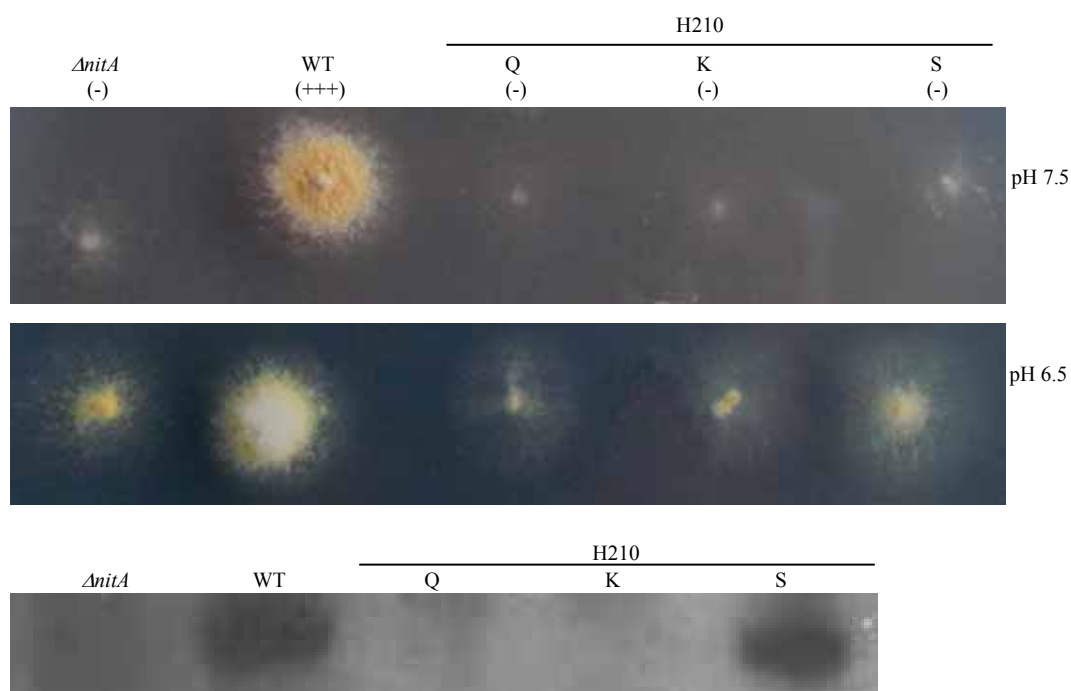


Figure 7.13 Growth and expression characteristics of mutants in H210 in NitA. Growth tests carried out as Figure 7.8. Grading as shown in Table 7.1.

7.2.9 Alteration of conserved asparagines

Alterations of N122 (Tm 3) to glutamine (conservative replacement), serine (slight reduction in size), lysine (increase in size and gain of positive charge), or aspartic acid (gain of negative charge) did not permit growth on 2 mM NaNO₂. This was also the case for N246 (NS-like motif, Tm 6). However, by changing N173 (FNT2, Tm 4) to alanine, cysteine, aspartic acid, lysine, glutamine, serine, threonine or tyrosine, growth was permitted to varying degrees, though none as wild-type (Figure 7.14, Table 7.1). Additionally, N214S mutant showed slight growth on nitrite, whereas growth was significantly improved for N214D and mutants N214K/Q lacked growth (Figure 7.14). Expression analyses showed that N122 and N246 mutants were not expressed in the membrane, with the exception of N246D (expressed to approximately wild-type levels, not shown).

¹³NO₂ assays were performed on N173A, N173Q and N173S (Figure 7.15a). One replicate of each mutant was performed in the concentration range 10-250 μM KNO₂ and strain N173S was repeated in the 10-2000 μM KNO₂ range (Figure 7.15b). While N173A and N173S both showed good growth on 2 mM NaNO₂ (Figure 7.14), ¹³NO₂ linear uptake kinetics were unexpected (Figure 7.15). Net nitrite assays were performed on these mutants to confirm or contradict this result.

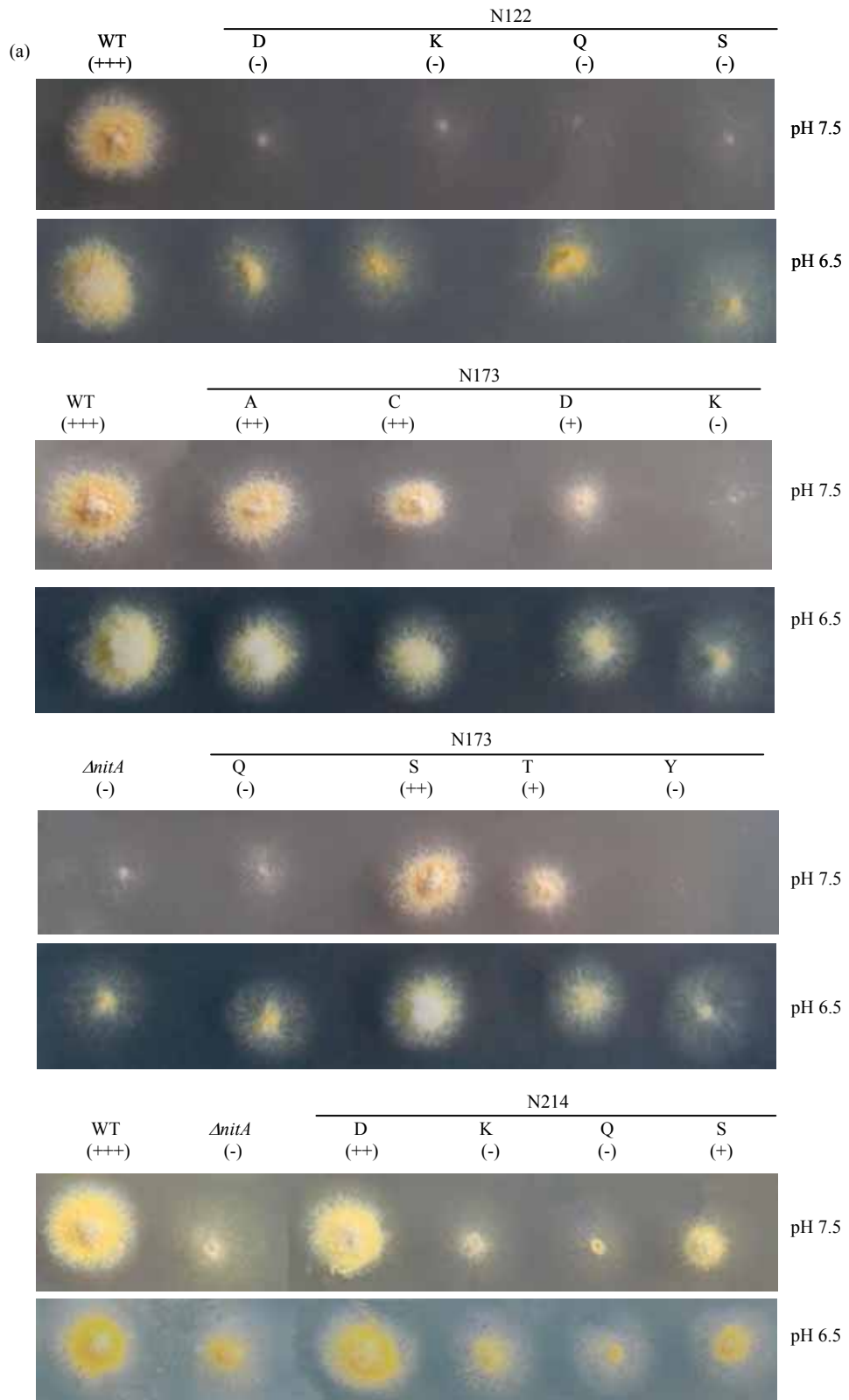


Figure 7.14 Legend on the following page.

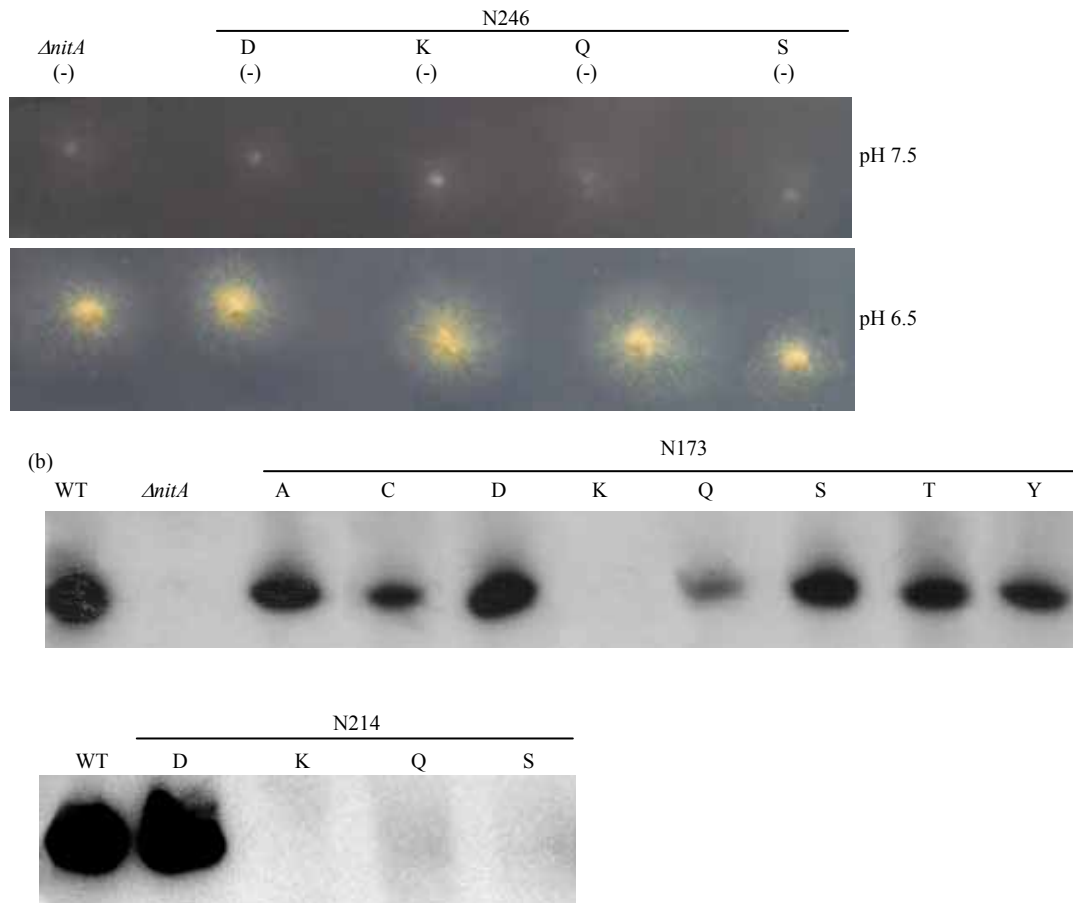


Figure 7.14 Growth and expression characteristics of mutants in N122, N173 and N246 (a) Growth tests shown here are as described in Figure 7.8 (b) Western blot showing the expression of the NitA protein in the membrane fraction of N173 and N214 mutant strains as described in Figure 7.8. Grading as Table 7.1.

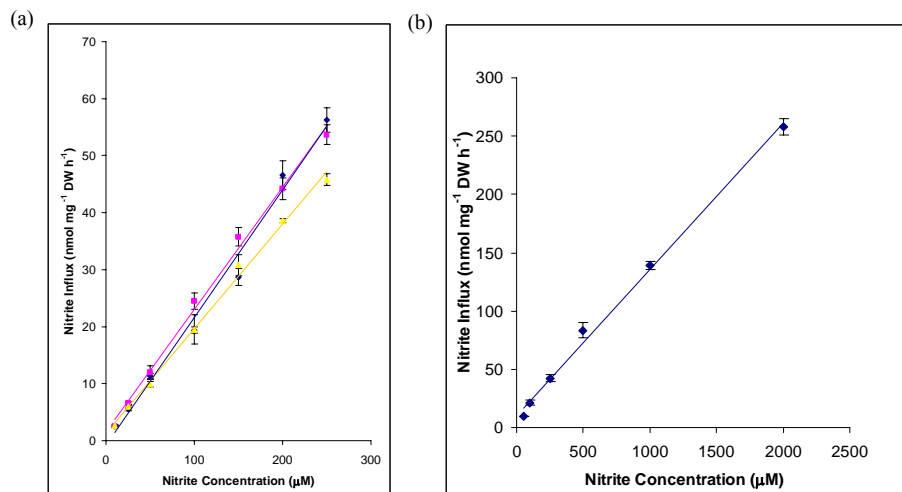


Figure 7.15 (a) ¹³NO₂⁻ flux assays for N173A, N173S and N173Q. All mutants displayed linear kinetics N173A, $r^2=0.996$ (yellow), N173Q, $r^2=0.996$ (pink), N173S, $r^2=0.988$ (blue). (b) An extended assay concentration range of 2 mM KNO₂ was performed on mutant N173S, shown here to illustrate that no plateau was reached, and thus,

indicating linear kinetics. Each mutant was assayed once; N173S was carried out twice, once for each concentration range (10-250 μM and 10-2000 μM). Strains were grown for 4 h on urea followed by 3 h induction by 5 mM KNO_2 before 10 min assays of 10-250 and 10-2000 μM KNO_2 .

7.2.10 Further expression analyses of N122 and N246

Protein expression in sequenced transformants was compared to a wild-type transformant with the C-terminal V5 epitope tag and *nitA* knock-out strain T26. In cases where no growth was found on 2 mM NaNO_2 and no expression on BN-PAGE, a further assessment of these proteins was carried out on 10 % SDS-PAGE to assess for protein which has not formed higher order structures. The Western blot data shown in Figure 7.16 shows these proteins from this electrophoresis and Western transfer. It would appear that no monomers are found.

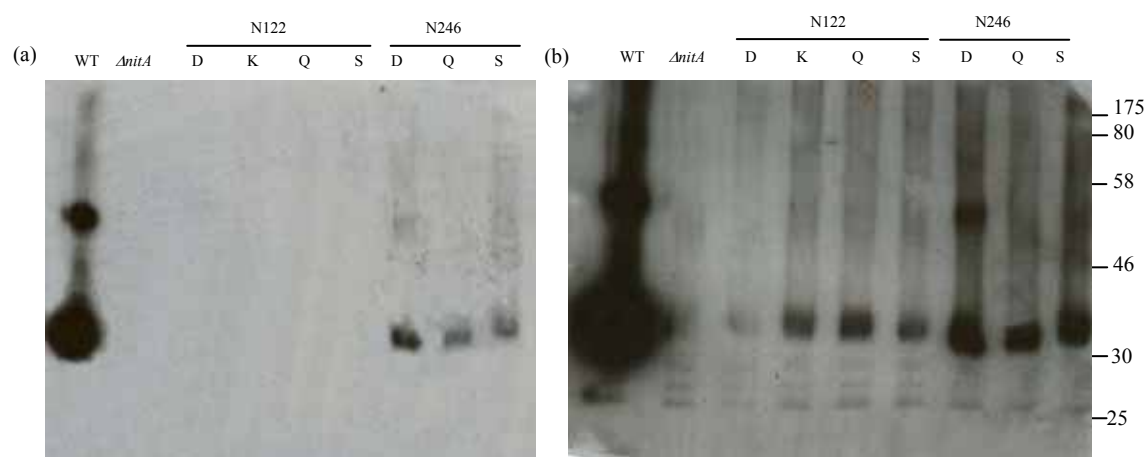


Figure 7.16 Expression characteristics of NitA proteins (10 % SDS-PAGE) which failed to show protein on BN-PAGE. Protein extracts were the same extracts as used for BN-PAGE. (a) Initial exposure (b) Extended exposure. Protein size marker measured in kDa.

7.2.11 Net nitrite assays

Net nitrite assays were performed on the wild-type *nitA* transformant (T5275), $\Delta nitA$ (T26), T110 (*nrtA747*, *nrtB110*), N173A and N173S as a check on $^{13}\text{NO}_2^-$ assay results. Initial assays (using 100 μM nitrite in the assay media) showed a slight elevation in uptake in mutant strains relative to the knock-out strain at pH 6.5 with 100 min 10 mM NaNO_3 induction (Table 7.3). Assays were also performed at pH 7.5 to reduce HNO_2 diffusion. However, these assays were unsuccessful with 100 μM or 2 mM nitrite.

Strain	Net nitrite uptake (nmol mg ⁻¹ DW h ⁻¹)
T26 (<i>ΔnitA</i>)	6.17 ± 1.92
T5275 (WT)	111.07 ± 2.07
T110	49.83 ± 4.45
N173A	25.27 ± 2.34
N173S	13.30 ± 2.35

Table 7.3 Net nitrite uptake in control strains and in NitA mutant strains N173A and N173S. Experiments were performed in triplicate.

7.2.12 Revertant studies

Using the random chemical *in vitro* mutagen NTG to target non-complementing NitA mutants, revertants were sought. Mutants targeted were N122Q, N173C, N173K, N173Q, H210S, N246Q and N246S. The *nitA* coding regions of putative revertants which grew on 2 mM NaNO₂ after mutagenesis were amplified by PCR and sequenced. However, no *bona fide* NitA suppressor strains were found. Supposed suppressors from N173Q and N173K mutants when sequenced showed the desired mutation (i.e. N173Q or K). However, they did not show any additional mutation in the *nitA* gene even though they showed improved growth relative to the non-mutagenised N173Q and N173K strains on nitrite agar, implying that these strains were mutant elsewhere in the genome.

7.3 Discussion

7.3.1 Determination of enzyme kinetics and regulation

This study represents an attempt to shed light on the workings of a previously unidentified protein in *A. nidulans* from the FNT family, NitA. There has been little research into members of FNT and an effort was made to elucidate some of the structure/function relationships that are present in this permease. Initially, a phenotype for this knock-out strain was sought to ascertain whether it was an exclusive nitrite carrier. This was demonstrated by complete non-growth on nitrite (Figure 7.1). Wang *et al* (2008) demonstrated both the initial kinetics of this permease in addition to its regulation by the *AreA* and *NirA* regulatory proteins showing that *nitA* is under the same regulation as nitrate transport proteins NrtA and NrtB (Unkles *et al.*, 2001). Preliminary uptake assays by Dr S.E. Unkles failed to show formate uptake *per se* using labelled formate, and therefore formate uptake by NitA was considered unlikely.

Kinetics from net nitrite transport assays (Wang *et al.*, 2008) were shown to be $4.2 \pm 1 \mu\text{M}$ and $168 \pm 21 \text{ nmol mg}^{-1} \text{ DW h}^{-1}$ for K_m and V_{max} respectively for NitA, however, tracer experiments (which are considered to be more accurate) showed K_m and V_{max} to be $19.17 \pm 0.88 \mu\text{M}$, $148.77 \pm 2.01 \text{ nmol mg}^{-1} \text{ DW h}^{-1}$ respectively. This discrepancy is unclear but may be due to difference in approaches which reflects differences in induction conditions. Net nitrite assays were performed using 10 mM nitrate for 100 min induction period vs. 3 h, 5 mM nitrite induction of $^{13}\text{NO}_2^-$ assays. In addition, there is a fundamental error in the net nitrite experiments as the measurement of nitrite depletion from the media measures both nitrite influx and efflux by comparison to the tracer assays which purely measure uptake and therefore it must be recognised that these are two different measurements. Thereby, using the tracer nitrite experiment as a comparison includes two experimental variables, the inducing conditions and the influx method. By comparison of induction conditions refer to Table 7.4, which shows uptake assays at 10 or 100 μM KNO_2 using 3 h, 5 mM KNO_2 and 100 min, 10 mM KNO_3 induction conditions. It appears that nitrite flux is higher in 3 h KNO_2 induction, probably due to a longer induction period.

	5 mM Nitrite Induction (3 h)		10 mM Nitrate Induction (100 min)	
	10 (μM)	100 (μM)	10 (μM)	100 (μM)
Nitrite Flux ($\text{nmol mg}^{-1} \text{ DW h}^{-1}$)	87.66 ± 1.34	209.91 ± 6.78	38.19 ± 2.50	47.80 ± 3.43

Table 7.4 Net nitrite uptake assays by comparison of induction conditions. Using strain T110 (*nrtA747*, *nrtB110*) as wild-type *nitA* strain. Induction conditions were 3 h 5 mM KNO_2 vs. 100 min 10 mM KNO_3 .

Net nitrite transport assays for NitA were also carried out by Wang *et al* (2008) on triple deletion mutant strain T26. Low influx values of $\sim 30 \text{ nmol mg}^{-1} \text{ DW h}^{-1}$ vs. $1000 \text{ nmol mg}^{-1} \text{ DW h}^{-1}$ were recorded for *nrtA* and *nrtB* single mutant strains. When pH was decreased, an increase in NO_2^- depletion was observed, due to the low pK_a of HNO_2 (3.6). NO_2^- converts to HNO_2 at low pH allowing passive diffusion of HNO_2 through the membrane. Figure 7.17 shows that with lower pH there appears to be increased $\text{NO}_2^-/\text{HNO}_2$ uptake when the concentration of HNO_2 is higher. Table 7.5 shows that the NitA protein has a comparatively lower capacity for nitrite (V_{max}) transport than both NrtA and NrtB but a higher affinity for nitrite (K_m) (Wang *et al.*, 2008).

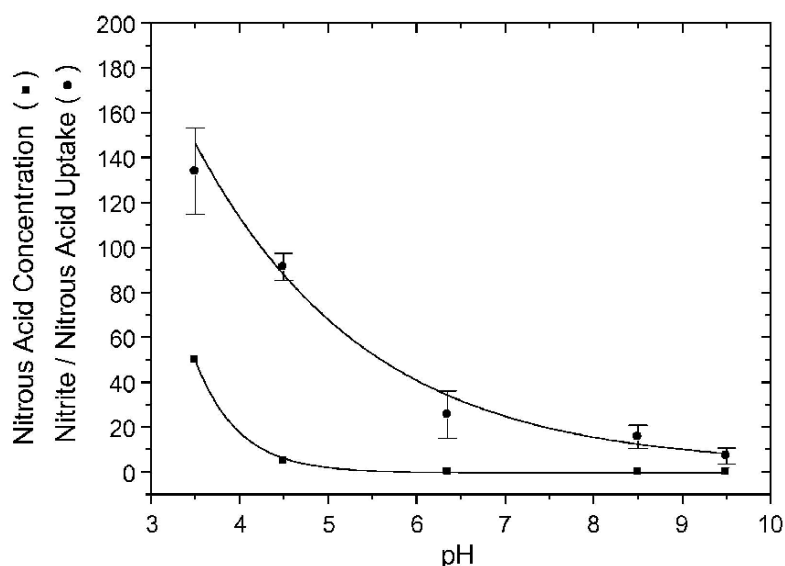


Figure 7.17 Assessment of HNO₂ concentration and NO₂ flux. This graph shows the effect of pH on HNO₂ concentration (µM) predicted from the Henderson-Hasselbalch equation on apparent NO₂ uptake (nmol mg⁻¹ DW h⁻¹) by triple mutant strain T26 from media initially containing 100 µM KNO₂. Essentially, the pattern of NO₂⁻ uptake mirrors HNO₂ concentration as pH decreases to the range of the pK_a for NO₂⁻. Graph taken from Wang *et al* (2008).

Strain	Transporter (s) present	K _m (µM)	V _{max} (nmol mg ⁻¹ DW h ⁻¹)	R ²
T26	-	-	~30	-
GO1	NrtA, NrtB, NitA	18.6 ± 1.8	915 ± 34	0.96
<i>nrtA747</i>	NrtB, NitA	11 ± 1	1147 ± 20	0.81
<i>nrtB110</i>	NrtA, NitA	16 ± 4	976 ± 82	0.91
<i>nrtA747, nrtB110</i>	NitA	4.2 ± 1	168 ± 21	0.81

Table 7.5 Kinetic data for nitrite flux of various *nrtA*, *nrtB* and *nitA* mutants. All strains were grown for 6 h in MM (pH 6.5) containing 5 mM urea; cells were induced for 100 min using NaNO₃. Net nitrite uptake was measured by depletion of NaNO₂ (10-100 µM) in assays over a 20 minute period. In mutants *nrtA747* and *nrtB110*, the kinetic data represents that of the NNP transporter in addition to that of the NitA transporter, therefore to determine an absolute value for nitrite uptake for both NrtA and NrtB the values for flux from *nrtA747 nrtB110* double mutant strain must be subtracted leaving V_{max} as 808 and 979 nmol mg⁻¹ DW h⁻¹ for NrtA and NrtB respectively. Data taken from Wang *et al* (2008).

7.3.2 Predicted secondary structure of NitA

Analysis of the NitA protein sequence using topology prediction software revealed NitA to be a 6 Tm FNT protein. There are three characteristic signature sequences of the FNT located in Tms 2, 4 and 5 (Galvan *et al.*, 2002). Their function is currently unknown, but constant presence across family members make it likely that they are involved with conformational changes and protein dynamics as in MFS proteins, which also contain specific sequences

characteristic to this family of proteins (Yamaguchi *et al.*, 1992; Jessen-Marshall *et al.*, 1995). In addition to these motifs, a sequence in Tm 6 exists that is not dissimilar to the NNP sequence of members of MFS subfamily NNP (Unkles *et al.*, 1991; Trueman *et al.*, 1996; Unkles *et al.*, 2001; Unkles *et al.*, 2004a). The conservation of the asparagine residue in this motif is of particular interest considering the structural/functional role of similar residues in NrtA (Unkles *et al.*, 2004a). A computational approach was taken to study NitA and nitrite and formate transporting homologs with an aim of identifying motifs characteristic of substrate. However, due to the small number of experimentally determined substrates it was not possible to develop a model for members of the FNT. With a larger sample set a characteristic motif or motifs could possibly be identified, this should be considered for future work.

NitA as a putative tetramer which likely operates with a single channel for substrate translocation. Thus, there are potentially four conserved asparagines from each monomer to interact with the substrate. It is likely that the NitA tetramer functions as a single binding site as a result of the characteristic hyperbolic curve. Transporters with more than one binding site generally show sigmoidal uptake kinetics (Thulasiraman *et al.*, 1998).

7.3.3 Mutagenesis

Fusion PCR was used to target mutant DNA constructs to the wild-type locus of *nitA* in VFS106 (*nrtA747*; *nrtB110*; *yA2*; *nkuA::argB*; *pyroA4*). This technique was developed for this study due to its high efficiency compared to the standard method used for NrtA integrations earlier in this thesis. In this method, employing an *nkuA* knock-out strain, authors had suggested that Southern blotting was not strictly necessary as integration was so efficient (> 90 % integration at target locus) (*J. R. Kinghorn personal communication*). Southern blotting did confirm, in this instance, successful integration of constructs. These mutant transformants were developed for biochemical assays. Two mutants were solely created as internal controls for this system, a 'reconstruction experiment'. Mutant L127V and C177T were successful in proving the efficient integration of this fusion PCR transformation system.

To build on our previous work, residues were identified which may be critical for the functioning of the permease. Charged amino acids are known to play pivotal roles in many transporters, either by directly binding the substrate, and/or participating in substrate translocation. Examples of proteins which employ crucial charged residues are LacY (Abramson *et al.*, 2003b), GlpT, (Huang *et al.*, 2003) NrtA (Unkles *et al.*, 2004a), OxlT

(Yang *et al.*, 2005) and the *E. coli* sodium proton anti-porter (NhaA) (Hunte *et al.*, 2005). In NitA, there are several highly conserved charged residues, for example D88, D209, K156 and K192.

Negatively charged residues in anion transporters contribute to salt-bridge formation (with positively charged residues) and protein dynamics (Mirza *et al.*, 2006; Law *et al.*, 2008). In Tm 2, there is a highly conserved negative charge (D88) which, in the majority of homologues (69 %) a glutamic acid resides, whereas in 24 % of homologues, like NitA an aspartic acid is present instead. Due to the negatively charged nature of D88 and D209 (Tm 5), these residues cannot be involved directly in anionic substrate binding. Consequently, residue D209 was not targeted in this study though its conservation is notable at the heart of Tm 5 next to conserved H210. The conservation of D88 suggests a role as a salt-bridge partner to charged amino acids within the protein. Mutations of D88 to polar amino acids permitted growth, albeit slightly reduced from wild-type, whereas the conservative alteration to glutamic acid permitted wild type growth. Expression of D88E and D88Q reflected the wild-type, whereas asparagine and serine were slightly reduced and D88V was not expressed (Figure 7.9a). Additional mutations to small amino acids serine and valine were carried out to test the necessity for side-chain bulk; these mutants showed reduced growth (Figure 7.9b). This suggests a requirement for both side-chain bulk and for charge in this position with charge being the main criterion. If D88 does act as a salt-bridge partner then it functions as wild-type with negatively charged glutamic acid in this position, there is no positively charged salt bridge partner candidate thus far. When D88 was altered to an uncharged amino acid (asparagine, glutamine, valine and serine) reduced transport was permitted, though it is thought that perhaps the tight binding of the permease structure is compromised, resulting in reduced transport as was found in GlpT (Law *et al.*, 2008). ¹³N assays did not show any significant alteration in Km or Vmax for any of these mutant proteins showing no direct substrate interaction (Figure 7.10 and 7.14). It is notable that in these assays at the high concentration end the kinetics seemed to be sigmoidal, i.e. they fell out of line with expected hyperbolic enzyme kinetics implying the presence of two binding sites, this had not been observed in enzyme kinetics for NitA previously, though when these values were removed the data reflected wild-type kinetics. The significance of these values is currently unknown.

Conserved positively charged residues are present throughout NitA though the highly conserved arginines of NrtA, LacY and GlpT which are essential mediators of substrate interactions (Abramson *et al.*, 2003b; Lemieux *et al.*, 2003; Unkles *et al.*, 2004a; Law *et al.*, 2008) are absent. Residues where charge was conserved in > 80 % of sites were studied. An

initial interpretation of the protein sequence and comparison to 51 homologues placed the highly conserved K192 firmly within Tm 5. This was a potential candidate for substrate binding, though phenotypic data does not support this notion (Figure 7.9a). Conserved lysines are important in GlpT (Law *et al.*, 2008) and OxlT (Wang *et al.*, 2006) for substrate binding and the formation of salt-bridges. With a larger alignment package (an increase of 51 to 373 sequences) plus a direct comparison to the FocA, K192 was moved out of the Tm, consistent with the phenotypic data not supporting a role in substrate binding, although it could still be involved with other cellular interactions in the cell as is implied by considering the strong purifying selection that has occurred at this site (Figure 7.12). It is possible that its position on a loop region of the intra cellular surface allows K192 to attract the anion as it moves through the pore, ensuring that the substrate moves quickly out of the binding site. This may explain why there is no kinetic alteration in the K192R mutant.

Again on the basis of conserved positive charge, K156 residing on the opposite side of the membrane to K192 was subjected to the same mutagenesis strategy. Alterations to glutamine, arginine and serine were made to represent changes in both charge and bulk. Again, these mutants were all expressed to wild-type levels in the membrane fraction; however growth was different from that of K192 alterations. While K156R maintained its wild-type growth, K156Q and K156S showed a lack of growth on agar (Figure 7.9a). This implies a direct function for K156 - a need for a positive charge at this position. The lack of growth in strain K156Q shows that it is not side-chain volume, but charge that is the controlling factor. As residue K156 is on the extra cellular surface of the membrane, it is possible that the charge is required to co-ordinate the anion as it moves into the pore as postulated for K192. $^{13}\text{NO}_2$ uptake assay results showed no reduction in K_m or V_{max} (Figure 7.12). Therefore, a direct involvement in substrate binding is unlikely. It is possible that residue K156 is involved in salt-bridge formation or co-ordination of the substrate as it travels towards the binding site.

The amino acid H210 (Tm 5) is a highly conserved residue which is usually considered as a positive charge, but depending on microenvironment pH, its imidazole side-chain can either be positively charged or polar, it has a pKa of 6. This amino acid is therefore unpredictable regarding potential interactions. As a positively charged residue it could be directly involved with binding the substrate or protein mobility and salt-bridge formation, or, as a polar amino acid with hydrogen bonding, either with the anion, or during translocation with residues elsewhere on the permease. Alterations in H210 were selected on the basis of minimal change to lysine and glutamine (accounting for the unknown nature of charge status) and a considerable alteration in size with the change to the polar amino acid serine. The question

here was therefore: in relation to this position is charge or polarity necessary for the normal functioning of NitA? If charge was indeed required a critical negatively charged salt-bridge partner may exist elsewhere in the protein. Conservative residues of glutamine and lysine did not produce growth, or protein expression (Figure 7.13). Further, while considerable change to serine did not permit growth, it was expressed in the membrane (Figure 7.13). To gain more of an insight into this protein it may be necessary to make further alterations with comparable side-chain bulk ideally polar amino acids, e.g. proline, or the large non-polar residue, phenylalanine. By changing histidine to lysine or glutamine, while charge was maintained the side-chain was lengthened, which may underlie the lack of expression as the protein was unable to insert or fold successfully in the membrane due to the appendage exceeding tight size restrictions. The change to serine, as expected, did not produce growth. Therefore, the bulk of the side-chain is probably necessary for function at this position. However no definite conclusions can be drawn currently as to what contribution charge makes at this position.

Random chemical mutagenesis to identify second site suppressors of H210S may identify amino acids that could compensate for this change located elsewhere in the protein. Unfortunately, this approach failed to unearth suppressors of H210S. This may indicate that there is no residue functionally capable of compensating for a knock-out of H210, attributing to its postulated essentiality in this position.

Within the GlpT protein H165 bears no obvious involvement with substrate binding, but, when protonated participates in substrate binding (Law *et al.*, 2008). Protonation stimulates an increased binding of charges at positions K80 and R269 and a destabilisation of a bond with R45 (Law *et al.*, 2008). Residue change of H165 to proline, produced a functional protein, though both transport and binding of the substrate were reduced (Law *et al.*, 2008). Proline is a similar size to histidine and this represented only a change in a protonation cycle and not a major physical alteration. Residue H168 in the UhpT transporter may have a similar function where the protonation state of histidine has the ability to alter the proteins' affinity for the substrate (Hall & Maloney, 2005). The position of histidine in UhpT and GlpT nearby the critical charged residues supports this theory (Hall & Maloney, 2005). Histidine has also been shown to be important in LacY (Law *et al.*, 2008) and TetA (Yamaguchi *et al.*, 1996). In regions of high aromatic density, the pKa of histidine can be elevated and thus encourage protonation by an increased propensity to react with aromatic residues (Dougherty, 1996; Tishmack *et al.*, 1997). However due to the lack of suitable models for NitA, the proximity of aromatics to H210 is unknown. The protonation of

histidine participates in channel closure of SoPIP2.1 (the spinach aquaporin) in response to flooding (Tornroth-Horsefield *et al.*, 2006) (Refer to Chapter Five, Figure 5.1). In SoPIP2.1 water management is controlled principally by phosphorylation of key serine residues at the opening of the pore. However, in conditions of flooding a highly conserved histidine residue is known to be protonated to close the channel and prevent an unwanted influx of water (Tornroth-Horsefield *et al.*, 2006).

The NitA protein has no perfectly conserved charged residues that when altered have modified kinetics as was shown for NrtA (Unkles *et al.*, 2004a). However, there are four very highly conserved asparagine residues, N122, N173, N214 and N246 which could theoretically co-ordinate their partial charges for the binding of the anion. Polar amino acids, such as asparagine, are known for their susceptibility to form hydrogen bonds as both donors and acceptors. There is the potential for asparagine to co-ordinate the partial negative charges of the oxygen atoms of nitrite and partial positive charges of the nitrogen. These amino acids may be the key to substrate binding and/or translocation considering their high conservation. Three conserved asparagines (N122, N173 and N246) were highlighted and targeted for mutagenesis. During a recent alignment, another asparagine which had previously been overlooked came to light, N214, this is why time constraints have meant Western analysis and $^{13}\text{NO}_2^-$ assays have not been performed on this strain. Initially, changes of asparagine in all four positions to aspartic acid, serine, glutamine and lysine were performed resulting in shifting of charge and bulk. N122 and N246 mutants showed no growth (Figure 7.14), and were not expressed in the membrane, with the exception of N246D which was expressed to wild-type levels (data not shown). It is possible that there are problems in the assembly of the quaternary structure of these proteins as conserved asparagines are known to contribute to the stabilisation of helix-helix interactions by hydrogen bonding (Rath & Deber, 2008). The expression pattern of N246D may be due to the near identical side chain volumes of aspartic acid and arginine aiding protein stability. All Western analyses were carried out using BN-PAGE. However, at the region of the gels where one would expect the transfer of monomers the gel was around 17 %. Thus, a problem may exist at this concentration for the efficient transfer of protein to the blotting membrane. This was repeated using controls for monomers on BN-PAGE though none were detected. As a final check, these mutant proteins were run on a standard 10 % SDS-PAGE to verify the complete absence of protein (Figure 7.16). Therefore, alterations in N122 and N246 do not produce membrane protein and do not grow on nitrite agar. Therefore, at this position, side-chain bulk is likely to be critical for correct membrane insertion and folding. No conclusions to the contribution of these residues can be drawn at this stage, other than the fact that they seem to be important in a structural capacity.

N214 mutants (aspartic acid, lysine, serine and glutamine) were found to grow on nitrite with varying growth phenotypes (Figure 7.14). Thus, alterations in this position are tolerated by the protein. However, only N214D appears to be expressed to wild-type levels in the membrane (Figure 7.14). N173 mutants grew to varying degrees and their expression levels were also variable (Figure 7.14). N173 was altered to aspartic acid, lysine, serine and glutamine, alanine, cysteine, threonine and tyrosine, accounting for reduction in size/loss of charge, slight reduction in size, and increase in size with the introduction of an aromatic side-chain. It was hoped that these mutants might answer the following questions: Is asparagine or the amide group mandatory at this position? Can a full charge compensate in this position? Are there side-chain bulk restrictions? Kinetic analyses of complementing mutants N173A and N173S were carried out to confirm a suspected role in substrate binding. At first glance of the phenotypic assessment of N173 mutants it would seem that space constraints may be important for this position in the heart of Tm 4 (Figure 7.14). With the exception of lysine and glutamine, all N173 mutant proteins appeared to be expressed to moderate levels (Figure 7.14b). N173K produced no protein and N173Q was significantly reduced. This does not appear to be a factor of side-chain bulk, as N173Y, which is considerably larger, was expressed to wild-type level in one instance and moderate levels in another. Net nitrite uptake assays using the radio-active tracer developed specifically for this work, however, showed linear kinetics for N173A and N173S. It was hoped that net nitrite assays as performed by Wang *et al* (2008) could be repeated at pH 7.5 with these mutants to generate a non tracer K_m . However, as shown (Table 7.3) preliminary results were generated at pH 6.5 as net uptake and not kinetic measurements and assays at pH 7.5 could not be optimised. Thus, no solid conclusion could be reached for nitrite uptake in these mutant strains. The lack of conclusive uptake data has left this study uncertain. Growth on agar of the majority of these mutants implies that hyperbolic uptake kinetics should be observed. These methods need to be optimised as they do not complement plate growth assay phenotypes. Hypotheses based purely on agar growth tests and expression studies indicate that there is potential for space constraints in position 173. This is presumably due to its position in the helix and the possibility that this residue faces into the binding site. Polar residues in the bilayer are often involved with helix-helix interactions; helix stability and large polar amino acids in particular are known to contribute to oligomerisation. All complementing mutants other than alanine are polar. However, the complementation of alanine rules out the possibility that residues are involved via hydrogen bonding during translocation, though the possibility of helix-helix interactions or an involvement with stability remains, as alanine is a small amino acid with no special conformational features like proline and glycine which could contribute to stability.

7.3.4 Revertant studies

The identification of missense mutations has been successfully employed in the study of LacY and NrtA (Bailey & Manoil, 1998; Kinghorn *et al.*, 2005) and indicated interesting relationships between amino acids, particularly directing studies toward important regions involved with substrate binding (Unkles *et al.*, 2004a). Mutant *nitA* strains which produced no growth and maintained two or more nucleotide changes in their mutant codons were targeted for random chemical mutagenesis using NTG (Adelberg *et al.*, 1965). This method of chemical mutagenesis can be particularly misleading. If contaminants occur they are taken as *bona fide* revertants and studied accordingly. Here, putative revertants did not harbour their original mutations, but other mutations in the *nitA* gene which suggested strains were contaminated. Further mutagenesis of mutants N173Q and N173K was carried out using NTG. Once more, putative revertants were generated, and while the original mutation remained, it appeared that no additional mutations occurred, even though growth was improved. It is possible that some other genetic component elsewhere was accommodating this mutation, e.g. another protein which, due to a minor modification, can alter its substrate or a mutant tRNA which could alter the protein translation from mRNA. Hopefully, this will be investigated further, in future NitA studies.

7.3.5 Previous reports of a nitrite transport gene in *A. nidulans*

Supposed nitrite transport in *A. nidulans* has been reported previously. Pombeiro-Sponchiado *et al* (1993) discussed nitrite uptake in a wild-type strain. Nitrite uptake in this strain would not be as a result of one individual transporter but of the combined permeases (Wang *et al.*, 2008). Additionally, the *nihB* gene was suggested to be a nitrite permease or involved in post-translational modifications of a nitrite permease (Pombeiro-Spondachio. R. C. *et al.*, 1993). As shown here NitA is the only nitrite permease and is located on chromosome 3, whereas *nihB* is located on chromosome 1. The toxicity as discussed by Pombeiro-Sponchiado *et al* (1993) of nitrite at higher concentrations may be due to the destruction/inactivation of PABA, required by the strain, by nitrite in the medium. Therefore, their observations were of PABA auxotrophic mutants which failed to grow in the presence of high concentrations of nitrite and therefore, lack of PABA, in the medium.

7.4 Summary

This study represents the first investigation into a member of the FNT proteins on a molecular level. By comparison to homologous proteins, this study has shown the conservation of amino acids providing a secondary structure model for future work; in addition it has probed further into the functionality of conserved residues. Though no substrate specific signature

sequences were identified by the bioinformatic approach, it is hoped that this will be achieved in the future once further sequences have been published.

No distinct roles have been found for conserved charge residues, though it is thought that D88 could be involved in the formation of salt bridges (pending the discovery of a salt bridge partner), due to the charge and possible side chain size restrictions at this point. Disappointingly charge status was not defined for histidine at position H210, though it is hoped that with further mutagenesis a role will be found for this highly conserved residue.

It is thought that of the conserved asparagine residues, position 173 holds the greatest potential for a role in nitrite trafficking; from this study it seems that there are space constraints at this position. However due to the tetrameric nature of this protein, work continues to establish the quaternary structure of mutant proteins that so far appear to not be expressed i.e. to ensure that where we see lack of expression on BN-PAGE is not just a lack of transfer of monomeric, dimeric or trimeric proteins. It is hoped that expression characteristics will be fine tuned in this regard for the final publication of this work.

Chapter Eight

Future work and perspectives

8.1 NrtA

The work described in Chapters Three, Four and Five discussed a site-directed mutagenesis approach which was used to target conserved amino acids of interest in NrtA. Altering every residue to all other possible amino acids would provide a vast amount of data, potentially indicating crucial amino acids. However, this approach would also produce several hundred useless mutants. It is therefore optimal to target residues thought to be important on the basis of conservation and presumptive functional importance, as performed here using complementary computational analyses.

The main aims of this thesis, regarding NrtA, were to understand motifs primarily in the first half of the protein and the putative phosphorylation sites in the central loop domain. Further mutagenesis, particularly on the nitrate signature and further putative phosphorylation sites, may provide vital information about residues involved with translocation processes. The next step would logically be to characterise the second nitrate signature of NrtA. This work is currently ongoing in our laboratory but is incomplete and thus is not discussed in detail here. It has been hypothesised that the nitrate signature of NrtA is primarily responsible for maintenance of structure and that N168 may perform another role. Cysteine scanning *in vitro* mutagenesis is currently underway on all Tms which seem to line the pore (i.e. all but Tm 3, 6, 9 and 12). This should provide novel insight into this uncharacterised region. Current assumptions are largely based on the crystal structure and mutagenesis work on other MFS proteins i.e. GlpT and LacY. It is hoped that with known dimensions, a role for the first nitrate signature could be defined in more detail, as a result of its position in relation to the other helices. In LacY, six critical residues for function were identified by cysteine scanning mutagenesis in combination with other site-directed mutants (Frillingos *et al.*, 1997; Frillingos *et al.*, 1998). This mutagenesis helped to elucidate information as regards helical packing, tilt, and ligand induced conformational changes. In addition, it allowed the development of a model for proton coupled β -galactosidase transport in LacY (Frillingos *et al.*, 1997; Frillingos *et al.*, 1998). This method may also be useful for the analysis of NitA, particularly as so little is known about its critical residues. Perhaps, like MFS proteins, this approach could help in the development of a transport model for NitA. Future work on the NrtA protein should target residues thought to be important in different facets of ion

translocation, e.g. in membrane targeting, tertiary and quaternary structure formation, structural maintenance, proton coupling, and substrate binding.

A crystal structure would of-course, be the ‘holy-grail’ of this work, though it would not provide all the information as regards substrate translocation, but more of a snap-shot of the permease. However, it would certainly direct future studies, providing new questions as to the structure and function of this protein. While awaiting crystal structures of NrtA, further modelling based on GlpT shall be pursued by our laboratory *in silico* using mutagenesis results described here and data from other studies to tailor the GlpT template to nitrate transport. This will facilitate further investigations on the structural and functional mechanisms of NrtA. In particular, residues for proton binding and translocation have yet to be identified in NrtA; from electrophysiological studies, protons are known to be important for energy provision and NrtA function (Zhou *et al.*, 2000b). Cysteine, scanning mutagenesis may hold the key to identifying these residues. The crystal structure of membrane proteins is notoriously difficult to achieve due to the metastable nature of transporters (Kaback *et al.*, 2001; Miller, 2003; Fleishman *et al.*, 2006). However, the publication of crystal structures of LacY and GlpT has provided an opportunity to develop crystallography in other membrane proteins. Again, in LacY the structure with bound substrate confirmed the model developed previously for translocation and defined interactive residues (Abramson *et al.*, 2003b; Huang *et al.*, 2003). Work on crystallography is underway for NitA and NrtA and orthologous proteins in my laboratory.

None of the putative phosphorylation residues targeted in Chapter Five provided an answer to whether or not NrtA is phosphorylated. The loop region was thought to be the most likely candidate for phosphorylation events to trigger conformational change. In AtNrt1.1, phosphorylation occurs at residue T101, much earlier in the protein, on an independent loop region separate from the central domain (Liu & Tsay, 2003). A further investigation should identify further putative phosphorylation sites elsewhere in the NrtA protein and knock-out the target phosphorylation residues. It is common to use mass spectrometry to identify phosphorylation sites in proteins; this could also be an interesting option should purified protein be available for NrtA. Also, an understanding of down regulation in NrtA would be interesting as it has been shown in YNT1 as this could explain the protein’s environmental response in fluctuating nitrate concentrations (Navarro *et al.*, 2006).

Putative ubiquitination sites were also investigated in Chapter Five. It was thought that this post-translational modification, if occurring on NrtA, could be involved in regulation of

conformational change or protein degradation. Computational approaches taken here were unsuccessful at identifying PEST sequences thought to be crucial, as in YNT1 (Navarro *et al.*, 2006). A specific investigation into the degradation of unwanted protein could give further depth to the understanding of nitrate transport and the NrtA permease.

As discussed in Chapter One, membrane proteins employ different mechanisms to permit membrane insertion and folding. While aromatic residues are known in the LamB channel for roles in substrate translocation (Dutzler *et al.*, 1996; Denker *et al.*, 2005) these residues are also known for their ability to aid membrane protein insertion (Kelkar & Chattopadhyay, 2006; Shank *et al.*, 2006). It is therefore interesting to note the high degree of aromatic residues in the first Tm of NrtA. Until thorough mutageneses of this region are completed, the function of this unusual domain shall remain a matter of speculation. This work is currently underway by another PhD student in the group. Since Tm 1 forms part of the pore, the role of these residues could be with anion co-ordination and partial binding as the ion translocates as in LamB (Denker *et al.*, 2005), or the function could solely be with membrane insertion as suggested here.

8.2 Nitrate signalling in *A. nidulans*

It is of critical importance to understand nitrate signalling in *A. nidulans*, as it represents a missing piece in the puzzle of nitrate assimilation. It seems that nitrate sensing in plants, yeast and bacteria differ in both regulation and putative signalling pathways. For example bacteria use a complex ‘dual component phosphorelay system’ which signals nitrate availability via membrane bound NarX and NarQ which signal their intra-cellular counterparts - NarL and NarP - via phosphorylation which in-turn control anaerobic gene expression (Rabin & Stewart, 1993; Walker & Demoss, 1993; Schroder *et al.*, 1994; Cavicchioli *et al.*, 1995; Darwin *et al.*, 1997, Noriega *et al.*, 2008). In *Arabidopsis*, homologues of *A. nidulans* *areA* and *nirA* have been pursued with no success, though shared domains with the *C. reinhardtii* gene *nit2* have been found (Crawford & Arst, 1993; Marzluf, 1997; Siverio, 2002; Camargo *et al.*, 2007). Nitrate repression in *C. reinhardtii* by *Nrg1* and *Nrg2* does not seem to be shared by *Arabidopsis* (Prieto *et al.*, 1996). It would be interesting to understand what methods fungi employ to detect nitrate. Other than Morozov and colleagues’ (2001) suggestion that nitrate signalling is multi-faceted, in addition to the regulated degradation of *areA* mRNA in response to ammonia and glutamine levels in the cell; little is currently known. Using the same approach discussed in Chapter Six, a further investigation into the development of the nitrate signalling minus mutants, and use of the constructed cosmid library seems to be the obvious avenue. Work has begun using strain T20

(*nrtA747*; *nrtB110*; *pyroA4*; *pabaA1*; *pTRAN3-1A::argB*), in an attempt to develop a thiourea resistant strain. A construct is to be prepared to transform this strain with two copies of the urea transport gene *ureA*, under the influence of the *nitA* gene promoter, using the *bar^R* gene as the selectable marker (Hynes & Davis, 2004). Mutagenesis in this strain to disrupt the signalling system would reduce the synthesis of mRNA of the thiourea gene along with the β -glucuronidase gene.

8.3 *NitA*

In Chapter Seven, a study was carried out to investigate nitrite transport in *A. nidulans*. As for NrtA, understanding post-translational modifications for NitA might help answer important functional questions. If these proteins are not inserted into the membranes effectively, are they ubiquitinated or targeted for proteasomal degradation? Does phosphorylation control conformational changes or the opening and closing of the putative translocation pore? Little speculation exists as to the role of post translational modifications in NitA. However, computational approaches employing prediction software identified putative recognition sites for kinases throughout extra-membrane regions. With further research on NitA homologues a model might be generated to predict the specific substrate of FNT members. As mentioned in Chapter One, the change in a single amino acid in the DMT1 transporter (i.e. G185R) altered a secondary iron transporter to a calcium channel (Xu *et al.*, 2004), revealing subtle sequence alterations which govern anion transport. Regarding the FNT, no dual function formate/nitrite transporters are currently known, but an interesting investigation would be to study how small changes in residue composition can change their preference for distinct substrates e.g. carbonate, formate and nitrite.

8.4 *Distribution and abundance of nitrate/nitrite transport permeases*

An interesting question posed as a result of this study is, where are these transporters in the mycelium and how many are there? This arose when considering environmental adaptations of protein transcription. It is likely that the number of copies of NrtA and NitA in the membrane is entirely environment dependant, part of the ecological plasticity discussed. When sufficient levels of nitrate or nitrite are available in the external environment, transcription is up-regulated increasing transport into the cells. One would also assume that transport would primarily occur at the hyphal tip where nutrients are sequestered by the organism. In *A. niger* the spatial differentiation of gene expression was investigated (Anderson & Levine, 1986). Authors found that, *niaD*, *niiA* and *nrtA* were expressed primarily in the zone of growth on a plate that represented the hyphal tips, even though nitrate was available evenly throughout the media (Anderson & Levine, 1986). It was therefore

concluded that nitrate assimilation gene expression was independent of media (Anderson & Levine, 1986). To study locality and frequency of proteins, it would seem that immunocytochemistry and microscopy would be an appropriate tool, employing fluorescent tags to study the spatial cellular distribution of proteins.

8.6 Evolution of NrtA

Assuming that a tandem intragenic duplication event did occur in the MFS (Henderson, 1990; Pao *et al.*, 1998; Gao-Rubinelli & Marzluf, 2004) what happened with the development of subfamily specific signature sequences? It is unlikely that the progenitor was solely a nitrate carrier, as the MFS proteins catalyse the translocation of such a diverse range of substrates (Pao *et al.*, 1998). These subfamily specificities are more likely to have evolved - more than 2 billion years ago - after the duplication of the progenitor 6 Tm protein - more than 3 billion years ago - as it is impossible that such an assorted set of transporters duplicated at the same time, maintaining their characteristic MFS signature and structural homology. It seems then that the 6 Tm protogene duplicated, then these genes fused to form the single 12 Tm ORF. Following a long period of evolutionary speciation and duplications the progenitor would have evolved into proteins with specialised functions for substrate translocation, and as a result, signature sequences are characteristic for function. There is no current evidence of monomeric 6 Tm MFS proteins which would support a second theory of evolution then duplication.

8.7 And finally.

The subject matter of this thesis has attempted to elucidate an understanding of nitrate/nitrite uptake in *A. nidulans*. For these membrane proteins, functional data can be generated only through laborious channels. Critical residues for substrate interaction and enzyme kinetics have been identified for both NrtA and NitA. This evidence, it is hoped, will be used for the development of models for each of these proteins which will provide an understanding as regards nitrate/nitrite use in *A. nidulans*. As discussed here, there is still considerable work to be completed for a thorough understanding of nitrogen use by plants, bacteria, fungi and algae though it is hoped that this work will help to direct future studies.

Appendix One

Amino Acid Reference

Amino Acid	Potential Codon(s)	Charge	Side-chain Volume	Structure
Alanine ¹ Ala, A	GCU GCA GCC GCG	Non-polar, hydrophobic	72	$ \begin{array}{c} \text{COO}^- \\ \\ ^+\text{H}_3\text{N}-\text{C}-\text{H} \\ \\ \text{CH}_3 \end{array} $
Arginine Arg, R	CGU CGC CGA CGG AGA AGG	Positive, hydrophilic	157	$ \begin{array}{c} \text{COO}^- \\ \\ ^+\text{H}_3\text{N}-\text{C}-\text{H} \\ \\ \text{CH}_2 \\ \\ \text{CH}_2 \\ \\ \text{CH}_2 \\ \\ \text{NH} \\ \\ \text{C}=\text{NH}_2^+ \\ \\ \text{NH}_2 \end{array} $
Asparagine Asn, N	AAU AAC	Polar, hydrophilic	115	$ \begin{array}{c} \text{COO}^- \\ \\ ^+\text{H}_3\text{N}-\text{C}-\text{H} \\ \\ \text{CH}_2 \\ \\ \text{C} \\ / \quad \backslash \\ \text{H}_2\text{N} \quad \text{O} \end{array} $
Aspartic Acid Asp, D	GAU GAC	Negative, hydrophilic	116	$ \begin{array}{c} \text{COO}^- \\ \\ ^+\text{H}_3\text{N}-\text{C}-\text{H} \\ \\ \text{CH}_2 \\ \\ \text{COO}^- \end{array} $
Cysteine ² Cys, C	UGU UGC	Polar, hydrophilic	104	$ \begin{array}{c} \text{COO}^- \\ \\ ^+\text{H}_3\text{N}-\text{C}-\text{H} \\ \\ \text{CH}_2 \\ \\ \text{SH} \end{array} $
Glutamic Acid Glu, E	GAA GAG	Negative, hydrophilic	130	$ \begin{array}{c} \text{COO}^- \\ \\ ^+\text{H}_3\text{N}-\text{C}-\text{H} \\ \\ \text{CH}_2 \\ \\ \text{CH}_2 \\ \\ \text{COO}^- \end{array} $

¹ Helix maker

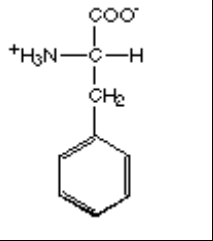
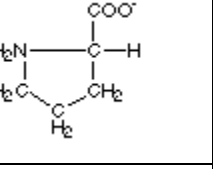
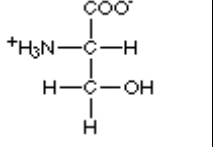
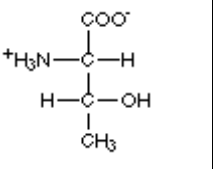
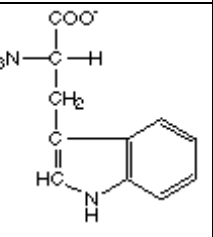
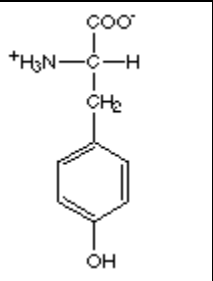
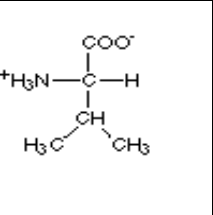
² Contains sulphur

Glutamine Gln, Q	CAA CAG	Polar, hydrophilic	129	$ \begin{array}{c} \text{COO}^- \\ \\ \text{}^+\text{H}_3\text{N}-\text{C}-\text{H} \\ \\ \text{CH}_2 \\ \\ \text{CH}_2 \\ \\ \text{C} \\ / \quad \backslash \\ \text{H}_2\text{N} \quad \text{O} \end{array} $
Glycine ³ Gly, G	GGU GGC GGA GGG	Non-polar, hydrophobic	58	$ \begin{array}{c} \text{COO}^- \\ \\ \text{}^+\text{H}_3\text{N}-\text{C}-\text{H} \\ \\ \text{H} \end{array} $
Histidine ⁴ His, H	CAU CAC	Positive, hydrophilic	138	$ \begin{array}{c} \text{COO}^- \\ \\ \text{}^+\text{H}_3\text{N}-\text{C}-\text{H} \\ \\ \text{CH}_2 \\ \\ \text{C} \\ // \quad \backslash \\ \text{HC} \quad \text{N}^+ \\ \quad \quad \\ \quad \quad \text{H} \end{array} $
Isoleucine Ile, I	AUU AUC AUA	Non-polar, hydrophobic	114	$ \begin{array}{c} \text{COO}^- \\ \\ \text{}^+\text{H}_3\text{N}-\text{C}-\text{H} \\ \\ \text{H}-\text{C}-\text{CH}_3 \\ \\ \text{CH}_2 \\ \\ \text{CH}_3 \end{array} $
Leucine Leu, L	UUA CUC UUG CUA CUU CUG	Non-polar, hydrophobic	114	$ \begin{array}{c} \text{COO}^- \\ \\ \text{}^+\text{H}_3\text{N}-\text{C}-\text{H} \\ \\ \text{CH}_2 \\ \\ \text{CH} \\ / \quad \backslash \\ \text{H}_3\text{C} \quad \text{CH}_3 \end{array} $
Lysine Lys, K	AAA AAG	Positive, hydrophilic	129	$ \begin{array}{c} \text{COO}^- \\ \\ \text{}^+\text{H}_3\text{N}-\text{C}-\text{H} \\ \\ \text{CH}_2 \\ \\ \text{CH}_2 \\ \\ \text{CH}_2 \\ \\ \text{CH}_2 \\ \\ \text{NH}_3^+ \end{array} $
Methionine ⁵ Met, M	AUG	Non-polar, hydrophobic	132	$ \begin{array}{c} \text{COO}^- \\ \\ \text{}^+\text{H}_3\text{N}-\text{C}-\text{H} \\ \\ \text{CH}_2 \\ \\ \text{CH}_2 \\ \\ \text{S} \\ \\ \text{CH}_3 \end{array} $

³ Helix breaker

⁴ Can be polar or positive depending upon the protonation of the imidazole side-chain

⁵ Contains sulphur

Phenylalanine Phe, F	UUU UUC	Non-polar, hydrophobic	148	
Proline ⁶ Pro, P	CCU CCC CCA CCG	Polar, hydrophobic	98	
Serine Ser, S	UCU UCC UCA UCG AGU AGC	Polar, hydrophilic	88	
Threonine Thr, T	ACU ACC ACA ACG	Polar, hydrophilic	102	
Tryptophan Trp, W	UGG	Non-polar, hydrophobic	187	
Tyrosine ⁷ Tyr, Y	UAU UAC	Polar*, hydrophilic	164	
Valine ⁸ Val, V	GUU GUC GUA GUG	Non-polar, hydrophobic	100	

⁶ Helix breaker

⁷ The side-chain of tyrosine is polar, but overall the amino acid is non-polar

⁸ β -sheet former

Appendix Two

Aspergillus Media and Solutions

Media Supplements

Solutions were sterilised by autoclaving at 15 lb inch⁻² for 20 min. When autoclaving was not possible solutions were filter-sterilised through a MILLEX[®] GP syringe driven filter unit (0.2 µm) (Millipore). Solutions were prepared in sterile distilled water.

Vitamin Solution (1000 x)

Vitamin	Weight (mg)
p-aminibenzoic acid	100
Pyrodoxine	500
Biotin	2
Pantothenic acid	200
Riboflavin	1000

1 L prepared with distilled water, filter sterilised and stored in a dark bottle at 4 °C

Trace Elements Solution (1000 x)

Component	Weight (g)
MnCl ₂ .4H ₂ O	0.4
ZnSO ₄	1.0
CuSO ₄	0.5
Na ₂ MoO ₄ .2H ₂ O	1.1
CoCl ₂ .H ₂ O	0.5
FeSO ₄ .7H ₂ O	0.5
HBO ₃	1.0
Citric Acid	3.72

Solution prepared in 800 ml distilled water, adjusted to pH 6.5 with 5 M KOH and made to 1 L volume with distilled water. Stored in a dark bottle at 4 °C and added to media where appropriate before sterilisation.

Nitrogen Sources

Nitrogen sources (proline, urea, ammonium tartrate, sodium nitrate, potassium nitrate, sodium nitrite, potassium nitrite) were prepared to a stock concentration of 1 M and were autoclaved where possible, or filter sterilised, and stored at 4 °C. These were added to minimal media to the concentration required, which was dependant on each experiment.

Media

Solid media was prepared by the addition of 1.2 % agar to the media described below. Media were sterilised by autoclaving at 15 lb inch⁻² for 20 min. The recipes for *Aspergillus* Minimal and Complete media were based on that described by Cove (1966), Clutterbuck (1974) and Unkles *et al* (2001), and are as follows:

Aspergillus Minimal Media (MM)

Component	Quantity L ⁻¹
Glucose	10 g
Trace Elements (x 1000)	1 ml
KCl	1.3 g
MgSO ₄ .7H ₂ O	1.3 g
KH ₂ PO ₄	3.8 g

Solution was prepared in 800 ml distilled water, adjusted to pH 6.5 with 5 M KOH and made to 1 L volume with distilled water.

Aspergillus Complete Media (CM)

Component	Quantity L ⁻¹
Glucose	10 g
Peptone	2 g
Yeast Extract	1 g
KCl	1.3 g
MgSO ₄ .7H ₂ O	1.3 g
KH ₂ PO ₄	3.8 g
Vitamins (x 1000)	1 ml
Trace Elements (x 1000)	1 ml
Casamino Acids	1 g

Solution was prepared in 800 ml distilled water, adjusted to pH 6.5 with 5 M KOH and made to 1 L volume with distilled water.

Aspergillus Transformation Media (TM)

As *Aspergillus* minimal media plus 1.2 M sorbitol.

Appendix Three

General primers used in this study

External primers used for mutagenesis and sequencing of *nrtA*

Primer	Sequence 5' - 3'
NrtAF1.1	TATTCAACCAGATCAGGCGAAT
NrtAF1.2	CCAGTGCCAAGCTTGGCTG
NrtAF1.3	TTCAACACATATGGCCGAGTCT
NrtAF1.4	TGCTTGCATTCTCTCATG
NrtAF1.5	AGTCTTTATCGGCCTACTG
NrtAF1.6	GTTGGGACAGCCAACTC
NrtAF1.7	CAACATTGTCGACCTTAGCTC
NrtAF1.8	CCATTCCCGACGTCGAAAAGAAAGGCA
NrtAF1.9	CTCCCGCAAGGAGGCTT
NrtAF1.10	ACGCAGACCGGTAAGTGGGCCG
NrtAR2.1	TCAGTCCGTTGTC
NrtAR2.2	GTGAGGTAACGAGGCCG
NrtAR2.3	TCGCAAGTGAAGAGCATGCC
NrtAR2.4	GAGCTAAGGTGACAATGTTG
NrtAR2.5	CGTTTGC GCGGAAGGCGTGC
NrtAR2.6	TGCCTTTCTTTTCGACGTCGGGAA
NrtAR2.7	GAGCAGGCGTAGGGGACT
NrtAR2.8	CGGCCCACTTACCGGTCTGCGA
NrtAR2.9	AGTAAGTACCAAACATAGTCGC
NrtAR2.10	CACGGCCATGGAAATAACACC
NrtAR2.11	GGAACAAAAGCTGGGTACCGGG
NrtAR2.12	GATATCGAATTCAACTAGGTGCTG

External primers used for mutagenesis and sequencing of *nitA*

Primer	Sequence 5' - 3'
NitAF1.2	CAGGCGAATTCGTGATTAGG
NitAF1.3	CGCCACTCGAGGTAGTCGAGTTTG
NitAF1.4	CAGCTGCTGCAATGCCTCCGTC
NitAF1.5	GGATGTCTGCTAGCACTGGCATGC
NitAF1.2	GACGCCCGAATTTACAGTATCTTC
NitAR2.1	CCCCGTAAGGGTGACCGGGTTGGT
NitAR2.2	GAAGATACTGTGAAATTCGGGCGTC
NitAR2.3	CCGCCGGGGCCCCCATCTTGCT

NitAR2.4	GATATCGAATTCAACTAGGTGCTG
----------	--------------------------

Primers used to produce fusion PCR product for transformation

Primer	Sequence 5' – 3'
FNitA1.1	GGCCCTATCTCTTATCAGTC
FNitA1.2	CCGTCTACAGTCTGGCGGGTC
FNitA1.3	CTAGGTTTCGACCACTCGAGCG
FNitA1.4	GTGGCCCTACGGCTAGAGGTG
FNitA1.5	GACGGAGGCATTGCAGCAGCTG
FNitA1.6	CATGGTCATAGCTGTTTCTGGGCGAAGATGTATGTTACCTC
FNitA1.7	CAGGAAACAGCTATGACCATG
FNitA1.8	GTTTTCCCAGTCACGAC
FNitA1.9	CAACGTCGTGACTGGGAAAACCAGCCCAGTCGCTCCATCCTC
FNitA1.10	GGCCCCAGCATTGGGCCTTTC

Primers used for the sequencing of the *ureA* gene

Primer	Sequence 5'-3'
UreA1.1	GTTGAGGTTGCTAGTTCTCCAC
UreA2.1	GCGAAGATGAAGATGATCACGACA
UreA1.2	CACCCTTTTCGGAGGCATTAA
UreA2.2	AGTTCTGCCCCCTCCAGACG
UreA1.3	TCTCTACCTTCTCATGGGCG
UreA 2.3	TAGCTAGCTGAACACACAACAA

Primers used for the sequencing of *uidA*, and promoter regions of the pTRAN3-1A transformants

Primer	Sequence 5'-3'
GlucF1	ATGTTACGTCCTGTAGAAACC
GlucF2	TAACGTGCTGATGGTGCACG
GlucR2	CGTGCACCATCAGCACGTTA
GlucR1	TCATTGTTTGCCTCCCTGCT
uidAbegR	TCGTTGTTACACAAAACGG
uidAmidR	CTTTAATCGCCTGTAAGTGC
uidAmidF	GGGCAACAAGCCGAAAGAAC
Prom2b	GTGCTGCAAGGCGATTAAGTT
Prom1b	GGTTCGCGGCCCCGCGGAGAT

Appendix Four

Mutagenic Primers

NitA

Mutant	Forward* Mutagenic Primers 5'-3'
D88E	CTT ACT GGT GCA <u>GAG</u> CTC TGC ACT GGC
D88N	CTT ACT GGT GCA <u>AAT</u> CTC TGC ACT GGC
D88Q	CTT ACT GGT GCA <u>CAA</u> CTC TGC ACT GGC
D88S	CTT ACT GGT GCA <u>TCC</u> CTC TGC ACT GGC
D88V	CTT ACT GGT GCA <u>GTG</u> CTC TGC ACT GGC
N122D	ACG TTT TGG GGG <u>GAT</u> CTT TGC GGC TCG
N122Q	ACG TTT TGG GGG <u>CAA</u> CTT TGC GGC TCG
N122S	ACG TTT TGG GGG <u>TCC</u> CTT TGC GGC TCG
N122K	ACG TTT TGG GGG <u>AAA</u> CTT TGC GGC TCG
L127V	C CTT TGC GGC TCG <u>GTC</u> TTC GTT GTC G
K156Q	A ACC AAG <u>CAG</u> CAA GTG ACG CC
K156R	A ACC AAG <u>CGA</u> CAA GTG ACG CC
K156S	A ACC AAG <u>TCA</u> CAA GTG ACG CC
N173A	GC ATC GGA TGC <u>GCC</u> TGG CTC GTC TGT
N173C	GC ATC GGA TGC <u>TGC</u> TGG CTC GTC TGT
N173D	GC ATC GGA TGC <u>GAT</u> TGG CTC GTC TGT
N173K	GC ATC GGA TGC <u>AAA</u> TGG CTC GTC TGT
N173Q	GC ATC GGA TGC <u>CAA</u> TGG CTC GTC TGT
N173S	GC ATC GGA TGC <u>TCC</u> TGG CTC GTC TGT
N173T	GC ATC GGA TGC <u>ACA</u> TGG CTC GTC TGT
N173Y	GC ATC GGA TGC <u>TAT</u> TGG CTC GTC TGT
C177T	C TGG CTC GTC <u>ACC</u> CTG GCG TGC TTC
K192Q	GAT ATG GCG TCT <u>CGA</u> ATA ATC GGC ATT
K192R	GAT ATG GCG TCT <u>CAA</u> ATA ATC GGC ATT
K192S	GAT ATG GCG TCT <u>TCA</u> ATA ATC GGC ATT
H210Q	CTG GGC TTT GAC <u>CAG</u> GTT GTT GCG AAC
H210S	CTG GGC TTT GAC <u>TCC</u> GTT GTT GCG AAC
H210K	CTG GGC TTT GAC <u>AAG</u> GTT GTT GCG AAC
N214D	C GTT GTT GCG <u>GAC</u> ATG ACA TTC AT
N214K	C GTT GTT GCG <u>AAG</u> ATG ACA TTC AT
N214Q	C GTT GTT GCG <u>CAA</u> ATG ACA TTC AT
N214S	C GTT GTT GCG <u>TCC</u> ATG ACA TTC AT
N246D	ACC TTG TTG GGA <u>GAT</u> ATA GTT GGG GGT
N246Q	ACC TTG TTG GGA <u>CAA</u> ATA GTT GGG GGT

N246S	ACC TTG TTG GGA <u>TCC</u> ATA GTT GGG GGT
N246K	ACC TTG TTG GGA <u>AAA</u> ATA GTT GGG GGT

* Reverse primers were the reverse complement of these

NrtA

Mutant	Forward* Mutagenic Primers 5'-3'
T83A	CT TTA CTA GCT <u>GCG</u> TAA GTT CC
T83S	CT TTA CTA GCT <u>AGG</u> TAA GTT CC
T83V	CT TTA CTA GCT <u>GTG</u> TAA GTT CC
T83Q	GCT TTA CTA GCT <u>CAG</u> TAA GTT CCC TGC A
T83R	GCT TTA CTA GCT <u>CGG</u> TAA GTT CCC TGC
G157A	AGT ATA GTT <u>GCA</u> ACA GCC AAC TCC
N160A	GTT GGG ACA GCC <u>GCC</u> TCC CTA GCT GCC
G165A	CC CTA GCT GCC <u>GCC</u> CTA GT AAC GC
L166A	TA GCT GCC GGT <u>GCA</u> GGT AAC GCT GG
L166F	TA GCT GCC GGT <u>TTC</u> GGT AAC GCT GG
L166T	TA GCT GCC GGT <u>ACA</u> GGT AAC GCT GG
L166W	TA GCT GCC GGT <u>TGG</u> GGT AAC GCT GG
G167A	CT GCC GGT CTA <u>GCC</u> AAC GCT GGT GG
N168A	C GGT CTA GGT <u>GCC</u> GCT GGT GGC GGT
N168S	CC GGT CTA GGT <u>TCC</u> GCT GGT GGC GGT
N168L	CC GGT CTA GGT <u>CTC</u> GCT GGT GGC GGT
N168Y	CC GGT CTA GGT <u>TCC</u> GCT GGT GGC GGT
G170N	TA GGT AAC GCT <u>AAT</u> GGC GGT ATC ACA
G170A	TA GGT AAC GCT <u>GCC</u> GGC GGT ATC ACA
G171A	GT AAC GCT GGT <u>GCT</u> GGT ATC ACA TA
G172A	AC GCT GGT GGC <u>GCC</u> ATC ACA TAC TTC
T224A	T GAC ACC CCG <u>GCC</u> GGA AAA TGG
S228A	ACT GGA AAA TGG <u>GCC</u> GAG CG
S255A	TCT GGT GCA CAG <u>GCC</u> TCC CG
S303A	TT GCC TCT CCC <u>GCC</u> CGC AAG GAG
N364R	TTC GGG TTC CTT <u>CGT</u> ATT GTC TGT CGG

* Reverse primers were the reverse complement of these

Appendix Five

SDS-PAGE and BN-PAGE Gel Composition

10 % SDS-PAGE (for the preparation of four 10 % SDS-PAGE gels using a multi-gel caster), gels were overlaid with water saturated iso-butanol.

Component	Separating Gel (ml)	Stacking Gel (ml)	Plug (ml)
1.5 M Tris pH 8.8	2.5	-	7
1 M Tris pH 6.8	-	1	-
10 % SDS	0.1	0.1	-
30 % (v/v) Acrylamide*	3.3	1.32	-
10 % (w/v) Ammonium persulphate	0.075	0.48	-
TEMED	0.0075	0.048	-
Glycerol	-	14	14
Bromophenol blue (water saturated)	-	-	0.1
Distilled water	4.1	5.2	-

*37.5:1 Acrylamide:Bisacrylamide (Flowgen, Nottinghamshire, U.K.)

For the preparation of four 5-17 % BN-PAGE gels using a multi-gel caster and a 15 ml gradient former

Component	Separating Gel (ml)		Stacking Gel (ml)	Plug (ml)
	5 %	17 %	4%	1 x
3 x Gel Buffer*	6.7	6.7	1.0	7
49.5 % w/v Acrylamide 1.5 % w/v Bisacrylamide	2.0	6.9	0.24	-
Glycerol	-	5.2	-	14
10 % (w/v) Ammonium persulphate	70	70	120	-
TEMED	7	7	12	-
Bromophenol blue (water saturated)	-	-	-	0.1
Distilled water	11.3	1.2	7.04	-

* Gel buffer (3 x) 150 mM BisTris (Fluka), 200 mM 6-amino hexanoic acid (Fluka) pH 7 at 4 °C.

Appendix Six

Accession numbers of proteins in NrtA alignment

Organism	Protein/locus	Accession Number
<i>A. fumigatus</i>	CrnA	CAD28427
<i>A. nidulans</i>	NrtA	P22152
<i>A. nidulans FGSC A4</i>	NrtB	XP_658003
<i>A. thaliana</i>	Nrt2.1	NP_172288
<i>A. thaliana</i>	Nrt2.2	AAF79836
<i>A. thaliana</i>	Nrt2.3	NP_200886
<i>A. thaliana</i>	Nrt2.4	NP_200885
<i>A. thaliana</i>	Nrt2.5	NP_172754
<i>A. thaliana</i>	Nrt2.6	NP_190092
<i>A. thaliana</i>	Nrt2.7	NP_196961
<i>Acinetobacter sp. ADP1</i>	ACIAD1911	YP_046561
<i>Aquifex aeolicus</i>	NasA	NP_213149
<i>Azoarcus sp.</i>	NarK1	CAI09722
<i>Azotobacter vinelandii AvOP</i>	AvinDRAFT_8460	ZP_00415179
<i>Bacillus clausii KSM-K16</i>	NarK	YP_175121
<i>Bacillus halodurans C-125</i>	BH0612	NP_241478
<i>Bacillus licheniformis ATCC 14580</i>	NasA	YP_077607
<i>Bacillus subtilis</i>	NarK	P46907
<i>Bacillus subtilis subsp. subtilis str. 168</i>	NasA	NP_388215
<i>Brassica napus</i>	Nrt2	CAC05338
<i>Burkholderia cenocepacia AU 1054</i>	Bcen_3861	YP_623726
<i>Burkholderia mallei ATCC 23344</i>	BMAA1087	YP_105750
<i>Burkholderia pseudomallei K96243</i>	BPSS1244	YP_111252
<i>Burkholderia sp. 383</i>	Bcep18194_B1343	YP_372101
<i>Burkholderia vietnamiensis G4</i>	Bcep1808_5661	YP_001114854
<i>C. fusiformis</i>	Nat2	AAD49572
<i>Caulobacter crescentus CB15</i>	narK	AAK22599
<i>Chlamydomonas reinhardtii</i>	Nrt2.1	CAA80925
<i>Chlorella sorokiniana</i>	NTR	AAK02066
<i>Chromobacterium violaceum ATCC 12472</i>	NarK1	NP_902215
<i>Clostridium perfringens str. 13</i>	NarK	NP_563190
<i>Corynebacterium diphtheriae</i>	narK	NP_938881
<i>Corynebacterium efficiens</i>	CE1416	NP_738026
<i>Cylindrotheca fusiformis</i>	Nat1	AAD49571
<i>Cytophaga hutchinsonii ATCC 33406</i>	CHU_1319	YP_677931
<i>Dechloromonas aromatica RCB</i>	Daro_0825	YP_284051

<i>Dunaliella salina</i>	NRT2	AAU87579
<i>E. coli</i>	NarU	P37758
<i>Escherichia coli</i>	NarK	CAA34126
<i>Geobacillus kaustophilus HTA426</i>	GK1865	YP_147718
<i>Geobacter metallireducens GS-15</i>	Gmet_0333	YP_383301
<i>Gibberella zeae PH-1</i>	FG00416.1	XP_380592
<i>Glycine max</i>	Nrt2.1	AAC09320.1
<i>H. polymorpha</i>	YNT1	CAA11229
<i>Hordeum vulgare</i>	BCH1	AAC49531
<i>H.vulgare</i>	BCH2	AAC49532
<i>H.vulgare</i>	BCH3	AAD28363
<i>H.vulgare</i>	BCH4	AAD28364
<i>Haloarcula marismortui ATCC 43049</i>	RrnAC2626	YP_137117
<i>Haloferax mediterranei</i>	NarK	CAF19043
<i>Halomonas halodenitrificans</i>	NarK1.1	BAB84307
<i>Hebeloma cylindrosporum</i>	Nrt2	CAB60009
<i>Lactobacillus plantarum</i>	NarK	CAD63937
<i>Lotus japonicus</i>	Nrt2.1	CAC35729
<i>Mesorhizobium sp. BNC1</i>	Meso_1450	YP_674011
<i>Methylibium petroleiphilum PM1</i>	Mpe_A2315	YP_001021506
<i>Methylobacillus flagellatus KT</i>	Mfla_0321	YP_544433
<i>Methylococcus capsulatus str. Bath</i>	MCA0594	YP_113110
<i>Mycobacterium tuberculosis</i>	NarK1	NP_216845
<i>M.tuberculosis</i>	NarK2	NP_216253
<i>Mycoplasma genitalium</i>	MG294	ABY79587
<i>Neurospora crassa</i>	CrnA	CAD71077
<i>Nicotiana plumbaginifolia</i>	NRT2.1	CAA69387
<i>Nostoc punctiforme PCC 73102</i>	Npun_R1527	YP_001865159
<i>Novosphingobium aromaticivorans DSM12444</i>	Saro_2970	YP_498239
<i>Oryza sativa</i>	Nrt2	EAY74469
<i>O. sativa</i>	Os01g0704100	NP_001044003
<i>O.sativa</i>	BCH2	NP_001045658
<i>P.patens</i>	Nrt2.2	BAE45926
<i>P.patens</i>	Nrt2.3	BAE45927
<i>P.patens</i>	Nrt2.4	BAE45928
<i>P.patens</i>	Nrt2.5	BAE45929
<i>Photobacterium profundum SS9</i>	PBPRA2521	YP_130705
<i>Phragmites australis</i>	NRT2	BAC76606
<i>Physcomitrella patens</i>	Nrt2.1	EDQ67083
<i>Polaromonas sp. JS666</i>	Bpro_3273	YP_550085
<i>Polaromonas sp. JS666</i>	Bpro_4597	YP_551378
<i>Populus tremula x Populus tremuloides</i>	tNit2.1	CAG26716
<i>P. tremula x P. tremuloides</i>	tNit2.2	CAG26717

<i>Pseudomonas aeruginosa</i>	NarK1	CAA75538
<i>Ps. aeruginosa</i>	nasT	AAD22549
<i>Ps. aeruginosa PAO1</i>	nasA	AAG05172
<i>Pseudomonas fluorescens</i>	NarK	AAG34372
<i>Pseudomonas fluorescens</i>	NarD	AAG34371
<i>Ps. fluorescens PfO-1</i>	PflO1_1783	YP_347515
<i>Pseudomonas putida F1</i>	Pput_3648	YP_001268956
<i>Pseudomonas sp. MT-1</i>	narM	BAD82905
<i>Pseudomonas syringae pv. tomato str. DC3000</i>	PSPTO_2304	NP_792123
<i>Psychrobacter arcticus 273-4</i>	Psyc_0601	YP_263895
<i>Ralstonia eutropha H16</i>	Nark1	NP_942903
<i>R. eutropha JMP134</i>	Reut_B4859	YP_299051
<i>R. eutropha JMP134</i>	Reut_B5000	YP_299192
<i>Ralstonia metallidurans CH34</i>	Rmet_4817	YP_586948
<i>Ralstonia solanacearum GMI1000</i>	RSp1223	NP_522784
<i>Rubrobacter xylanophilus</i>	GK0766	YP_643982
<i>S. lycopersicum</i>	Nrt2.2	AAF00054
<i>S. lycopersicum</i>	Nrt2.3	AAK72402.1
<i>Saccharophagus degradans</i>	Sde_2278	YP_527750
<i>S. degradans 2-40</i>	Sde_2277	YP_527749
<i>Sinorhizobium meliloti 1021</i>	SMb20436	NP_436962
<i>Skeletonema costatum</i>	Nat	AAL85928
<i>Solanum lycopersicum</i>	Nrt2.1	AAF00053
<i>Staphylococcus aureus</i>	NarK	ABD22550
<i>S. carnosus</i>	NarT	AAC45758
<i>Streptomyces coelicolor</i>	SCO0213	NP_624546
<i>S.coelicolor A3(2)</i>	Nark	CAB72205
<i>Synechococcus sp. PCC 7002</i>	NrtP	AAD45941
<i>Synechococcus sp. WH 7803</i>	NapA	AAG45172
<i>Synechococcus sp. WH 8103</i>	NrtP	AAQ86991
<i>T. aestivum</i>	NRT2.2	AAK19519.1
<i>T. aestivum</i>	NRT2.3	AAL11016.1
<i>Thermus thermophilus</i>	NarK1	CAB65479
<i>Thiobacillus denitrificans ATCC 25259</i>	Tbd_1401	YP_315159
<i>Trichodesmium erythraeum IMS101</i>	Tery_1069	YP_720911
<i>Triticum aestivum</i>	NRT2.1	AAG01172
<i>Ustilago maydis 521</i>	UM03849.1	XP_759996
<i>Xanthomonas campestris pv. campestris</i>	Xccb100_2306	YP_001903710
<i>Zea Mays</i>	Nrt2.1	AAN05088

Web References¹

Bailey, T. L and Gribskov, M. Motif Alignment and Search Tool (MAST) [Online] <http://meme.sdsc.edu/meme/mast.html> Accessed: 4th December 2008

Bailey, T. L. and Elkan, C. Motif-based sequence analysis tools Multiple Em for Motif Elicitation (MEME) [Online] <http://meme.sdsc.edu/meme/intro.html> Accessed: 4th December 2008

Blom, N., Gammeltoft, S., Brunak, S. NetPhos Eukaryotic phosphorylation site prediction software [Online] <http://www.cbs.dtu.dk/services/NetPhos/> Accessed: 4th December 2008

Broad Institute – *Aspergillus nidulans* Aspergillus comparative database [Online] http://www.broad.mit.edu/annotation/fungi/aspergillus_nidulans Accessed 4th December 2008

Cuff, A. L., Sillitoe, I., Lewis, T., Redfern, O.C., Garratt, R., Thornton, J., Orengo, C. CATH Database v 3.2.0. Protein Structure Classification 2008 [Online] <http://www.cathdb.info/> Accessed: 18th December 2008.

Delano, W.L. Pymol Molecular visualisation software [Online] <http://www.pymol.org> Accessed: 4th December 2008

Dundee Sequencing Service [Online] <http://www.dnaseq.co.uk> Accessed: 4th December

European Bioinformatics Institute 2008 [Online] <http://www.ebi.ac.uk> Accessed: 4th December 2008

Expert Protein Analysis System proteomics 2008 [Online] <http://www.expasy.org> Accessed: 4th December 2008

¹ Where web references are shown here, if an author's name is stated the relevant publication should be sought in the reference list.

Hulo, N., Bairoch, A., Bulliard, V., Cerutti, L., Cuče, B. A., de Castro, E., Lachaize, C., Langendijk-Genevaux, P. S., Sigrist, C. J. A. Prosite Database of protein domains, families and functional sites [Online] <http://www.expasy.ch/prosite/> Accessed: 4th December 2008

Macrogen Sequencing Service [Online] <http://www.macrogen.com> Accessed: 4th December

Pagni, M., Ioannidis, V., Cerutti, L., Zahn, Zabal, M., Jongeneel, C. V., Falquet, L. MyHits Protein sequence and motif analysis tools [Online] <http://myhits.isb-sib.ch/cgi-bin/index> Accessed: 4th December 2008

Rechsteiner, M., Rogers, S. W. EMBnet Austria PEST Find [Online] <https://embl.bcc.univie.ac.at/toolbox> Accessed: 4th December 2008

TOPCONS Consensus prediction of membrane protein topology Stockholm Bioinformatics Centre 2008 [Online] <http://topcons.net/> Accessed: 4th December 2008

Transport Classification Database 2008 [Online] <http://www.tcdb.org> Accessed: 4th December 2008

References

- Abramson, J., Kaback, H. R. & Iwata, S. 2004 Structural comparison of lactose permease and the glycerol-3-phosphate antiporter: members of the major facilitator superfamily. *Current Opinion in Structural Biology* **14**, 413-419.
- Abramson, J., Smirnova, I., Kasho, V., Verner, G., Iwata, S. & Kaback, H. R. 2003a The lactose permease of *Escherichia coli*: overall structure, the sugar-binding site and the alternating access model for transport. *FEBS Letters* **555**, 96-101.
- Abramson, J., Smirnova, I., Kasho, V., Verner, G., Kaback, H. R. & Iwata, S. 2003b Structure and mechanism of the lactose permease of *Escherichia coli*. *Science* **301**, 610-615.
- Accardi, A. & Miller, C. 2004 Secondary active transport mediated by a prokaryotic homologue of ClC Cl⁻ channels. *Nature* **427**, 803-807.
- Adelberg, E. A., Mandel, M. & Chen, G. C. C. 1965 Optimal conditions for mutagenesis by N-methyl-N'-nitrosoguanidine in *Escherichia coli* K12. *Biochemical and Biophysical Research Communications* **18**, 788-795.
- Alboresi, A., Gestin, C., Leydecker, M., -T., Bedu, M., Meyer, C. & Truong, H., -N. 2005 Nitrate, a signal relieving seed dormancy in *Arabidopsis*. *Plant, Cell and Environment* **28**, 500-512.
- Amarasinghe, B., de Bruxelles, G. L., Braddon, M., Onyeocha, I., Forde, B. G. & Udvardi, M. K. 1998 Regulation of GmNRT2 expression and nitrate transport activity in roots of soybean (*Glycine max*). *Planta* **206**, 44-52.
- Anantharaman, V., Balaji, S. & Aravind, L. 2006 The signaling helix: a common functional theme in diverse signaling proteins. *Biology Direct* **1**.
- Anderson, I. C. & Levine, J. S. 1986 Relative Rates of Nitric-Oxide and Nitrous-Oxide Production by Nitrifiers, Denitrifiers, and Nitrate Respirers. *Applied and Environmental Microbiology* **51**, 938-945.
- Andrews, S. C., Berks, B. C., McClay, J., Ambler, A., Quail, M. A., Golby, P. & Guest, J. R. 1997 A 12-cistron *Escherichia coli* operon (hyf) encoding a putative proton-translocating formate hydrogenlyase system. *Microbiology-Uk* **143**, 3633-3647.
- Andrianopoulos, A., Kourambas, S., Sharp, J. A., Davis, M. A. & Hynes, M. J. 1998 Characterization of the *Aspergillus nidulans nmrA* gene involved in nitrogen metabolite repression. *Journal of Bacteriology* **180**, 1973-1977.
- Appleman, J. A., Chen, L. L. & Stewart, V. 2003 Probing conservation of HAMP linker structure and signal transduction mechanism through analysis of hybrid sensor kinases. *Journal of Bacteriology* **185**, 4872-4882.

- Appleman, J. A. & Stewart, V. 2003 Mutational analysis of a conserved signal-transducing element: the HAMP linker of the *Escherichia coli* nitrate sensor NarX. *Journal of Bacteriology* **185**, 89-97.
- Appleyard, M. V. C. L., McPheat, W. L. & Stark, M. J. R. 2000 A novel 'two-component' protein containing histidine kinase and response regulator domains required for sporulation in *Aspergillus nidulans*. *Current Genetics* **37**, 364-372.
- Arbely, E., Granot, Z., Kass, I., Orly, J. & Arkin, I. T. 2006 A trimerizing GxxxG motif is uniquely inserted in the severe acute respiratory syndrome (SARS) coronavirus spike protein transmembrane domain. *Biochemistry* **45**, 11349-11356.
- Arst, H. N. & Cove, D. J. 1973 Nitrogen metabolite repression in *Aspergillus nidulans*. *Molecular & General Genetics* **174**, 89-100.
- Arst, H. N., Tollervey, D. W. & Sealy Lewis, H. M. 1982 A possible regulatory gene for the molybdenum-containing cofactor in *Aspergillus nidulans*. *Journal of General Microbiology* **128**, 1083-1093.
- Auer, M., Kim, M. J., Lemieux, M. J., Villa, A., Song, J., Li, X. & Wang, D. N. 2001 High-yield expression and functional analysis of *Escherichia coli* glycerol-3-phosphate transporter. *Biochemistry* **40**, 6628-6635.
- Avila, J., Gonzalez, C., Brito, N., Machin, F., Perez, M. D. & Siverio, J. M. 2002 A second Zn(II)(2)Cys(6) transcriptional factor encoded by the *YNA2* gene is indispensable for the transcriptional activation of the genes involved in nitrate assimilation in the yeast *Hansenula polymorpha*. *Yeast* **19**, 537-544.
- Avila, J., Gonzalez, C., Brito, N. & Siverio, J. M. 1998 Clustering of the *YNA1* gene encoding a Zn(II)(2)Cys(6) transcriptional factor in the yeast *Hansenula polymorpha* with the nitrate assimilation genes *YNT1*, *YNII* and *YNRI*, and its involvement in their transcriptional activation. *Biochemical Journal* **335**, 647-652.
- Bailey, J. & Manoil, C. 1998 Missense mutations that inactivate *Escherichia coli* lac permease. *Journal of Molecular Biology* **277**, 199-213.
- Bailey, T. L. & Elkan, C. 1995 Fitting a mixture model by expectation maximization to discover motifs in biopolymers, Proceedings of the second international conference on intelligent systems for molecular biology, August (ed. R. B. Altman, Brutlag, D.L., Karp, P.D., Lathrop, R.H., Searls, D.B.), pp. 28-36. Menlo Park, CA: AAAI Press.
- Bailey, T. L., Williams, N., Misleh, C. & Li, W. W. 2006 MEME: discovering and analysing DNA and protein sequence motifs. *Nucleic Acids Research* **34**, W369-W373.
- Bal, J., Kajtaniak, E. M. & Pieniasek, N. J. 1977 4-Nitroquinoline-1-oxide: a good mutagen for *Aspergillus nidulans*. *Mutation Research* **56**, 153-156.

- Ballance, D. J., Buxton, F. P. & Turner, G. 1983 Transformation of *Aspergillus nidulans* by the orotidine-5'-phosphate decarboxylase gene of *Neurospora crassa*. *Biochemical and Biophysical Research Communications* **112**, 284-289.
- Barnett, J. A., Payne, R. W. & Yarrow, D. 1990 *Yeasts: Characteristics and Identification* Cambridge: Cambridge University Press.
- Beguín, P., Nagashima, K., Nishimura, M., Gonoï, T. & Seino, S. 1999 PKA-mediated phosphorylation of the human K_{ATP} channel: separate roles of Kir6.2 and SUR1 subunit phosphorylation *EMBO Journal* **18**, 4722-4732.
- Berg, J. M., Tymoczko, J. L. & Stryer, L. 2007, *Biochemistry* (ed. **J. M. Berg**). New York: W.H. Freeman.
- Bernreiter, A. B., Ramon, A., Fernandez-Martinez, J., Berger, H., Araujo-Bazan, L., Espeso, E. A., Pachlinger, R., Gallmetzer, A., Anderl, I., Scazzocchio, C. & Strauss, J. 2007 Nuclear export of the transcription factor NirA is a regulatory checkpoint for nitrate induction in *Aspergillus nidulans*. *Molecular and Cellular Biology* **27**, 791-802.
- Bibb, J. A., Snyder, G. L., Nishi, A., Yan, Z., Meijer, L., Fienberg, A. A., Tsai, L. H., Kwon, Y. T., Girault, J. A., Czernik, A. J., Haganir, R. L., Hemmings, H. C., Nairn, A. C. & Greengard, P. 1999 Phosphorylation of DARPP-32 by Cdk5 modulates dopamine signalling in neurons. *Nature* **402**, 669-671.
- Blom, N., Gammeltoft, S. & Brunak, S. 1999 Sequence and structure-based prediction of eukaryotic protein phosphorylation sites. *Journal of Molecular Biology* **294**, 1351-1362.
- Bowie, J. U. 2005 Solving the membrane protein folding problem. *Nature* **438**, 581-589.
- Boyd, J., Gradmann, D. & Boyd, C. M. 2003 Transinhibition and voltage-gating in a fungal nitrate transporter. *Journal of Membrane Biology* **195**, 109-120.
- Brakhage, A. A. & Van den Brulle, J. 1995 Use of reporter genes to identify recessive trans-acting mutations specifically involved in the regulation of *Aspergillus nidulans* penicillin biosynthesis genes. *Journal of Bacteriology* **177**, 2781-2788.
- Breyton, C., Haase, W., Rapoport, T. A., Kuhlbrandt, W. & Collinson, I. 2002 Three-dimensional structure of the bacterial protein-translocation complex SecYEG. *Nature* **418**, 662-665.
- Brownlee, A. G. & Arst, H. N. 1983 Nitrate uptake in *Aspergillus nidulans* and involvement of the 3rd gene of the nitrate assimilation gene-cluster. *Journal of Bacteriology* **155**, 1138-1146.
- Buchel, D. E., Gronenborn, B. & Mullerhill, B. 1980 Sequence of the lactose permease gene. *Nature* **283**, 541-545.

- Burger, G., Strauss, J., Scazzocchio, C. & Lang, B. F. 1991 *nirA*, the pathway-specific regulatory gene of nitrate assimilation in *Aspergillus nidulans*, encodes a putative GAL4-type zinc finger protein and contains four introns in highly conserved regions. *Molecular and Cellular Biology* **11**, 5746-5755.
- Bywater, R. P., Thomas, D. & Vriend, G. 2001 A sequence and structural study of transmembrane helices. *Journal of Computer-Aided Molecular Design* **15**, 533-552.
- Camargo, A., Llamas, A., Schnell, R. A., Higuera, J. J., Gonzalez-Ballester, D., Lefebvre, P. A., Fernandez, E. & Galvan, A. 2007 Nitrate signaling by the regulatory gene *NIT2* in *Chlamydomonas*. *Plant Cell* **19**, 3491-3503.
- Casselton, L. & Zolan, M. 2002 The art and design of genetic screens: Filamentous Fungi. *Nature Reviews Genetics* **3**, 683-697.
- Catic, A., Collins, C., Church, G. M. & Ploegh, H. L. 2004 Preferred *in vivo* ubiquitination sites. *Bioinformatics* **20**, 3302-3307.
- Cavicchioli, R., Chiang, R. C., Kalman, L. V. & Gunsalus, R. P. 1996 Role of the periplasmic domain of the *Escherichia coli* NarX sensor-transmitter protein in nitrate-dependent signal transduction and gene regulation. *Molecular Microbiology* **21**, 901-911.
- Cavicchioli, R., Schroder, I., Constanti, M. & Gunsalus, R. P. 1995 The NarX and NarQ sensor-transmitter proteins of *Escherichia coli* each require 2 conserved histidines for nitrate-dependent signal-transduction to NarL. *Journal of Bacteriology* **177**, 2416-2424.
- Chau, V., Tobias, J. W., Bachmair, A., Marriott, D., Ecker, D. J., Gonda, D. K. & Varshavsky, A. 1989 A multiubiquitin chain is confined to specific lysine in a targeted short-lived protein. *Science* **243**, 1576-1583.
- Chenna, R., Sugawara, H., Koike, T., Lopez, R., Gibson, T. J., Higgins, D. G. & Thompson, J. D. 2003 Multiple sequence alignment with the Clustal series of programs. *Nucleic Acids Research* **31**, 3497-3500.
- Chou, P. Y. & Fasman, G. D. 1974 Prediction of Protein Conformation. *Biochemistry* **13**, 222-245.
- Clarkson, D. T. & Luttge, U. 1991 Mineral nutrition: inducible and repressible nutrient transport systems. *Progress in Botany* **52**, 61-83.
- Claros, M. G. & von Heijne, G. 1994 Toppred-Ii - an improved software for membrane protein structure predictions. *Computer Applications in the Biosciences* **10**, 685-686.
- Clegg, S., Yu, F., Griffiths, L. & Cole, J. A. 2002 The roles of the polytopic membrane proteins NarK, NarU and NirC in *Escherichia coli* K-12: two nitrate and three nitrite transporters. *Molecular Microbiology* **44**, 143-155.

- Clutterbuck, A. J. 1974 *Aspergillus nidulans*, Handbook of Genetics (ed. R. C. King), pp. 447-510. New York: Plenum Press.
- Cohen, P. 2002 The origins of protein phosphorylation. *Nature Cell Biology* **4**, E127-E130.
- Cohen, S. N., Chang, A. C. Y. & Hsu, L. 1972 Nonchromosomal antibiotic resistance in bacteria - Genetic transformation of *Escherichia coli* by R-factor DNA. *Proceedings of the National Academy of Sciences of the United States of America* **69**, 2110-&.
- Cove, D. J. 1966 The induction and repression of nitrate reductase in the fungus *Aspergillus nidulans*. *Biochimica et Biophysica Acta*.
- Cove, D. J. 1979 Genetic studies of nitrate assimilation in *Aspergillus nidulans*. *Biological Reviews of the Cambridge Philosophical Society* **54**, 291-327.
- Crawford, N. M. 1995 Nitrate - Nutrient and signal for plant growth. *Plant Cell* **7**, 859-868.
- Crawford, N. M. & Arst, H. N. 1993 The molecular genetics of nitrate assimilation in fungi and plants. *Annual Review of Genetics* **27**, 115-146.
- Crawford, N. M. & Glass, A. D. M. 1998 Molecular and physiological aspects of nitrate uptake in plants. *Trends in Plant Science* **3**, 389-395.
- Crowley, K. S., Reinhart, G. D. & Johnson, A. E. 1993 The signal sequence moves through a ribosomal tunnel into a noncytoplasmic aqueous environment at the ER membrane early in translocation. *Cell* **73**, 1101-1115.
- Cuff, A. L., Sillitoe, I., Lewis, T., Redfern, O. C., Garratt, R., Thornton, J. & Orengo, C. 2008 The CATH classification revisited—architectures reviewed and new ways to characterize structural divergence in superfamilies. *Nucleic Acids Research*, 1-5.
- Daniel-Vedele, F., Filleur, S. & Caboche, M. 1998 Nitrate transport: a key step in nitrate assimilation. *Current Opinion in Plant Biology* **1**, 235-239.
- Danielli, J. F. & Davson, H. 1935 A contribution to the theory of permeability of thin films. *Journal of Cellular and Comparative Physiology* **5**, 495-508.
- Darby, N., J., & Creighton, T., E. 1993. In *In Focus*, Protein Structure (ed. D. Rickwood), pp. 7-8. Oxford: IRL Press.
- Darwin, A. J., Tyson, K. L., Busby, S. J. W. & Stewart, V. 1997 Differential regulation by the homologous response regulators NarL and NarP of *Escherichia coli* K-12 depends on DNA binding site arrangement. *Molecular Microbiology* **25**, 583-595.
- Dean, M., Rzhetsky, A. & Allikmets, R. 2001 The human ATP-binding cassette (ABC) transporter superfamily. *Genome Research* **11**, 1156-1166.
- DeFelice, L. J. 2004 Transporter structure and mechanism. *Trends in Neurosciences* **27**, 352-359.
- DeFelice, L. J. & Blakely, R. D. 1996 Pore models for transporters? *Biophysical Journal* **70**, 579-580.

- Delano, W. L. 2002 The PyMOL Graphics System: DeLano Scientific, San Carlos, CA, USA.
[www://www.pymol.org](http://www.pymol.org).
- Delomenie, C., Foti, E., Floch, E., Diderot, V., Porquet, D., Dupuy, C. & Bonaly, J. 2007 A new homolog of FocA transporters identified in cadmium-resistant *Euglena gracilis*. *Biochemical and Biophysical Research Communications* **358**, 455-461.
- Denker, K., Orlik, F., Schiffler, B. & Benz, R. 2005 Site-directed mutagenesis of the greasy slide aromatic residues within the LamB (maltoporin) channel of *Escherichia coli*: Effect on ion and maltopentose transport. *Journal of Molecular Biology* **352**, 534-550.
- Deshais, R. J. & Schekman, R. 1987 A yeast mutant defective at an early stage in import of secretory protein precursors into the endoplasmic reticulum. *Journal of Cell Biology* **105**, 633-645.
- Dougherty, D. A. 1996 Cation- π interactions in chemistry and biology: a new view of benzene, Phe, Tyr and Trp. *Science* **271**, 163-168.
- Doyle, D. A., Cabral, J. M., Pfuetzner, R. A., Kuo, A. L., Gulbis, J. M., Cohen, S. L., Chait, B. T. & MacKinnon, R. 1998 The structure of the potassium channel: Molecular basis of K⁺ conduction and selectivity. *Science* **280**, 69-77.
- Duce, R. A., LaRoche, J., Altieri, K., Arrigo, K. R., Baker, A. R., Capone, D. G., Cornell, S., Dentener, F., Galloway, J., Ganeshram, R. S., Geider, R. J., Jickells, T., Kuypers, M. M., Langlois, R., Liss, P. S., Liu, S. M., Middelburg, J. J., Moore, C. M., Nickovic, S., Oschlies, A., Pedersen, T., Prospero, J., Schlitzer, R., Seitzinger, S., Sorensen, L. L., Uematsu, M., Ulloa, O., Voss, M., Ward, B. & Zamora, L. 2008 Impacts of atmospheric anthropogenic nitrogen on the open ocean. *Science* **320**, 893-897.
- Dumas, F., Koebnik, R., Winterhalter, M. & Van Gelder, P. 2000 Sugar transport through maltoporin of *Escherichia coli* - Role of polar tracks. *Journal of Biological Chemistry* **275**, 19747-19751.
- Dupre, S., Urban-Grimal, D. & Haguenaer-Tsapis, R. 2004 Ubiquitin and endocytic internalisation in yeast and animal cells. *Biochimica et Biophysica Acta-Molecular Cell Research* **1695**, 89-111.
- Dutzler, R., Campbell, E. B., Cadene, M., Chait, B. T. & MacKinnon, R. 2002 X-ray structure of a CIC chloride channel at 3.0 angstrom reveals the molecular basis of anion selectivity. *Nature* **415**, 287-294.
- Dutzler, R., Wang, Y. F., Rizkallah, P. J., Rosenbusch, J. P. & Schirmer, T. 1996 Crystal structures of various maltooligosaccharides bound to maltoporin reveal a specific sugar translocation pathway. *Structure* **4**, 127-134.

- Elbaz, Y., Salomon, T. & Schuldiner, S. 2008 Identification of a glycine motif required for packing in EmrE, a multidrug transporter from *Escherichia coli*. *Journal of Biological Chemistry* **283**, 12276-12283.
- Engelman, D. M. 2005 Membranes are more mosaic than fluid. *Nature* **438**, 578-580.
- Ermolova, N. V., Smirnova, I. N., Kasho, V. N. & Kaback, H. R. 2005 Interhelical packing modulates conformational flexibility in the lactose permease of *Escherichia coli*. *Biochemistry* **44**, 7669-7677.
- Esguerra, M., Wang, J., Foster, C. D., Adelman, J. P., North, R. A. & Levitan, I. B. 1994 Cloned Ca²⁺-dependent K⁺ channel modulated by functionally associated protein kinase. *Nature* **369**, 563-565.
- Eubel, H., Braun, H. P. & H., M. A. 2005 Blue-native PAGE in plants: a tool in analysis of protein-protein interactions. *Plant Methods* **1**.
- Feinberg, A. P. & Vogelstein, B. 1983 A technique for radiolabeling DNA restriction endonuclease fragments to high specific activity. *Analytical Biochemistry* **132**, 6-13.
- Fernandez, E. & Galvan, A. 2007 Inorganic nitrogen assimilation in *Chlamydomonas*. *Journal of Experimental Botany* **58**, 2279-2287.
- Ferris, P. J., Armbrust, E. V. & Goodenough, U. W. 2002 Genetic structure of the mating-type locus of *Chlamydomonas reinhardtii*. *Genetics* **160**, 181-200.
- Filleur, S. & Daniel-Vedele, F. 1999 Expression analysis of a high-affinity nitrate transporter isolated from *Arabidopsis thaliana* by differential display. *Planta* **207**, 461-469.
- Fincham, J. R. S. 1989 Transformation in fungi. *Microbiological Reviews* **53**, 148-170.
- Finn, R. D., Mistry, J., Schuster-Bockler, B., Griffiths-Jones, S., Hollich, V., Lassmann, T., Moxon, S., Marshall, M., Khanna, A., Durbin, R., Eddy, S. R., Sonnhammer, E. L. L. & Bateman, A. 2006 Pfam: clans, web tools and services. *Nucleic Acids Research* **34**, D247-D251.
- Fisk, H. A. & Yaffe, M. P. 1999 A role for ubiquitination in mitochondrial inheritance in *Saccharomyces cerevisiae*. *Journal of Cell Biology* **145**, 1199-1208.
- Fleishman, S. J., Unger, V. M. & Ben-Tal, N. 2006 Transmembrane protein structures without X-rays. *Trends in Biochemical Sciences* **31**, 106-113.
- Forde, B. G. 2000 Nitrate transporters in plants: structure, function and regulation. *Biochimica Et Biophysica Acta-Biomembranes* **1465**, 219-235.
- Forde, B. G. 2002 Local and long-range signaling pathways regulating plant responses to nitrate. *Annual Review of Plant Biology* **53**, 203-224.
- Forst, D., Welte, W., Wacker, T. & Diederichs, K. 1998 Structure of the sucrose-specific porin ScrY from *Salmonella typhimurium* and its complex with sucrose. *Nature Structural Biology* **5**, 37-46.

- Fraisier, V., Gojon, A., Tillard, P. & Daniel-Vedele, F. 2000 Constitutive expression of a putative high-affinity nitrate transporter in *Nicotiana plumbaginifolia*: evidence for post-transcriptional regulation by a reduced nitrogen source. *Plant Journal* **23**, 489-496.
- Frelet, A. & Klein, M. 2006 Insight in eukaryotic ABC transporter function by mutation analysis. *FEBS Letters* **580**, 1064-1084.
- Frillingos, S., Gonzalez, A. & Kaback, H. R. 1997 Cysteine-scanning mutagenesis of helix IV and the adjoining loops in the lactose permease of *Escherichia coli*: Glu126 and Arg144 are essential. *Biochemistry* **36**, 14284-14290.
- Frillingos, S., Sahin-Toth, M., Wu, J. H. & Kaback, H. R. 1998 Cys-scanning mutagenesis: a novel approach to structure-function relationships in polytopic membrane proteins. *FASEB Journal* **12**, 1281-1299.
- Fugslang, A. T., Visconti, S., Drumm, K., Jahn, T., Stensballe, A., Mattei, B., Jensen, O. N., Aducci, P. & Palmgren, M. G. 1999 Binding of 14-3-3 protein to the plasma membrane H⁺-ATPase AHA2 involves the three C-terminal residues Tyr946-Thr-Val and requires phosphorylation of Thr947. *Journal of Biological Chemistry* **274**, 36774-36780.
- Furukawa, K., Katsuno, Y., Urao, T., Yabe, T., Yamada-Okabe, T., Yamada-Okabe, H., Yamagata, Y., Abe, K. & Nakajima, T. 2002 Isolation and functional analysis of a gene, *tsbB*, encoding a transmembrane hybrid-type histidine kinase from *Aspergillus nidulans*. *Applied and Environmental Microbiology* **68**, 5304-5310.
- Galagan, J. E., Calvo, S. E., Cuomo, C., Ma, L. J., Wortman, J. R., Batzoglou, S., Lee, S. I., Basturkmen, M., Spevak, C. C., Clutterbuck, J., Kapitonov, V., Jurka, J., Scazzocchio, C., Farman, M., Butler, J., Purcell, S., Harris, S., Braus, G. H., Draht, O., Busch, S., D'Enfert, C., Bouchier, C., Goldman, G. H., Bell-Pedersen, D., Griffiths-Jones, S., Doonan, J. H., Yu, J., Vienken, K., Pain, A., Freitag, M., Selker, E. U., Archer, D. B., Penalva, M. A., Oakley, B. R., Momany, M., Tanaka, T., Kumagai, T., Asai, K., Machida, M., Nierman, W. C., Denning, D. W., Caddick, M., Hynes, M., Paoletti, M., Fischer, R., Miller, B., Dyer, P., Sachs, M. S., Osmani, S. A. & Birren, B. W. 2005 Sequencing of *Aspergillus nidulans* and comparative analysis with *A. fumigatus* and *A. oryzae*. *Nature* **438**, 1105-1115.
- Galan, J. M. & Haguenuer-Tsapis, R. 1997 Ubiquitin Lys63 is involved in ubiquitination of a yeast plasma membrane protein. *EMBO Journal* **16**, 5847-5854.
- Galloway, J. N., Townsend, A. R., Erisman, J. W., Bekunda, M., Cai, Z. C., Freney, J. R., Martinelli, L. A., Seitzinger, S. P. & Sutton, M. A. 2008 Transformation of the

- nitrogen cycle: Recent trends, questions, and potential solutions. *Science* **320**, 889-892.
- Galvan, A. & Fernandez, E. 2001 Eukaryotic nitrate and nitrite transporters. *Cellular and Molecular Life Sciences* **58**, 225-233.
- Galvan, A., Quesada, A. & Fernandez, E. 1996 Nitrate and nitrite are transported by different specific transport systems and by a bispecific transporter in *Chlamydomonas reinhardtii*. *Journal of Biological Chemistry* **271**, 2088-2092.
- Galvan, A., Rexach, J., Mariscal, V. & Fernandez, E. 2002 Nitrite transport to the chloroplast in *Chlamydomonas reinhardtii*: molecular evidence for a regulated process. *Journal of Experimental Botany* **53**, 845-853.
- Gan, Y. B., Filleur, S., Rahman, A., Gotensparre, S. & Forde, B. G. 2005 Nutritional regulation of ANR1 and other root-expressed MADS-box genes in *Arabidopsis thaliana*. *Planta* **222**, 730-742.
- Gao-Rubinelli, F. & Marzluf, G. A. 2004 Identification and characterization of a nitrate transporter gene in *Neurospora crassa*. *Biochemical Genetics* **42**, 21-34.
- Giles, J. 2005 Nitrogen study fertilizes fears of pollution. *Nature* **433**, 791-791.
- Glass, A. D. M., Britto, D. T., Kaiser, B. N., Kinghorn, J. R., Kronzucker, H. J., Kumar, A., Okamoto, M., Rawat, S., Siddiqi, M. Y., Unkles, S. E. & Vidmar, J. J. 2002 The regulation of nitrate and ammonium transport systems in plants. *Journal of Experimental Botany* **53**, 855-864.
- Goder, V. & Speiss, M. 2001 Topogenesis of membrane proteins: determinants and dynamics. *FEBS Letters* **504**, 87-93.
- Gorter, E. & Grendel, F. 1925 On biomolecular layers of lipoids on the chromocytes of the blood. *Journal of Experimental Medicine* **41**, 439-422.
- Gouaux, E. & MacKinnon, R. 2005 Principles of selective ion transport in channels and pumps. *Science* **310**, 1461-1465.
- Govers, R., ten Broeke, T., van Kerkhof, P., Schwartz, A. L. & Strous, G. J. 1999 Identification of a novel ubiquitin conjugation motif, required for ligand-induced internalisation of the growth hormone receptor. *EMBO Journal* **18**, 28-36.
- Green, A. L., Hrodey, H. A. & Brooker, R. J. 2003 Evidence for structural symmetry and functional asymmetry in the lactose permease of *Escherichia coli*. *Biochemistry* **275**, 11226-11233.
- Griffith, J. K., Baker, M. E., Rouch, D. A., Page, M. G., Skurray, R. A., Paulsed, I. T., Chater, K., F., Baldwin, S. A. & Henderson, P. J. 1992 Membrane transport proteins: implications of sequence comparisons. *Current Opinion in Cell Biology* **4**, 684-695.

- Guan, L. & Kaback, H. R. 2006 Lessons from lactose permease. *Annual Review of Biophysics and Biomolecular Structure* **33**, 67-91.
- Guan, L., Mirza, O., Verner, G., Iwata, S. & Kaback, H. R. 2007 Structural determination of wild-type lactose permease. *Proceedings of the National Academy of Sciences of the United States of America* **104**, 15294-15298.
- Guan, L., Murphy, F. D. & Kaback, H. R. 2002 Surface-exposed positions in the transmembrane helices of the lactose permease of *Escherichia coli* determined by intermolecular thiol cross-linking. *Proceedings of the National Academy of Sciences of the United States of America* **99**, 3475-3480.
- Guerra, G., Petrov, V. V., Allen, K. E., Miranda, M., Pardo, J. P. & Slayman, C. W. 2007 Role of transmembrane segment M8 in the biogenesis and function of yeast plasma-membrane H⁺-ATPase. *Biochimica Et Biophysica Acta* **1768**, 2383-2392.
- Guo, F. O., Young, J. & Crawford, N. M. 2003 The nitrate transporter AtNRT1.1 (CHL1) functions in stomatal opening and contributes to drought susceptibility in *Arabidopsis*. *Plant Cell* **15**, 107-117.
- Guo, F. Q., Wang, R. C., Chen, M. S. & Crawford, N. M. 2001 The *Arabidopsis* dual-affinity nitrate transporter gene AtNRT1.1. (CHL1) is activated and functions in nascent organ development during vegetative and reproductive growth. *Plant Cell* **13**, 1761-1777.
- Guo, F. Q., Wang, R. C. & Crawford, N. M. 2002 The *Arabidopsis* dual-affinity nitrate transporter gene AtNRT1.1 (CHL1) is regulated by auxin in both shoots and roots. *Journal of Experimental Botany* **53**, 835-844.
- Gutman, N., Steiner-Mordoch, S. & Schuldiner, S. 2003 An amino acid cluster around the essential Glu-14 is part of the substrate- and proton-binding domain of EmrE, a multidrug transporter from *Escherichia coli*. *Journal of Biological Chemistry* **278**, 16082-16087.
- Hall, J. A. & Maloney, P. C. 2005 Altered oxyanion selectivity in mutants of UhpT, the Pi-linked sugar phosphate carrier of *Escherichia coli*. *Journal of Biological Chemistry* **280**, 3376-3381.
- Han, M., Groesbeek, M., Sakmar, T. P. & Smith, S. O. 1997 The C9 methyl group of retinal interacts with glycine-121 in rhodopsin. *Proceedings of the National Academy of Sciences of the United States of America* **94**, 13442-13447.
- Han, M., Lin, S. W., Smith, S. O. & Sakmar, T. P. 1996 The effects of amino acid replacements of glycine 121 on transmembrane helix 3 of rhodopsin. *Journal of Biological Chemistry* **271**, 32330-32336.

- Hanks, S. K. & Hunter, T. 1995 Protein Kinases 6. The eukaryotic protein-kinase superfamily - Kinase (Catalytic) domain-structure and classification. *FASEB Journal* **9**, 576-596.
- Hardie, D. G. 1993 *Protein Phosphorylation: A practical approach*: Oxford University Press.
- Hardin, S. C. & Huber, S. C. 2004 Proteasome activity and the post-translational control of sucrose synthase stability in maize leaves. *Plant Physiology and Biochemistry* **42**, 197-208.
- Hardin, S. C., Tang, G. Q., Scholz, A., Holtgraewe, D., Winter, H. & Huber, S. C. 2003 Phosphorylation of sucrose synthase at serine 170: occurrence and possible role as a signal for proteolysis. *Plant Journal* **35**, 588-603.
- Hardin, S. C., Winter, H. & Huber, S. C. 2004 Phosphorylation of the amino terminus of maize sucrose synthase in relation to membrane association and enzyme activity. *Plant Physiology* **134**, 1427-1438.
- Henderson, P. J. 1990 Proton-linked sugar transport transport systems in bacteria. *Journal of Bioenergetics and Biomembranes* **22**, 571-592.
- Henry, G. D. & Sykes, B. D. 1990 Structure and dynamics of detergent-solubilised M13 coat protein (an integral membrane protein) determined by ¹³C and ¹⁵N nuclear magnetic resonance spectroscopy. *Biochemistry and Cell Biology* **68**, 318-329.
- Hershko, A. & Ciechanover, A. 1998 The ubiquitin system. *Annual Review of Biochemistry* **67**, 425-479.
- Hessa, T., Kim, H., Bihlmaier, K., Lundin, C., Boekel, J., Andersson, H., Nilsson, I., White, S. H. & von Heijne, G. 2005 Recognition of transmembrane helices by the endoplasmic reticulum translocon. *Nature* **433**, 377-381.
- Hessa, T., Meindl-Beinker, N. M., Bernsel, A., Kim, H., Sato, Y., Lerch-Bader, M., Nilsson, I., White, S. H. & von Heijne, G. 2007 Molecular code for transmembrane-helix recognition by the Sec61 translocon. *Nature* **450**, 1026-U2.
- Heymann, J. A. W., Hirai, T., Shi, D. & Subramaniam, S. 2003 Projection structure of the bacterial oxalate transporter OxIT at 3.4 angstrom resolution. *Journal of Structural Biology* **144**, 320-326.
- Heymann, J. A. W., Sarker, R., Hirai, T., Shi, D., Milne, J. L. S., Maloney, P. C. & Subramaniam, S. 2001 Projection structure and molecular architecture of OxIT, a bacterial membrane transporter. *EMBO Journal* **20**, 4408-4413.
- Hicke, L. 2001 Protein regulation by monoubiquitin. *Nature Reviews Molecular Cell Biology* **2**, 195-201.
- Hicke, L. & Dunn, R. 2003 Regulation of membrane protein transport by ubiquitin and ubiquitin-binding proteins. *Annual Review of Cell and Developmental Biology* **19**, 141-172.

- Hildebrand, P. W., Lorenzen, S., Goede, A. & Preissner, R. 2006 Analysis and prediction of helix-helix interactions in membrane channels and transporters. *Proteins-Structure Function and Bioinformatics* **64**, 253-262.
- Hirai, T., Heymann, J. A. W., Maloney, P. C. & Subramaniam, S. 2003 Structural model for 12-helix transporters belonging to the major facilitator superfamily. *Journal of Bacteriology* **185**, 1712-1718.
- Hirai, T. & Subramaniam, S. 2004 Structure and transport mechanism of the bacterial oxalate transporter OxIT. *Biophysical Journal* **87**, 3600-3607.
- Hoege, C., Pfander, B., Moldovan, G. L., Pyrowolakis, G. & Jentsch, S. 2003 RAD6 dependent DNA repair is linked to modification of PCNA by ubiquitin and SUMO. *Yeast* **20**, S147-S147.
- Hollenstein, K., Dawson, R. J. P. & Locher, K. P. 2007 Structure and mechanism of ABC transporter proteins. *Current Opinion in Structural Biology* **17**, 412-418.
- Holowka, D., Goose, J.A., Hammond, A. T., Han, X., Sengupta, P., Smith, N.L et al. 2005 Lipid segregation and IgE receptor signalling: a decade of progress. *Biochimica et Biophysica Acta* **1746**, 252-259.
- Horak, J. 2003 The role of ubiquitin in down-regulation and intracellular sorting of membrane proteins: insights from yeast. *Biochimica Et Biophysica Acta-Biomembranes* **1614**, 139-155.
- Huang, H. D., Lee, T. Y., Tzeng, S. W. & Horng, J. T. 2005 KinasePhos: a web tool for identifying protein kinase-specific phosphorylation sites. *Nucleic Acids Research* **33**, W226-W229.
- Huang, N. C., Liu, K. H., Lo, H. J. & Tsay, Y. F. 1999 Cloning and functional characterization of an *Arabidopsis* nitrate transporter gene that encodes a constitutive component of low-affinity uptake. *Plant Cell* **11**, 1381-1392.
- Huang, Y. F., Lemieux, M. J., Song, J. M., Auer, M. & Wang, D. N. 2003 Structure and mechanism of the glycerol-3-phosphate transporter from *Escherichia coli*. *Science* **301**, 616-620.
- Huber, S. C. & Hardin, S. C. 2004 Numerous post-translational modifications provide opportunities for the intricate regulation of metabolic enzymes at multiple levels. *Current Opinion in Plant Biology* **7**, 318-322.
- Hulo, N., Bairoch, A., Bulliard, V., Cerutti, L., Cuče, B. A., de Castro, E., Lachaize, C., Langendijk-Genevaux, P. S. & Sigrist, C. J. A. 2008 The 20 years of PROSITE. *Nucleic Acids Research* **36**, D245-D249.

- Hulo, N., Bairoch, A., Bulliard, V., Cerutti, L., De Castro, E., Langendijk-Genevaux, P. S., Pagni, M. & Sigrist, C. J. A. 2006 The PROSITE database. *Nucleic Acids Research* **34**, D227-D230.
- Hunte, C., Screpanti, E., Venturi, M., Rimon, A., Padan, E. & Michel, H. 2005 Structure of a Na^+/H^+ antiporter and insights into mechanism of action and regulation by pH. *Nature* **435**, 1197-1202.
- Hynes, M. J. & Davis, M., A. . 2004 Regulation of the *amdS* gene in *Aspergillus nidulans*, vol. 3, The Mycota: Biochemistry and Molecular Biology (ed. R. Branmbel & G. A. Marzluf), pp. 421-435. Berlin and Heidelberg: Springer-Verlag.
- Jardetzky, O. 1966 Simple Allosteric Model for membrane pumps. *Nature* **211**, 969-970.
- Javadpour, M. M., Eilers, M., Groesbeek, M. & Smith, S. O. 1999 Helix packing in polytopic membrane proteins: role of glycine in transmembrane helix association. *Biophysical Journal* **77**, 1609-1618.
- Jefferson, R. A. 1989a Gene encoding the transport protein glucuronide permease allows cellular uptake of beta-glucuronide(s) and detection of beta-glucuronidase activity.
- Jefferson, R. A. 1989b The Gus Reporter Gene System. *Nature* **342**, 837-838.
- Jessen-Marshall, A. E., Paul, N. J. & Brooker, R. J. 1995 The conserved motif, $\text{Gxxx(D/E)(R/K)XG[X](R/K)(R/K)}$, in hydrophilic loop-2/3 of the lactose permease. *Journal of Biological Chemistry* **270**, 16251-16257.
- JessenMarshall, A. E., Parker, N. J. & Brooker, R. J. 1997 Suppressor analysis of mutations in the loop 2-3 motif of lactose permease: Evidence that glycine-64 is an important residue for conformational changes. *Journal of Bacteriology* **179**, 2616-2622.
- Jia, W. & Cole, J. A. 2005 Nitrate and nitrite transport in *Escherichia coli*. *Biochemical Society Transactions* **33**, 159-161.
- Jiang, Y. X., Lee, A., Chen, J. Y., Cadene, M., Chait, B. T. & MacKinnon, R. 2002 Crystal structure and mechanism of a calcium-gated potassium channel. *Nature* **417**, 515-522.
- Jin, J., Guffanti, A. A., Beck, C. & Krulwich, T. A. 2001 Twelve trans membrane segment (TMS) version (*TMS VII-VIII)of the 14-TMS Tel(L) antibiotic resistance protein retains monovalent cation transport modes but lacks tetracycline efflux capacity. *Journal of Bacteriology* **183**, 2667-2671.
- John, M. A. & Peberdy, J. F. 1984 Transformation of *Aspergillus nidulans* using the *argB* gene. *Enzyme and microbial technology* **6**, 386-389.
- Johnson, E. S. 2002 Ubiquitin branches out. *Nature Cell Biology* **4**, E295-E298.
- Johnstone, I. L., McCabe, P. C., Greaves, P., Gurr, S. J., Cole, G. E., Brow, M. A. D., Unkles, S. E., Clutterbuck, A. J., Kinghorn, J. R. & Innis, M. A. 1990 Isolation and

- characterisation of the *crnA-niiA-niaD* gene cluster for nitrate assimilation in *Aspergillus nidulans*. *Gene* **90**, 181-192.
- Jung, K., Jung, H., Colacurcio, P. & Kaback, H. R. 1995 Role of glycine residues in the structure and function of lactose permease, an *Escherichia coli* membrane transport protein. *Biochemistry* **34**, 1030-1039.
- Kaback, H. R. 1976 Molecular biology and energetics of membrane transport. *Journal of Cellular Physiology* **89**, 575-593.
- Kaback, H. R. 2005 Structure and mechanism of the lactose permease. *Comptes Rendus Biologies* **328**, 557-567.
- Kaback, H. R., Frillingos, S., Jung, H., Jung, K., Prive, G. G., Ujwal, M. L., Weitzman, C., Wu, J. H. & Zen, K. 1994 The lactose permease meets Frankenstein. *Journal of Experimental Biology* **196**, 183-195.
- Kaback, H. R., Sahin-Toth, M. & Weinglass, A. B. 2001 The kamikaze approach to membrane transport. *Nature Reviews Molecular Cell Biology* **2**, 610-620.
- Kaback, H. R. & Wu, J. 1999 What to do while awaiting crystals of a membrane protein and thereafter. *Accounts of Chemical Research* **32**, 805-813.
- Kabouridis, P. S. 2006 Lipid rafts in T-cell receptor signalling. *Molecular Membrane Biology* **23**, 49-57.
- Kasahara, T. & Kasahara, M. 2000 Interaction between the critical aromatic amino acid residues Tyr(352) and Phe(504) in the yeast Gal2 transporter. *FEBS Letters* **471**, 103-107.
- Kay, B. K., Williamson, M. P. & Sudol, P. 2000 The importance of being proline: the interaction of proline rich motifs in signalling proteins with their cognate domains. *FASEB Journal* **14**, 231-241.
- Kelkar, D. A. & Chattopadhyay, A. 2006 Membrane interfacial localization of aromatic amino acids and membrane protein function. *Journal of Biosciences* **31**, 297-302.
- Kielland, K. 1994 Amino acid absorption by Arctic plants - Implications for plant nutrition and nitrogen cycling. *Ecology* **75**, 2373-2383.
- Kim, S., Chamberlain, A. K. & Bowie, J. U. 2004 Membrane channel structure of *Helicobacter pylori* vacuolating toxin: Role of multiple GXXXG motifs in cylindrical channels. *Proceedings of the National Academy of Sciences of the United States of America* **101**, 5988-5991.
- Kim, S., Jeon, T. J., Oberai, A., Yang, D., Schmidt, J. J. & Bowie, J. U. 2005 Transmembrane glycine zippers: Physiological and pathological roles in membrane proteins. *Proceedings of the National Academy of Sciences of the United States of America* **102**, 14278-14283.

- Kinghorn, J. R. 1989 Genetic, biochemical and structural organisation of the *Aspergillus nidulans crnA-niiA-niaD* gene cluster, *Molecular and Genetic Aspects of Nitrate Assimilation* (ed. J. Wray & J. R. Kinghorn), pp. 69-87: Oxford Science Publications.
- Kinghorn, J. R., Sloan, J., Kana'n, G. J. M., DaSilva, E. R., Rouch, D. A. & Unkles, S. E. 2005 Missense mutations that inactivate the *Aspergillus nidulans nrtA* gene encoding a high-affinity nitrate transporter. *Genetics* **169**, 1369-1377.
- Kinghorn, J. R. & Unkles, S. E. 1994 Molecular genetics and expression of foreign proteins in the genus *Aspergillus*. In *Biotechnology Handbooks*, vol. 7, *Aspergillus* (ed. J. E. Smith), pp. 65-100. Glasgow: Plenum Press.
- Kisselev, A. F., Akopian, T. N., Woo, K. M. & Goldberg, A. L. 1999 The sizes of peptides generated from protein by mammalian 26 and 20 S proteasomes - Implications for understanding the degradative mechanism and antigen presentation. *Journal of Biological Chemistry* **274**, 3363-3371.
- Kozakiewicz, Z. & Smith, D. 1994 Physiology of *Aspergillus*. In *Biotechnology Handbooks*, vol. 7, *Aspergillus* (ed. J. E. Smith), pp. 23-40. Glasgow: Plenum Press.
- Krogh, A., Larsson, B., von Heijne, G. & Sonnhammer, E. L. L. 2001 Predicting transmembrane protein topology with a hidden Markov model: Application to complete genomes. *Journal of Molecular Biology* **305**, 567-580.
- Kronzucker, H. J., Siddiqi, M. Y. & Glass, A. D. M. 1995 Compartmentation and flux characteristics of nitrate in spruce. *Planta* **196**, 674-682.
- Kruger, E., Kuckelkorn, U., Sijts, A. & Kloetzel, P. M. 2004 The components of the proteasome system and their role in MHC class I antigen processing. *Reviews of Physiology, Biochemistry and Pharmacology, Vol 148* **148**, 81-104.
- Kudla, B., Caddick, M. X., Langdon, T., Martinez-Rossi, N. M., Bennett, C. F., Sibley, S., Davis, R. W. & Arst, H. N. 1990 The regulatory gene *areA* mediating nitrogen metabolite repression in *Aspergillus nidulans*. Mutations affecting specificity of gene activation alter a loop residue of a putative zinc finger. *EMBO Journal* **9**, 1355-1364.
- Kurtzman, C. P. 1984 Synonymy of the yeast genera *Hansenula* and *Pichia* demonstrated through comparisons of desoxyribonucleic acid relatedness. *Antonie Van Leeuwenhoek* **50**, 209-217.
- Kwak, Y.-G., Navarro-Polanco, R. A., Grobaski, T., Gallagher, D. J. & Tamkan, M. M. 1999 Phosphorylation is required for alteration of Kv1.5K⁺ channel function by the Kvβ1.3 subunit. *Journal of Biological Chemistry* **274**, 25355-25361.
- Lafont, F. & van der Goot, F. G. 2005 Bacterial invasion via lipid rafts. *Cellular Microbiology* **7**, 613-620.

- Lalonde, S., Boles, E., Hellmann, H., Barker, L., Patrick, J. W., Frommer, W. B. & Ward, J. M. 1999 The dual function of sugar carriers: Transport and sugar sensing. *Plant Cell* **11**, 707-726.
- Law, C. J., Almqvist, J., Bernstein, A., Goetz, R. M., Huang, Y., Soudant, C., Laaksonen, A., Hovmoller, S. & Wang, D. N. 2008 Salt-bridge dynamics control substrate induced conformational change in the membrane transporter GlpT. *Journal of Molecular Biology* **378**, 826-837.
- le Coutre, J. & Kaback, H. R. 2000 Structure-function relationships of integral membrane proteins: Membrane transporters vs channels. *Biopolymers* **55**, 297-307.
- Lear, J. D., Gratkowski, H., Adamian, L., Liang, J. & DeGrado, W. F. 2003 Position-dependence of stabilizing polar interactions of asparagine in transmembrane helical bundles. *Biochemistry* **42**, 6400-6407.
- Lee, A. I., Delgado, A. & Gunsalus, R. P. 1999 Signal-dependent phosphorylation of the membrane-bound NarX two-component sensor-transmitter protein of *Escherichia coli*: Nitrate elicits a superior anion ligand response compared to nitrite. *Journal of Bacteriology* **181**, 5309-5316.
- Lee, R. B. 1979 Effect of Nitrite on Root-Growth of Barley and Maize. *New Phytologist* **83**, 615-622.
- Lefevre, F., Remy, M. G. & Masson, J. M. 1997 Alanine-scanning mutagenesis: a simple and efficient method to probe protein structure and function. *Nucleic Acids Research* **25**, 447-448.
- Lemieux, M. J., Huang, Y. F. & Wang, D. N. 2004 Glycerol-3-phosphate transporter of *Escherichia coli*: Structure, function and regulation. *Research in Microbiology* **155**, 623-629.
- Lemieux, M. J., Song, J. M., Kim, M. J., Huang, Y. F., Villa, A., Auer, M., Li, X. D. & Wang, D. N. 2003 Three-dimensional crystallization of the *Escherichia coli* glycerol-3-phosphate transporter: A member of the major facilitator superfamily. *Protein Science* **12**, 2748-2756.
- Lewis, C. W., Anderson, J. G. & Smith, J. E. 1994 Health-related aspects of the genus *Aspergillus*. In *Biotechnology Handbooks*, vol. 7, *Aspergillus* (ed. J. E. Smith). Glasgow: Plenum Press.
- Li, S. C., Goto, N. K., Williams, K. A. & Deber, C. M. 1996 alpha-Helical, but not beta-sheet, propensity of proline is determined by peptide environment. *Proceedings of the National Academy of Sciences of the United States of America* **93**, 6676-6681.
- Lin, H. & Goodenough, U. W. 2007 Gametogenesis in the *Chlamydomonas reinhardtii* minus mating type is controlled by two genes, *MID* and *MTD1*. *Genetics* **176**, 913-925.

- Little, D. Y., Rao, H., Oliva, S., Daniel-Vedele, F., Krapp, A. & Malamy, J. E. 2005 The putative high affinity nitrate transporter Nrt2.1 represses lateral root initiation in response to nutritional cues. *Proceedings of the National Academy of Sciences of the United States of America* **102**, 1005-1013.
- Liu, J. F. & Rost, B. 2001 Comparing function and structure between entire proteomes. *Protein Science* **10**, 1970-1979.
- Liu, K. H., Huang, C. Y. & Tsay, Y. F. 1999 CHL1 is a dual-affinity nitrate transporter of arabidopsis involved in multiple phases of nitrate uptake. *Plant Cell* **11**, 865-874.
- Liu, K. H. & Tsay, Y. F. 2003 Switching between the two action modes of the dual-affinity nitrate transporter CHL1 by phosphorylation. *EMBO Journal* **22**, 1005-1013.
- Liu, Y., Engelman, D.M., Gerstein, M. 2002 Genomic analysis of membrane protein families: abundance and conserved motifs. *Genome Biology* **3**, 0054.1–0054.12.
- Liu, Y., Gerstein, M. & Engelman, D. M. 2004 Transmembrane protein domains rarely use covalent domain recombination as an evolutionary mechanism. *Proceedings of the National Academy of Sciences of the United States of America* **101**, 3495-3497.
- Llamas, A., Igeno, M. I., Galvan, A. & Fernandez, E. 2002 Nitrate signalling on the nitrate reductase gene promoter depends directly on the activity of the nitrate transport systems in *Chlamydomonas*. *Plant Journal* **30**, 261-271.
- Locher, K. P., R.B., B. & D.C., R. 2003 Breaching the barrier. *Science* **301**, 603-604.
- MacArthur, M. W. & Thornton, J. M. 1991 Influence of proline residues on protein conformation. *Journal of Molecular Biology* **218**, 397-412.
- Machin, F., Medina, B., Navarro, F. J., Perez, M. D., Veenhuis, M., Tejera, P., Lorenzo, H., Lancha, A. & Siverio, J. M. 2004 The role of Ynt1 in nitrate and nitrite transport in the yeast *Hansenula polymorpha*. *Yeast* **21**, 265-276.
- Machin, F., Perdomo, G., Perez, M. D., Brito, N. & Siverio, J. M. 2001 Evidence for multiple nitrate uptake systems in the yeast *Hansenula polymorpha*. *FEMS Microbiology Letters* **194**, 171-174.
- MacKinnon, R. 2004 Potassium channels and the atomic basis of selective ion conduction (Nobel lecture). *Angewandte Chemie-International Edition* **43**, 4265-4277.
- Maiden, M. C. J., Davis, E. O., Baldwin, S. A., Moore, D. C. M. & Henderson, P. J. F. 1987 Mammalian and bacterial sugar-transport proteins are homologous. *Nature* **325**, 641-643.
- Majumdar, D. S., Smirnova, I., Kasho, V., Nir, E., Kong, X. X., Weiss, S. & Kaback, H. R. 2007 Single-molecule FRET reveals sugar-induced conformational dynamics in LacY. *Proceedings of the National Academy of Sciences of the United States of America* **104**, 12640-12645.

- Manes, S., del Real, G. & Martinez, A. C. 2003 Pathogens: raft hijackers. *Nature Reviews Immunology* **3**, 557-568.
- Manes, S. & Viola, A. 2003 Lipid rafts in lymphocyte activation and migration *Molecular Membrane Biology* **23**, 59-69.
- Mann, M. & Jensen, O. N. 2003 Proteomic analysis of post-translational modifications. *Nature Biotechnology* **21**, 255-261.
- Mann, M., Ong, S. E., Gronborg, M., Steen, H., Jensen, O. N. & Pandey, A. 2002 Analysis of protein phosphorylation using mass spectrometry: deciphering the phosphoproteome. *Trends in Biotechnology* **20**, 261-268.
- Manoil, C. & Bailey, J. 1997 A simple screen for permissive sites in proteins: Analysis of *Escherichia coli* lac permease. *Journal of Molecular Biology* **267**, 250-263.
- Mansey, S. S., Schrum, J. P., Krishnamurthy, M., T., S., , Treco, D. A. & Szostak, J. W. 2008 Template-directed synthesis of a genetic polymer in a model protocell. *Nature* **454**, 122-125.
- Margelis, S., D'Souza, C., Small, A., Hynes, M. J., Adams, T. H. & Davis, M. A. 2001 Role of glutamine synthase in nitrogen metabolite repression in *Aspergillus nidulans*. *Journal of Bacteriology* **183**, 5826-5833.
- Marger, M. D. & Saier, M. H. 1993 A major superfamily of transmembrane facilitators that catalyze uniport, symport and antiport. *Trends in Biochemical Sciences* **18**, 13-20.
- Mariscal, V., Moulin, P., Orsel, M., Miller, A. J., Fernandez, E. & Galvan, A. 2006 Differential regulation of the *Chlamydomonas* *Nar1* gene family by carbon and nitrogen. *Protist* **157**, 421-433.
- Mariscal, V., Rexach, J., Fernandez, E. & Galvan, A. 2004 The plastidic nitrite transporter NAR1;1 improves nitrate use efficiency for growth in *Chlamydomonas*. *Plant Cell and Environment* **27**, 1321-1328.
- Martinelli, S. D. 1994 *Aspergillus nidulans* as an experimental organism, vol. 29, *Aspergillus: 50 years on* (ed. S. D. Martinelli & J. R. Kinghorn), pp. 33-58: Elsevier.
- Marzluf, G. A. 1997 Genetic regulation of nitrogen metabolism in the fungi. *Microbiology and Molecular Biology Reviews* **61**, 17-32.
- Matlack, K. E. S., Misselwitz, B., Plath, K. & Rapoport, T. A. 1999 BiP acts as a molecular ratchet during posttranslational transport of prepro-alpha factor across the ER membrane. *Cell* **97**, 553-564.
- McElfresh, M. W., Meeks, J. C. & Parks, N. J. 1979 Synthesis of N-13-labeled nitrite of high specific activity and purity. *Journal of Radioanalytical Chemistry* **53**, 337-344.

- McKone, E. F., Emerson, S. S., Edwards, K. L. & Aitken, M. L. 2003 Effect of genotype on phenotype and mortality in cystic fibrosis: a retrospective cohort study *Lancet* **316**, 1671-1676.
- Meyer, J. E. W., Hofnung, M. & Schulz, G. E. 1997 Structure of maltoporin from *Salmonella typhimurium* ligated with a nitrophenyl-maltotrioxide. *Journal of Molecular Biology* **266**, 761-775.
- Miller, A. J. & Cramer, M. D. 2005 Root nitrogen acquisition and assimilation. *Plant and Soil* **274**, 1-36.
- Miller, A. J., Fan, X. R., Orsel, M., Smith, S. J. & Wells, D. M. 2007 Nitrate transport and signalling. *Journal of Experimental Botany* **58**, 2297-2306.
- Miller, C. 2000 Ion channels: doing hard chemistry with hard ions. *Current Opinion in Chemical Biology* **4**, 148-151.
- Miller, G. 2003 The puzzling portrait of a pore. *Science* **300**, 2020-2022.
- Mirza, O., Guan, L., Verner, G., Iwata, S. & Kaback, H. R. 2006 Structural evidence for induced fit and a mechanism for sugar/H⁺ symport in LacY *Embo Journal* **25**, 1177-1183.
- Mitaku, S., Ono, M., Hirokawa, T., Boon-Chieng, S. & Sonoyama, M. 1999 Proportion of membrane proteins in proteomes of 15 single-cell organisms analysed by the SOSUI prediction system. *Biophysical Chemistry* **82**, 165-171.
- Mitchell, P. 1961 Coupling of phosphorylation to electron and hydrogen transfer by a chemi-osmotic type of mechanism. *Nature* **191**, 144-148.
- Morozov, I. Y., Galbis-Martinez, M., Jones, M. D. & Caddick, M. 2001 Characterisation of nitrogen metabolite signalling in *Aspergillus* via the regulated degradation of *areA* mRNA. *Molecular Microbiology* **42**, 269-277.
- Muro-Pastor, M. I., Gonzalez, R., Strauss, J., Narendja, F. & Scazzocchio, C. 1999 The GATA factor AreA is essential for chromatin remodelling in a eukaryotic bidirectional promoter. *EMBO Journal* **18**, 1584-1597.
- Murray, J., Marusich, M. F., Capaldi, R. A. & Aggeler, R. 2004 Focused proteomics: Monoclonal antibody-based isolation of the oxidative phosphorylation machinery and detection of phosphoproteins using a fluorescent phosphoprotein gel stain. *Electrophoresis* **25**, 2520-2525.
- Naujokat, C., Fuchs, D. & Berges, C. 2007 Adaptive modification and flexibility of the proteasome system in response to proteasome inhibition. *Biochimica Et Biophysica Acta-Molecular Cell Research* **1773**, 1389-1397.
- Naujokat, C. & Hoffmann, S. 2002 Role and function of the 26S proteasome in proliferation and apoptosis. *Laboratory Investigation* **82**, 965-980.

- Navarro, F. J., Machin, F., Martin, Y. & Siverio, J. M. 2006 Down-regulation of eukaryotic nitrate transporter by nitrogen-dependent ubiquitinylation. *Journal of Biological Chemistry* **281**, 13268-13274.
- Navarro, F. J., Perdomo, G., Tejera, P., Medina, B., Machin, H., Guillen, R. M., Lancha, A. & Siverio, J. M. 2003 The role of nitrate reductase in the regulation of the nitrate assimilation pathway in the yeast *Hansenula polymorpha*. *FEMS Yeast Research* **4**, 149-155.
- Navarro, M. T., Guerra, E., Fernandez, E. & Galvan, A. 2000 Nitrite reductase mutants as an approach to understanding nitrate assimilation in *Chlamydomonas reinhardtii*. *Plant Physiology* **122**, 283-289.
- Nelson, N., Sacher, A. & Nelson, H. 2002 The significance of molecular slips in transport systems. *Nature Reviews Molecular Cell Biology* **3**, 876-881.
- Nie, Y., Ermolova, N. & Kaback, H. R. 2007 Site-directed alkylation of LacY: Effect of the proton electrochemical gradient. *Journal of Molecular Biology* **374**, 356-364.
- Nijman, S. M. B., Luna-Vargas, M. P. A., Velds, A., Brummelkamp, T. R., Dirac, A. M. G., Sixma, T. K. & Bernards, R. 2005 A genomic and functional inventory of deubiquitinating enzymes. *Cell* **123**, 773-786.
- Noriega, C. E., Schmidt, R., Gray, M. J., Chen, L. L. & Stewart, V. 2008 Autophosphorylation and dephosphorylation by soluble forms of the nitrate-responsive sensors NarX and NarQ from *Escherichia coli* K-12. *Journal of Bacteriology* **190**, 3869-3876.
- Okamoto, M., Kumar, A., Li, W. B., Wang, Y., Siddiqi, M. Y., Crawford, N. M. & Glass, A. D. M. 2006 High-affinity nitrate transport in roots of *Arabidopsis* depends on expression of the NAR2-like gene AtNRT3.1. *Plant Physiology* **140**, 1036-1046.
- Okamoto, M., Vidmar, J. J. & Glass, A. D. M. 2003 Regulation of NRT1 and NRT2 gene families of *Arabidopsis thaliana*: Responses to nitrate provision. *Plant and Cell Physiology* **44**, 304-317.
- Okamoto, P. M. & Marzluf, G. A. 1993 Nitrate reductase of *Neurospora crassa* - the functional role of individual amino acids in the heme domain as examined by site directed mutagenesis. *Molecular & General Genetics* **240**, 221-230.
- Orengo, C., Michie, A. D., Jones, D. T. & Swindells, M. B., Thornton, J.M. 1997 CATH: A hierarchic classification of protein domain structures. *Structure* **5**, 1093-1108.
- Orsel, M., Chopin, F., Leleu, O., Smith, S. J., Krapp, A., Daniel-Vedele, F. & Miller, A. J. 2006 Characterization of a two-component high-affinity nitrate uptake system in

- Arabidopsis. Physiology and protein-protein interaction. *Plant Physiology* **142**, 1304-1317.
- Orsel, M., Filleur, S., Fraissier, V. & Daniel-Vedele, F. 2002 Nitrate transport in plants: which gene and which control? *Journal of Experimental Botany* **53**, 825-833.
- Orzaez, M., Salgado, J., Gimenez-Giner, A., Perez-Paya, E. & Mingarro, I. 2004 Influence of proline residues in transmembrane helix packing. *Journal of Molecular Biology* **335**, 631-640.
- Osborne, A. R., Rapoport, T. A. & van den Berg, B. 2005 Protein translocation by the Sec61/SecY channel. *Annual Review of Cell and Developmental Biology* **21**, 529-550.
- Ostermeier, C., Harrenga, A., Ermler, U. & Michel, H. 1997 Structure at 2.7 angstrom resolution of the *Paracoccus denitrificans* two-subunit cytochrome c oxidase complexed with an antibody F-V fragment. *Proceedings of the National Academy of Sciences of the United States of America* **94**, 10547-10553.
- Pagni, M., Ioannidis, V., Cerutti, L., Zahn-Zabal, M., Jongeneel, C. V. & Falquet, L. 2004 MyHits: a new interactive resource for protein annotation and domain identification. *Nucleic Acids Research* **32**, W332-W335.
- Pao, S. S., Paulsen, I. T. & Saier, M. H. 1998 Major facilitator superfamily. *Microbiology and Molecular Biology Reviews* **62**, 1-34.
- Parton, R. G. & Richards, A. A. 2003 Lipid rafts and caveolae as portals for endocytosis: new insights and common mechanisms. *Traffic* **4**, 724-738.
- Pateman, J. A., Cove, D. J., Rever B. M. & B., R. D. 1964 A common co-factor for nitrate reductase and xanthine dehydrogenase which also regulates the synthesis of nitrate reductase. *Nature* **201**, 58-60.
- Pauling, L., Corey, R. B. & Branson, H. R. 1951 The structure of proteins: two hydrogen-bonded helical configurations of the polypeptide chain. *Proceedings of the National Academy of Sciences of the United States of America* **37**, 205-211.
- Pawson, T. 1994 Introduction - Protein-Kinases. *Faseb Journal* **8**, 1112-1113.
- Pazdernik, N. J., Jessen-Marshall, A. E. & Brooker, R. J. 1997 Role of conserved residues in hydrophilic loop 8-9 of the lactose permease. *Journal of Bacteriology* **179**, 735-741.
- Pazdernik, N. J., Matzke, E. A., Jessen-Marshall, A. E. & Brooker, R. J. 2000 Roles of charges residues in the conserved motif, G-X-X-X-D/E-R/K-X-G-[X]-R/K-R/K, of the lactose permease of *Escherichia coli*. *Journal of Membrane Biology* **174**, 31-40.
- Peakman, T., Crouzet, J., Mayaux, J. F., Busby, S., Mohan, S., Harborne, N., Wootton, J., Nicolson, R. & Cole, J. 1990 Nucleotide-sequence, organisation and structural-analysis of the products of genes in the Nirb-Cysg region of the *Escherichia coli* K-12 chromosome. *European Journal of Biochemistry* **191**, 315-323.

- Peberdy, J. F. 1989 Fungi without coats - Protoplasts as tools for mycological research. *Mycological Research* **93**, 1-20.
- Peng, J. M. 2008 Evaluation of proteomic strategies for analysing ubiquitinated proteins. *Bmb Reports* **41**, 177-183.
- Peng, J. M., Schwartz, D., Elias, J. E., Thoreen, C. C., Cheng, D. M., Marsischky, G., Roelofs, J., Finley, D. & Gygi, S. P. 2003 A proteomics approach to understanding protein ubiquitination. *Nature Biotechnology* **21**, 921-926.
- Perez, M. D., Gonzalez, C., Avila, J., Brito, N. & Siverio, J. M. 1997 The YNT1 gene encoding the nitrate transporter in the yeast *Hansenula polymorpha* is clustered with genes YNI1 and YNR1 encoding nitrite reductase and nitrate reductase, and its disruption causes inability to grow in nitrate. *Biochemical Journal* **321**, 397-403.
- Perozo, E., Cortes, D. M. & Cuello, L. G. 1999 Structural rearrangements underlying K⁺ channel activation gating. *Science* **285**, 73-78.
- Picot, D., Loll, P. J. & Garavito, R. M. 1994 The X-ray structure of the membrane protein prostaglandin H2 synthetase-1. *Nature* **367**, 243-249.
- Pierce, S. K. 2002 Lipid rafts and B-Cell activation *Nature Reviews Immunology* **2**, 96-105.
- Pike, L. J. 2004 Lipid rafts: heterogeneity on the high seas. *Biochemical Journal* **378**, 281-292.
- Platt, A., Langdon, T., Arst, H. N., Kirk, D., Tollervey, D., Sanchez, J. M. M. & Caddick, M. X. 1996 Nitrogen metabolite signalling involves the C-terminus and the GATA domain of the *Aspergillus* transcription factor AREA and the 3' untranslated region of its mRNA. *EMBO Journal* **15**, 2791-2801.
- Pombeiro-Spondachio, R. C., Rossi, A., Han, S. W. & Martinez-Rossi, N.M. 1993 Kinetic studies of nitrite uptake by *Aspergillus nidulans*. *Brazilian Journal of Medical Biology Research* **26**.
- Pontecorvo, G. 1953 The genetics of *Aspergillus nidulans*. *Advances in Genetics* **5**, 141-238.
- Popot, J. L. & Engelman, D. M. 1990 Membrane-Protein Folding and Oligomerization - the 2-Stage Model. *Biochemistry* **29**, 4031-4037.
- Popot, J. L. & Engelman, D. M. 2000 Helical membrane protein folding, stability, and evolution. *Annual Review of Biochemistry* **69**, 881-922.
- Pozuelo, M., Merchan, F., Macias, M. I., Beck, C. F., Galvan, A. & Fernandez, E. 2000 The negative effect of nitrate on gametogenesis is independent of nitrate assimilation in *Chlamydomonas reinhardtii*. *Planta* **211**, 287-292.
- Prieto, R., Dubus, A., Galvan, A. & Fernandez, E. 1996 Isolation and characterization of two new negative regulatory mutants for nitrate assimilation in *Chlamydomonas*

- reinhardtii* obtained by insertional mutagenesis. *Molecular & General Genetics* **251**, 461-471.
- Promega. 1991 Promega Protocols and Applications Guide pp. 54.
- Punt, P. J., Greaves, P. A., Kuyvenhoven, A., Vandeutekom, J. C. T., Kinghorn, J. R., Pouwels, P. H. & Van den Hondel, C. A. M. J. J. 1991 A twin-reporter vector for simultaneous analysis of expression signals of divergently transcribed, contiguous genes in filamentous fungi. *Gene* **104**, 119-122.
- Punt, P. J., Strauss, J., Smit, R., Kinghorn, J. R., Vandenhondel, C. & Scazzocchio, C. 1995 The intergenic region between the divergently transcribed *niiA* and *niaD* genes of *Aspergillus nidulans* contains multiple *nirA* binding sites which act bidirectionally. *Molecular and Cellular Biology* **15**, 5688-5699.
- Punt, P. J., van Biezen, N., Conesa, A., Albers, A., Mangnus, J. & Van den Hondel, C. 2002 Filamentous fungi as cell factories for heterologous protein production. *Trends in Biotechnology* **20**, 200-206.
- Quesada, A., Galvan, A. & Fernandez, E. 1994 Identification of nitrate transporter genes in *Chlamydomonas reinhardtii*. *Plant Journal* **5**, 407-419.
- Quesada, A., Hidalgo, J. & Fernandez, E. 1998 Three Nrt2 genes are differentially regulated in *Chlamydomonas reinhardtii*. *Molecular and General Genetics* **258**, 373.
- Quesada, A., Krapp, A., Trueman, L. J., Daniel-Vedele, F., Fernandez, E., Forde, B. G. & Caboche, M. 1997 PCR-identification of a *Nicotiana plumbaginifolia* cDNA homologous to the high-affinity nitrate transporters of the *crnA* family. *Plant Molecular Biology* **34**, 265-274.
- Rabin, R. S. & Stewart, V. 1992 Either of two functionally redundant sensor proteins NarX and NarQ, is sufficient for nitrate regulation in *Escherichia coli*. *Proceedings of the National Academy of Sciences of the United States of America* **89**, 8419-8423.
- Rabin, R. S. & Stewart, V. 1993 Dual response regulators (NarL and NarP) interact with dual sensors (NarX and NarQ) to control nitrate-regulated and nitrite-regulated gene-expression in *Escherichia coli* K-12. *Journal of Bacteriology* **175**, 3259-3268.
- Rapoport, T. A., Goder, V., Heinrich, S. U. & Matlack, K. E. S. 2004 Membrane-protein integration and the role of the translocation channel. *Trends in Cell Biology* **14**, 568-575.
- Rapoport, T. A., Jungnickel, B. & Kutay, U. 1996 Protein transport across the eukaryotic endoplasmic reticulum and bacterial inner membranes. *Annual Review of Biochemistry* **65**, 271-303.
- Rath, A. & Deber, C. A. 2008 Surface recognition elements of membrane protein oligomerization. *Proteins-Structure Function and Bioinformatics* **70**, 786-793.

- Rechsteiner, M. & Rogers, S. W. 1996 PEST sequences and regulation by proteolysis. *Trends in Biochemical Sciences* **21**, 267-271.
- Remans, T., Nacry, P., Pervent, M., Filleur, S., Diatloff, E., Mounier, E., Tillard, P., Forde, B. G. & Gojon, A. 2006 The Arabidopsis NRT1.1 transporter participates in the signaling pathway triggering root colonization of nitrate-rich patches. *Proceedings of the National Academy of Sciences of the United States of America* **103**, 19206-19211.
- Rexach, J., Fernandez, E. & Galvan, A. 2000 The *Chlamydomonas reinhardtii* Nar1 gene encodes a chloroplast membrane protein involved in nitrite transport. *Plant Cell* **12**, 1441-1453.
- Rexach, J., Llamas, A., Fernandez, E. & Galvan, A. 2002 The activity of the high-affinity nitrate transport system I (NRT2;1, NAR2) is responsible for the efficient signalling of nitrate assimilation genes in *Chlamydomonas reinhardtii*. *Planta* **215**, 606-611.
- Rexach, J., Montero, B., Fernandez, E. & Galvan, A. 1999 Differential regulation of the high affinity nitrite transport systems III and IV in *Chlamydomonas reinhardtii*. *Journal of Biological Chemistry* **274**, 27801-27806.
- Riach, M. B. R. & Kinghorn, J. R. 1996 Genetic transformation and vector developments in filamentous fungi. In *Mycology* vol. 13, Fungal Genetics: Principles and Practice (ed. C. J. Bos.), pp. 209-234. New York: Marcel Dekker, Inc.
- Riezman, H. 2002 Cell biology - The ubiquitin connection. *Nature* **416**, 381-383.
- Roepe, P. D., Zbar, R. T. S., Sarkar, H. K. & Kaback, H. R. 1989 A five residue sequence near the carboxyl terminus of the polytopic membrane protein lac permease is required for stability within the membrane. *Proceedings of the National Academy of Sciences of the United States of America* **86**, 3992-3996.
- Rogers, S., Wells, R. & Rechsteiner, M. 1986 Amino acid sequences common to rapidly degraded proteins: the PEST hypothesis. *Science* **234**, 364-368.
- Ruiz-Diez, B. 2002 Strategies for the transformation of filamentous fungi. *Journal of Applied Microbiology* **92**, 189-195.
- Russ, W. P. & Engelman, D. M. 2000 The GxxxG motif: A framework for transmembrane helix-helix association. *Journal of Molecular Biology* **296**, 911-919.
- Sahin-Toth, M., Karlin, A. & Kaback, H. R. 2000 Unraveling the mechanism of the lactose permease of *Escherichia coli*. *Proceedings of the National Academy of Sciences of the United States of America* **97**, 10729-10732.
- Sahin-Toth, M., le Coutre, J., Kharabi, D., le Maire, G., Lee, J. C. & Kaback, H. R. 1999 Characterization of Glu126 and Arg144, two residues that are indispensable for substrate binding in the lactose permease of *Escherichia coli*. *Biochemistry* **38**, 813-819.

- Saier, M. H. 2000 A functional-phylogenetic classification system for transmembrane solute transporters. *Microbiology and Molecular Biology Reviews* **64**, 354-411.
- Salaun, C., James, D. J. & Chamberlain, L. H. 2004 Lipid rafts and the regulation of exocytosis. *Traffic* **5**, 255-264.
- Salghetti, S. E., Caudy, A. A., Chenoweth, J. G. & Tansey, W. P. 2001 Regulation of transcriptional activation domain function by ubiquitin. *Science* **293**, 1651-1653.
- Sambrook, J., Fritsch, E. F. & Maniatis, T. 1989 *Molecular Cloning: A laboratory manual*: Cold Spring Harbour Laboratory Press.
- Samson, R. A. 1994 Taxonomy - Current Concepts of *Aspergillus* Systematics. In *Biotechnology Handbooks*, vol. 7, *Aspergillus* (ed. J. E. Smith), pp. 1-22. Glasgow: Plenum Press.
- Schagger, H. & van Jagow, G. 1991 Blue native electrophoresis for isolation of membrane protein complexes in enzymatically active form. *Analytical Biochemistry* **199**, 223-231.
- Schauser, L., Roussis, A., Stiller, J. & Stougaard, J. 1999 A plant regulator controlling development of symbiotic root nodules. *Nature* **402**, 191-195.
- Schauser, L., Wieloch, W. & Stougaard, J. 2005 Evolution of NIN-Like proteins in *Arabidopsis*, rice, and *Lotus japonicus*. *Journal of Molecular Evolution* **60**, 229-237.
- Scheible, W. R., Gonzalez-Fontes, A., Lauerer, M., Muller-Rober, B., Caboche, M. & Stitt, M. 1997a Nitrate acts as a signal to induce organic acid metabolism and repress starch metabolism in tobacco. *Plant Cell* **9**, 783-798.
- Scheible, W. R., Lauerer, M., Schulze, E. D., Caboche, M. & Stitt, M. 1997b Accumulation of nitrate in the shoot acts as a signal to regulate shoot-root allocation in tobacco. *Plant Journal* **11**, 671-691.
- Scheible, W. R., Morcuende, R., Czechowski, T., Fritz, C., Osuna, D., Palacios-Rojas, N., Schindelasch, D., Thimm, O., Udvardi, M. K. & Stitt, M. 2004 Genome-wide reprogramming of primary and secondary metabolism, protein synthesis, cellular growth processes, and the regulatory infrastructure of *Arabidopsis* in response to nitrogen. *Plant Physiology* **136**, 2483-2499.
- Schiff, M. L., Siderovski, D. P., Jordan, J. D., Brothers, G., Snow, B., De Vries, L., Oriz, D. F. & Diverse-Pierluissi, M. 2000 Tyrosine kinase-dependent recruitment of RGS12 to the N-type calcium channel. *Nature* **408**, 723-727.
- Schnell, R. A. & Lefebvre, P. A. 1997 The *Chlamydomonas NIT2* locus encodes an activator of nitrate assimilation genes that is unusually rich in amino acid homopolymers. *Plant Physiology* **114**, 1282-1282.

- Schroder, I., Wolin, C. D., Cavicchioli, R. & Gunsalus, R. P. 1994 Phosphorylation and dephosphorylation of the NarQ, NarX, and NarL proteins of the nitrate-dependent 2-component regulatory system of *Escherichia coli*. *Journal of Bacteriology* **176**, 4985-4992.
- Schulenberg, B., Goodman, T. N., Aggeler, R., Capaldi, R. A. & Patton, W. F. 2004 Characterization of dynamic and steady-state protein phosphorylation using a fluorescent phosphoprotein gel stain and mass spectrometry. *Electrophoresis* **25**, 2526-2532.
- Senes, A., Engel, D. E. & DeGrado, W. F. 2004 Folding of helical membrane proteins: the role of polar, GxxxG-like and proline motifs. *Current Opinion in Structural Biology* **14**, 465-479.
- Senes, A., Gerstein, M. & Engelman, D. M. 2000 Statistical analysis of amino acid patterns in transmembrane helices: The GxxxG motif occurs frequently and in association with beta-branched residues at neighboring positions. *Journal of Molecular Biology* **296**, 921-936.
- Sengupta, P., Baird, B. & Holowka, D. 2007 Lipid rafts, fluid/fluid phase separation, and their relevance to plasma membrane structure and function. *Seminars in Cell & Developmental Biology* **18**, 583-590.
- Shank, L. P., Broughman, J. R., Takeguchi, W., Cook, G., Robbins, A. S., Hahn, L., Radke, G., Iwamoto, T., Schultz, B. D. & Tomich, J. M. 2006 Redesigning channel-forming peptides: Amino acid substitutions that enhance rates of supramolecular self-assembly and raise ion transport activity. *Biophysical Journal* **90**, 2138-2150.
- Sharp, P. A., Sugden, B. & Sambrook, J. 1973 Detection of 2 restriction endonuclease activities in *Haemophilus parainfluenzae* using analytical agarose ethidium bromide electrophoresis. *Biochemistry* **12**, 3055-3063.
- Siddiqi, M. Y., Glass, A. D. M., Ruth, T. J. & Fernando, M. 1989 Studies of the regulation of nitrate influx by Barley seedlings using (NO₃⁻¹)-N-13. *Plant Physiology* **90**, 806-813.
- Simon, S. M. & Blobel, G. 1991 A protein-conducting channel in the endoplasmic-reticulum. *Cell* **65**, 371-380.
- Simons, K. & Ikonen, E. 1997 Functional rafts in cell membranes. *Nature* **387**, 569-572.
- Singer, S. J. & Nicolson, G. L. 1972 Fluid mosaic model of structure of cell-membranes. *Science* **175**, 720-731.
- Siverio, J. M. 2002 Assimilation of nitrate by yeasts. *FEMS Microbiology Reviews* **26**, 277-284.
- Smil, V. 1999 Detonator of the population explosion. *Nature* **400**, 415-415.

- Smirnova, I., Kasho, V., Choe, J. Y., Altenbach, C., Hubbell, W. L. & Kaback, H. R. 2007 Sugar binding induces an outward-facing conformation of LacY. *Proceedings of the National Academy of Sciences of the United States of America* **104**, 16504-16509.
- Smirnova, I. N. & Kaback, H. R. 2003 Mutation in the lactose permease of *Escherichia coli* that decreases conformational flexibility and increases protein stability. *Biochemistry* **42**, 3025-3031.
- Snapp, E. L., Reinhart, G. A., Bogert, B. A., Lippincott-Schwartz, J. & Hegde, R. S. 2004 The organization of engaged and quiescent translocons in the endoplasmic reticulum of mammalian cells. *Journal of Cell Biology* **164**, 997-1007.
- Southern, E. M. 1975 Detection of specific sequences among DNA fragments separated by gel electrophoresis. *Journal of Molecular Biology* **98**, 503-517.
- Staub, O., Gautschi, I., Ishikawa, T., Brietschopf, K., Ciechanover, A., Schild, L. & Rotin, D. 1997 Regulation of stability and function of the epithelial Na⁺ channel (ENaC) by ubiquitination *EMBO Journal* **16**, 6325-6336.
- Stewart, V. 1994 Regulation of nitrate and nitrite reductase in enterobacteria. *Antonie Van Leeuwenhoek* **66**, 37-45.
- Stewart, V., Chen, L. L. & Wu, H. C. 2003 Response to culture aeration mediated by the nitrate and nitrite sensor NarQ of *Escherichia coli* K-12. *Molecular Microbiology* **50**, 1391-1399.
- Strauss, J., Muro-Pastor, M. I. & Scazzocchio, C. 1998 The regulator of nitrate assimilation in ascomycetes is a dimer which binds a nonrepeated, asymmetrical sequence. *Molecular and Cellular Biology* **18**, 1339-1348.
- Stryer, L. 1999 Membrane Channels and Pumps, *Biochemistry* (ed. L. Stryer), pp. 316-317. New York: W.H Freeman and Company.
- Suppmann, B. & Sawers, G. 1994 Isolation and characterization of hypophosphite-resistant mutants of *Escherichia coli* - Identification of the FocA protein, encoded by the Pfl operon, as a putative formate transporter. *Molecular Microbiology* **11**, 965-982.
- Svennelid, F., Olsson, A., Pitrowski, M., Rosenquist, M., Ottman, C., Larsson, C., oecking, C. & Sommarin, M. 1999 Phosphorylation of Thr-948 at the C terminus of the plasma membrane H⁺-ATPase creates a binding site for the regulatory 14-3-3 protein. *Plant Cell* **11**, 2379-2392.
- Szentpetery, Z., Kern, A., Liliom, K., Sarkadi, B. & Varadi, A. 2004 The role of the conserved glycines of ATP-binding cassette signature motifs of MRP1 in the communication between the substrate-binding site and the catalytic centres. *Journal of Biological Chemistry* **279**, 41670-41678.

- Szewczuk, E., Nayak, T., Oakley, C. E., Edgerton, H., Xiong, Y., Taheri-Talesh, N., Osmani, S. A. & Oakley, B. R. 2006 Fusion PCR and gene targeting in *Aspergillus nidulans*. *Nature Protocols* **1**, 3111-3120.
- Thrower, J. S., Hoffman, L., Rechsteiner, M. & Pickart, C. M. 2000 Recognition of the polyubiquitin proteolytic signal. *EMBO Journal* **19**, 94-102.
- Thulasiraman, P., Newton, S. M. C., Xu, J. D., Raymond, K. N., Mai, C., Hall, A., Montague, M. A. & Klebba, P. E. 1998 Selectivity of ferric enterobactin binding and cooperativity of transport in Gram-negative bacteria. *Journal of Bacteriology* **180**, 6689-6696.
- Tilburn, J., Scazzocchio, C., Taylor, G. G., Zabickyzissman, J. H., Lockington, R. A. & Davies, R. W. 1983 Transformation by integration in *Aspergillus nidulans*. *Gene* **26**, 205-221.
- Timberlake, W. E. & Marshall, M. A. 1989 Genetic engineering of filamentous fungi. *Science* **244**, 1313-1317.
- Tischner, R. 2000 Nitrate uptake and reduction in higher and lower plants. *Plant Cell and Environment* **23**, 1005-1024.
- Tishmack, P. A., Bashford, D., Harms, E. & Van Etten, R. L. 1997 Use of ¹H NMR spectroscopy and computer simulations to analyse histidine pKa changes in a protein tyrosine phosphatase: experimental and theoretical determination of electrostatic properties in a small protein *Biochemistry* **36**, 11984-11944.
- Tollervey, D. W. & Arst, H. N. 1981 Mutations to constitutivity and derepression are separate and separable in a regulatory gene of *Aspergillus nidulans* *Current Genetics* **4**, 63-68.
- Tomsett, A. B. & Cove, D. J. 1979 Deletion mapping of the *niiA niaD* gene region of *Aspergillus nidulans*. *Genetical Research* **34**, 19-&.
- Tong, Y., Zhou, J. J., Li, Z. S. & Miller, A. J. 2005 A two-component high-affinity nitrate uptake system in barley. *Plant Journal* **41**, 442-450.
- Tornroth-Horsefield, S., Wang, Y., Hedfalk, K., Johanson, U., Karlsson, M., Tajkhorshid, E., Neutze, R. & Kjellbom, P. 2006 Structural mechanism of plant aquaporin gating. *Nature* **439**, 688-694.
- Trueman, L. J., Richardson, A. & Forde, B. G. 1996 Molecular cloning of higher plant homologues of the high - affinity nitrate transporters of *Chlamydomonas reinhardtii* and *Aspergillus nidulans*. *Gene* **175**, 223-231.
- Tsezou, A., KitsiouTzeli, S., Galla, A., Gourgiotis, D., Papageorgiou, J., Mitrou, S., Molybdas, P. A. & Sinaniotis, C. 1996 High nitrate content in drinking water: Cytogenetic effects in exposed children. *Archives of Environmental Health* **51**, 458-461.

- Unkles, S. E., Hawker, K. L., Grieve, C., Campbell, E. I., Montague, P. & Kinghorn, J. R. 1991 *crnA* encodes a nitrate transporter in *Aspergillus nidulans*. *Proceedings of the National Academy of Sciences of the United States of America* **88**, 204-208.
- Unkles, S. E., Hawker, K. L., Grieve, C., Campbell, E. I., Montague, P. & Kinghorn, J. R. 1995 *crnA* encodes a nitrate transporter in *Aspergillus nidulans* (Vol 88, Pg 204, 1991). *Proceedings of the National Academy of Sciences of the United States of America* **92**, 3076-3076.
- Unkles, S. E., Rouch, D. A., Wang, Y., Siddiqi, M. Y., Glass, A. D. M. & Kinghorn, J. R. 2004a Two perfectly conserved arginine residues are required for substrate binding in a high-affinity nitrate transporter. *Proceedings of the National Academy of Sciences of the United States of America* **101**, 17549-17554.
- Unkles, S. E., Rouch, D. A., Wang, Y., Siddiqi, M. Y., Okamoto, M., Stephenson, R. M., Kinghorn, J. R. & Glass, A. D. M. 2005 Determination of the essentiality of the eight cysteine residues of the NrtA protein for high-affinity nitrate transport and the generation of a functional cysteine-less transporter. *Biochemistry* **44**, 5471-5477.
- Unkles, S. E., Smith, J., Kanan, G., Millar, L. J., Heck, I. S., Boxer, D. H. & Kinghorn, J. R. 1997 The *Aspergillus nidulans* *cnxABC* locus is a single gene encoding two catalytic domains required for synthesis of precursor Z, an intermediate in molybdenum cofactor biosynthesis. *Journal of Biological Chemistry* **272**, 28381-28390.
- Unkles, S. E., Wang, R. C., Wang, Y., Glass, A. D. M., Crawford, N. M. & Kinghorn, J. R. 2004b Nitrate reductase activity is required for nitrate uptake into fungal but not plant cells. *Journal of Biological Chemistry* **279**, 28182-28186.
- Unkles, S. E., Zhou, D., Siddiqi, M. Y., Kinghorn, J. R. & Glass, A. D. M. 2001 Apparent genetic redundancy facilitates ecological plasticity for nitrate transport. *EMBO Journal* **20**, 6246-6255.
- van den Berg, B., Clemons, W. M., Collinson, I., Modis, Y., Hartmann, E., Harrison, S. C. & Rapoport, T. A. 2004 X-ray structure of a protein-conducting channel. *Nature* **427**, 36-44.
- Van Gelder, P., Dumas, F., Bartoldus, I., Saint, N., Prilipov, A., Winterhalter, M., Wang, Y. F., Philippsen, A., Rosenbusch, J. P. & Schirmer, T. 2002 Sugar transport through maltoporin of *Escherichia coli*: Role of the greasy slide. *Journal of Bacteriology* **184**, 2994-2999.
- Vazquez-Ibar, J. L., Guan, L., Weinglass, A. B., Verner, G., Gordillo, R. & Kaback, H. R. 2004 Sugar recognition by the lactose permease of *Escherichia coli*. *Journal of Biological Chemistry* **279**, 49214-49221.

- Vermeer, I. T. M. & van Mannen, J. M. S. 2001 Nitrate exposure and the endogenous formation of carcinogenic nitrosamines in humans. *Reviews on Environmental Health* **16**, 105-116.
- Vidmar, J. J., Zhuo, D. G., Siddiqi, M. Y. & Glass, A. D. M. 2000 Isolation and characterization of HvNRT2.3 and HvNRT2.4, cDNAs encoding high-affinity nitrate transporters from roots of barley. *Plant Physiology* **122**, 783-792.
- Vogelstein, B. & Gillespie, D. 1979 Preparative and Analytical Purification of DNA from Agarose. *Proceedings of the National Academy of Sciences of the United States of America* **76**, 615-619.
- von Heijne, G. 2007 Formation of trans membrane helices *in vivo* - Is hydrophobicity all that matters? *Journal of General Physiology* **129**, 353-356.
- Vonheijne, G. 1991 Proline Kinks in Transmembrane Alpha-Helices. *Journal of Molecular Biology* **218**, 499-503.
- Waldispuhl, J., O'Donnell, C. W., Devadas, S., Clote, P. & Berger, B. 2008 Modeling ensembles of transmembrane beta-barrel proteins. *Proteins* **71**, 1097-1112.
- Walker, M. S. & Demoss, J. A. 1993 Phosphorylation and dephosphorylation catalyzed *in vitro* by purified components of the nitrate sensing system, NarX and NarL. *Journal of Biological Chemistry* **268**, 8391-8393.
- Wang, R. C., Okamoto, M., Xing, X. J. & Crawford, N. M. 2003 Microarray analysis of the nitrate response in *Arabidopsis* roots and shoots reveals over 1,000 rapidly responding genes and new linkages to glucose, trehalose-6-phosphate, iron, and sulphate metabolism. *Plant Physiology* **132**, 556-567.
- Wang, R. C., Xing, X. J. & Crawford, N. 2007 Nitrite acts as a transcriptome signal at micromolar concentrations in *Arabidopsis* roots. *Plant Physiology* **145**, 1735-1745.
- Wang, X. C., Sarker, R. I. & Maloney, P. C. 2006 Analysis of substrate-binding elements in OxlT, the oxalate : formate antiporter of *Oxalobacter formigenes*. *Biochemistry* **45**, 10344-10350.
- Wang, Y.-T., Yu, X.-M. & Salter, M. W. 1996 Ca²⁺-independent reduction of N-methyl-D-aspartate channel activity by protein tyrosine phosphatase *Proceedings of the National Academy of Sciences of the United States of America* **93**, 1721-1725.
- Wang, Y., Li, W., Siddiqi, Y., Symington, V.F., Kinghorn, J.R., Unkles, S.E. & Glass, A. D. M. 2008 Nitrite transport is mediated by the nitrite-specific high-affinity NitA transporter and by nitrate transporters NrtA, NrtB in *Aspergillus nidulans*. *Fungal Genetics and Biology* **45**, 94-102.

- Wang, Y. F., Dutzler, R., Rizkallah, P. J., Rosenbusch, J. P. & Schirmer, T. 1997 Channel specificity: Structural basis for sugar discrimination and differential flux rates in maltoporin. *Journal of Molecular Biology* **272**, 56-63.
- Ward, J. M. 2001 Identification of novel families of membrane proteins from the model plant *Arabidopsis thaliana*. *Bioinformatics* **17**, 560-563.
- Warrens, A. N., Jones, M. D. & Lechler, R. I. 1997 Splicing by overlap extension by PCR using asymmetric amplification: An improved technique for the generation of hybrid proteins of immunological interest. *Gene* **186**, 29-35.
- White, S. H. & von Heijne, G. 2004 The machinery of membrane protein assembly. *Current Opinion in Structural Biology* **14**, 397-404.
- White, S. H. & von Heijne, G. 2005 Transmembrane helices before, during and after insertion. *Current Opinion in Structural Biology* **15**, 378-386.
- White, W. B. & Ferry, J. G. 1992 Identification of formate dehydrogenase-specific messenger-RNA species and nucleotide-sequence of the Fdhc gene of *Methanobacterium formicicum*. *Journal of Bacteriology* **174**, 4997-5004.
- Wickner, W. 1988 Mechanisms of membrane assembly: general lessons from the study of M13 coat protein and *Escherichia coli* leader peptidase. *Biochemistry* **27**, 1081-1086.
- Wilkinson, K. D. 2000 Ubiquitination and deubiquitination: Targeting of proteins for degradation by the proteasome. *Seminars in Cell & Developmental Biology* **11**, 141-148.
- Williams, R. W., Chang, A., Juretic, D. & Loughran, S. 1987 Secondary structure predictions and medium range interactions. *Biochimica Et Biophysica Acta* **916**, 200-204.
- Williams, S. B. & Stewart, V. 1997 Discrimination between structurally related ligands nitrate and nitrite controls autokinase activity of the NarX transmembrane signal transducer of *Escherichia coli* K-12. *Molecular Microbiology* **26**, 911-925.
- Wilmot, C. M. & Thornton, J. M. 1988 Analysis and prediction of the different types of beta-turn in proteins. *Journal of Molecular Biology* **203**, 221-232.
- Wimley, W. C. 2002 Toward genomic identification of β -barrel membrane proteins: composition and architecture of known structures. *Protein Science* **11**, 301-312.
- Wimley, W. C. 2003 The versatile β -barrel membrane protein *Current Opinion in Structural Biology* **13**, 404-411.
- Wirth, J., Chopin, F., Santoni, V., Viennois, G., Tillard, P., Krapp, A., Lejay, L., Daniel-Vedele, F. & Gojon, A. 2007 Regulation of root nitrate uptake at the NRT2.1 protein level in *Arabidopsis thaliana*. *Journal of Biological Chemistry* **282**, 23541-23552.

- Wolf, D. H. & Hilt, W. 2004 The proteasome: a proteolytic nanomachine of cell regulation and waste disposal. *Biochimica Et Biophysica Acta-Molecular Cell Research* **1695**, 19-31.
- Wolin, C. D. & Kaback, H. R. 2001 Functional estimation of loop-helix boundaries in the lactose permease of *Escherichia coli* by single amino acids deletion analysis. *Biochemistry* **20**, 1996-2003.
- Wong, K. H., Hynes, M. J. & Davis, M., A. 2008 Recent advances in nitrogen regulation: a comparison between *Saccharomyces cerevisiae* and filamentous fungi. *Eukaryotic Cell* **7**, 917-925.
- Wood, N. J., Alizadeh, T., Richardson, D. J., Ferguson, S. J. & Moir, J. W. B. 2002 Two domains of a dual function NarK protein are required for nitrate uptake, the first step of denitrification in *Paracoccus pantotrophus*. *Molecular Microbiology* **44**, 157-170.
- Xu, H. X., Jin, J., DeFelice, L. J., Andrews, N. C. & Clapham, D. E. 2004 A spontaneous, recurrent mutation in divalent metal transporter-1 exposes a calcium entry pathway. *Plos Biology* **2**, 378-386.
- Yamaguchi, A., ASamejima, T., Kimura, T. & Sawai, T. 1996 His257 is a uniquely important histidine for tetracycline/H⁺ antiport function but not mandatory for full activity of the transposon Tn10-encoded metal-tetracycline/H⁺ antiporter. *Biochemistry* **35**, 4359-4364.
- Yamaguchi, A., Someya, Y. & Sawai, T. 1992 Metal-Tetracycline/H⁺ antiporter of *Escherichia coli* encoded by transposon Tn10 - the role of a conserved sequence motif, GXXXXRXGRR, in a putative cytoplasmic loop between helices 2 and 3. *Journal of Biological Chemistry* **267**, 19155-19162.
- Yamashita, A., Singh, S. K., Kawate, T., Jin, Y. & Gouaux, E. 2005 Crystal structure of a bacterial homologue of Na⁺/Cl⁻ dependent neurotransmitter transporters. *Nature* **437**, 215-223.
- Yang, Q., Wang, X. C., Ye, L. W., Mentrikoski, M., Mohammadi, E., Kim, Y. M. & Maloney, P. C. 2005 Experimental tests of a homology model for OxIT, the oxalate transporter of *Oxalobacter formigenes*. *Proceedings of the National Academy of Sciences of the United States of America* **102**, 8513-8518.
- Yarden, Y., Escobedo, J. A., Kuang, W. J., Yangfeng, T. L., Daniel, T. O., Tremble, P. M., Chen, E. Y., Ando, M. E., Harkins, R. N., Francke, U., Fried, V. A., Ullrich, A. & Williams, L. T. 1986 Structure of the receptor for platelet-derived growth-factor helps define a family of closely related growth-factor receptors. *Nature* **323**, 226-232.

- Yelton, M. M., Hamer, J. E. & Timberlake, W. E. 1984 Transformation of *Aspergillus nidulans* by using a Trpc plasmid. *Proceedings of the National Academy of Sciences of the United States of America-Biological Sciences* **81**, 1470-1474.
- Yerushalmi, H., Lebendiker, M. & Schuldiner, S. 1995 EmrE, an *Escherichia coli* 12-kDa multidrug transporter, exchanges toxic cations and H⁺ and is soluble in organic solvents. *Journal of Biological Chemistry* **270**, 6856-6863.
- Yerushalmi, H. & Schuldiner, S. 2000 An essential glutamyl residue in EmrE, a multidrug antiporter from *Escherichia coli*. *Journal of Biological Chemistry* **275**, 5264-5269.
- Zhang, H. M. & Forde, B. G. 2000 Regulation of *Arabidopsis* root development by nitrate availability. *Journal of Experimental Botany* **51**, 51-59.
- Zhang, W., Guan, L. & Kaback, H. R. 2002 Helices VII and X in the lactose permease of *Escherichia coli*: Proximity and ligand-induced distance changes. *Journal of Molecular Biology* **315**, 53-62.
- Zheng, L., Kostrewa, D., Berneche, S., Winkler, F.K. & Li, X. D. 2004 The mechanism of ammonia transport based on the crystal structure of MntB of *Escherichia coli*. *PNAS* **101**, 17090-17095.
- Zhou, J. J., Fernandez, E., Galvan, A. & Miller, A. J. 2000a A high affinity nitrate transport system from *Chlamydomonas* requires two gene products *FEBS Letters* **466**, 225-227.
- Zhou, J. J., Trueman, L. J., Boorer, K. J., Theodoulou, F. L., Forde, B. G. & Miller, A. J. 2000b A high affinity fungal nitrate carrier with two transport mechanisms. *Journal of Biological Chemistry* **275**, 39894-39899.
- Zhou, Y. F., Morais-Cabral, J. H., Kaufman, A. & MacKinnon, R. 2001 Chemistry of ion coordination and hydration revealed by a K⁺ channel-Fab complex at 2.0 angstrom resolution. *Nature* **414**, 43-48.
- Zhou, Y. G., Guan, L., Freites, J. A. & Kaback, H. R. 2008 Opening and closing of the periplasmic gate in lactose permease. *Proceedings of the National Academy of Sciences of the United States of America* **105**, 3774-3778.
- Zhuo, D. G., Okamoto, M., Vidmar, J. J. & Glass, A. D. M. 1999 Regulation of a putative high-affinity nitrate transporter (Nrt2;1At) in roots of *Arabidopsis thaliana*. *Plant Journal* **17**, 563-568.